EPA-600/4-77-010
February 1977

MESOSCALE AIR POLLUTION TRANSPORT IN SOUTHEAST WISCONSIN

by

Walter A. Lyons
University of Wisconsin-Milwaukee
Milwaukee, Wisconsin 53201

Grant R-800873

Project Officer

Paul A. Humphrey
Environmental Sciences Research Laboratory
Research Triangle Park, North Carolina 27711

Environmental Sciences Research Laboratory
Office of Research and Development
U.S. Environmental Protection Agency
Research Triangle Park, NC 27711

RESEARCH REPORTING SERIES

Research reports of the Office of Research and Development, U.S. Environmental Protection Agency, have been grouped into five series. These five broad categories were established to facilitate further development and application of environmental technology. Elimination of traditional grouping was consciously planned to foster technology transfer and a maximum interface in related fields. The five series are:

1. Environmental Health Effects Research
2. Environmental Protection Technology
3. Ecological Research
4. Environmental Monitoring
5. Socioeconomic Environmental Studies

This report has been assigned to the ENVIRONMENTAL MONITORING series. This series describes research conducted to develop new or improved methods and instrumentation for the identification and quantification of environmental pollutants at the lowest conceivably significant concentrations. It also includes studies to determine the ambient concentrations of pollutants in the environment and/or the variance of pollutants as a function of time or meteorological factors.

This document is available to the public through the National Technical Information Service, Springfield, Virginia 22161.

DISCLAIMER

This report has been reviewed by the Environmental Sciences Research Laboratory, U.S. Environmental Protection Agency, and approved for publication. Approval does not signify that the contents necessarily reflect the views and policies of the U.S. Environmental Protection Agency, nor does mention of trade names or commercial products constitute endorsement or recommendation for use.

PREFACE

During the period 1970-1976, the University of Wisconsin-Milwaukee's Air Pollution Analysis Laboratory (College of Engineering and Applied Science) engaged in extensive studies on the mesometeorology of the Great Lakes. In spite of the fact that these massive bodies of water are convenient natural laboratories for the study of mesoscale air mass transformation, the body of scientific knowledge relating to such phenomena as lake breezes, snow squalls, etc., was surprisingly small. The extreme climatic and weather fluctuations generated by the lakes are of great importance to the region. The Great Lakes themselves cover an area of 246,000 km^2. Over 15% of the total U.S. population, and more than 25% of the nation's industrial capacity, is located near or on their shorelines.

The U.S. Environmental Protection Agency (1972) funded a large program to further investigate the effects of lake induced meteorological systems upon air pollution diffusion and transport using the western shore of Lake Michigan (near Milwaukee) as the test site. This program was then integrated into a much larger effort studying the Great Lakes' mesometeorology as a whole. The lake effects on the atmosphere in general must be first understood in greater detail before it is possible to better define the behavior of air pollutants. The combined research programs

sponsored by the National Aeronautics and Space Administration, the National Science Foundation, U.S. E.P.A., Office of Water Resources Research, the UWM Center for Great Lakes Studies, and several utilities, generated over three dozen papers, project reports, theses and films (totally almost 2000 pages of text). Obviously summarization, even of only that portion pertinent to air pollution becomes very difficult if one wishes to keep the document to readible dimensions. This report acts more as an "executive summary" of the pollution related aspects of the program rather than a complete stand-alone final report.The reader will be directed to the appropriate documents for details that may be of interest (see Appendix).

A reasonably complete summary of lake effects upon air pollution was published under the auspices of the American Meteorological Society (Lyons, 1975) in "Lectures on Air Pollution and Environmental Impact Analysis." Chapter 5 of this book, "Turbulent Diffusion and Pollutant Transport in Shoreline Environments" is also a fairly extensive review of what is known about Great Lakes mesometeorology.

This paper has been written to highlight the important findings of six years of Great Lakes air pollution related research. Those more recent developments not covered in the AMS review paper will be presented in somewhat greater detail.

It is felt that the results reported herein will be used not only by those responsible for environmental planning on the Great Lakes but also generalized for use along the entire 26,000 km of the United States coastline.

ABSTRACT

This research program comprised a comprehensive study of mesoscale meteorological regimes on the western shore of Lake Michigan and their effect upon air pollution dispersion and transport. It is felt that the results are applicable in a generic way to other mid-latitude coastal zones.

Continuous fumigation from elevated sources in shoreline zones during stable daytime onshore flow was intensively investigated by a large scale field program. A model was proposed, constructed, validated and calibrated. It was shown that the fumigation spot, while causing very high surface SO_2 concentrations, was so highly mobile as to generally reduce dosages below the three-hour standard (at least for the plants studied).

Instrumented aircraft profiles the structure of the thermal internal boundary layer (using $^{1/3}$ measurements). An acoustic sounder at 1 km from the Milwaukee shoreline revealed drastically reduced daytime mixing depths.

An intensive case study of a lake breeze was performed. Data were used as input to a Kinematic Diagnostic Model (KDM) which simulated mesoscale trajectories for pollutants released within the coastal zone.

Both mesoscale and synoptic scale transport of photochemical oxidants were found to be a significant problem in the Milwaukee area.

CONTENTS

FIGURES

ACKNOWLEDGEMENTS

Though the bulk of the results reported herein were the direct result of funding fromthe U.S. Environmental Protection Agency under Grant No. R-800873, it must be remembered that this research formed a major subset of an intensive and comprehensive study of Great Lakes mesometeorological systems. Thus the facilities, data and techniques used and developed were an integrated whole. For this reason the support of other organizations and agencies must be gratefully acknowledged, including: National Aeronautics and Space Administration, the National Science Foundation, the Graduate School of the University of Wisconsin-Milwaukee, and the UWM Center for Great Lakes Studies, and the UWM Social Science Research Facility, the National Center for Atmospheric Research, Commonwealth Edison Company, and Wisconsin Electric Power Company. This final report was produced using the facilities of COMPUMET/Meteorological and Environmental Services, Minneapolis, Minnesota.

Graduate students at the Air Pollution Analysis Laboratory at the University of Wisconsin-Milwaukee, deserve special thanks for making significant contributions to both the data gathering and analysis phases. In particular, Dr. Cecil S. Keen (now, University of Cape Town) served as field coordinator and developer of the Kinematic Diagnostic Program. Jerome Schuh super-

vised general software development, and in particular, the GLUMP Diffusion Model. John C. Dooley and Kenneth R. Rizzo labored long hours in equipment maintenance and data abstraction. Others including Eugene M. Rubin, Norman Knox, and as many as twenty additional undergraduate and graduate students played key roles in this effort.

In particular,the assistance of Professor Henry S. Cole, University of Wisconsin-Parkside, is hereby acknowledged for his role as co-principal investigator.

Other agencies, organizations and individuals who were most helpful in various phases of data collection include: Wisconsin Department of Natural Resources, Milwaukee County Department of Air Pollution Control, First Wisconsin Center, Towne Realty, Miller's Brewery, Johnston Candy Co., Milwaukee Water Works, City of Waukegan, Illinois Toll Highway Authority, Waukesha County Airport, and the Milwaukee County Institutions.

Technical manuscript preparation was admirably handled by Kathleen Walker.

SECTION 1

INTRODUCTION

GREAT LAKES MESOMETEOROLOGY

Covering almost a quarter of a million square kilometers, and with a shoreline extending 5,600 km, the Great Lakes represent the largest reservoir of fresh water in the world. Their thermal mass, represented by a volume of 22,910 km^3 makes them a tremendous heat source or sink, depending on the temperature of the overlying air mass. Since the region possesses a distinctly continental climate with recorded temperature extremes ranging from +47C to -53C, the Lakes are the generator of dramatic mesoscale air mass transformations. Thus the meteorology of Great Lakes shoreline regions provides an excellent natural laboratory for studying pollution diffusion and transport under conditions of transitional stability and complex mesoscale circulation regimes. But this opportunity is of more than academic importance inasmuch as fully 25% of the U.S. industrial capacity lies in areas affected. The Lake Michigan shoreline alone counts over 25 power plants.

During the winter (cold season), frigid continental air masses stream southwards over the largely unfrozen waters. Extensive observational (Lenschow, 1973) and theoretical studies (Lavoie, 1972) of lake snow squalls exist. Lyons and Pease (1972)

presented pictures of "steam devils" over Lake Michigan as -25°C air flowed over +2°C water, indicative of the extreme instability that can be found over and near the lakes during such events. This of course would have significant impact on the diffusion of effluents released into such a highly modified boundary layer.

The summer (warm season) has not been as extensively researched since the phenomena produced by the lakes are far less spectacular. In fact often the lakes eliminate rather than cause phenomena, such as total suppression of convective cloud systems over the water and downwind shoreline (Lyons, 1966). Bellaire (1965) was among the first to document the extreme but shallow (less than 150 m) conduction inversions which can form as warm tropical air advects over the cold water, which in the center of Lake Michigan can remain as cold as 4°C well into June. Lyons (1971) developed a model for such conduction inversions. Since low-level thermal stabilities are equivalent to those found within the polar night they would allow effluents to travel long distances virtually undiluted. As the stabilized air mass advects inland over the downwind shore on a sunny day, intense remodification occurs. Herkoff (1969) used surface temperature patterns obtained via an instrumented automobile to show that ground heating restores the temperature to typical inland values often within 20 km. Bierly (1963) studied the vertical aspect of this thermal remodification on the eastern Lake Michigan shoreline. The top of this modified layer, the thermal internal boundary layer (TIBL), marks the upward extent of newly generated

penetrative convection. Collins (1971) and Van der Hoven (1967), along with Hewson, et al. (1963) were among the first to point out that the generation of a TIBL could lead to the continuous (dynamic) fumigation of plumes released at an elevated level into the stable onshore flowing air (see Figure 1-1). Lyons and Cole (1973) further refined the concept and proposed a Gaussian type model for the phenomenon. The implications were that since unusually high concentrations of pollutants would be mixed to the surface for many consecutive hours, continuous fumigation potentially represented the most serious (and frequent) possible cause of exceedences of three-hour federal standards for such pollutants as SO_2.

The early studies of fumigation presumed a simple gradient onshore flow. The addition of a shoreline lake/sea breeze circulation compounds the problem many orders of magnitude. This diurnal mesoscale wind regime has been known since the time of the Greeks (Baralt and Brown, 1965) and appears in American scientific literature in almost Revolutionary times (Endicott,1799). It is only in the last decade or so that its rather profound impact upon shoreline air quality has begun to be recognized. It is still possible to find occasional state implementation documents or air quality advisories in which the presumption is made that a lake breeze will result in the onshore advection of clean air and thus the alleviation of a pollution episode. Lyons and Olsson (1972) used mesoscale data analyses and photography to show how, that in spite of apparently good ventilation, shoreline

lake breezes could cause serious degradation of urban shoreline air quality. An addition to continuous fumigation and generally severely limited mixing depths within roughly 20 km of the shore, it appeared that pollutants could recirculate within the lake breeze cell. Indeed, in Chicago and Milwaukee it was found that the highest values of most pollutants tended to occur during those months when lake breezes were most frequent. Figure 1-2 is a schematic of the lake breeze structure and its possible effects upon air pollutants. It becomes immediately apparent that conventional air quality models, which assume a steady-state homogeneous wind field, would fail in such cases. Furthermore, aerosols of various sizes could be expected to travel along different paths due to size sorting effects (Lyons and Keen, 1976a). And while Figure 1-2 is necessarily a two-dimensional representation, as shown by the Chicago tetroon experiments of 1967 (Lyons and Olsson, 1973), the complex transport phenomena within lake breezes are eminently three-dimensional.

Also apparent from numerous studies (Lyons, 1975a) was the fact that conventionally gathered meteorological data were totally inadequate to describe the atmosphere in coastal environments. Radiosonde derived mean mixing depth climatologies such as those generated by Holzworth (1967, 1972) had little validity within 20 km of a coastline, precisely were most of the Great Lakes air pollution sources (and receptors) were located. The need for improved mesoscale climatologies of wind, stability and mixing depths became imperative.

The several projects undertaken by the UWM Air Pollution Analysis Laboratory were aimed at arriving at some first solutions to the problems discussed above.

With regards to fumigation, it was necessary to actually test and validate and calibrate the model proposed by Lyons and Cole (1973). It was necessary to first expand the model to a multi-source configuration, out of which grew the GLUMP Regional Fumigation Model. Field studies in 1974 essentially validated the basic geometry, at least for high stack shoreline plumes. Urban scale fumigation was found to be indeed important in causing higher air pollution levels. Studies of the mixing depth profiles revealed the TIBL formation to be complex and its height and shape extremely significant in determining surface pollution concentrations. It was furthermore found that the "fumigation" spot exhibited a high degree of mobility, making the calculation of total dosages received at any one point a difficult problem.

The lake breeze structure was further studied and new details were revealed. Most importantly, it was possible to acquire extensive data showing the concept of recirculation and complex transport phenomena to be correct. A kinematic diagnostic model was developed which shed further light on how mesoscale shoreline flow regimes effect pollutants emitted from a variety of sources.

The following sections will detail the most significant results from these studies.

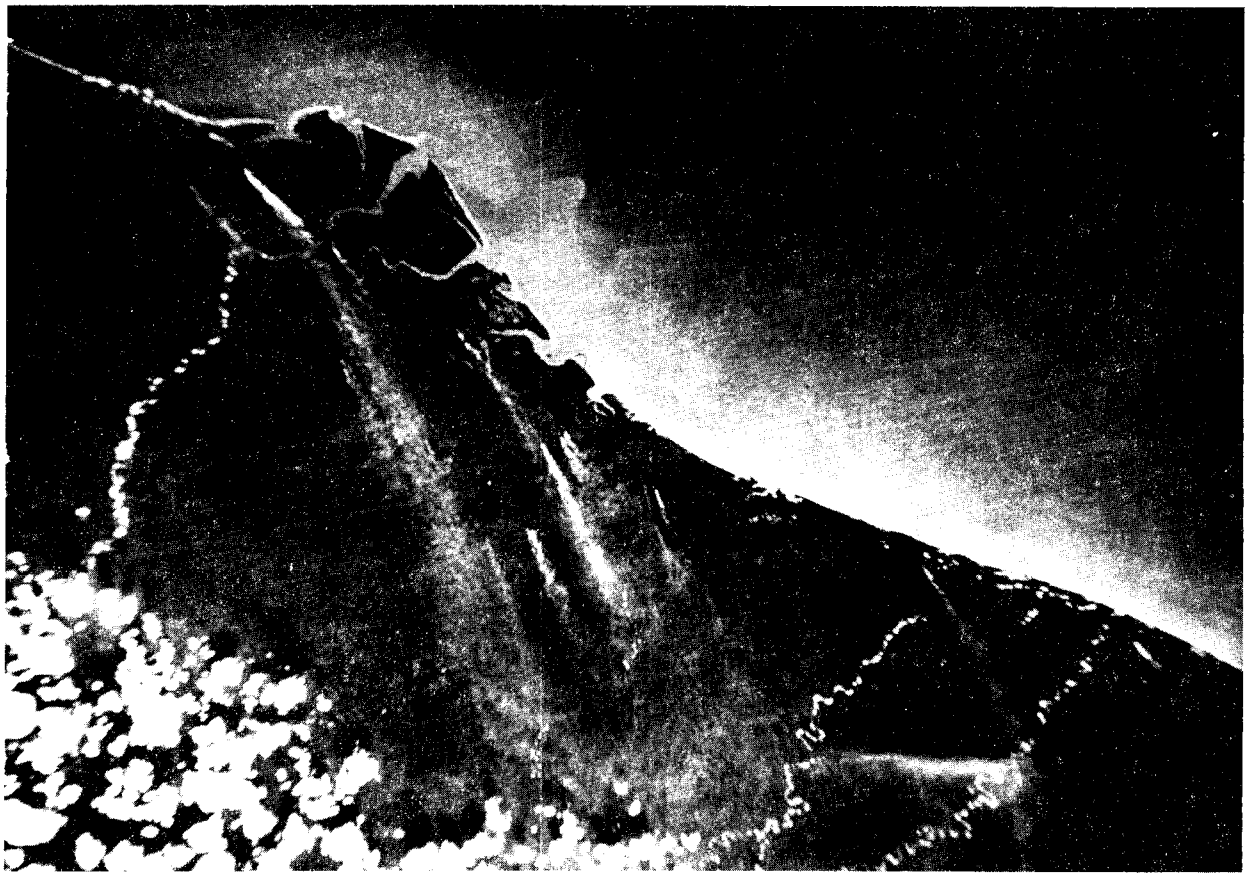

Figure 1-1. Photograph taken during Gemini manned orbital mission of a coastal region during midday. A fully developed boundary layer is present inland several tens of kilometers as marked by cumulus convection. However smoke released from numerous points undoubtedly experiences fumigation as it passes inland through a zone of rapidly changing atmospheric stabilities.

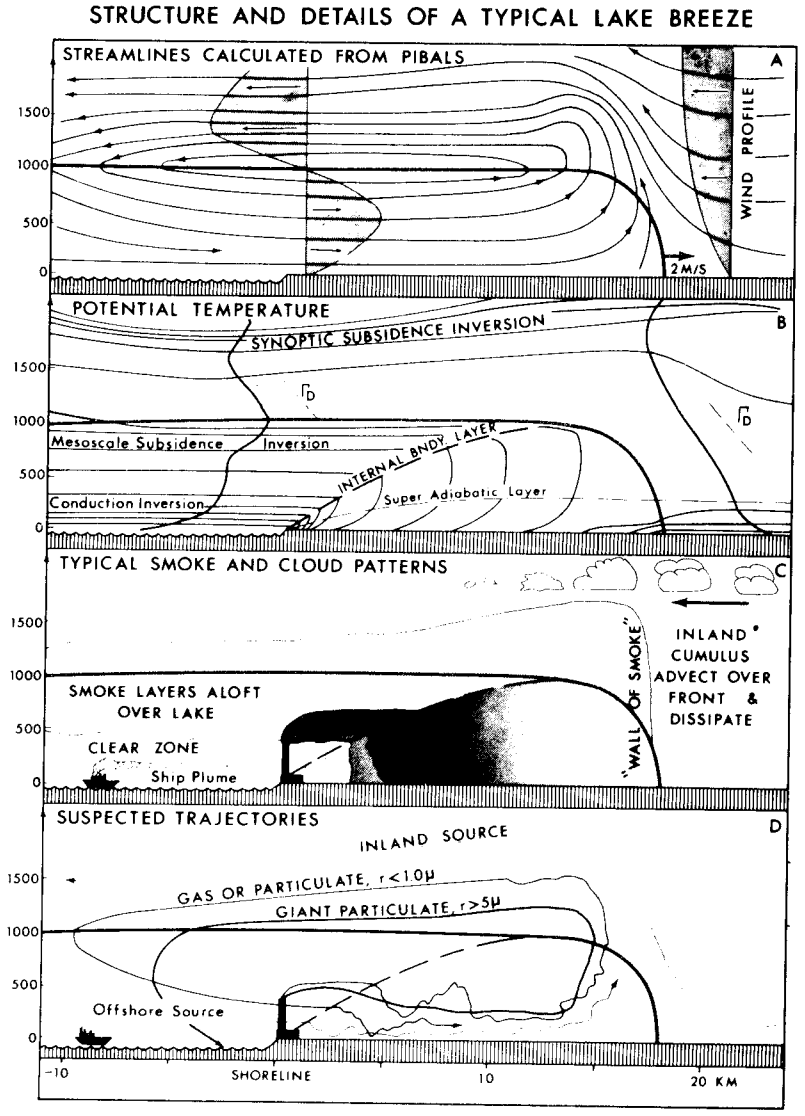

Figure 1-2. (a) Typical streamline patterns in a well developed lake breeze cell during mid-afternoon. The heavy line represents the top boundary of the inflow. View is looking south, with the lake on the left. (b) Schematic isopleths of potential temperature with packing indicating synoptic and mesoscale inversions. Typical temperature soundings over land and lake are shown compared to the dry adiabatic lapse. (c) General smoke patterns found, including the fumigating plume from an elevated shoreline point source. (d) Hypothesized trajectories of both fine and large particulate aerosols emitted in the area.

SECTION 2

CONCLUSIONS AND RECOMMENDATIONS

While considerable information was generated regarding lake-induced effects upon air pollution transport and diffusion in coastal zones, if anything, the phenomena were shown to be even more complex and multi-faceted than originally anticipated.

An extensive field program on the western shore of Lake Michigan during the summer of 1974 essentially validated the fumigation model proposed by Lyons and Cole (1973). The three regime plume geometry was indeed found using helicopter and aircraft measurements. These data also showed the necessity of employing split-simga modeling inasmuch as plume lateral and vertical spreads were often as much as three Pasquill-Gifford stability classes apart (the effect of wind shear the primary factor in causing enhanced lateral spread). The fumigation phenomenon is highly dependent on the shape and depth of the Thermal Internal Boundary Layer (TIBL). Aircraft profiling of the eddy dissipation rate ($\varepsilon^{1/3}$) proved most effective in gathering TIBL data, a highly complex, temporally and spatially, variable phenomenon. Actual power plant plume SO_2 measurements showed high surface concentrations. However, the fumigation spots moved rapidly about the landscape at speeds upward of 10 kmph, reducing dosages at any given point significantly. Extreme vertical direction wind shears frequently caused plumes to travel along separate axes. Any fumigation model for multi-stack power plants must take account of this effect or gross overestimates of concentration/dosages could

occur. For ascertaining "worst case" surface concentrations of fumigating power plant plumes, mobile monitoring (vans, aircraft, helicopter) is superior to the establishment of a fixed ground network. The size of the fumigation spot is too small, perhaps making the required network density prohibitively expensive for adequate data return in a reasonable amount of time.

The GLUMP Fumigation Model was calibrated for multi plume power plants with a range dependent calibration factor. The model predicts within a factor of two in the cases studied, even before the calibration is applied. The model was extended to cover regional patterns (Milwaukee County) and shows the fumigation regime significant enhances ground level pollution concentrations. Surface data and emission inventories were unfortunately insufficient to allow calibration of the model in the regional mode.

Studies of lake meteorology showed that even during supposedly "steady state" onshore gradient flows, there are complicated wind patterns, including the development of low level jet streams associated with intense inversion layers. The strong wind direction shears at plume level,highlight the essential invalidity of surface or even tower wind data for modeling individual cases. It is necessary to know exactly how the wind is behaving at the height of each individual plume through time.

The acoustic sounder is highly useful in showing the structure of lakeshore environment. For example, five straight days of severely reduced mixing depths occurred during one period of onshore flow. Conventional data would have suggested excellent dispersion conditions, when in fact quite the opposite was true.

A climatology of mixing depths at 1 km inland found the mean hourly daytime mixing depth (clear and scattered skies) to be reduced 2.73 times during onshore as opposed to offshore flow during summer (656 vs 240 m). Mid-day mixing depths could be suppressed by more than a factor of five.

An extensive analysis of a lake breeze illustrated via aircraft and tetroon data the recirculatory nature of lake breeze circulations. The pibal data obtained was used as input into the Kinematic Diagnostic Model (KDM), designed to use real rather than numerically generated wind data to simulate lake breeze transport. It proved a most useful experimental technique, confirming pollutant recirculation, aerosol size sorting, the role of the convergence zone in redistributing pollutants, and the essential futility of using surface data in predicting the spread of hazardous materials and pollutants in coastal zones.

Satellite data were shown highly useful in monitoring mesoscale, regional and synoptic scale transport. Individual plumes were detected for more than 150 km over Lake Michigan by Landsat, whereas SMS imaged a major sulfate haze aerosol episode over the central U.S. Also lake effects complicate even further mesoscale and synoptic scale transport. A model was proposed to explain the inland band of elevated ozone levels running parallel to the shoreline. The Chicago metropolitan area was shown to be a major contributor to the high oxidant levels recorded in southeastern Wisconsin. Also, aircraft monitoring of the Chicago urban plume revealed interstate transport of 25 tons per hour of SO_2 from Illinois into Wisconsin on one occasion. With regards to photo-

chemical oxidants and sulfates, the concept of Air Quality Control Regions clearly has to be severely modified or abandoned altogether.

In general, most required meteorological data taking in coastal environments is highly unrelated to the true needs of describing the atmosphere into which effluents are released. Needless to say, the inapplicability of most existing short term prediction models in coastal zones is painfully evident!

SECTION 3

DATA COLLECTION AND FIELD EXPERIMENTS

CHRONOLOGY

Each summer from 1970 through 1974 inclusive, some field data gathering took place in the Milwaukee area in direct or indirect support of this project.

The 1970 program was limited to a few aircraft photo-reconnaissance flights inspecting the plumes of local sources under differing regimes. These however quickly identified the continuous fumigation and plume trapping potentials of the Lake Michigan shoreline environment. The result was the proposed model of Lyons and Cole (1973).

The summer of 1971 saw a two week field program in the first half of August. An instrumented Queen Air was supplied by the National Center for Atmospheric Research. The prime objective was aerosol monitoring in conjunction with limited pibal wind measurements of lake breeze structure. Only limited success resulted due to highly unfavorable weather conditions along with malfunctions of both sensors and recording devices on the aircraft. Valuable qualitative data was obtained however with regards to the structure of the TIBL during stable onshore flow situations. In fact, one of the best developed TIBLs ever monitored (5 August 1971) was mapped (Lyons, 1975a). In addition, a rough correlation between aircraft sensed turbulence and the shape and depth of the thermal internal boundary layer was developed.

Also noted were some definite relationships between surface ozone levels and lake breeze frontal passages (Lyons and Cole, 1976).

The 1972 season saw relatively limited field data gathering other than pibal wind soundings for climatological purposes.

The summer of 1973 was dedicated to the testing of new techniques for data gathering and the development of instrumentation packages. An airborne meteorological/air quality monitoring and data logging package was designed and test flown. The Wisconsin Department of Natural Resources (DNR) graciously allowed the use of a twin engine Cessna 337 for this task. There was limited data acquisition, in part due to relatively uneventful weather, but also due to several electronic component failures within the data logging system that were inconspicuous only until post-program data analysis. Several test flights of optically-tracked tetroons were made in order to establish firm procedures for weigh-off, balloon release, and tracking via double theodolites. Software was developed and tested for analyses of tetroon and pibal balloon data. Field sites were selected for pibal releases. Attempts at offshore releases of pibals and tetroons were made but found to be operationally difficult to coordinate. Pollution photography techniques were improved upon. Data gathered during mid-July proved most useful in the analysis of an ozone episode along the western shore of the lake (Lyons and Cole, 1976). Also, a more complete model study of power plant fumigation potential was carried out using field data gathered on 16 July 1973 (Lyons and Dooley, 1974). The most important result of the 1973 effort was to prepare for a highly successful

summer of 1974.

THE 1974 SUMMER FIELD PROGRAMS

With additional sponsorship of Wisconsin Electric Power, a three month long field program was mounted to study both the mechanism of continuous fumigation and lake breeze phenomena along the western shore of Lake Michigan. The first phase of the project was conducted in and around Waukegan, Illinois from 3 June through 28 June 1974. The prime target of study was the four stack shoreline Waukegan Power Plant (WPP) on the shoreline. The project moved to the Milwaukee area from 16 July through 4 September 1974 where the four stack shoreline Oak Creek Power Plant plume was intensively monitored, along with the general urban pollution patterns. A total of 21 days of intensive field data gathering were undertaken. As many as 37 individuals were employed in various phases of the data taking and processing. An extensive summary of the equipment and data processing procedures used appears in Lyons, et al. (1974). However, a brief summary is presented here.

The Milwaukee Area

Figure 3-1 is a map of the various sites for the second and more complete stage of the field program. In addition, within this area were nine DNR air quality monitoring stations (not shown) which provided additional data on such pollutants as SO_2, CO, HC, NO_x and oxidants, as well as partial meteorological data (wind and temperature). In addition to maintaining a file of all National Weather Service (NWS) hourly and synoptic teletype,

transmissions, NAFAX facsimile charts, and SMS, DMSP, and pertinent Landsat satellite images were archived. The base of operations in Milwaukee was the 12th floor Air Pollution Analysis Laboratory at UWM. On the roof top directly above was constructed an observation platform (Figure 3-2) for siting the radiosonde, FM communications, and acoustic sounder antennae, optical theodolites for tetroon and pibal tracking, and camera systems.

The Waukegan Area

The first phase of the project was directed from a mobile laboratory established in Waukegan, Illinois, just south of the Wisconsin-Illinois state line. Figure 3-3 shows the deployment of instruments. The main attraction of this site was a ten station telemetered SO_2/wind monitoring network around the coal burning Waukegan power plant (WPP). A base station was established 3 km from the lakeshore on the grounds of the Jack Benny Junior High School (JBJHS). Figure 3-4 shows the headquarters which housed one of the two wiresonde tethered balloons, the white sound baffle for the acoustic sounder, radio, and radiosonde antennae, etc.

Instrumentation

During 1974 a Cessna 182 was instrumented to monitor air quality and meteorological variables (temperature, relative humidity, pressure altitude). A Sign-X fast response conductimetric sensor was used for SO_2. A two-channel Royco particle counter sampled the airstream isokinetically. A Universal Indicating Turbulence System (UITS) was installed which produces a linear

output from 0.0 to 10.0 units which is equivalent to $\varepsilon^{1/3}$, where ε is the eddy dissipation rate. The output closely corresponds to the turbulence sensed by the aircraft passengers and thus is comparable to the subjective methods used to locate the TIBL. In addition, DME, air speed and two VOR signals were acquired. All data were recorded on magnetic tape cartridge for later ground processing by MODCOMP II/25 computer. Back-up strip charts for SO_2 and particulate data were also available. The aircraft instrument package is shown in Figure 3-5.

An instrumentation package was designed for use in either a Bell 47J or 206 Jet Ranger helicopter. A Sign-X SO_2 monitor with a strip chart electrostatic recorder also monitored pressure height. Dry and wet bulb temperatures were recorded on a second chart. Tests showed that in normal flying configuration rotor downwash did not interfere with any of the sensors.

A mobile van was supplied by Environmental Research and Technology, Inc., which contained a fast response flame photometric SO_2 sensor. The van was held in place for at least ten minutes for each reading beneath a fumigating plume. A second car was instrumented with a temperature probe and routinely measured the air temperature gradients normal to the shoreline.

All the above were in constant UHF FM communication with a base station and each other. The aircraft was generally used to spot the location of the fumigation zone and to vector the others to it.

A chain of four single theodolite pibal wind stations was established in a line normal to the shoreline to roughly 30 km

inland. Thirty gram helium filled balloons were tracked at 30 second intervals, and data were processed by the Univac 1110 computer yielding mean wind speeds and direction in roughly 100 m thick layers.

A monostatic acoustic sounder was operated continuously at the Waukegan base station and then later at the Milwaukee base, which was atop the 60 m building about 1.5 km inland.

Two wiresondes were constructed for temperature profiles in the lowest 350 m. Radiation shielded YSI precision thermistors were attached to 600-ft^3 finned balloons. Temperature accuracy was estimated to better than 0.3°C. Actual heights were determined with the aid of balloon zenith angle measurements made by a theodolite. In Waukegan, wiresondes were stationed at the shoreline (WPP) and at the 3 km base station. In Milwaukee, they were located at the shoreline and at a site 16 km inland. Additional data was gathered by an RD-65 portable radiosonde used at both the Waukegan and Milwaukee base stations. Generally three soundings were made each operational day.

Considerable photographic data were taken. Standard 35 mm cameras were used on board the aircraft and helicopter. A time-lapse all sky fish eye camera was placed beneath the WPP stacks to record smoke behavior. Also conventional 16 mm time-lapse movies were made of smoke and cloud patterns from both base stations. In addition, hourly 360° cloud panoramas were made at each base station. The use of polarizing filters and/or color infrared films often produced superior photographs of clouds and smoke

patterns that were otherwise obscured in the hazy atmosphere.

Lagrangian air trajectories were determined using 2.5 m^3 constant volume super pressured balloons (tetroons) made of 2-mil thickness mylar, filled with a helium air mixture. By following certain inflation procedures, it was possible to set the tetroon to drift with the wind on a predetermined isopycnic surface (nominally weighted to float at 250 or 300 m AGL), towed to these altitudes by two or three pilot balloons. Figure 3-6 shows a balloon in flight.

Tetroons were tracked by two theodolites using 25-power standard theodolites atop tall buildings (Figure 3-7). The base-line between the theodolite pair was 3740 m. Azimuth and elevation angles were recorded every 30 seconds to 0.1° resolution. Two-way radio communication assured the synchronous coordination of readings. The double theodolite computer program gave x, y, and z positions (in shoreline coordinates and absolute UTM co-ordinates) and computed the u, v, and w wind components at 30 sec intervals.

The tetroons have a free lift on the order of 1500 gm, which is sufficient to fly a standard radiosonde package from beneath the balloon. A standard NWS/VIZ radiosonde was modified to cycle automatically through temperature, humidity, and reference contacts (Figure 3-8). Analysis of the data from the RASOT (Radiosonde-tetroon) technique gave a three-dimensional picture of the winds, as well as the temperature and humidity variations over time and space.

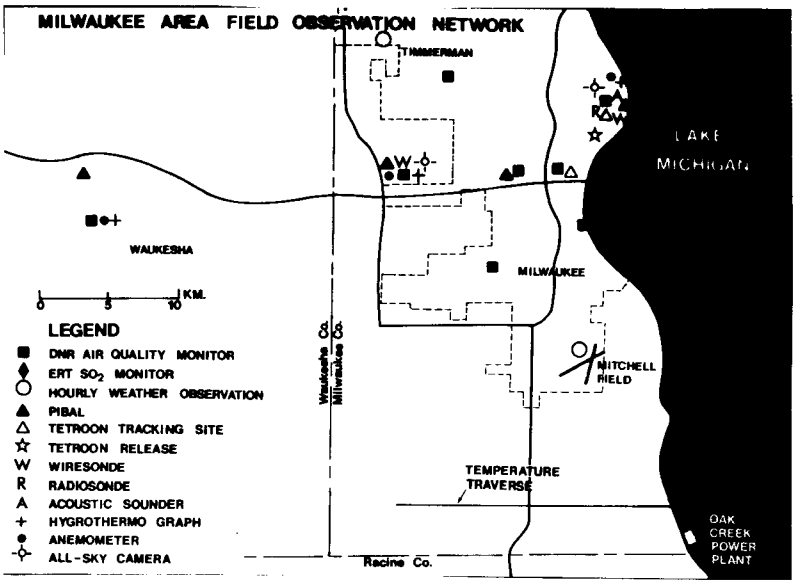

Figure 3-1. The Milwaukee area field program network, summer 1974. Not shown are nine air quality monitoring stations operated by the state of Wisconsin, Department of Natural Resources.

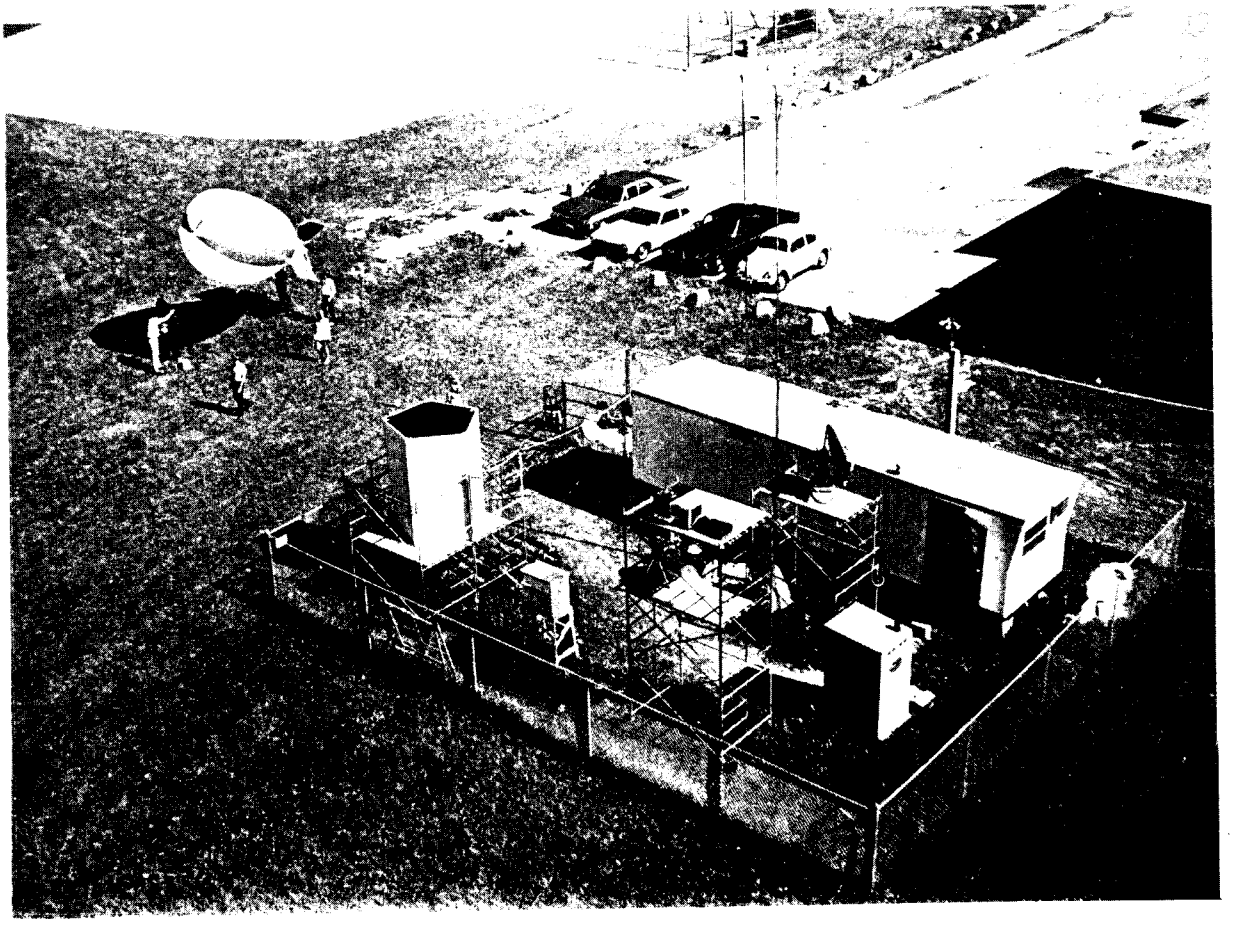

Figure 3-2. Aerial view of Jack Benny Jr. High School (JBJHS) base station in Waukegan. The large trailer houses both office space and storage space, especially for the wiresonde balloon. The acoustic sounder shelter is visible on the scaffold at the lower left of the enclosure.

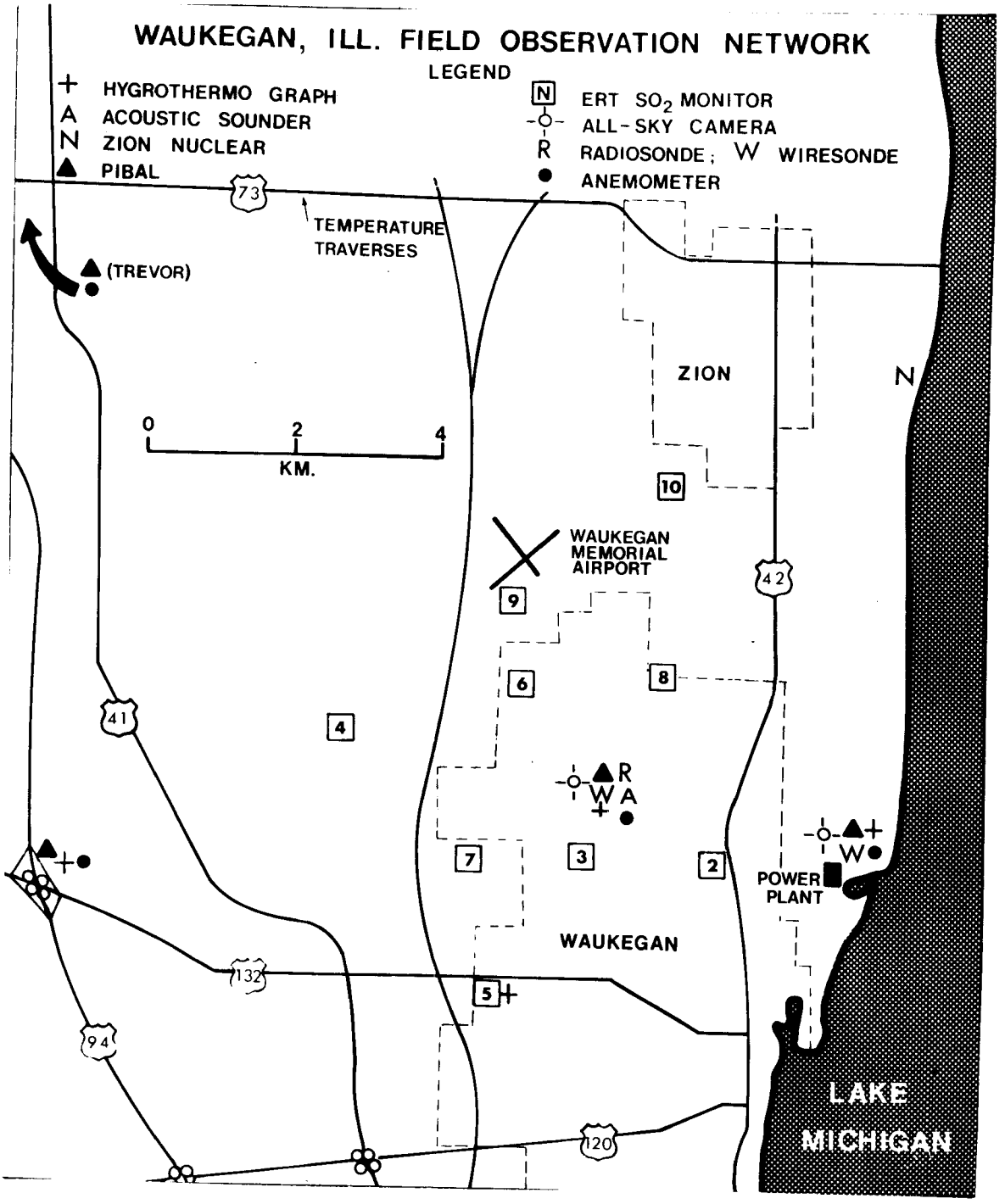

Figure 3-3. The Waukegan, Illinois field program network, summer 1974.

Figure 3-4. Widelux wide angle camera view from top of UWM Science Complex building, as viewed from the north. Tetroon tracks and the 16 mm and 35 mm cameras visible. The radiosonde antenna is located to the right of the picture.

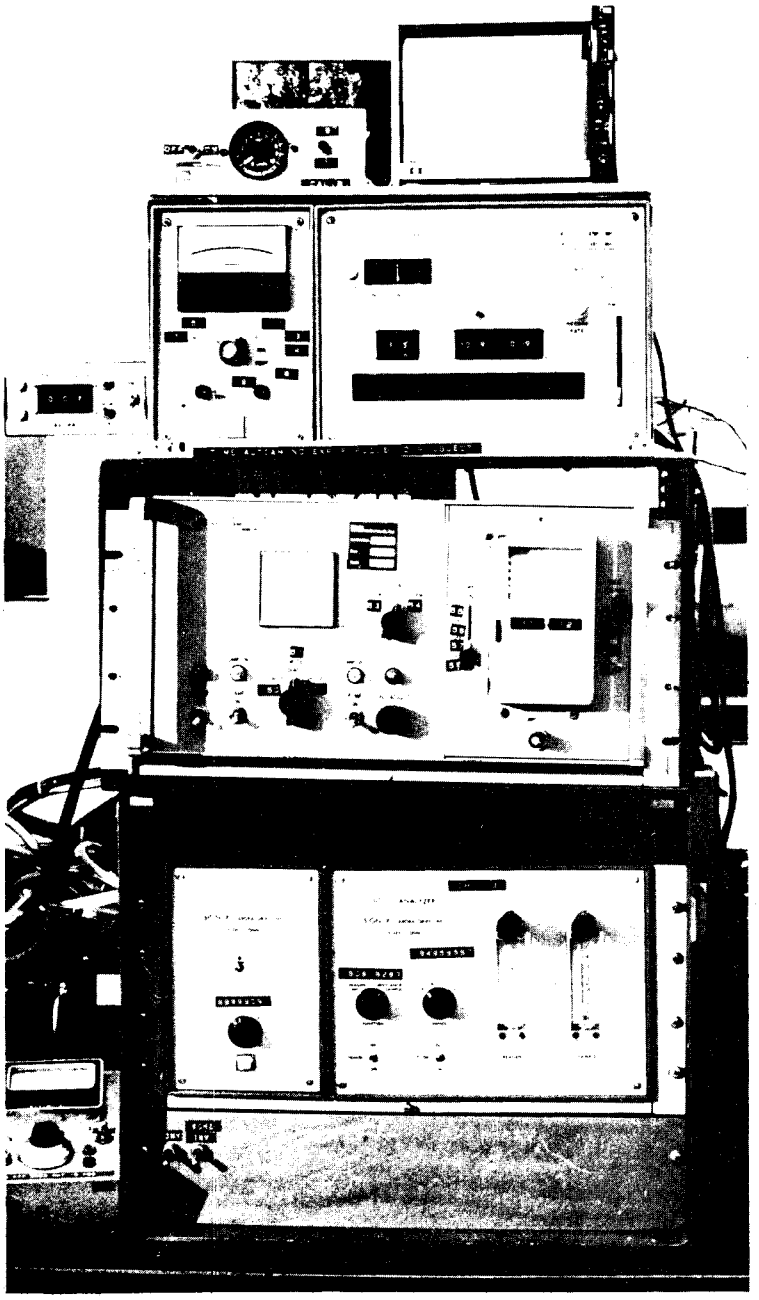

Figure 3-5. Cessna 182 instrumentation and data acquisition system. Sign-X at bottom with Royco above. The UITS read-out dial is on upper left, next to HP multichannel recorder used for hard copy of SO_2 traces.

Figure 3-6. A tetroon being towed to its neutral density level by two pilot balloons floating over Lake Michigan just east of the University of Wisconsin-Milwaukee campus. The RASOT (modified radiosonde package) can be seen dangling below.

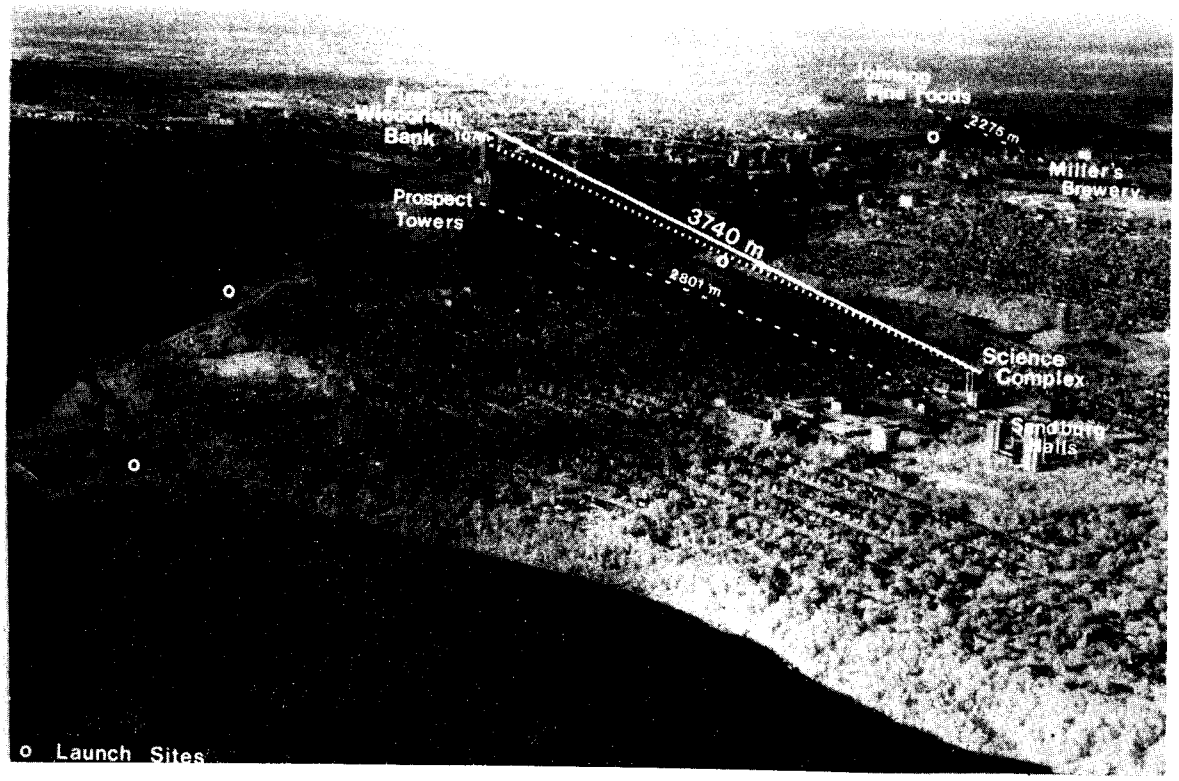

Figure 3-7. Aerial view showing various launch and tracking sites for tetroons and pibals around Milwaukee. The laser range finder determined base lines for the tetroon trailings are indicated.

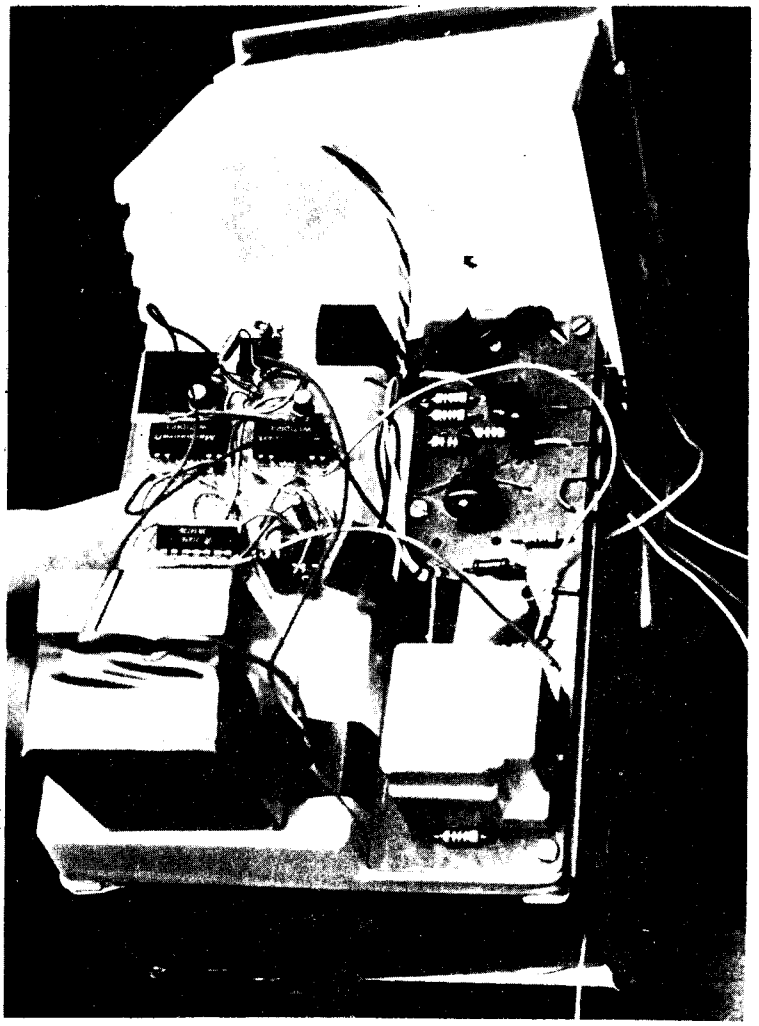

Figure 3-8. Specially modified NWS-VIZ radiosonde, a RASOT, used with tetroon system.

SECTION 4

FUMIGATION AND THE THERMAL INTERNAL BOUNDARY LAYER

GENERAL COMMENTS

An airmass that advects over a colder water surface is both conductively cooled from below in the lowest 100-150 m (Lyons, 1971) and not destabilized by the penetrative convective heat transport that is present over land during periods of solar insolation (Lyons and Wilson, 1968). When this stabilized airmass reaches a down wind shoreline on a sunny day, it experiences an almost step function jump in surface roughness lengths and heat input. In an analogy to laboratory flow experiments over a heated plate, a thermal internal boundary layer (TIBL) develops. This has in fact been extensive physically modeled (Ogawa, 1973). It has been shown (Raynor, et al., 1974) that even before land fall, stabilized marine air has diffusion characteristics substantially different from those deduced from over-land diffusion experiments under equivalent thermal stabilities. When this airmass reaches land, the diffusion in a highly transitional stability state becomes even more complex and atypical.

The implications of variable diffusion characteristics in such shoreline "transitional states" was gradually recognized by a number of researchers, perhaps beginning with Munn (1959). Turner (1969) adequately described nocturnal radiation inversion breakup fumigation, a phenomenon which typically produces high

surface concentrations from elevated plumes for periods of on the order of 30 minutes. As early as 1962, Bierly and Hewson discussed "Type III Fumigation" occurring when plume matter is emitted into an elevated stable layer at the shoreline and then intensely mixed downward as the convective turbulence generated during overland travel reaches plume altitude. They further illustrated and discussed this as the result of field experiments on the Lake Michigan shoreline (Hewson, Gill, and Walke, 1963). Limited studies on the west coast (Robinson, Eberly and Cramer, 1965) further focused attention on the possible serious implications of what is now called continuous (dynamic) fumigation of high-stack plumes in coastal zones. Bierly (1968) studied the characteristics of lakeshore internal boundary layers, though with relatively little emphasis on pollution aspects. Van der Hoven (1967) and Collins (1971) made summary studies of what was known about fumigation and presented simple models to account for the formation of TIBLs. Figure 4-1 is a dramatic photograph of the stable plume from a lakeshore power plant drifting inland on a typical fumigation day: strong insolation and onshore flow of stable lake-modified air. The view taken in the opposite direction (downwind) shows no plume matter - it having been rapidly convected to the surface in the vicinity of the photographer by the fumigation mechanism. Accurately modeling this dynamic process was the first major goal of these projects.

A FUMIGATION MODEL

As a result of a limited field study in which shoreline

power plant plumes were photographed, Lyons and Cole (1973) extended Turner's (1969) fumigation modeling procedure to the case of continuous (dynamic) fumigation. The model was phenomenologically rather simple. Complete details of the model as applied to a single point source are contained in the original paper. Figure 4-2 however, highlights its basic characteristics. Three regimes are postulated. In the first (Figure 4-2a), the plume from a high stack is emitted into a stable layer and drifts inland with relatively little diffusion, and plume σs are chosen characteristically. At a given point X_b, the top of the TIBL penetrative convection intersects the base of the plume (at the 10% of plume centerline concentration level), and begins mixing plume mass downward. This process, which defines the transition or fumigation zone, continues until point X_e where the entire plume has been convectively mixed within the deeping boundary layer. While the horizontal concentration profile remains Gaussian, the vertical profile within the mixed layer is considered linear and constant with height. The third regime is one of modified lid trapping in which both lateral and vertical diffusion continues, but under a deeping lid, and with σ_z characteristic of the inland unstable air mass. Hirt et al. (1971) also found a similar behavior in helicopter studies of Toronto area power plant plumes. The Lyons and Cole model is essentially Gaussian in nature, assumes uniform steady state wind, flat terrain and non-varying surface roughness lengths, uses a "4 sigma" approach (a split-sigma σ_y/σ_z for both the stable and unstable portions

of the process), and yields concentrations presumably consistent with ten minute sample averages. Needed, in addition to the usual model input parameters are specified effective plume heights and most importantly, the depth of the top of the TIBL as a function distance along the plume centerline. The distance between X_b and X_e is called the "fumigation zone" and the quasi-elliptical area with the 50% of χ_{max} isopleth is termed the "fumigation spot."

In that first paper, using estimated input parameters, including a crudely determined TIBL profile, it was calculated that maximum surface SO_2 concentrations from the OCPP could exceed 1.00 PPM. It should be noted that all four stack effluents were combined into one plume. This high level, plus the possibility of the mechanism continuing for over six hours, raised the speculation of widespread exceedences of the federal three-hour SO_2 standards downwind of shoreline power plants. However it was also pointed out that the model needed extensive field testing, validation, and calibration.

A FURTHER APPLICATION

Even before extensive field testing, additional computations based on the Lyons and Cole model revealed the fumigation phenomena to be far more complex than perhaps originally envisioned.

While the plume(s) from a shoreline tall stack may indeed fumigate for many hours on end, fluctuations in wind direction and speed, plume rise(s), and the height and shape of the thermal

internal boundary layer (TIBL) cause the location of the highest ground level concentrations (the fumigation spot) to move about the landscape with great speed, therefore reducing significantly the total dosage received by any given receptor.

To aid in the design of a 10-station SO_2 network, a modeling effort to show fumigation patterns from a coal burning power plant at Waukegan, Illinois was conducted (Lyons and Dooley, 1974). The simulation covers an 8-hour period and uses both actual and estimated meteorological data for 16 July 1973. This day, assumed to approximate a "worst case" example was simulated on an hour-by-hour basis, the time history of the fumigation patterns from a multi-plume source then being integrated to show final concentrations and dosages.

The coal-burning 964 MWe Waukegan power plant (WPP) is located on the western Lake Michigan shoreline halfway between Chicago, Illinois and Milwaukee, Wisconsin. It has four stacks of 102, 121, 137, and 137 m height above ground. The two tallest stacks had nearly identical emission parameters, and were considered to form a single combined plume. The annual average SO_2 emission rate for the three plumes was 485, 448, and 2220 gm/sec, thus making the combined plume from the tallest stacks predominant. Calculated plume rise showed considerable variation with wind speed, from as low as 30 m for the middle stack at 10 m/sec wind to as great as 780 m on the combined plume at 1 m/sec wind speed.

From those days during the summer of 1973 when hourly shoreline pibal wind data were available in Milwaukee, 16 July

was chosen as most likely having "worst case" characteristics, that is, causing the most intense and long lasting fumigation potential. A high pressure cell centered over lower Michigan maintained fair skies and light gradient easterly flow over Wisconsin and Illinois. Landsat-1 high resolution images of the area during mid-morning revealed cumuli forming 10-16 km inland from the western shore. Though no lake breeze per se developed, a probable mesohigh over the lake caused the usual clockwise rotation of the low level winds. Figure 4-3 is a hodograph of the pibal measured winds at 271 m over the Milwaukee shoreline between 0900 and 1600 CST. It was assumed that all three plume axes lay along these azimuths at each hour. Thus neither velocity nor directional shear is accounted for in these calculations. Due to the lack (at that time) of adequate aircraft turbulence data, the profile of the top of the TIBL was estimated on an hourly basis (Figure 4-4). P-G class F was assumed in the stable air while P-G class C was used in the unstable air.

Figure 4-5 is a plot of the SO_2 isopleths of the three plumes at 1100 CST. More importantly is the combined pattern of all three plumes at the time of maximum fumigation intensity (1300 CST) showing the average maximum concentration of 1.30 PPM, some 4.6 km from the power plant. The fumigation spot is very small, however, with concentrations greater than 0.5 PPM covering only 2.7 km^2. Figure 4-6 is a time history plot of the SO_2 concentrations from each of the three plumes showing the large area affected during this 8 hour period. Federal three-hour SO_2 quality standards are expressed in terms of total dosage received

at any one point. Figure 4-9 shows the reconctructed trace of an SO_2 sensor that might have been located at the point of maximum concentration. It was assumed that the surface plume concentration pattern remained steady state during a two-hour period while rotating clockwise with the winds past this receptor point. The resulting dosage calculated is 1.04 PPM*Hr, considerably less than the three-hour standard of 1.50 PPM*Hr. The 24-hour average of 0.14 PPM (or 3.36 PPH*Hr) was not even remotely approached.

Virtually all of the assumptions used in this model have been shown to be highly conservative. No doubt locally high values of pollution do occur beneath fumigating plumes. However, due to the rapid movement of the fumigation spots, the potential for exceeding three-hour dosage standards at any given point are smaller than might be expected based on a mere analysis of instantaneous concentration values. While fumigation effects most certainly must be carefully considered in any environmental impact assessment for an elevated source in the shoreline environment, proper modeling may reveal that some such sources can be legally operated within federal standards. Those occasional times when limits might be exceeded would be prime candidates for the application of supplementary emission control strategies (fuel switching, etc.). This study also revealed that fixed monitoring sites would only poorly resolve the nature of the fumigation processes.

It must also be remembered that in all of the above, no validating field data was available, and no correction factors have yet been applied to the predicted concentrations. The 1974

field program was directed at alleviating these problems.

THERMAL INTERNAL BOUNDARY LAYERS - TIBLs

Clearly the most sensitive input parameter into a fumigation model is the shape of the top of the thermal internal boundary layer. Laboratory experiments (Ogawa, et al., 1973) and some field investigators (Weismann and Hirt, 1975) have assumed its shape to be parabolic and assymptotically approaching a maximum depth equivalent to the inland mixing layer depth. Eariler investigations however *a priori* assumed the top of the layer to be linear, and the models of Van der Hoven (1967) and Collins (1971) proceeded accordingly. In fact, the Lake Michigan field studies showed the measured TIBLs to have a variety of shapes with no easy parameterization scheme apparent.

A fundamental question must be raised as to how the TIBL is defined within the context of a measurement program. In fact, separate boundary layers develop in terms of moisture, heat, moisture flux, etc. as the lake air flows inland and is modified (Bierly, 1968). For the purposes of defining elevated plume fumigation, the parameter of importance is vertical mixing generated by columnar penetrative convective elements raising from the superadiabatically stratified ground layer (Warner and Telford, 1967). The top of the TIBL in fact marks the level of maximum penetration of these convective motions. Inferring this structure from conventional meteorological data is definitely not straightforward. Surface temperatures, chilled by passage over the cold lake generally are restored to inland values after

10-30 km of overland fetch, as shown in Figure 4-8. But this type of information gives little clue as to vertical structure above. A way is needed to discriminate between "laminar" and turbulent atmospheric flow regimes. The former refers to stabilized lake air masses which have minimal turbulent fluctuations due to either thermal or mechanically generated eddies. The latter is characterized by both mechanical but primarily thermally driven eddy motions. In level flight in a small aircraft, this sharp distinction can be readily noted by an observer. Crossing into the TIBL results in the flight transforming from generally smooth to rather bouncy. A field experiment, using an NCAR Queen Air, refined this simple TIBL detection approach used in the original Lyons and Cole (1973) paper. Data were collected on 5 August 1971 during a series of east-west traverses normal to the Milwaukee shoreline during mid-afternoon with strong sunshine and stable onshore flowing non-lake breeze winds. The potential temperature analysis (Figure 3-9) shows the development of the TIBL. A corresponding plot of the observers subjective characterization of encountered turbulence (Figure 4-10) shows a very strong correlation indeed. The power plant plume under study that day was seen to begin fumigating at about the point where it was engulfed by turbulence of "level II", noticeable bouncing of the aircraft.

This, and other similar experiences, lead to the decision to define the TIBL not by radiosondes, etc., but rather by aircraft turbulence monitoring. The development of the Universal Indicating Turbulence System (UITS) by MacCready (1964) suggested

a fairly simple method of profiling the TIBL from a light aircraft. The UITS, a wing mounted gust probe essentially senses $\varepsilon^{1/3}$, where ε is the eddy dissipation rate of turbulent energy within the inertial subrange. Experience has shown that the "feel" of turbulence to an aircraft observer is very closely correlated to the $\varepsilon^{1/3}$ values. The $\varepsilon^{1/3}$ values recorded on tape (and monitored via dial by the aircraft observer) are independent of aircraft speed. Values of $\varepsilon^{1/3}$ below 0.3-0.5 $cm^{2/3}sec^{-1}$ were associated with "smooth" air. As $\varepsilon^{1/3}$ approached 1.0 $cm^{2/3}sec^{-1}$ noticeable bouncing would be felt, which would be described as the onset of "light turbulence" by an experienced pilot. This level of turbulence, almost always found to be associated with penetrative convection (often made visible by rising columns of smoke) was chosen as the criteria for defining the top of the TIBL. Values above 3.5 $cm^{2/3}sec^{-1}$, occasionally found within lake breeze convergence zones and beneath growing cumulus, would be characterized by a pilot as marginally heavy turbulence.

Aircraft flight tracks were chosen to fly east-west traverses normal to the shoreline at various altitudes, in part to measure the $\varepsilon^{2/3}$ patterns. Experience showed that they were remarkably revealing of the gross structure of the atmospheric boundary layer. Figure 4-11 is a good example. Isopleths of $\varepsilon^{1/3}$ drawn therein must be properly interpreted however. Rather than representing lines of equal $\varepsilon^{1/3}$ value, they should rather be considered "envelopes" within which the values indicated frequently and repeatedly reoccurred. Thus outside the 0.5 $cm^{2/3}$ sec^{-1} isopleth one finds no exceedences of the value (smooth air),

and within 3.0 $cm^{2/3}sec^{-1}$ there are wild fluctuations of $\varepsilon^{1/3}$, many exceeding that value. Again, the top of the TIBL was assumed to be roughly equivalent to the 1.0 $cm^{2/3}sec^{-1}$ isopleth.

The 27 June 1974 case shown in Figure 4-11 represent early morning, near noon, and mid-afternoon traverses of the shoreline in the Waukegan area. On this day, a weak lake breeze did in fact form. The front was clearly delineated by a vertical wall of turbulence, indicated by the $\varepsilon^{1/3}$ gradient several kilometers inland. Rapidly increasing southeasterly gradient winds however quickly destroyed the lake breeze and the last vestiges of its return flow by 1000 CDT. By mid-day one could almost invision a "plume" of turbulent heated air starting at the shoreline.

This technique proved quite successful and numerous TIBL profiles were obtained under varying conditions. As Figure 4-12 reveals, a plot of ten typical mid-afternoon profiles of TIBL tops shows that they can be highly variable indeed, ranging from linear to parabolic to hyperbolic, etc. The shape and depth of the TIBL was found to be very complex and clearly a function of many factors including initial potential temperature lapse of the onshore flow, vertical wind speed and direction profiles, insolation, intensity angle of the mean flow to the shoreline and shoreline shape itself, etc. An appempt was made to correlate the depth of the TIBL at 5 km inland fetch with the shoreline potential temperature lapse (as suggested by Van der Hoven). Linear regression analysis yielded (Figure 4-13) a poor correlation coefficient of 0.35 (which was the best of any relationship found). Despite the wide scatter, a trend could be noted showing that

the TIBL would be deeper at 5 km the less the initial stability of the lake airmass. This is due to the fact that penetrative convection will grow more rapidly the less of an overlying inversion it needs to destroy. This also means that fumigation potentials are likely to be higher for onshore flows which are just barely stable, rather than those which are the most stable, a fact not always appreciated by those dealing with the phenomenon.

An interesting observation was made on 28 June 1974. The aircraft was flying just at the top of the haze layer through which columns of smoke could be seen protruding. As each was traversed the turbulence values rose accordingly (Figure 4-14), as did the fine aerosol particle count and the SO_2 concentration. This graphically illustrates the role that penetrative convection can play in vertical transport of atmospheric pollutants as well as the successful use of $\varepsilon^{1/3}$ as a first approximation to the upward limit of vertical mixing.

Figure 4-1. Print made from a polarized color infrared 35 mm slide, 1330 CDT, 28 June 1974, on Ground at Waukegan Airport. The Waukegan Power Plant Plume (dominated by stack 5) was stratifying west-southwestward before fumigating.

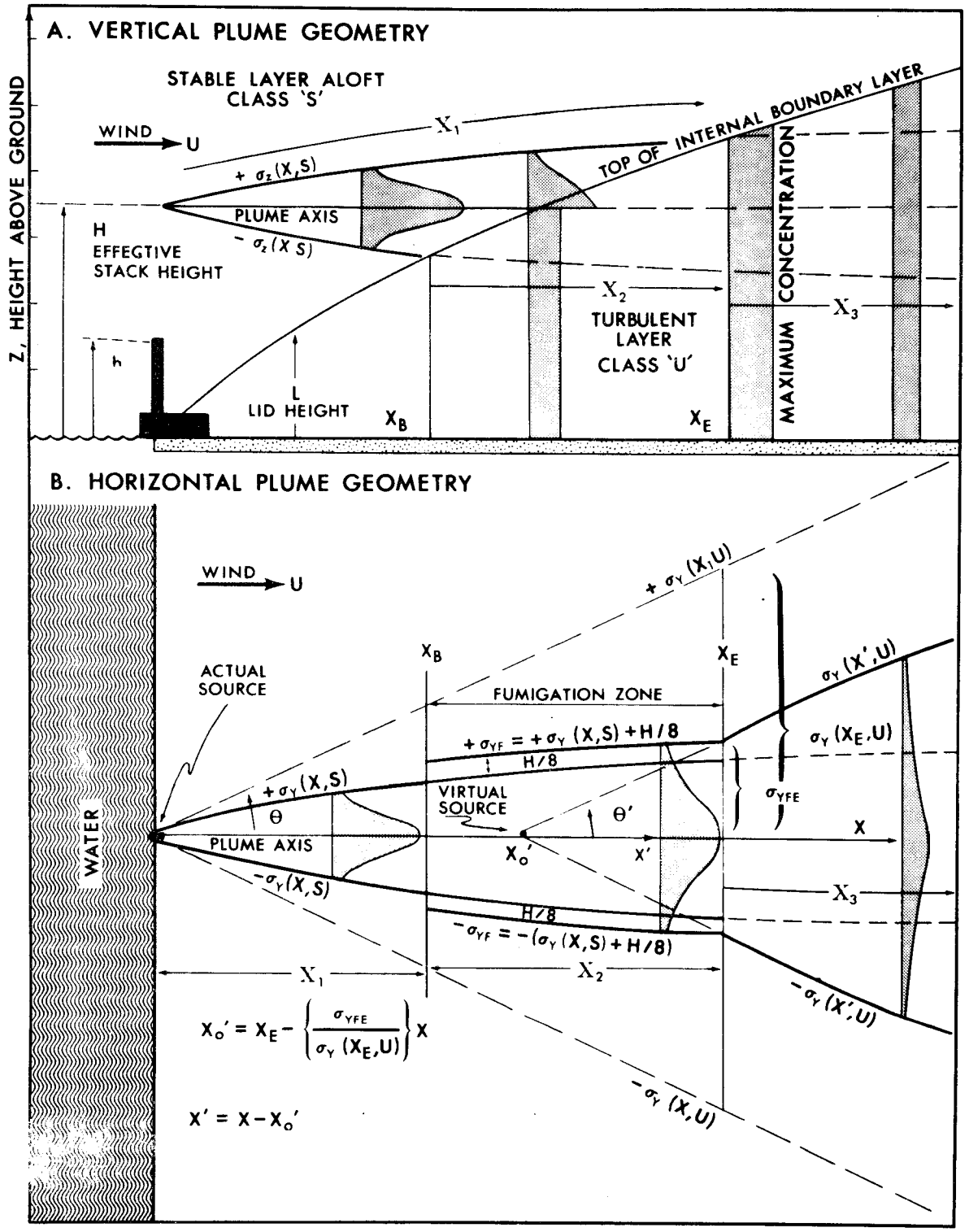

Figure 4-2. (a) Schematic of plume geometry in vertical (XZ) plane used in modeling continuous fumigation, (b) horizontal (XY) plume geometry used in the Lyons and Cole continuous fumigation model.

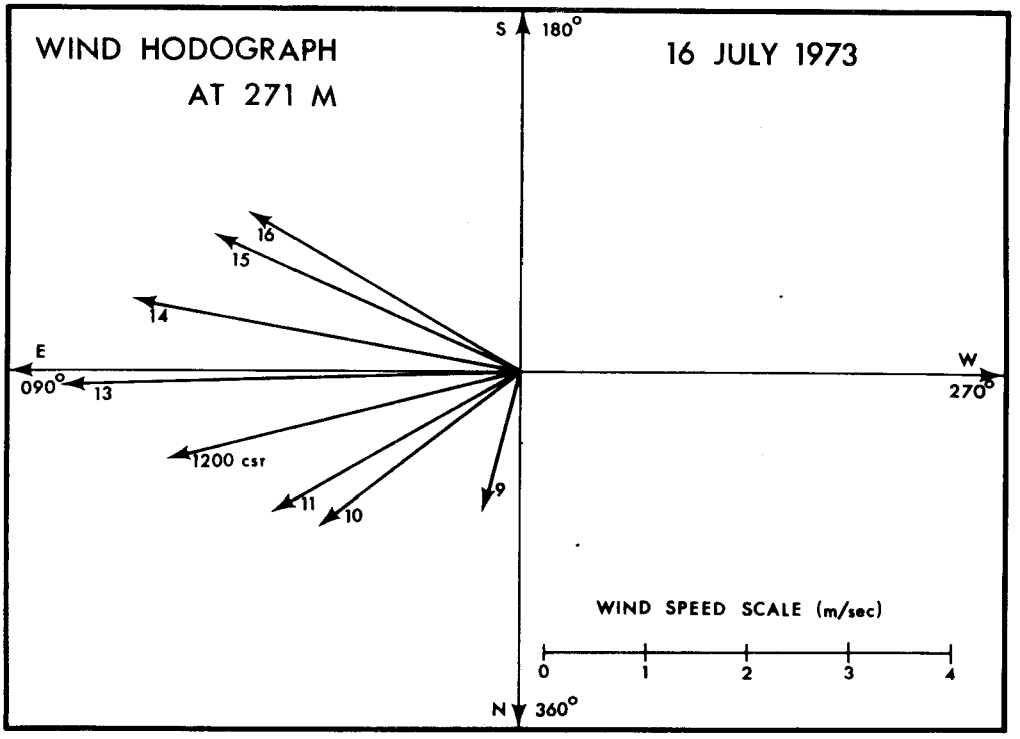

Figure 4-3. Wind hodograph at 271 m AGL, 0900-1600 CST, 16 July 1973 along Lake Michigan shoreline at Milwaukee, Wisconsin.

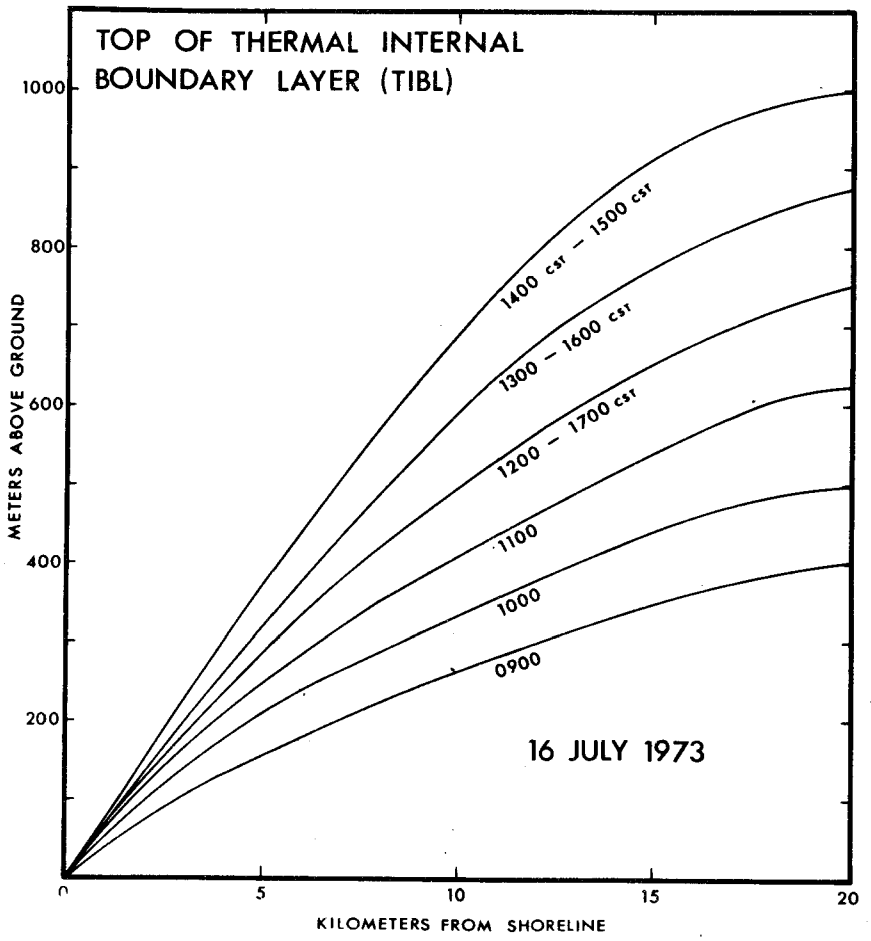

Figure 4-4. Estimated profiles of the top of the thermal internal boundary layer (TIBL) used in calculations.

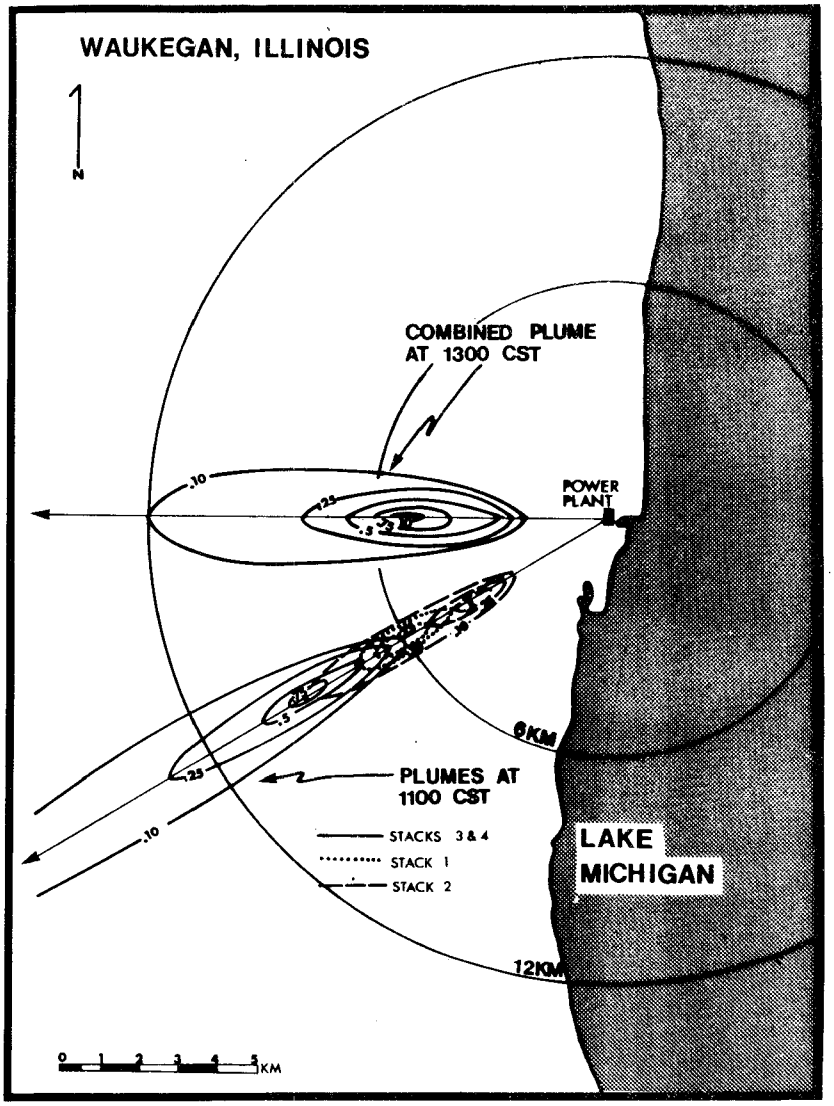

Figure 4-5. Calculated surface SO_2 concentrations (in PPM) at 1100 CST (showing three fumigation spots along same axis) and combined total for three plumes at 1300 CST, the time of the maximum predicted surface concentrations.

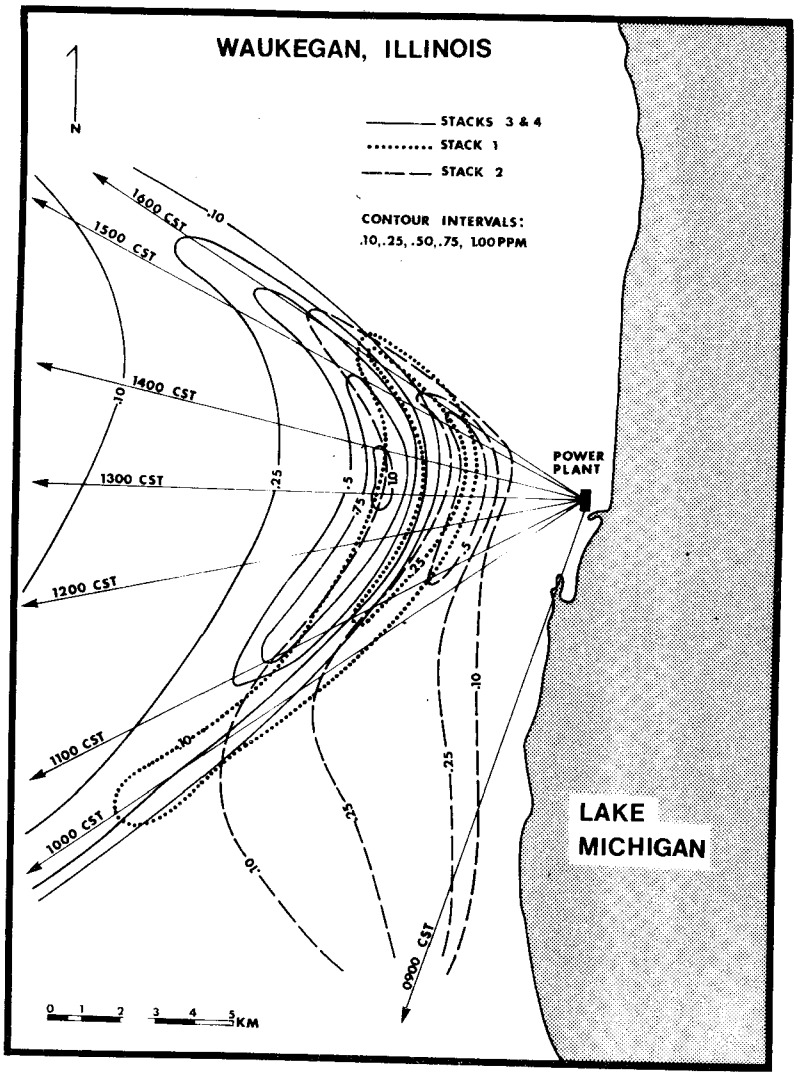

Figure 4-6. Time history diagram of predicted fumigation patterns from three power plant plumes (0900-1600 CST, 16 July 1973). Plume azimuths shown at hourly intervals. Interpretation: at a point on a given concentration isopleth, SO_2 levels were predicted to have reached the indicated level at least for one instant during that period.

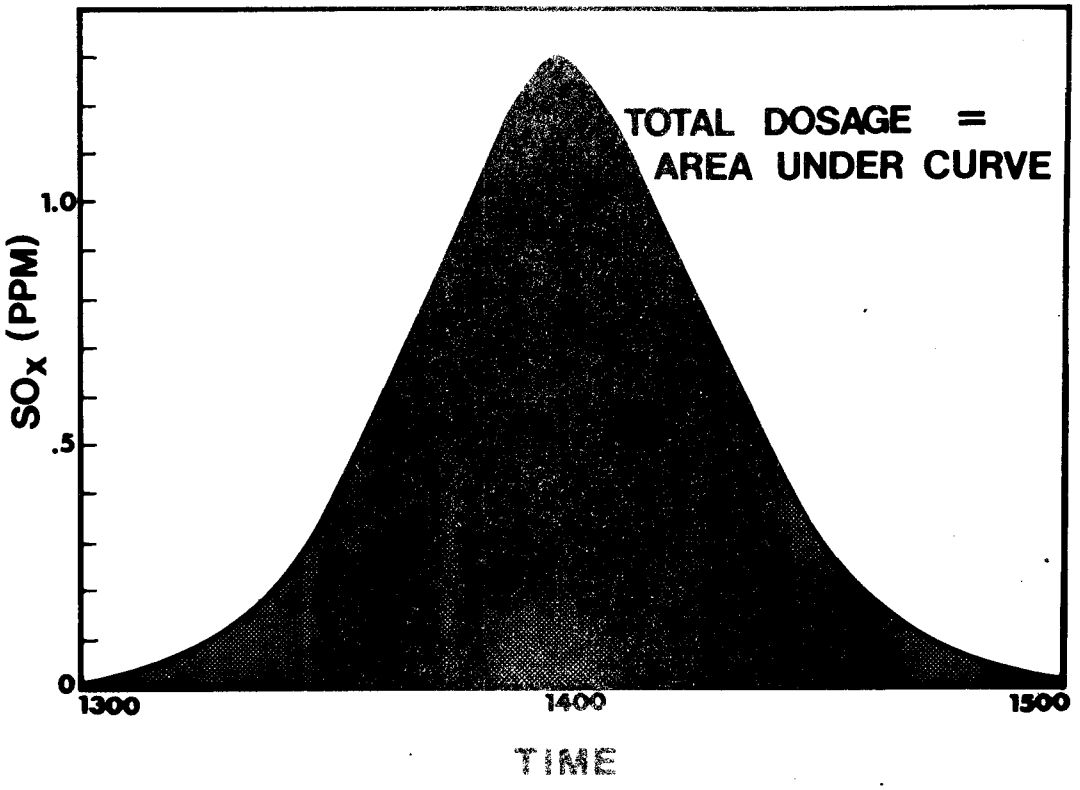

Figure 4-7. Predicted time history of SO_2 concentrations at receptor point receiving highest instantaneous concentration (1.30 PPM). Total dosage received during the approximately 2 hours necessary for fumigation spot passage was 1.04 PPM*Hr.

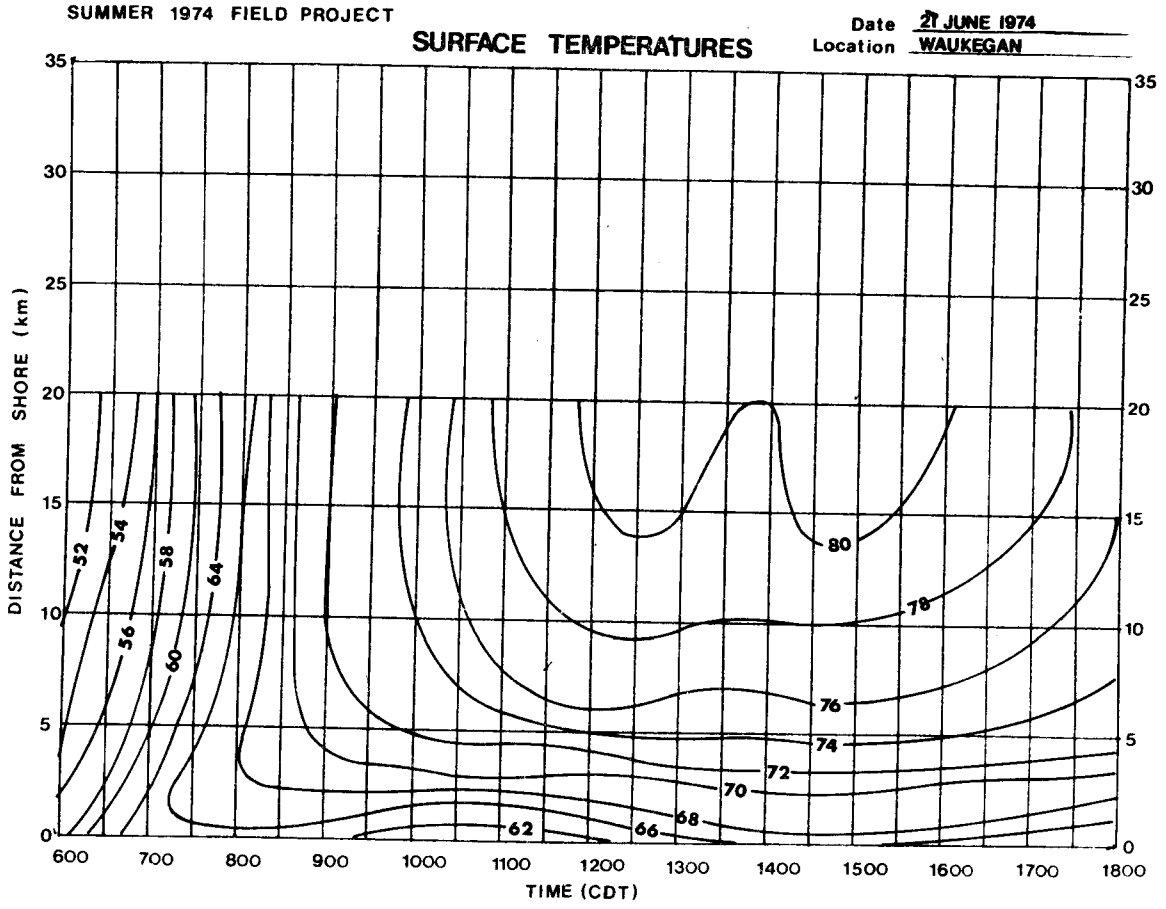

Figure 4-8. Surface temperature time versus distance from lakeshore (2 °F isotherm), Waukegan, 27 June 1974.

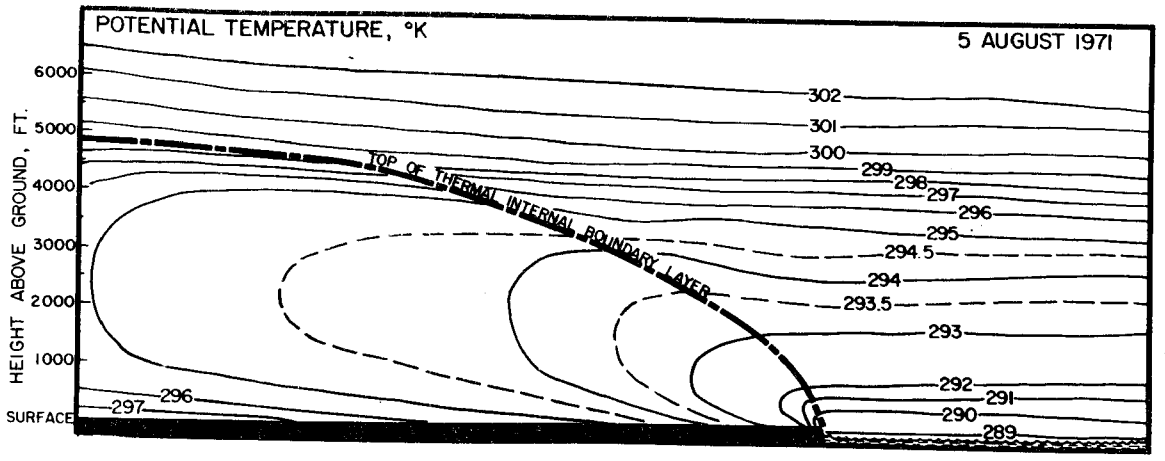

Figure 4-9. Potential temperature cross section was made following an east-west traverse of Lake Michigan shoreline at Oak Creek, Wisconsin, 5 August 1971, with NCAR instrumented Queen Air. A weak conduction inversion is capped by a stable layer over the lake, with an elevated synoptic subsidence inversion above 4000 ft. The heavy line denotes the top of the layer heated by penetrative convection from the surface: the thermal internal boundary layer (TIBL).

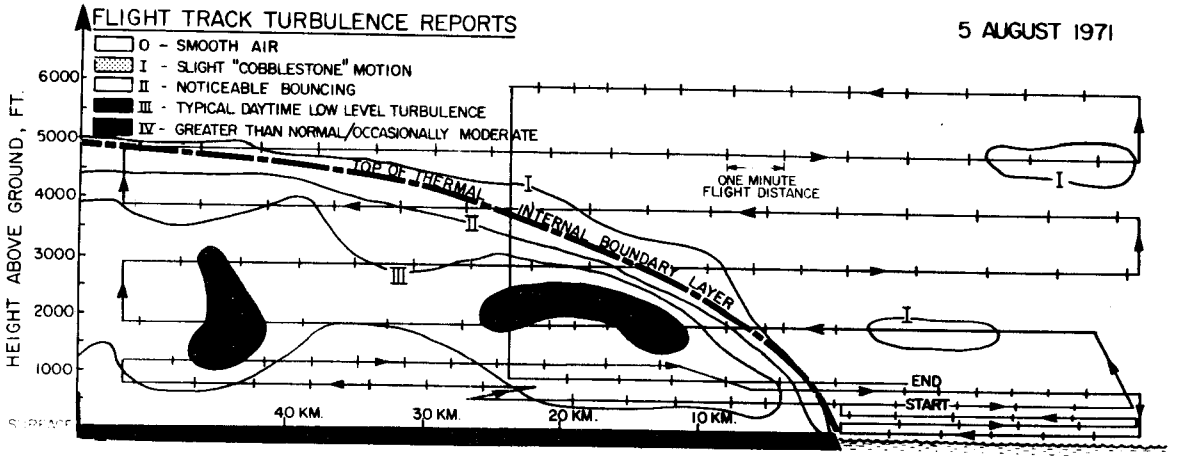

Figure 4-10. Flight track turbulence reports. Plots of relative turbulence values noted by observer in aircraft taken during the same time period as Figure 4-9. Turbulence described as "noticeable bouncing" seems to closely fit the TIBL upper limit. This in turn is roughly equivalent to a $\varepsilon^{1/3}$ value of 1.0 $cm^{2/3}$ sec^{-1} as measured by the UITS system on the UWM instrumented Cessna 182 aircraft.

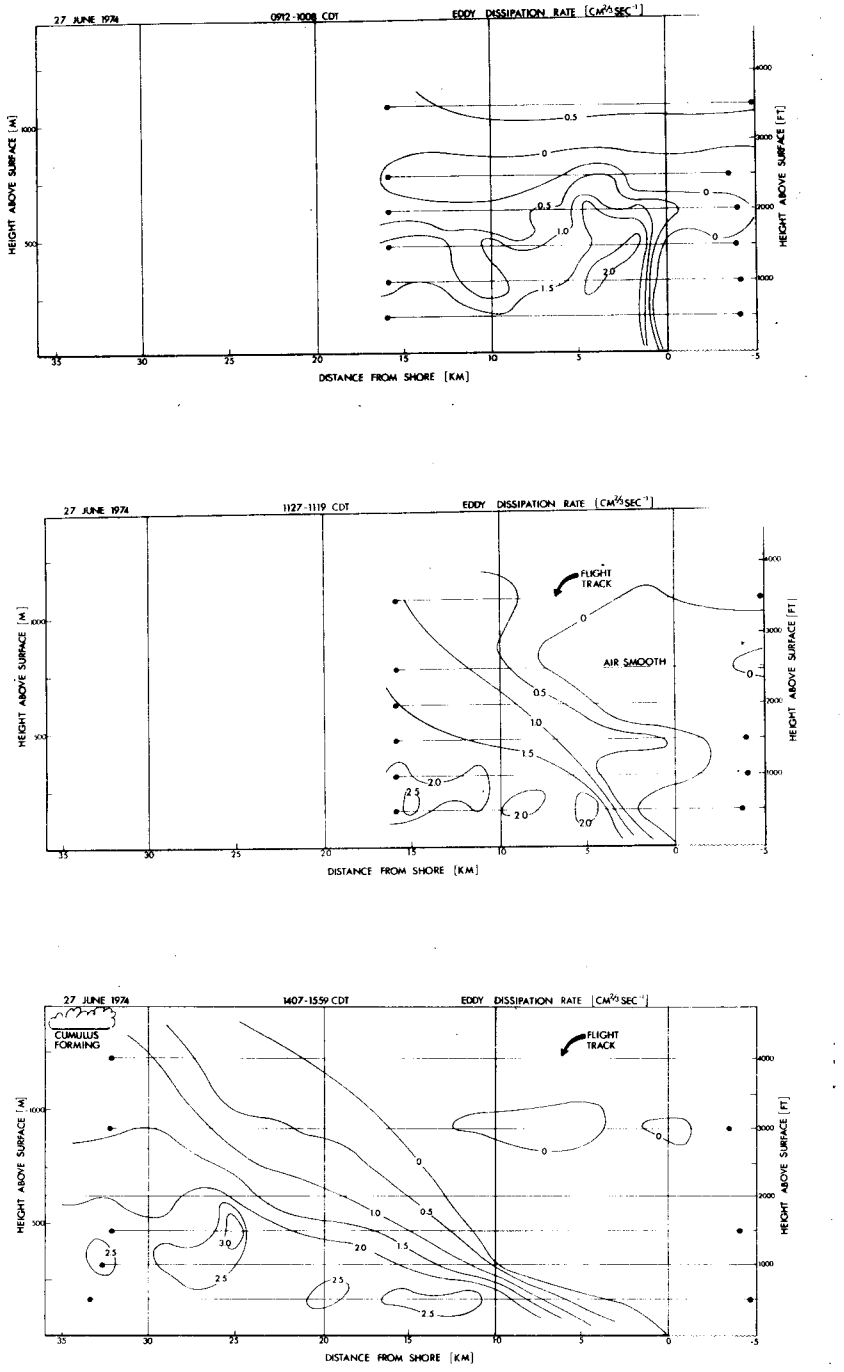

Figure 4-11. (top) Aircraft measurement of eddy dissipation rate ($\varepsilon^{1/3}$, $cm^{2/3}sec^{-1}$) on an east-west traverse near the Illinois-Wisconsin border, at 0912-1008 CDT, 27 June 1974. (middle) same, but for 1127-1119 CDT. (bottom) same, but for 1407-1559 CDT.

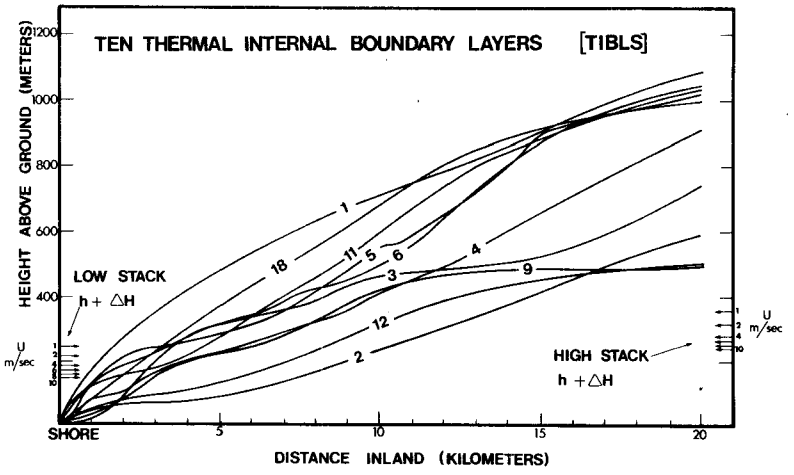

Figure 4-12. Ten selected TIBL tops monitored by aircraft during mid-afternoon during 1974 field program. Shown also are computed effective stack heights (H) for highest and lowest OCPP stacks with wind speed varying from 1 to 10 m/sec.

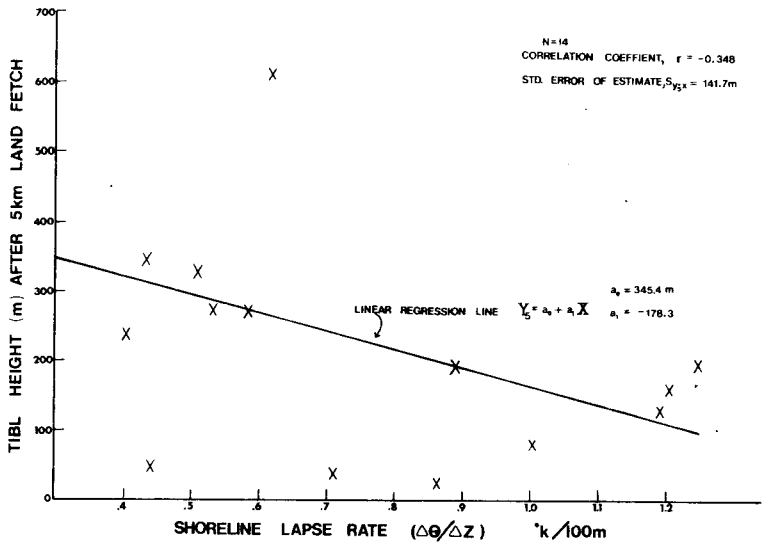

Figure 4-13. Linear regression analysis between TIBL depth at 5 km fetch and initial shoreline potential lapse.

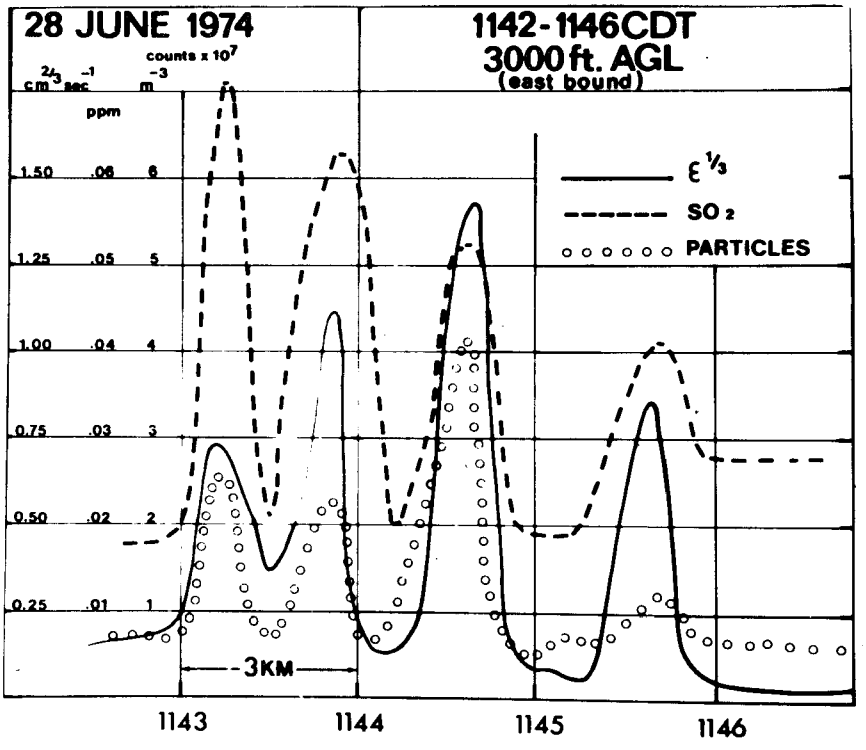

Figure 4-14. Plots of $\mathcal{E}^{1/3}$, SO_2, and 0.3-1.3 micrometer aerosol concentrations for a four minute section of flight just at the top of the mixed layer showing the turbulent and polluted columns of air just penetrating into the stable layer above at 3000 ft AGL.

SECTION 5

THE GLUMP REGIONAL FUMIGATION MODEL

GENERAL COMMENTS

The 1973 Waukegan analysis showed the clear necessity of treating separately the several plumes of a multi-stack power plant. Differences in plume effective stack height and the effect of the strong directional wind shear could cause the fumigation spots from plumes of a "point source" to be separated by many kilometers at any given instant.

The model was tailored to compute the plume characteristics separately and then sum the results. Conceptually, the step to a large and distributed number of point and area sources was a simple one. The GLUMP Regional Diffusion Model was therefore developed for the western shoreline of Lake Michigan. It can, of course, be reconfigured for any other shoreline area that is relatively straight and has quasi-uniform coastal terrain.

MODEL CHARACTERISTICS

The point source model of Lyons & Cole (1973) served as the basis for a regional model. The GLUMP Model (Great Lakes UWM Mesometeorology Project) is in many ways similar to steady state Gaussian approaches that have been employed in the past, but with one major difference. It was specifically designed to model shoreline fumigation, predicting resultant concentrations from

several hundred point and area sources at a given point in time.

A 1970 emission inventory of SO_2 and suspended particulates for southeastern Wisconsin was available for use. Figure 5-1 shows the major point sources of SO_2 in Milwaukee County, circa 1970. Note that they cluster along the shoreline and the east-west industrial valley. The model also separately simulates the individual plumes from multi-stack sources, such as a power plant.

The GLUMP model was programmed for the University of Wisconsin System Univac 1110 dual processor computer. At maximum, it requires 190 k words of core, and 30+ minutes of run time.

The program is constructed in a modular fashion. Plume rise can be calculated from any number of equations. Typically, large sources are estimated by Briggs' formulae (Briggs, 1969). Other equations can be used depending on atmospheric conditions and source characteristics (cold plumes, etc.).

The model was designed to be versatile. The number of receptor grids is variable, with over 100,000 points used if the computations require. Most of the examples shown herein used a 129(X), 153(Y), 6(Z) grid, or 118,422 receptors. Also, the computational grid size is arbitrarily chosen, perhaps as small as 100 m or larger than 5 km. The source emission and the receptor grids are independent of one another. Typically all sources within the seven counties of southeastern Wisconsin and extreme northeast Illinois are available for use. The receptor grid is positioned by assigning the location of a movable base point (the upper left hand grid point). UTM coordinates are used throughout. Figure 5-2 is a horizontal schematic of the model.

The number of vertical layers is also arbitrary, with six being most frequently used. Each layer has its own wind speed and direction, P-G stability class for both σ_z and σ_y (a "split sigma" approach), temperature, pressure, and background level of the source effective plume height is calculated, it is assigned to a given layer, and diffuses with the conditions at that level. Thus for a multi-plume power plant, it is possible to diffuse each plume in different directions, etc. This partially corrects for the inability to simulate wind shear effects found in some Gaussian plume models.

Area sources are given pre-assigned effective plume heights and are treated as virtual sources.

Figure 5-3 is a schematic showing the vertical structure of the model.

In order to reduce computation time, several steps are undertaken. When a TIBL is entered, it extends from the lake shore to 20 km inland,at 0.1 km increments. TIBL heights beyond 20 km are calculated by extrapolating the TIBL's slope in the 19.3-20.0 km zone. A "TIBL wind" is assigned which allows the computation of the TIBL height along a mean wind vector from the shore. Thus, full mixing depths may be attained after 20 km fetch over the heated land -- but this may be very close to the lake shore for a north-northeast flow and actually 20 km inland for a due east flow. The presence of an irregular shoreline often creates some highly distorted TIBL surfaces as winds depart from the easterly direction (Figure 5-4).

The first step computes all receptor fetches with respect to the lake shore, yielding the height of the TIBL at that point. After calculation of H, this allows the plume to be assigned to the proper computational scheme (conventional dispersion, fumigation, or lid trapping). With this information, the plume's limits are computed. One solves for a lateral (Y) and a downwind (X) distance along the plume centerline, at which the concentration drops off below a minimum desired cutoff. This approach cuts down the number of computations or throws out the source entirely if it does not enter the receptor grid. The cutoff concentration of SO_2 used was 0.0002 PPM. Along with these computations, two other factors are computed, x_B and x_E, the points at which fumigation begins and ends. These are distances downwind from the source, not necessarily (and not usually) equivalent to the "fetch" of the "TIBL wind" from the shoreline.

MODEL INPUT DATA REQUIREMENTS

The following is a listing of the information needed to run the GLUMP model for shoreline fumigation.

1. One must specify the receptor grid base point, grid spacing, x and y dimensions, number and height of the various layers, and a plume concentration cut-off value.

2. The shore is entered in UTM coordinates with the number of points being some multiple of 2^n, where n is greater than 3 but less than or equal to 11. This requirement is derived from the fact that a smooth shoreline profile is determined by a modified binary-lookup technique employing a maximum of n searches. The

shoreline from the northern edge of Milwaukee County to just south of Waukegan is specified by 2048 points and is assumed straight north and south of these points.

3. The emission inventory consists of all-point sources (over 200) with their UTM location, physical stack height, inside stack diameter, exit velocity, stack temperature, emission rate, company name, and hours per year of operation. These are updated on an hour-by-hour basis for the power plant plumes simulated here. Area sources, if used, must be specified by location, size, source strength, and effective stack height.

4. The TIBL height is read in at 0.1 km increments to 20 km of inland fetch along the "TIBL wind."

5. The "environment" is specified for the number of layers chosen with wind speed, wind direction, background level, temperature, mean pressure, $\sigma_y(s)$ and $\sigma_z(s)$ in the stable air above the TIBL, and $\sigma_y(u)$ and $\sigma_z(u)$ in the unstable air below the TIBL.

6. Concentration isopleth levels for the output contour routines must be selected.

MODEL OUTPUT FORMATS

Much of the utility of the GLUMP model lies in its versatile output routines.

1. A map is generated showing all points used in the calculations and also the points rejected due to insufficiently large Q, or lack of interception of any receptor points with above the cut-off level.

2. Each plume computed is listed along with all relevant data such as Q, ΔH, H, lateral spread, plume centerline concentration χ at 0.5 km increments downwind, and location of x_e and x_b.

3. A statistical table is generated giving the maximum and minimum χ at each level, along with mean and standard deviations of all non-zero receptor points.

4. A printer plot echoes the TIBL profile as a function of fetch along the "TIBL wind." (Figure 5-4).

5. More useful is a CALCOMP plot of the TIBL surface with contours every 50 meters showing the actual pattern of mixing heights over the region.

6. If desired, a 3-D plot of a TIBL surface can be generated, with the perspective of the viewing angle being a variable.

7. Pollution concentrations can be generated in any xy, yz, or xz plane used in the three-dimensional receptor grid, including:

i. Standard numerical grid print output, showing actual values,

ii. Printer plots which can be very effective for viewing individual plumes,

iii. CALCOMP plots with any desired isopleth contour levels, scaled to overlay directly a 1:62500 USGS topographic map, etc.,

iv. 3-D surfaces of concentrations.

Once a series of computations are made, the values obtained at each receptor are stored on magnetic tape for any later reference.

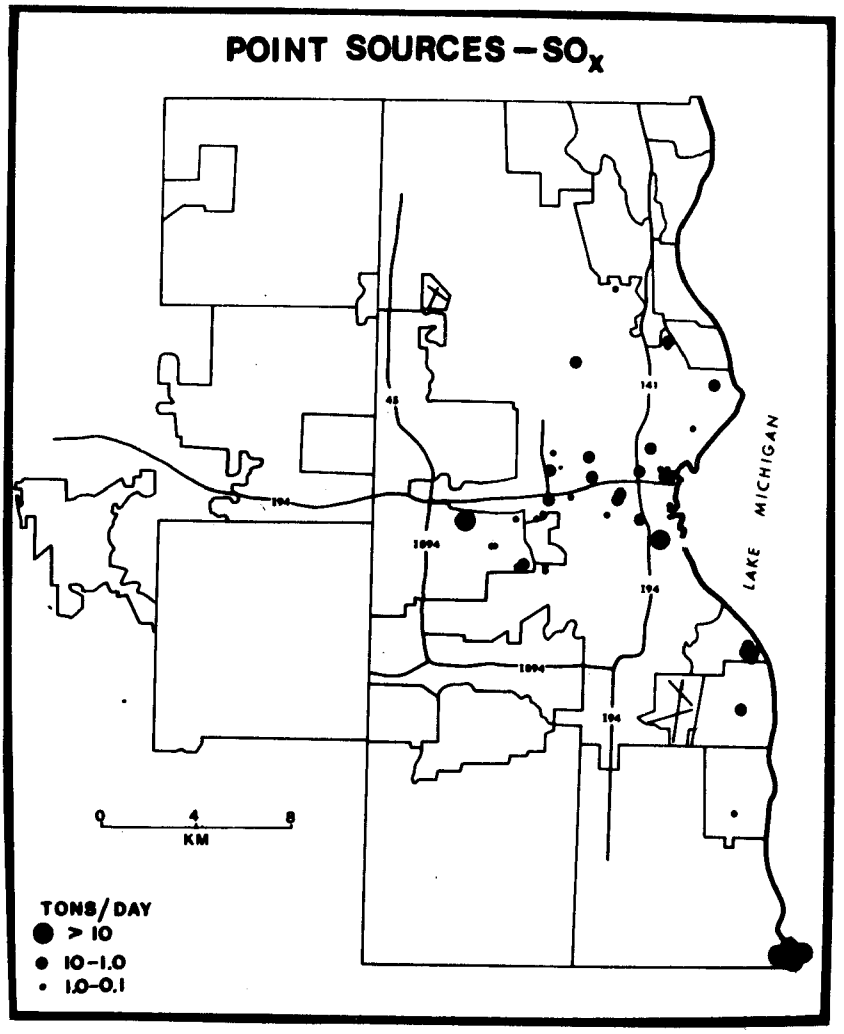

Figure 5-1. Portion of 1970 emission inventory of SO_2 sources in southeastern Wisconsin, showing Milwaukee County major point sources. Particulate emissions have a similar geographic distribution.

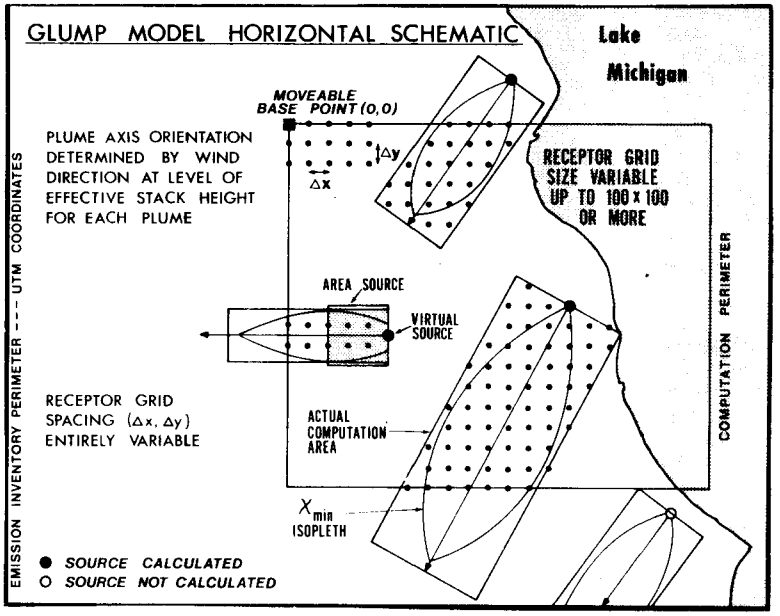

Figure 5-2. Horizontal schematic of GLUMP model. The receptor grid shown has arbitrary dimensions and grid spacing. Its location is selected by assigning a "base point" for the upper left corner. Each point and area source is then tested for the maximum lateral and downwind distance to which a pre-determined cut-off level for concentration is applied. Thus, only points with concentrations above this minimum and lying within the receptor grid are calculated. This eliminates numerous unnecessary computations.

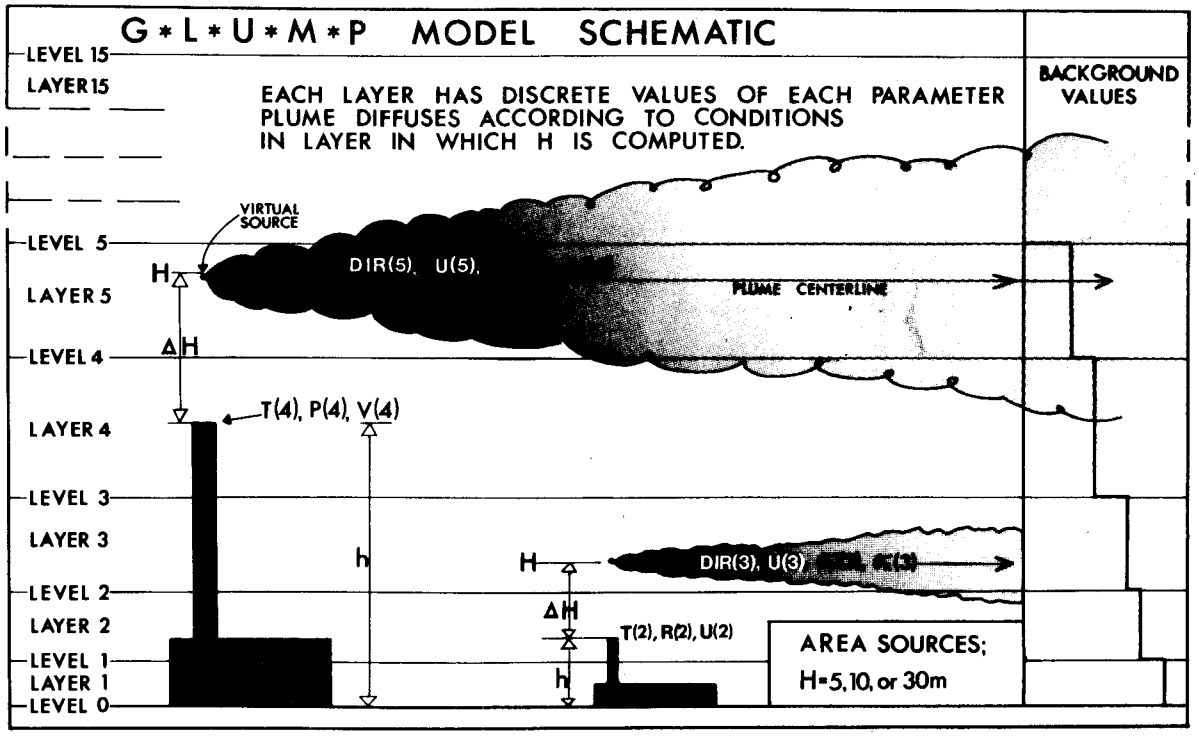

Figure 5-3. Representation of vertical structure of the GLUMP model. Each individual effective plume height is computed. The plume is assigned to a given level having its own wind speed and direction, background level, σ_y and σ_z for stable and unstable portions of its fetch. N levels (of arbitrary spacing) can be employed.

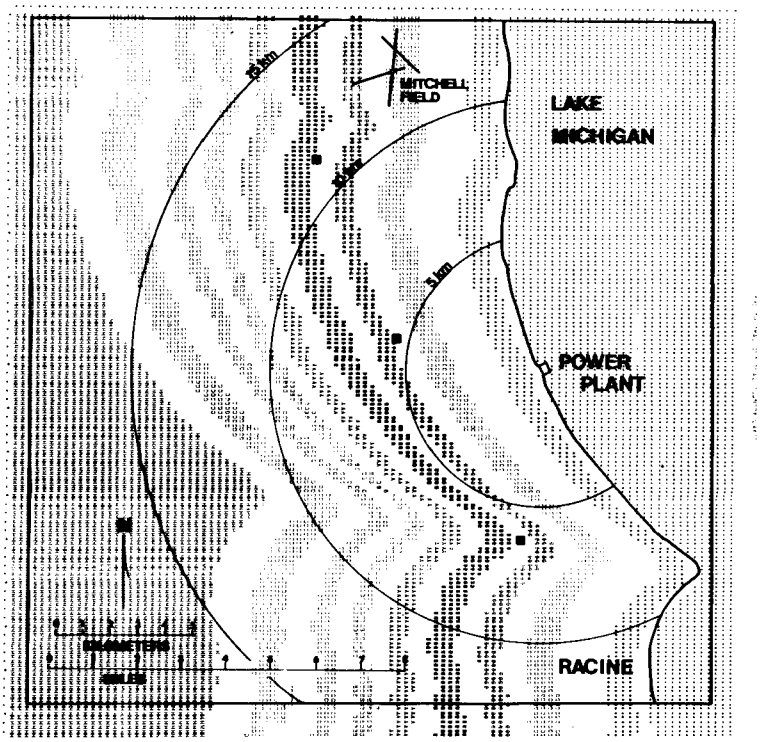

Figure 5-4. Printer plot of a typical TIBL top profile with an east-southeasterly flow. As flow becomes more parallel to the shore, TIBL top profiles become increasingly complex and distorted.

SECTION 6

MODEL CALIBRATION AND VALIDATION

GENERAL COMMENTS

All numerical models of geophysical phenomena are simplified approximations of reality and are assemblages of assumptions, compromises, parameterizations, and idealizations, tying together a conceptualization hopefully based upon the phenomenon as it actually occurs and not how it is merely perceived. Accuracy, whether relative or absolute, is never presumed, merely hoped for. In general a model would be considered successful if the assumptions and techniques are chosen in such a way as to consistently over/under predict in such a manner as to be subjected to a rational calibration scheme. The 1974 Lake Michigan field programs attempted to validate the basic assumptions made in the model and to find proper calibration factors so that the computations could be used with confidence for planning purposes.

PLUME GEOMETRY

The most extensively studied day of the 1974 Milwaukee portion of the field programs was 8 August 1974. Nearly ideal fumigation conditions were combined with unusually high data acquisition rates. A high pressure ridge over the eastern U.S. resulted in light southeasterly gradient flow over Lake Michigan. No lake breeze formed. Pibal ascents showed that even at that, low level wind profiles were complex and exhibited great spatial

and temporal changes. Wind speeds near plume altitudes generally decreased from over 5 m/sec to under 2 m/sec by late afternoon. Considerable wind direction shear in the vertical caused the separate plumes of the OCPP occasionally to be distinct, although they were more cohesive than many other days studied. Winds at plume levels early in the day were east-northeast, shifted to southeast, and then returned to northeast by late afternoon. Insolation was strong. Cumulus clouds formed about 10-15 km inland during the afternoon, and a maximum mixing depth of 1250 m was attained by 15 km inland. The onshore flowing airmass was only slightly stable inasmuch as lake water temperature was considerably warmer than in the early summer and spring. A rather weak but persistent elevated inversion was found through the day with a base ranging from 50 to 150 m. Inland wiresonde runs showed a ground-based 100 m deep superadiabatic layer during the greater portion of the day.

Though the east-west aircraft traverses were not designed to monitor SO_2 plumes per se, chance allowed the plane to fly nearly along the mean plume axes during mid-afternoon. Figure 6-1 shows an excellent resemblence to the profiles hypothesized by Lyons and Cole (1973). Values above 3 ppm were found aloft. It should be remembered that the plumes were actually drifting through the aircraft track at angles of up to several tens of degrees. Yet the overall pattern is obvious.

In order to test the correspondence between measured horizontal and vertical plume profiles and the GLUMP model predic-

tions, specific aircraft and helicopter data taking traverses were run. A complete study of model calibration and validation is made by Dooley (1976).

Figures 6-2, 6-3, and 6-4 are plots of the vertical helicopter soundings made on 8 August 1974. Sounding number one (Figure 6-2) was taken 0.9 km northwest of the power plant and shows the plumes traveling downwind. The lower plume has layered out between 125 and 275 m while a portion of the upper plume is centered at 350 meters. This is typical of a pre-fumigation sounding. By 6.3 km (Figure 6-3), the lower plumes have fumigated but the upper plume, above the TIBL, is still layered just below 500 meters. At a distance of 11.4 km (Figure 6-4), all the SO_2 has been thoroughly mixed below the TIBL and is reaching a nearly vertically uniform concentration profile. A nearly identical sequence was recorded on the prior day (Dooley, 1976). Thus, there is an excellent qualitative agreement between observation and model (see Figure 4-2). In particular measured and computed x_e and x_b values were satisfyingly similar.

Horizontal plume traverses likewise conform to the model. Figure 6-5 is the plot of the observed SO_2 concentrations in a series of north-south sections during mid-day at 2.3, 4.5, and 11.8 km downwind of the Oak Creek Power Plant. Each individual cross section has a vertical scale for reference. The two closer runs were made by the Cessna 182 and have their lowest travers at 152 m AGL (500 ft). The helicopter made the 11.8 km traverse and it was able to traverse from 30 m to 760 m AGL at 30 m increments. North on this cross section is to the right.

There are some obvious features in the cross sections. The first is that the plumes are expanding with distance, and the maximum concentrations decrease as the plume diffuses. Second, by 11.8 km, vertical SO_2 concentrations are quasi-homogeneous. Finally, the plume and its maximum concentration tilt slightly to the north. Brown and Michael (1974) noted that if no other outside forces acted on the plume, the veering action of the wind alone would cause the distinct tilt observed. A direct consequence of this shear is to spread the plumes over a greater horizontal width when projected onto a plan service. Dooley (1976) shows that the changes in horizontal plume width, as specified by chosing two σ rates (one in the stable air and a second in the mixing zone related to a virtual source) likewise show a satisfactory degree of comparison between observed and modeled.

CALIBRATION PROCEDURE

While geometric similarity between modeled and observed plumes is necessary, is not sufficient to assure that computed concentrations are accurate. The values generated must be scaled (calibrated) by comparison with actual measurements.

The concentrations predicted by Gaussian plume models are typically held to be representative of ten minute averages. It is unlikely that this is the case for a fumigation regime. The mobile van, positioned by the aircraft and helicopter in a fumigation spot, took SO_2 readings for a full ten minutes. Very rapid fluctuations about a mean occurred associated with both the azimuthal and range variations of the spot and with thermal convective eddies.

Figure 6-6, from a telemetered surface station beneath the OCPP plumes on 8 August is a good example.

The mobile van data from seven days representing fumigation conditions were examined. The ratios of the observed ten minute means to instantaneous peaks were plotted as a function of range from the power plant. While there is considerable scatter, a curve visually fitted through the data seems to represent the observed trent (Figure 6-7).

The ratio $R_{10}(x)$, approached 0.9 beyond 15 km. For the few readings within 5 km of the stacks, values fluctuated around 0.5. The greatest scatter is found between 6 and 15 km, the zone where the most active fumigation would be expected. The plume matter thus becomes more nearly vertically homogeneous as the distance from the power plant increases. This confirms the patterns measured by the helicopter and aircraft.

The following method appears a reasonable and generally conservative calibration technique.

It is assumed that the GLUMP Model predicts essentially the instantaneous concentrations that are measured by the fast response sensors on the helicopter, aircraft, or the peaks monitored by the van. The conversion to ten minute average SO_2 values at the ground, $\chi_{10}(x)$, is given by:

$$\chi_{10}(x) = \chi_G * R_{10}(x)/\Omega$$

where $R_{10}(x)$ is the distant dependent ratio of the 10-minute mean to peak concentration, χ_G is the prediction of the GLUMP Model,

and Ω is a calibration factor.

The Ω term is essentially the ratio of the maximum χ_G predicted by the GLUMP Model at a given time to the maximum instantaneous concentrations obtained by either the ERT Van or one of the fixed monitors. There were five hours during which it is reasonably certain that the measured SO_2 peaks were the highest peaks. Of these, four were on 8 August, and the fifth was on 28 June. The average value of Ω was found to be 1.28, with all values higher than 1.00. Thus, as expected, the GLUMP Model tends to over-predict surface concentrations, by factors ranging from over 2.5 within 5 km to less than 1.5 at 15-20 km downwind. Note that in examples shown below, the computer values are uncorrected and represent χ_G.

PLUME MASS BALANCE

It has been assumed above that measured SO_2 values were in fact accurate. All ground sensors were of course frequently caligrated. In particular the flame photometric unit in the mobile van was checked at least daily against a calibration source. The conductometric instruments in the Cessna 182 and the helicopters were also calibrated before each days flights began. Yet numerous errors can be expected in airborne sampling programs. One method to assure that instruments are working satisfactorily, the data are analysed properly, and that all plume matter was monitored, is to perform a plume mass balance.

In order to perform the balance we need as input data: the emissions from the power plant, the reconstructed plume cross

section, and the wind field into which the plume was emitted. Six cross sections were selected for this analysis, five taken on 8 August, the day most intensively investigated. The sixth section was from 6 August, when the flow was offshore and the plume was over the lake.

The mass balance consisted of digitizing the cross section and arriving at a total amount of SO_2 (gm) contained therein. Then, using the winds obtained from the pibal sites at the shoreline, 7 km, and 15 km sites, the travel time fromthe power plant to the location of the cross section could be estimated, and the emission for the hour nearest the sample would be used then in the balance.

In attempting this type of mass balance there are several factors influencing the final results. The first factor will be the analysis of the plume SO_2. The technique of extrapolating a series of horizontal traverses through the plume into a continuous concentration field lends itself to the possibility of sampling errors. The exact centerline value may be missed using this method and this would reduce the total SO_2 mass. In lieu of some remote sensing technique, this method, while practical, is crude, and clearly needs improvement. The response of the SO_2 monitor is not instantaneous and this too could introduce some errors, especially in large gradients of SO_2 concentrations. Thirdly, SO_2 undergoes transformation to aerosol in the plume and this factor is not incorporated in the mass balance. Finally, it is to be remembered that power plant emissions themselves are

only rough estimates.

With these possible errors in mind, Figure 6-8 shows the results. Computed SO_2 mass captured from the aircraft/helicopter traverse data ranged from 74.5 to 101.0% (at distances from 2.3 to 11.8 km). The average was 87.3%. This is felt to be acceptable in light of the various factors mentioned above.

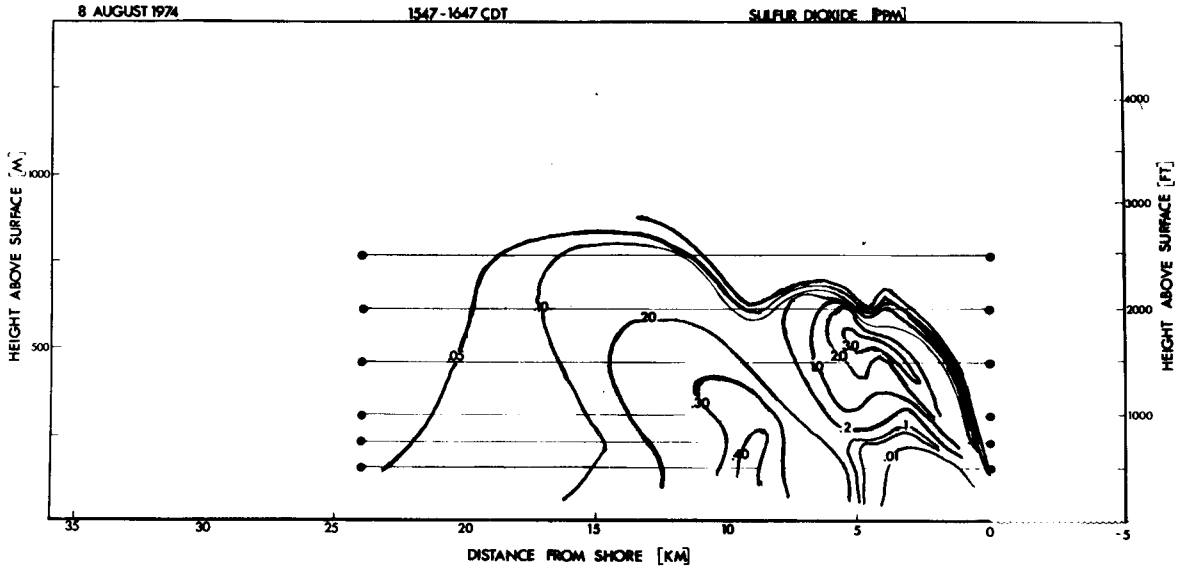

Figure 6-1. East-west aircraft SO_2 traverse, roughly down mean plume centerline path, 1547 CDT, 8 August 1974. Peak values in excess of 3.0 PPM remained well aloft.

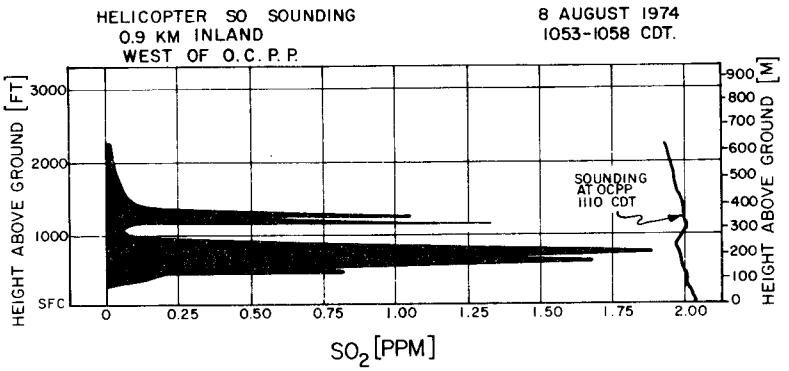

6-2

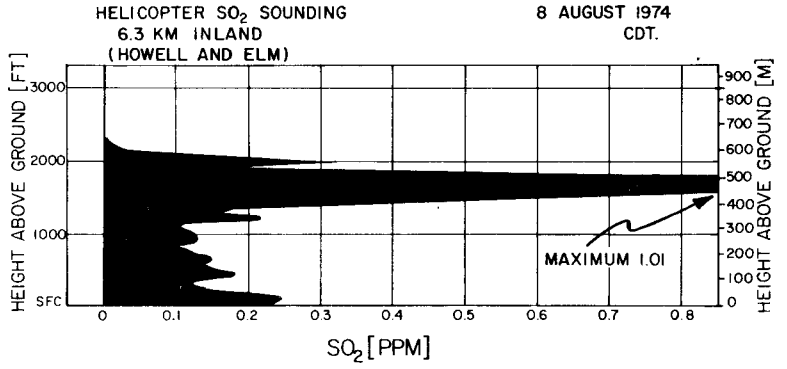

6-3

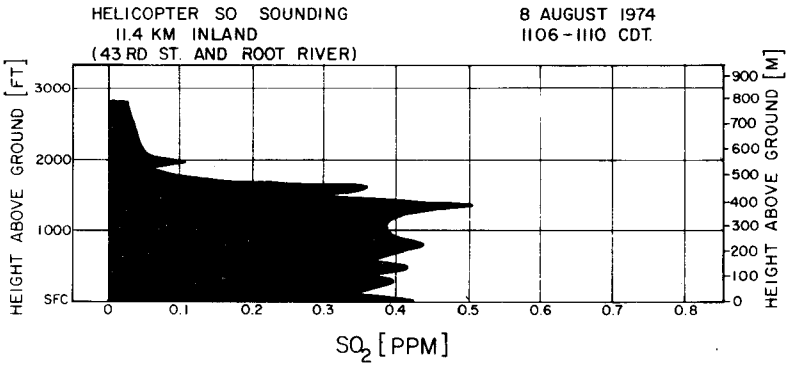

6-4

Figure 6-2. Helicopter SO_2 sounding, 0.9 km downwind of power plant, 1053-1058 CDT, 8 August 1974. Figure 6-3, same, at 6.3 km downwind, 1116-1120 CDT. Figure 6-4, same, at 11.4 km, 1106-1110 CDT.

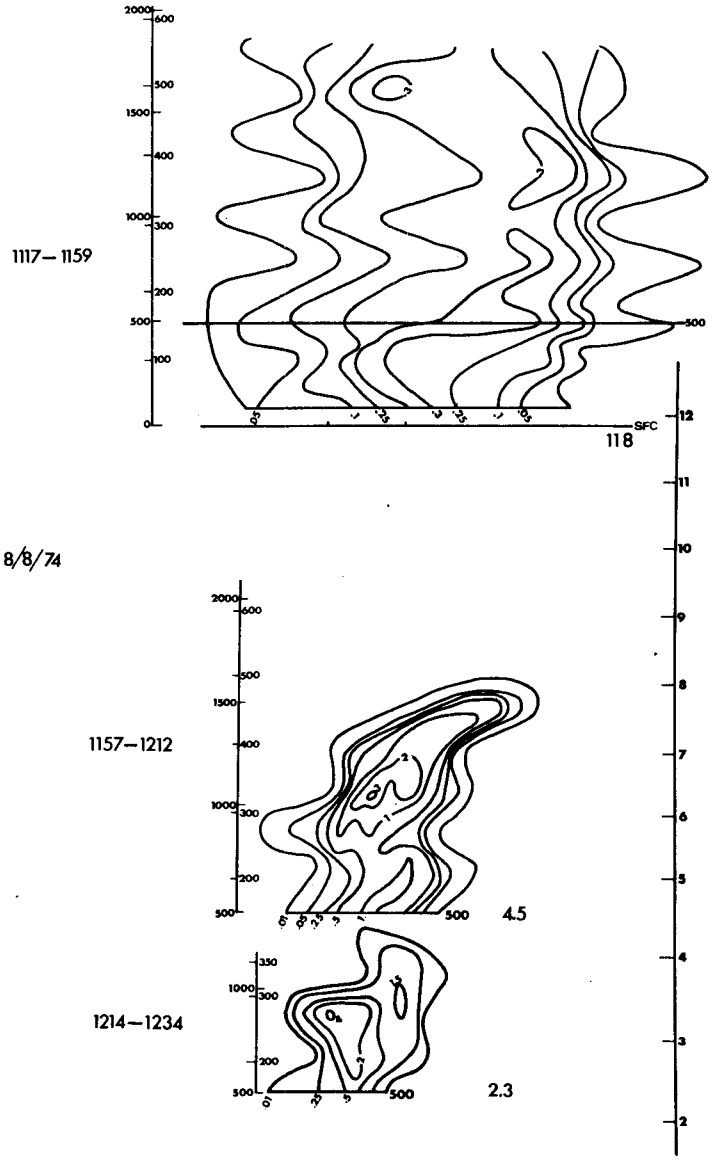

Figure 6-5. Composite of the 2.3, 4.5, and 11.8 km SO_2 Traverses on 8 August 1974. The right hand scale is the distance from the power plant in km. Each individual traverse has its own vertical scale for reference but each scale is the same. Isopleths at .01, .05, .25, .50, 1.0, 2.0, 2.0 ppm.

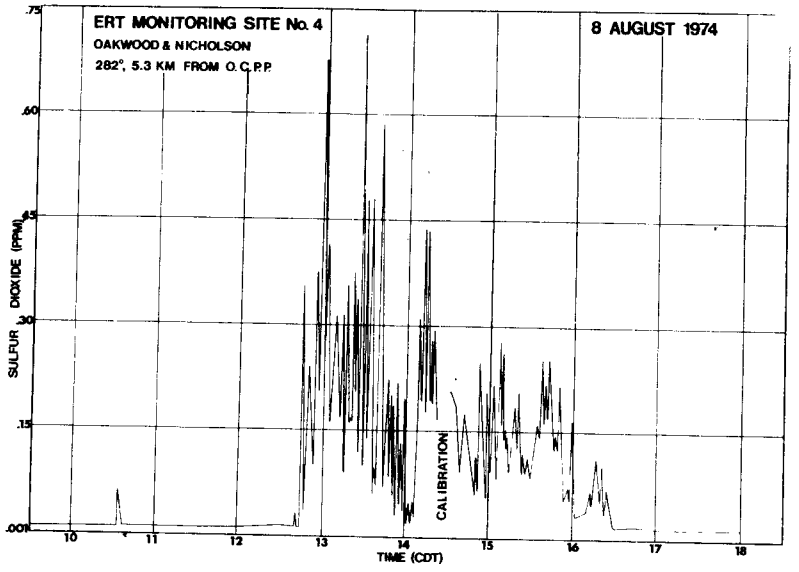

Figure 6-6. SO_2 record from the ERT fixed site monitor located 5.3 km from the Oak Creek power plant. This trace on 8 August 1974 is typical of the record of fumigation measured at a point. Note that fumigation began shortly after the end (1234 CDT) of the 4.5 km traverse.

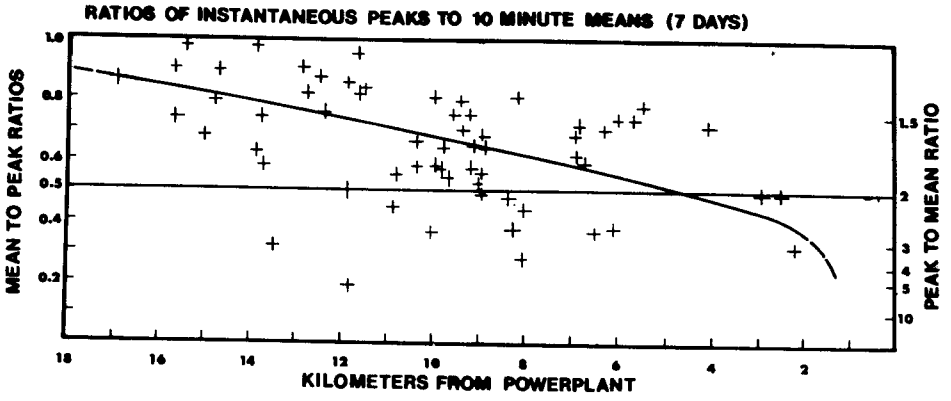

Figure 6-7. Ratio of ten minute average to instantaneous peak SO_2 values measured by ERT mobile van. All fumigation measurements for seven days in Oak Creek and Waukegan were plotted. The line is a rough fit of the data as a function of distance from the power plant.

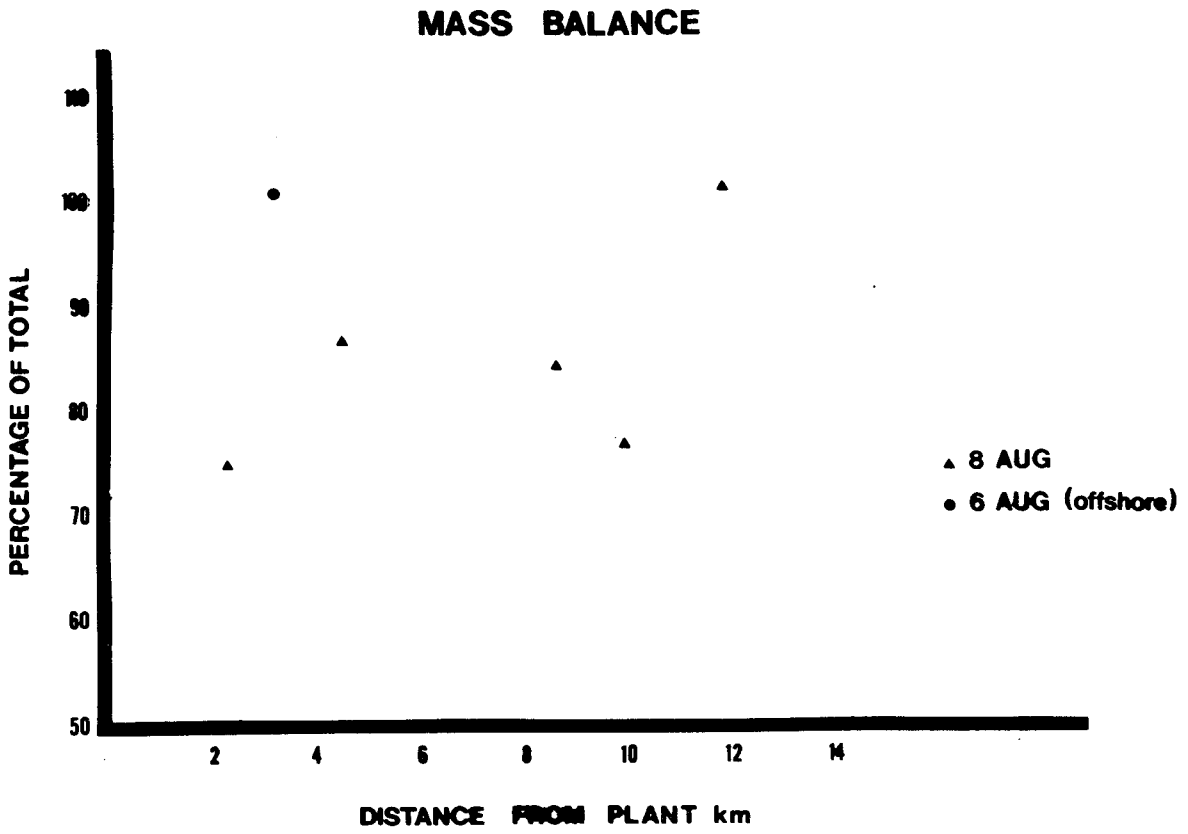

Figure 6-8. Mass balance for six selected plumes. The solid triangles are the five plumes that had complete data on 8 August 1974. The circle represents an offshore flow case. Traverse density, instrument response, and sulfate aerosol formation are all probably errors that were not taken into account.

SECTION 7

STUDIES OF ELEVATED POINT SOURCE PLUME FUMIGATION

OVERALL FINDINGS

The field studies did indeed confirm that continuous fumigation of high-stack shoreline power plant plumes could produce significant surface SO_2 concentrations. Both the field data and the refined modeling efforts made it very clear in addition that the rapid movement of the fumigation spot resulted in much lower dosages than originally expected. This is not to say that shoreline fumigation is not a serious problem, but that a sufficiently detailed model and the proper input data are required to assess its true impact. The phemenon is in fact an extremely complex one.

The use of fixed surface networks in order to study shoreline fumigation is likely to be frustrating unless one is prepared to accept an unusually long data gathering period (several years?) or install a very dense network (prohibitively expensive). The ten station network around the Waukegan Power Plant, designed in part to monitor its fumigating plume, only sporadically had any of its stations intercepted by the "fumigation spot" itself. Similarly for several monitors installed near the Oak Creek Power Plant. On only several occasions during a three-month summer 1974 period did any site clearly record the passage of the spot. Yet on many days, high surface concentrations of SO_2 were present somewhere within the several hundred square kilometer area of potential

impact.

The strategy of using aircraft and helicopters to locate the fumigation spot, and to deploy a mobile van via FM radio voice link proved to be correct. It was not necessarily easy however. The spot moved rapidly and of course not along roads that the van necessarily had to use. All problems aside, several dozen readings on excellent fumigation days were obtained, which were adequate for model calibration.

Certainly obvious was that conventionally acquired meteorological data (on 200 ft towers, etc.) is totally inadequate to define the atmospheric structure resulting in fumigation. The exact orientation of the several plumes from a multi-stack power plant must be known. Even the serial pibal chains with hourly ascents insufficiently defined the details of the wind which had a major impact on surface concentrations during supposedly "steady state" gradient onshore flows. In any case, a 60 m tower will not yield wind directions relevant to a plume with an effective stack height of 300 m. So marked were the temperature inversions and vector wind shears with height that little could be infered from near-surface observations. Plume diffusive characteristics likewise were totally unrelated to the P-G stability classes that might be estimated by using surface data alone and Turner's (1969) simplified classification scheme. In fact, even temperature lapse rates determined by radiosonde/wiresonde proved useful only in the grossest sense of the word. In particular horizontal plume spread was poorly correlated to temperature lapse due to the marked effect of vertical wind direction shear.

8 AUGUST 1974

As mentioned in Section 6, the most intensely studied day was 8 August 1974, which was nearly a "classic" in terms of fumigation potential. A weak high pressure ridge was stalled over the Greal Lakes; there was no lake breeze, but the apparent steadiness of the onshore flow from the synoptic charts was however partly illusory. Mean wind directions varied from 070° during the morning to 135° by mid-afternoon, and back to 085° by late afternoon. These fluctuations are brought about in part by the development of a highly ageostrophic wind component associated with a lake mesohigh (Lyons, 1970). Vertical wind direction shears, which on this day were comparatively small, acting on the highest and lowest plumes can have a significant impact on the location of fumigation spots. Velocity shears, associated with wind speed maxima similar to "low level jets" also result in plumes emitted at different levels having markedly differing plume rise and dilution factors (Figure 7-1). Very telling is a wind hodograph (Figure 7-2) of the azimuth of the highest plume from OCPP. This was constructed by calculating the effective plume height on an hourly basis and then interpolating the wind direction and speed from the shoreline pibal-derived winds. Each of the four plumes had similar but still distinctly different hodographs.

By early August the lake had become considerably warmer, with surface temperatures approaching 20 °C. The onshore flow was thus not as severely stabilized as in early summer and spring. The shoreline radiosonde measured slightly stable layers aloft,

and generally P-G stability Class E prevailed at the shoreline. The maximum surface temperature differential between the shore and the inland sites was only about 4.5 °C. The wiresonde located 15 km inland generally measured D stabilities in the lower 300 m during the bulk of the day. Had not a rather thick sulfate haze covered the area, the surface temperature remodification would undoubtedly have been stronger, and the TIBL even deeper. The acoustic sounder showed little indication of significant low-level stability during the day. It is important to note that the minimal initial stability played a key role in the relatively rapid deepening of the TIBL, even under reduced insolation. Had an intense low level inversion been present, it would have taken considerably greater fetch before the weak insolation could have caused penetrative convection to erode the overlying stable air while flowing inland.

Various plume measurements on this day are seen in Section 6 above. Figure 7-3 is a horizontal traverse of the SO_2 plume made by the aircraft during mid-afternoon. Of some interest is the plume's rather sharp bend to the left after reaching approximately 10 km inland. This could very well be a manifestation of two phenomena. The first is that as the plume experiences vertical mixing due to convection, the vertical direction wind shear also enhances lateral spread. The second point is that there appears to be a "wobble" on the entire boundary layer that occurs during the stable onshore flow situation. It appears to be something of a higher speed version of a typical stable flow meander, and the entire boundary layer appears to undergo alterations of wind

direction of several tens of degrees at a frequency of several times per hour. It should be noted on many days with stable onshore flow, the plume cannot be tracked as easily as might be suggested by Figure 7-3. On some days the intense vertical wind direction shear had the four plumes fanning off in entirely separate directions, in one case with axes separated by up to 120°. Even a fast moving aircraft is incapable of adequately mapping SO_2 fields under these circumstances.

MODEL RESULTS

The GLUMP model was employed to produce hour-by-hour simulations of the four Oak Creek Power Plant plumes, each treated separately. Brigg's stable plume rise equation estimated effective stack height for each plume, adjusted by observations when available. The effective stack heights of the four plumes ranged from less than 200 meters to above 525 meters in the time period under discussion. in almost all cases but one (discussed below) there were at least several degrees of wind direction shear between the four plumes. A typical plot of surface SO_2 concentrations (uncalibrated, instantaneous values) is shown in Figure 7-4a for 1400 CDT. In this case there appear to be two distinct fumigation spots on the surface. A ten minute computed value of 0.47 ppm (calibrated) is found, while the mobile van reported a 10-minute average of .42 ppm. In this case the two lower plumes had azimuths of 124° with upper plume azimuths being 137°. By 1600 CDT (Figure 7-4b) the winds became more easterly, but more importantly, for a short time, there was relatively little wind

direction shear, less than 1° between the upper and lower plumes. Thus all four plumes coincidentally lay along the same azimuth resulting in almost the maximum additive effect. The uncalibrated SO_2 surface concentrations were approximately 1.06 ppm (similar to those reported by Lyons and Cole (1973) in their initial case studies). It was during this hour that the highest surface values were monitored by the mobile van, 0.79 PPM (instantaneous).

While both observations and computations suggest very high instantaneous SO_2 values at the ground, the maximum one hour average recorded by the fixed monitor 5.3 km west of the power plant was only .16 PPM. This is a manifestation of the fact that the fumigation spots are moving about the surface with great speed lowering dosage at any given point. Figure 7-5 represents a summation of the computations for OCPP stack 1.

The diagram was produced by overlaying all the plumes from this stack for all hours and drawing isopleths around concentrations of equal value. In other words, any point within the 0.50 PPM contour had values in excess of that figure for at least one instant during the period 1000 to 1730 CDT. The heavy line connects the center of the fumigation spot for the plume. Figure 7-6 is the same presentation except for the highest stack (number 4) which also has had the highest SO_2 emissions. (The extremely rapid motion of the four separate fumigation spots around the area is evident.) The patterns from stack 1 and stack 4 were similar but by no means identical. It is imperative that for multi-plume sources that each plume be treated separately with the final SO_2

concentrations achieved by summation. Figure 7-7 is another time/history diagram of the integrated behavior of all four plumes during the time period 1300-1730 CDT. The tracks of the primary and, when present, secondary fumigation spots, are noted. The pattern is clearly dominated by the peak calculated at 1600 CDT, which may be a partial artifact of the pibal wind data. It seems likely that a 15-20 km^2 area experienced maximum instantaneous SO_2 values in excess of 0.70 PPM. Upon application of the 1.28 Ω calibration factor, and a mean distance of $R_{10(x)}$ of 0.75, the $\chi_{10(x)}$ value resulting is about 0.45 PPM. Especially in view of the speed at which fumigation spots travel (see below) it seems certain that the values exceeding the 3-hour 0.50 PPM standard did not occur on this day.

FUMIGATION SPOT CHARACTERISTICS

Using the model computations for 8 August 1974 plume simulation, the fumigation spots were investigated in greater detail. For purposes of definition, a fumigation spot is the area enclosed within the isopleth representing half of the peak surface SO_2 concentration.

Figure 7-8 shows the fumigation spots and areas for each plume on 8 August 1974. Each spot generally covered an area less than 20 km^2, and occasionally less than 5 km^2. Thus the area affected at any given instance is quite small. The area of a fumigation spot is largely determined by the slope of the TIBL at the point where it intersects a given plume. If the TIBL is rising rapidly, the area will be quite small, although peak surface

Thus it can be concluded that, unless actual observations of plume σ_y's are at hand, modeling efforts in the shoreline boundary layer should include corrective terms for σ_y to account for shear diffusion phenomena.

Figure 7-11 shows all observed σ_y's as a function of distance downwind from the power plant. What becomes clear is that the main line through all of these data does not appear to follow the general curve slope, but rather shows a distance-dependent decrease in the rate of vertical spread. Thus the data appear to be illustrating the significant effect of active diffusion due to the plume's inherent initial turbulence at emission into the atmosphere for the first several kilometers. Aircraft $\varepsilon^{1/3}$ measurements within plumes the first several kilometers downwind found values equivalent to that in a fully developed boundary layer. The fact that the plume was actively entraining environmental air could be seen by the turbulent nature of the plume. Only after several kilometers did the plume become smoothly stratified (as long as it remained above the TIBL). Thus while it has not been incorporated into the GLUMP model, it would be wise to investigate the use of a σ_z correction term to account for the initial active diffusion in such plumes before only passive pollution takes hold. A final note.

Even though the fumigation case studies made throughout this program refer to power plants at the immediate shoreline, lake fumigation effects can be a significant factor in determining worst-case surface concentrations for five or more kilometers inland. This was shown in great detail in the analysis of the

concentrations will be higher.

Figure 7-9 charts the speed of the fumigation spots across the landscape through the day showing a range from less than two to almost 10 kilometers per hour. The higher stacks (numbers 3 and 4) of course moved faster, since they intersect the TIBL at greater heights than the lower, thus at greater range, and a given angular variation results in a higher surface translational speed. On this day, which was probably rather typical of many summer days, these spots traversed the landscape approximately four kilometers per hour. The difficulty in obtaining an adequate 10-minute sample for a spot perhaps less than a kilometer in width is obvious.

It should be reemphasized that if a lake breeze were in progress all of the above described fumigation spot behaviors would be even more erratic and complex. Wind shears within the lake breeze circulation cell are considerably greater, and winds are more temporally and spatially inhomogeneous. Fumigation spots would then be found over a much wider area and travel at even greater speeds, making tracking all the more difficult, and interpretation of fixed station monitoring data almost impossible.

SPLIT SIGMAS

Dooley (1976) studied the 1974 field data to determine the validity and/or necessity of employing the split sigma approach in the GLUMP Fumigation Model. Based on initial visual observations that plume lateral spread seemed to be disproportionately large in comparison to the vertical spread within the lake en-

vironment, Lyons and Cole (1973) allowed the option of using different P-G stability classes in their single point model. This capability was continued in the GLUMP Regional Fumigation Model.

In general it was found that the measured σ_z values were often close to, but sometimes a class or more greater than the expected based on vertical temperature lapse rate. But the plume lateral spreads σ_y were often much larger than the temperature might lead one to expect. This effect is undoubtedly due largely to the vertical directional wind shear. Tyldesley and Wallington (1975) could account almost entirely for the horizontal diffusion of plumes. Brown and Michael (1974) noted wind shear effects from power plant plumes to be significant within Long Island sea breezes.

Figure 7-10 shows the observed plume σ_z's plotted as a function of the observed plume σ_y's. Note that in no case did they fall within the same P-G stability class. Of those studied, 29% were one P-G class apart, 33% were two P-G classes apart, and 38% were three or more P-G classes apart. The use of a σ_y belonging to the same stability class as the σ_z can often result in an overestimate of concentrations in excess of a factor of 2.5 in the case of a three class overestimate of a σ_y stability. Brown and Michael (1974) noted that power plant plume σ_y's increased as a function of vertical wind direction shear. The data shown in Figure 7-10 were stratified with respect to wind shear and it was found that those having a cross separation of one or two, had an average vertical wind shear of .08°/meter, whereas those being three or more classes apart had a vertical wind shear of .16°/meter.

projected Pleasant Prairie power plant (Wisconsin Electric Power, southwest of Kenosha, Wisconsin) in Lyons et al. (1974). In this particular case, a very slowly developing TIBL remained below the top of the proposed physical stack height for much of 27 June 1974. This resulted in a classic case of fumigation at a point five kilometers further inland. Again, quite high instantaneous surface SO_2 concentrations were predicted, but the plume's extreme meandering effects discussed above prevented any predicted exceedences of 1, 3, or 24-hour standards.

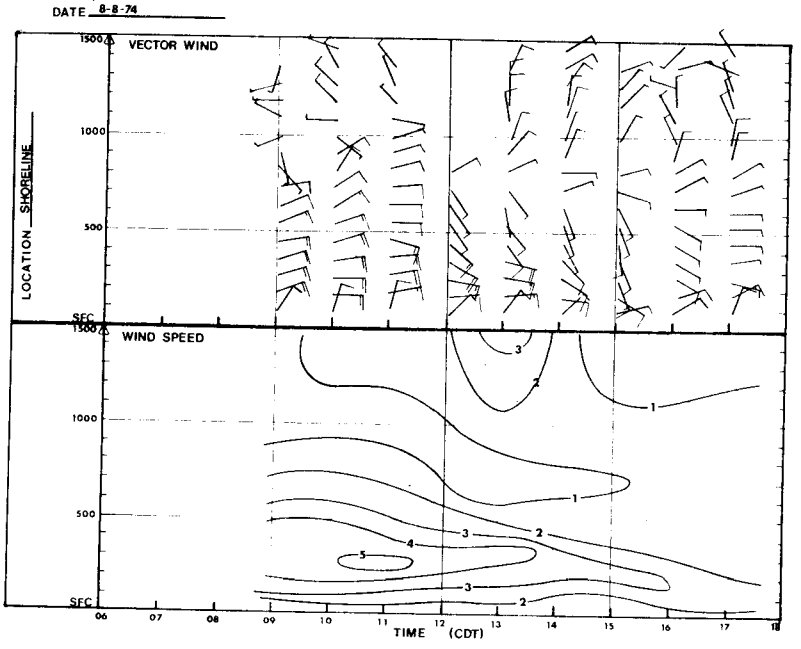

Figure 7-1. Hourly pibal ascents at the Milwaukee shoreline, 8 August 1974. Top shows plotted winds (1 barb = 2.5 m/sec), Wind speed (u) in 1 m/sec isopleths shown at the bottom.

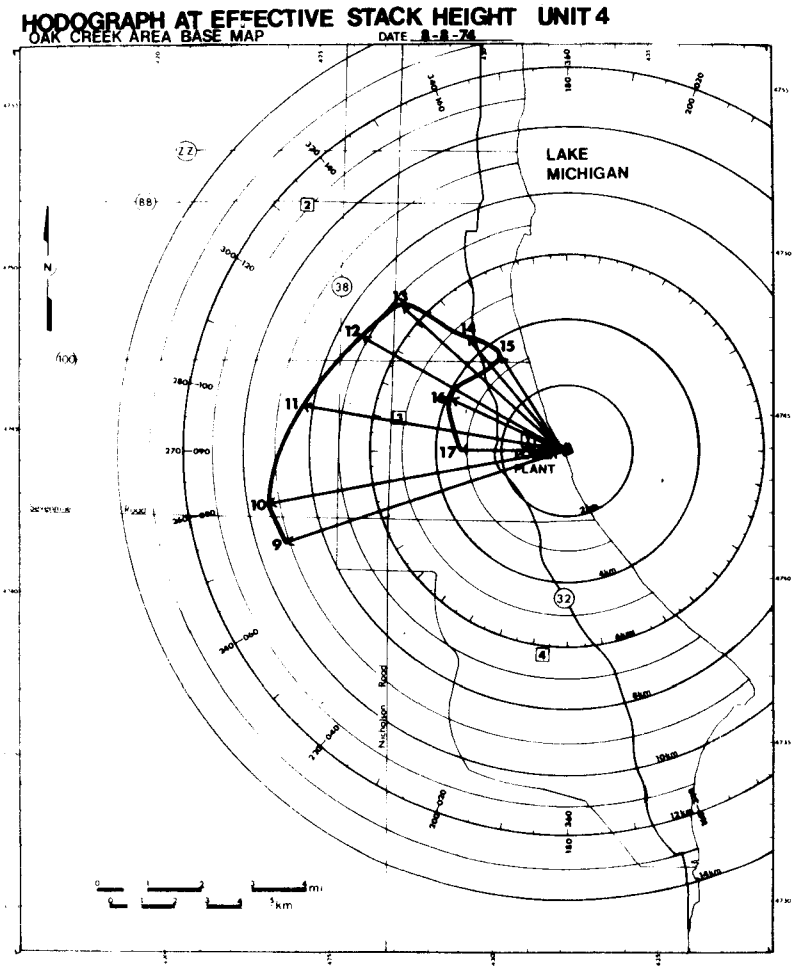

Figure 7-2. Hourly hodograph of wind at effective stack height (H) for OCPP stack 4. The hodographs for each of the four plumes were similar but by no means identical.

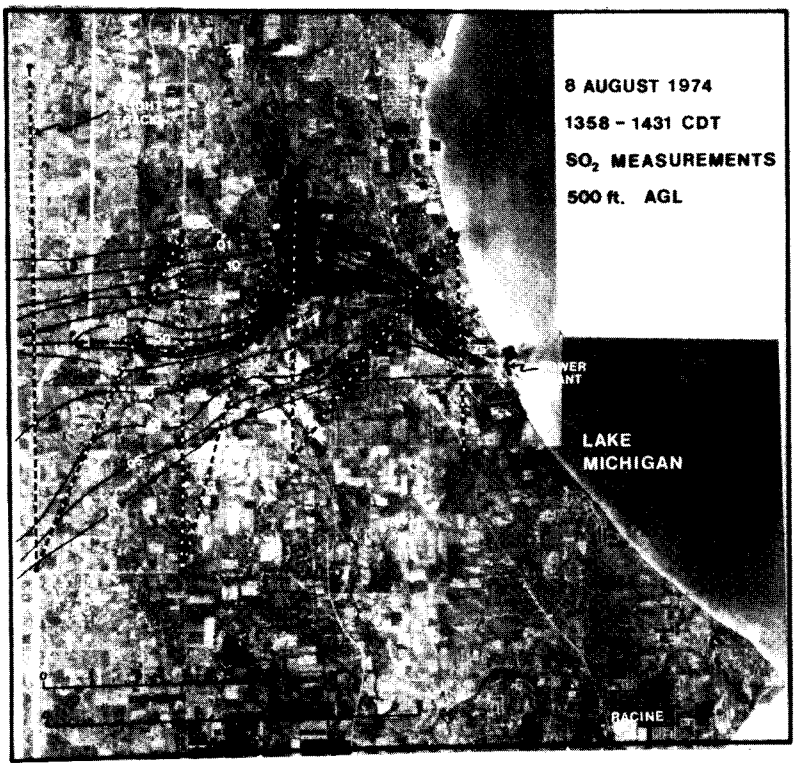

Figure 7-3. Shows the horizontal SO_2 patterns measured in a saw tooth trajectory flown west of OCPP at 150 m AGL between 1358 CDT and 1431 CDT. Once again, as at Waukegan, a sharp bend in the plume axis appears. This is probably the result of a shift in the boundary layer wind direction associated with the meander phenomenon discussed above. The peak values of SO_2 noted in the fumigation zone were between 0.5 and 0.6 ppm.

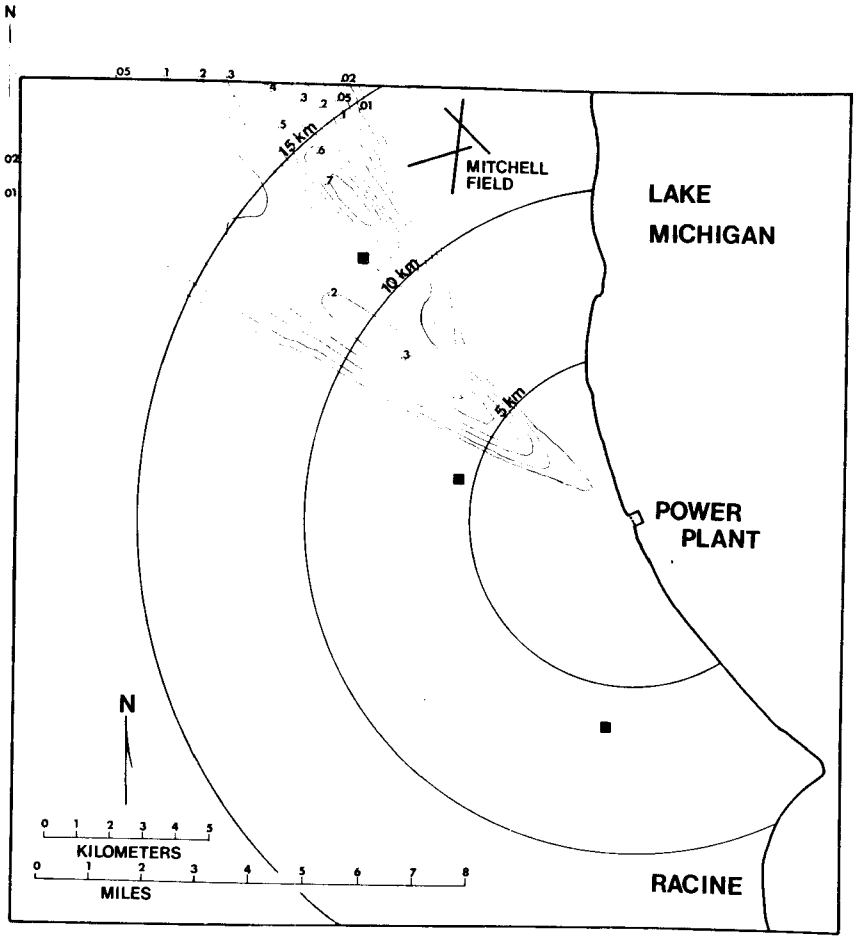

Figure 7-4a. GLUMP model predictions of surface SO_2 concentrations (uncalibrated, instantaneous readings) at 1400 CDT, 8 August 1974 in Oak Creek area showing double fumigation spots due to large wind shear.

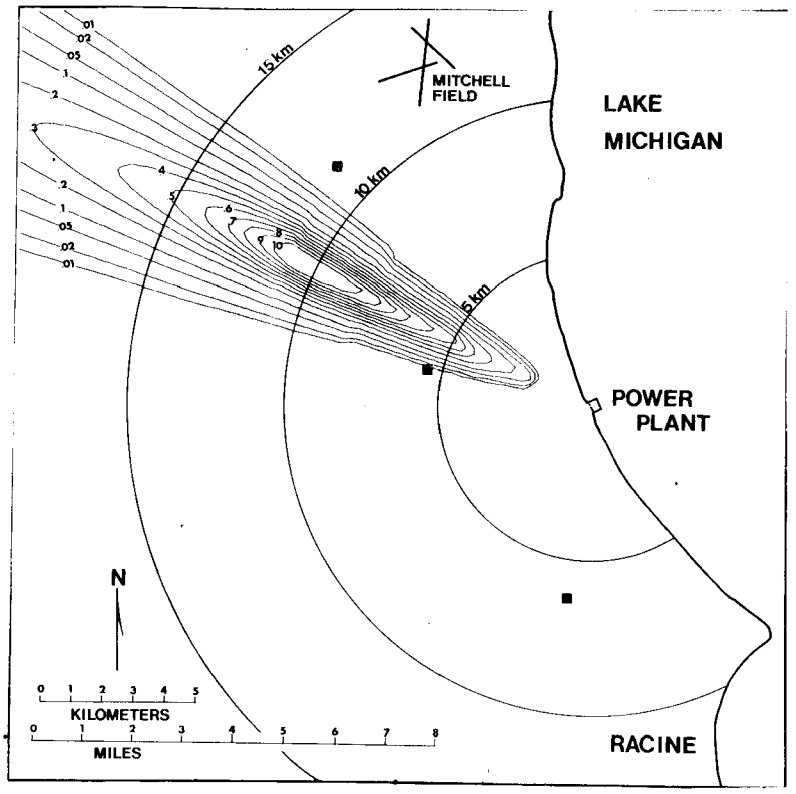

Figure 7-4b. GLUMP model prediction of surface SO_2 concentration, 1600 CDT, 8 August 1974, in Oak Creek. (The figure shows a single fumigation spot with 1.06 ppm maximum during a period of negligible directional wind shear in vertical.) The values shown here are uncalibrated instantaneous predictions.

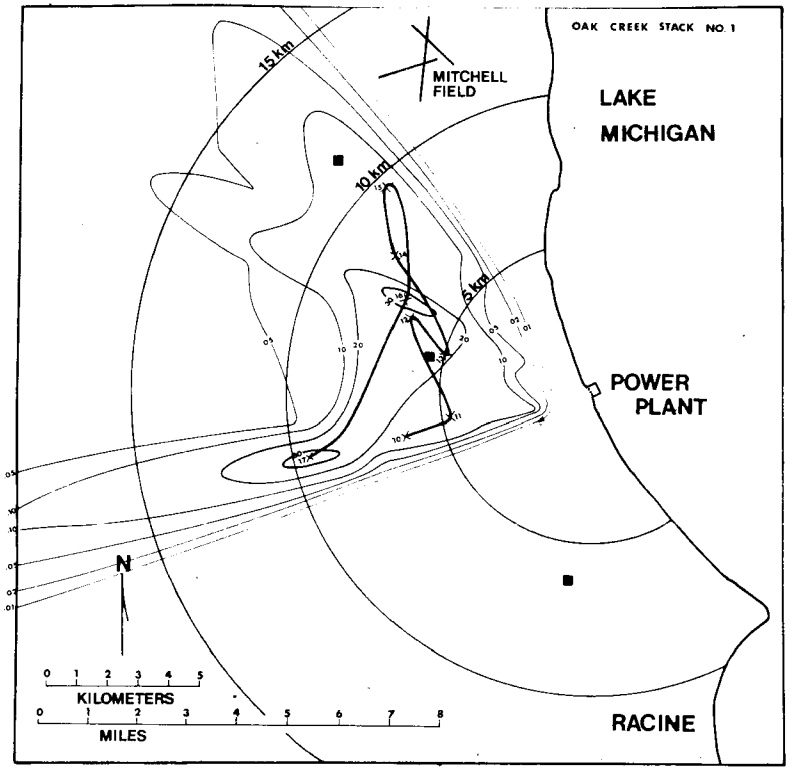

Figure 7-5. Represents a summation of the predicted maximum χ_G for the plume from OCPP Stack 1. The diagrams were produced by overlaying all of the plumes from a given stack for all hours and drawing isopleths around concentrations of equal value. In other words, any point within the 0.50 ppm contour had values in excess of 0.50 ppm for at least one time during the period 1000 to 1730 CDT. A heavy line connects the centers of the fumigation spots for each plume. The extremely rapid motion of the four separate fumigation spots around the area is evident.

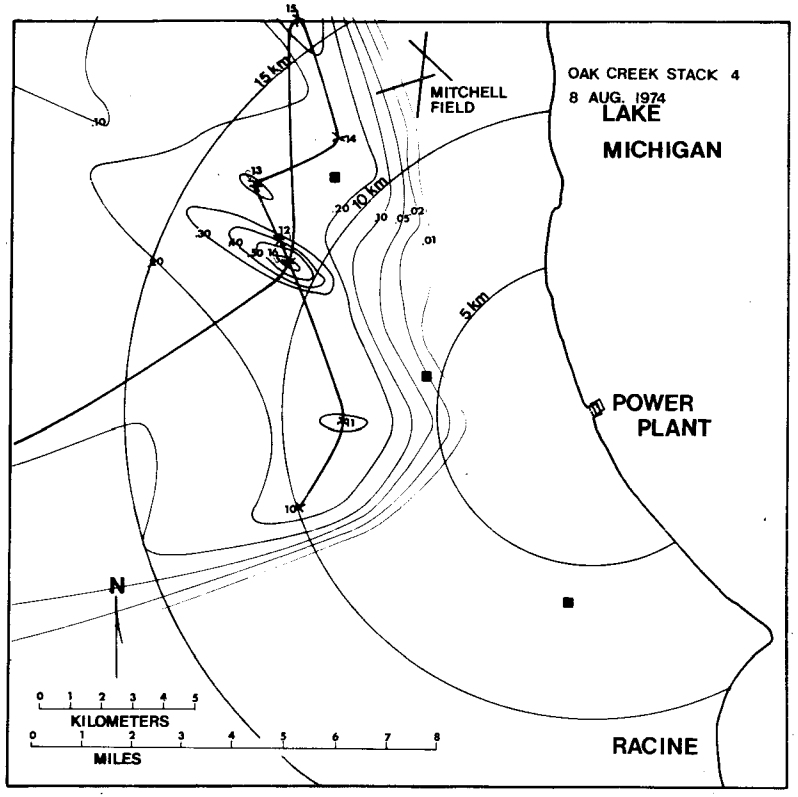

Figure 7-6. Same as Figure 7-5, but for OCPP Stack 4.

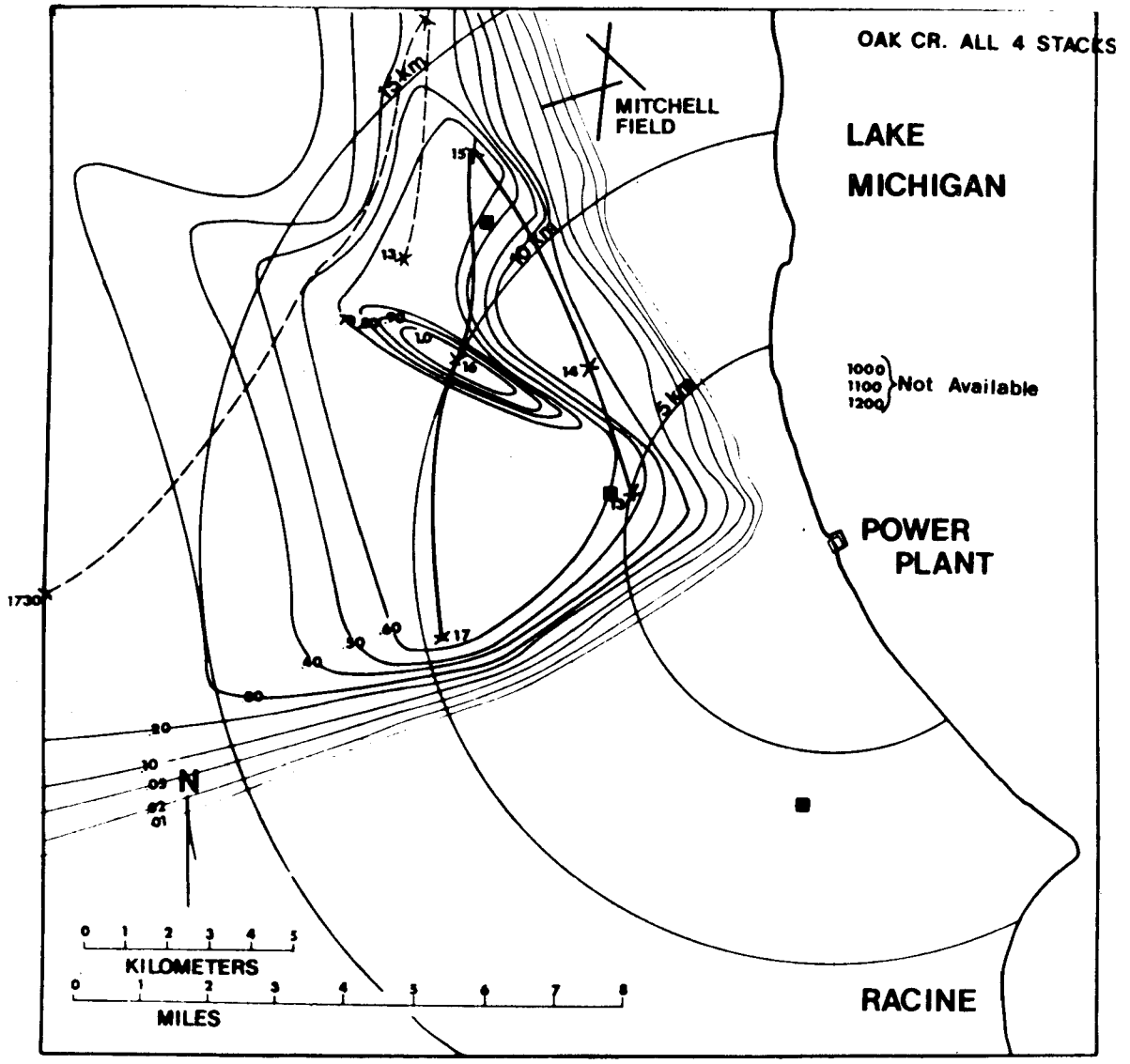

Figure 7-7. Time history of predicted surface SO_2 χG values for the sum of all four OCPP stacks, 1300-1730 CDT, 8 August 1974. Plume fumigation track is heavy line, and a secondary is shown as dashed.

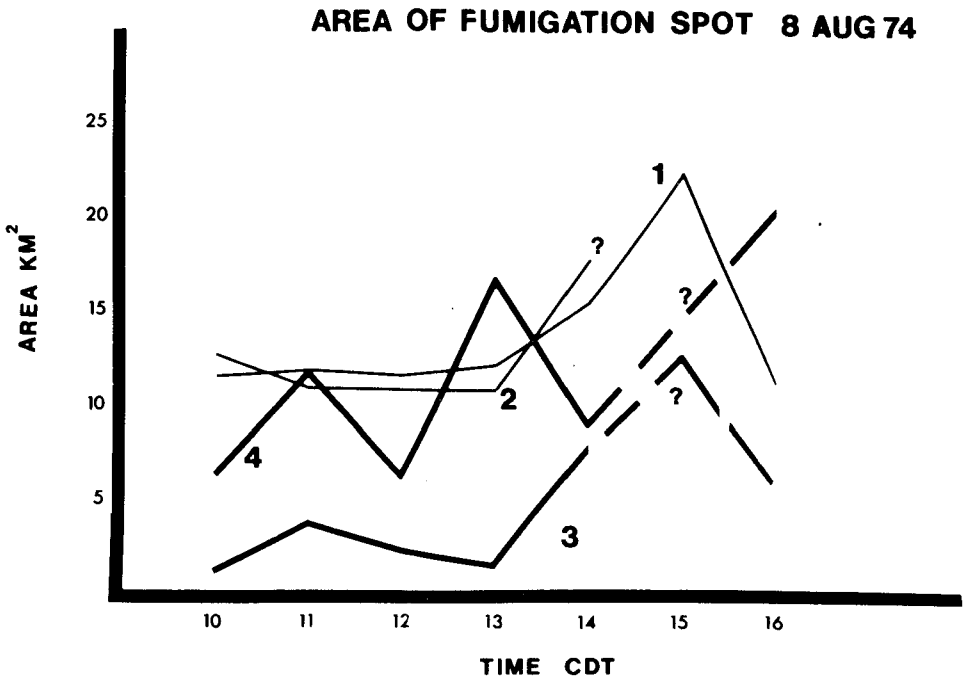

Figure 7-8. The areas of the individual fumigation spots on 8 August 1974. The areas of fumigation at 1500 CDT were not available because portions of the plumes were outside of the computational grid.

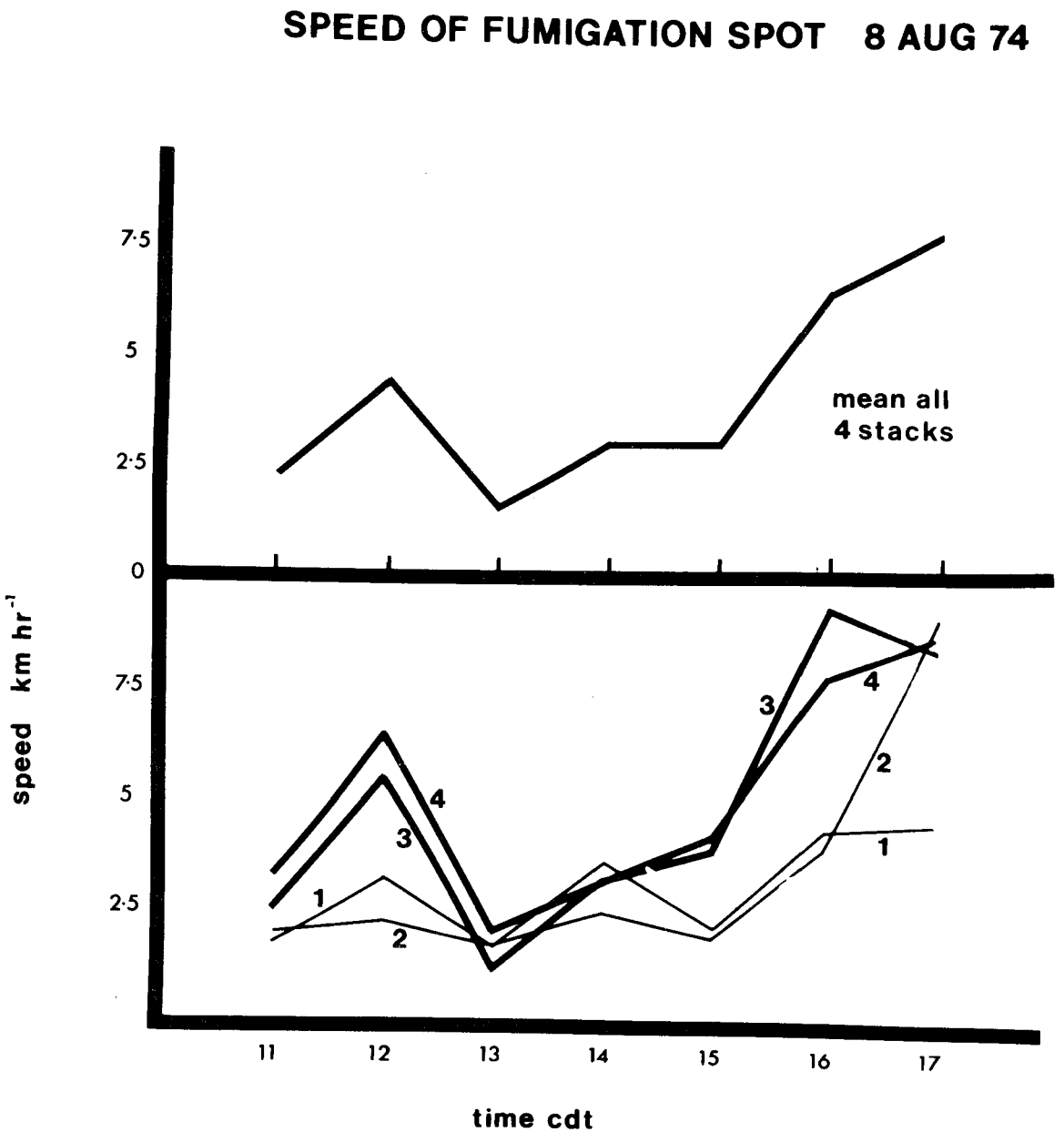

Figure 7-9. The speed at which the fumigation spots moved on 8 August 1974. The upper graph is the mean speed for all four plumes and the lower is for each individual plume.

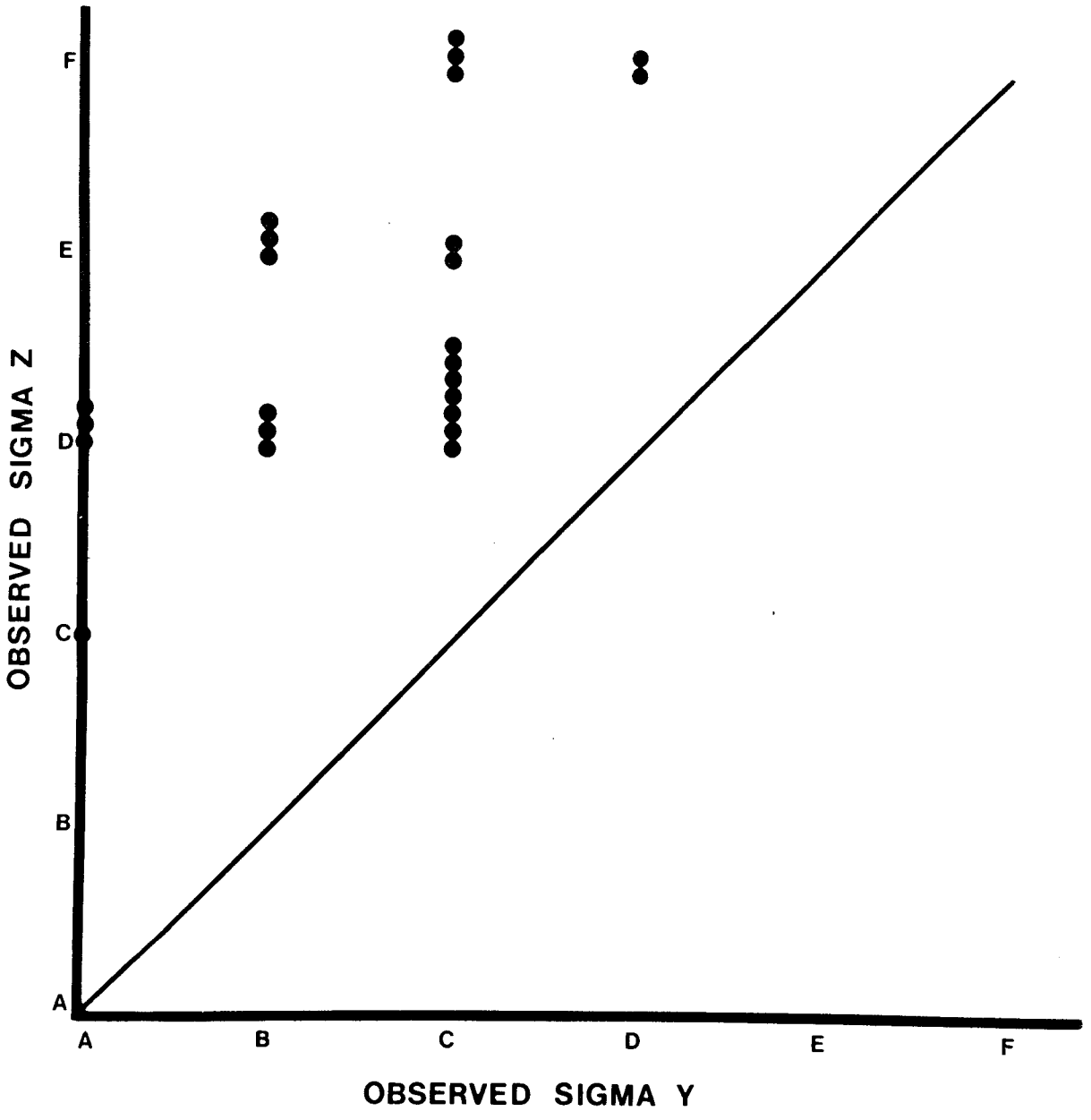

Figure 7-10. σ_z plotted as a function of σ_y. Note that if a model did not use split sigma then most of the observed values would have to fall along the diagonal line.

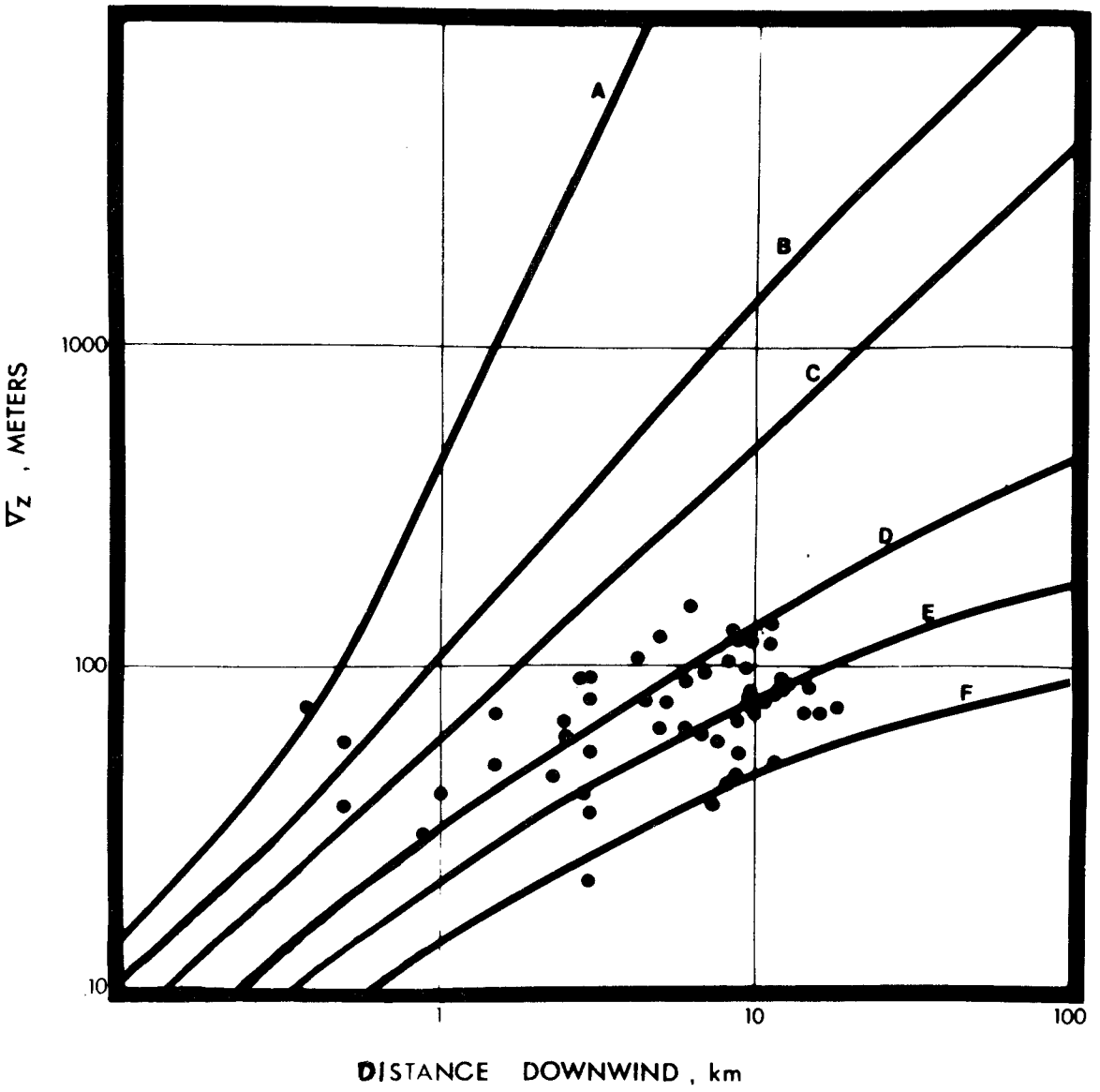

Figure 7-11. σ_z measurements made during the course of the 1974 summer field project.

SECTION 8

URBAN SCALE POLLUTION PATTERNS

EXTENSION FROM POINT TO REGIONAL MODELING

This report so far has discussed fumigation from single or multi-plume "point" sources. What happens when an entire urbanized area undergoes continuous fumigation? The GLUMP model was designed to simulate this phenomena. The mesometeorological data gathered on 28 June and 8 August 1974 were used in predicting SO_2 and suspended particulate patterns at the surface over Milwaukee County and environs for several selected hours. Only point source calculations are shown here (since the accuracy of the area source emission inventory available was questionable). In face, it is fairly certain that the 1970 emission inventory for point sources had become invalid by 1974 due to rather major changes in fuel combustion patterns in Milwaukee County in that time period. Thus no calibration of the model was attempted. The calculations are still useful of course for the manner in which they illustrate the deleterious effects of onshore flow in a heavily industrialized urban area. The complete model and results are described in Schuh (1975).

RESULTS

The urban model is essentially that described in Section 5 and used in Section 7, except that over 75 major point sources of

SO_2 and particulates were introduced. A 0.33 km horizontal grid spacing was used, resulting in a receptor grid 43 km in the x direction, 51 km in the y direction, and with 6 levels (118,422 receptor points). Except where noted, plume rise is computed using Briggs' equation based on hourly inputs of emission factors (when available), wind speed and direction from pibals, aircraft-measured TIBL profiles (Figure 8-1), wiresonde temperature profiles (for plume rise), etc. Pasquill-Gifford stability classes for each level above and below the TIBL, were those used in discussing the power plant plume fumigations.

Figure 8-2 shows the predicted (and uncalibrated) ground level concentrations of SO_2 for 1100 CDT, 28 June 1974. The top portion of the illustration are the predicted concentrations for essentially a plume (lid) trapping regime with the lid constant everywhere at 700 m. The bottom portion shows the fumigation regime values for identical conditions except the TIBL surface rising along curve b (Figure 8-1) to a final height of 700 m. In essence, this compares the difference between lid trapping and fumigation on a regional basis. Careful examination shows that the fumigation regime is indeed a more restrictive one in terms of surface air quality. Peak values for fumigation are noted in excess of 0.50 PPM. The typical CALCOMP concentration isopleth plots are somewhat difficult to use when attempting to visualize the overall pattern. Thus the GLUMP model output data are preferably presented as three-dimensional surfaces covering the same area as Figure 8-2 but viewed from above and to the southwest.

Figures 8-3 through 8-8 have all been smoothed to eliminate, among other things, "orifice errors", that is, extreme values resulting from a receptor grid being unusually close to a source.

Figure 8-3 is the exact same information as shown in Figure 8-2. It is clear that substantially higher surface SO_2 values should be expected during the fumigation episode as compared to lid trapping. Similar area averaged SO_2 levels were 0.018 vs. 0.009 PPM. That is to say, average SO_2 readings over Milwaukee County can be 100% higher during fumigation episodes (at least under this set of meteorological conditions). The suspended particulate computations (Figure 8-4) show a similar pattern. Fumigation peak values of 4552 $\mu gm/m^3$ are compared to 1362 $\mu gm/m^3$ for lid trapping. Areal averages show fumigation levels from point source emissions 30% above those for lid trapping.

Figures 8-5 and 8-6 show much the same for 1600 CDT, 8 August 1974, when the final depth of the TIBL was deeper (almost 1000 m). For SO_2, peak surface values for fumigation were 31% higher than for lid trapping, and areal average concentrations were 42% higher. It should be noted that during "fumigation episodes" not all sources, especially low-level ones, actually experience fumigation. They do, however, diffuse within very limited and slowly increasing mixing depths for the first 10 to 20 km of inland drift.

Figure 8-7 and 8-8 are for 8 August 1974, but for 1730 CDT, when increasing high cloudiness causes a rapid reduction in TIBL depth to a maximum of less than 400 m (there was also a sharp

drop-off in wind speed and a shift to more northeasterly direction). For SO_2, peak values for fumigation were actually less than for lid trapping. This is partly an artifact of the plume rise computational scheme which caused several large power plant plumes to remain entirely aloft. But the areal average for fumigation was a full 144% above that for lid trapping. Areal averages of particulates (Figure 8-8) were 41% greater for the fumigation case.

Thus it appears that, for short-term or "worst case" episodes, continuous fumigation from both isolated sources and for entire urban areas must be considered a major concern in any potential violation of standards. The regional computations also show that the lake effects of fumigation are insignificant beyond about 20 km under most circumstances (note, major differences in concentrations are most pronounced near the shoreline).

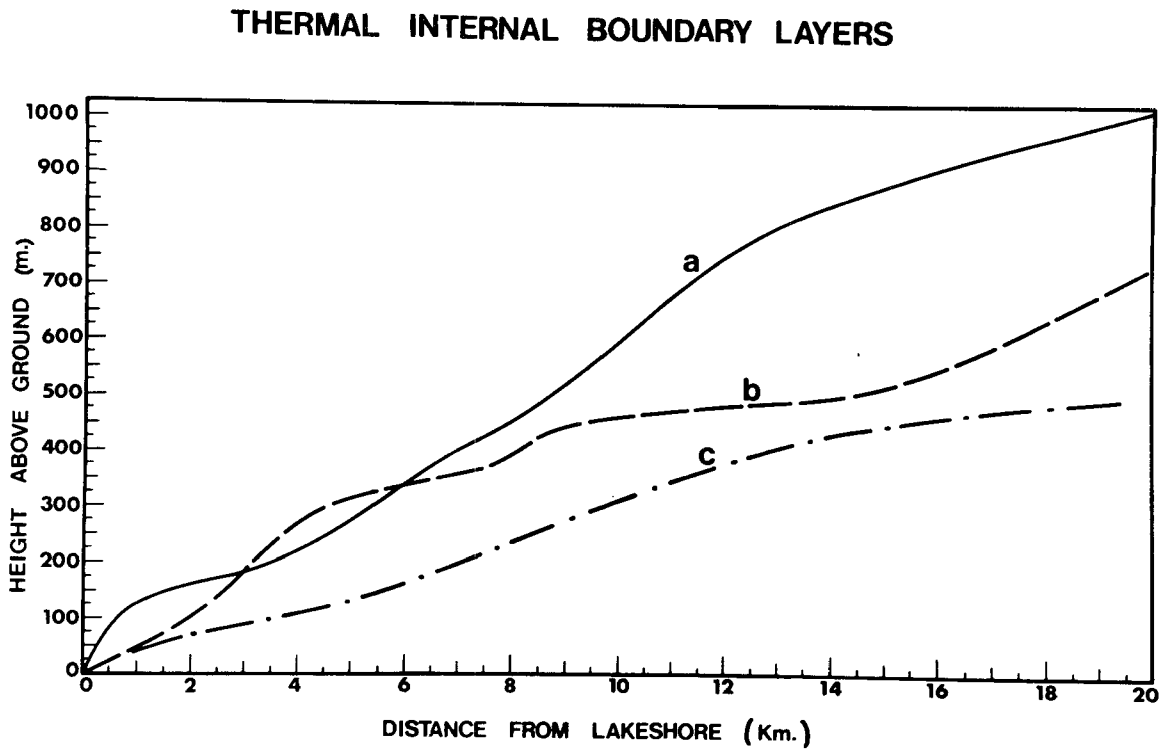

Figure 8-1. Three TIBL tops used in regional computations. (a) 1600 CDT, 8 August 1974, (b) 1100 CDT, 28 June 1974, and (c) 1730 CDT, 8 August 1974.

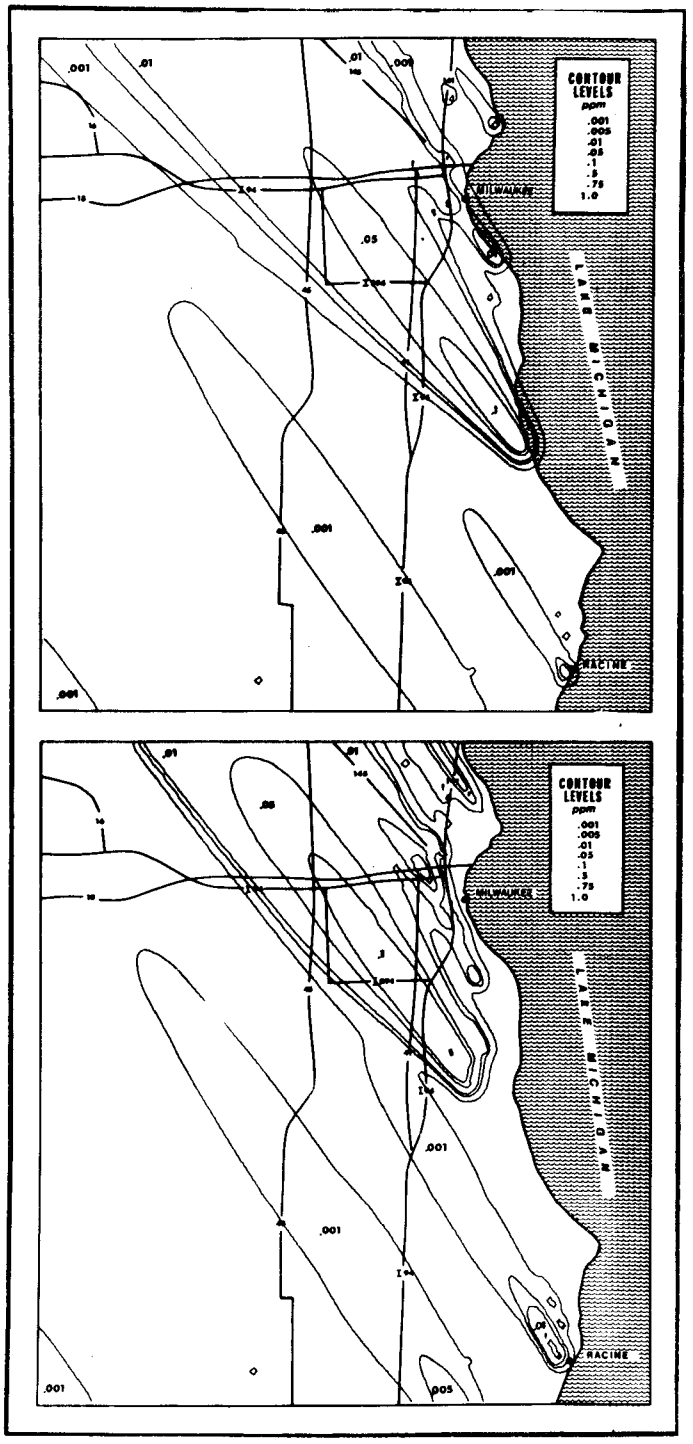

Figure 8-2. CALCOMP contour plots of uncalibrated GLUMP model surface SO_2 concentrations for 1100 CDT, 28 June 1974 for a uniform 700 m deep mixing layer (top) or for a variable depth TIBL (bottom) yielding fumigation.

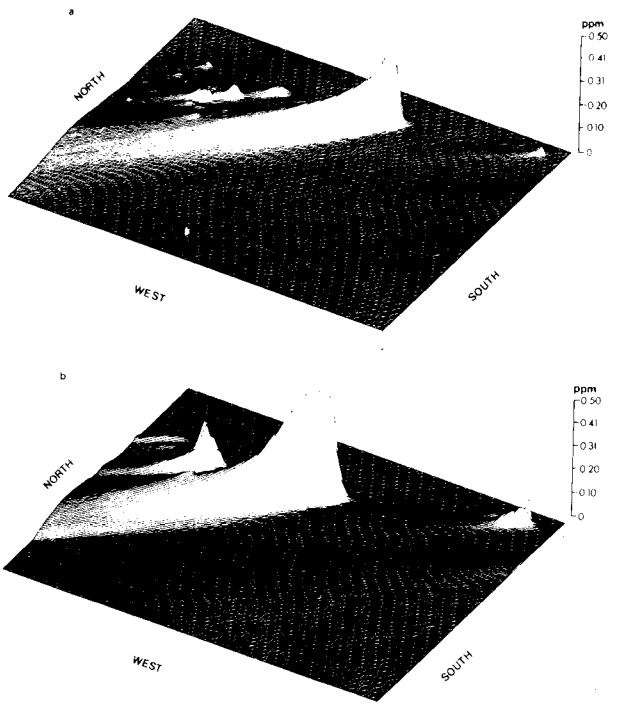

Figure 8-3. Three-dimensional surface of SO_2 concentrations predicted by GLUMP model for Milwaukee County with (top) a uniform 700 m lid, and (bottom) fumigation according to conditions of 1100 CDT, 28 June 1974.

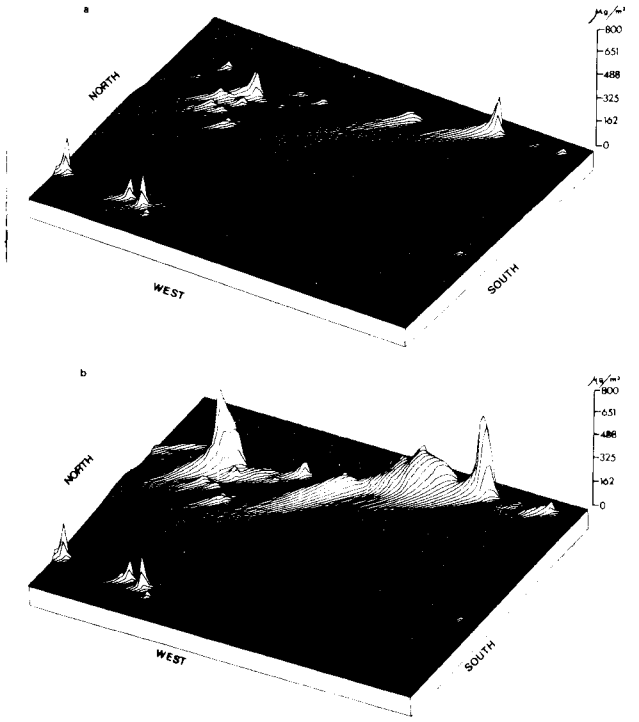

Figure 8-4. Same as Figure 8-3, except for suspended particulates.

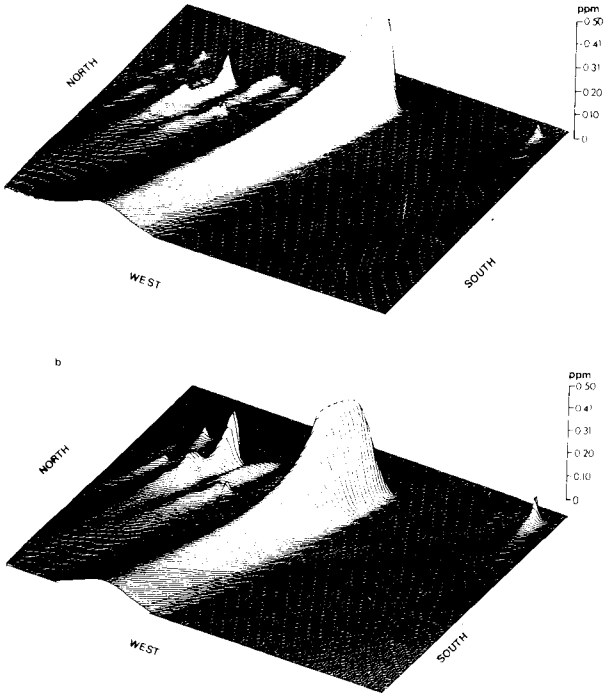

Figure 8-5. Three-dimensional surface of SO_2 concentrations predicted by GLUMP model for Milwaukee County with (top) a uniform lid of 1000 m, and (bottom) fumigation according to conditions at 1600 CDT, 8 August 1974.

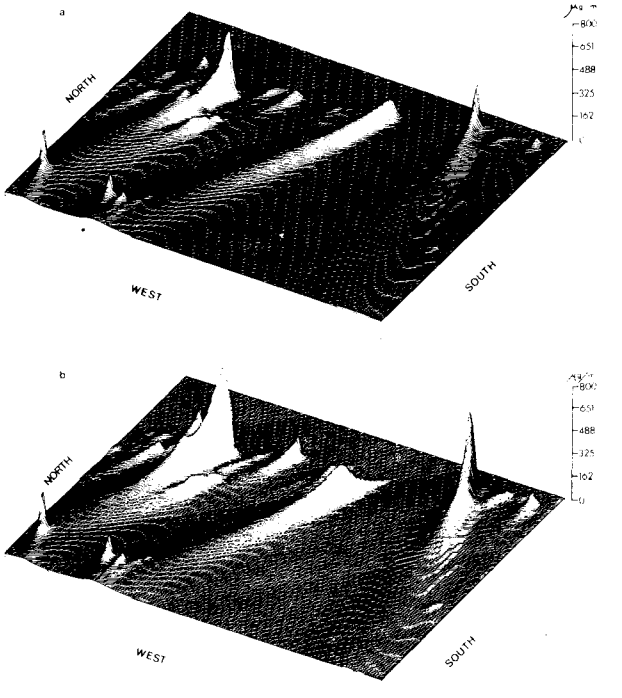

Figure 8-6. Same as Figure 8-5,except for suspended particulates.

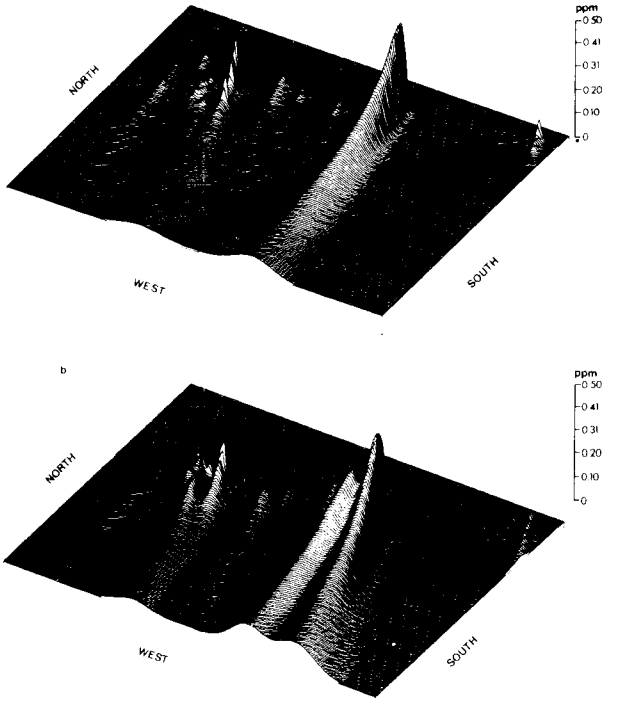

Figure 8-7. Same as Figure 8-5, but for (top) 400 m lid, and (bottom) fumigation according to condition at 1730 CDT, 8 August 1974.

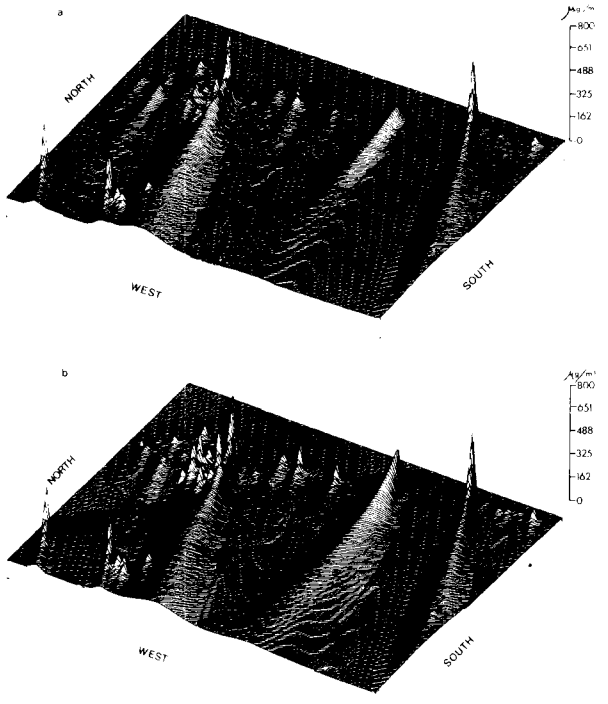

Figure 8-8. Same as Figure 8-7, except for suspended particulates.

SECTION 9

ACOUSTIC SOUNDER DERIVED MIXING DEPTHS

COASTAL CLIMATOLOGY

The vast amount of meteorological data collected in this country serves the needs of aviation and National Weather Service numerical forecast models. Air pollution meteorologists, when in need of climatological data have had two choices: make do with existing networks, or install their own sensors and wait a considerable amount of time. When attempting to define aeral distributions of mean mixing depths for instance, the synoptic radiosonde network is all that is available to use (Holzworth, 1972). It is known that the numbers derived are highly unrepresentative of mountainous regions, cities, and of course coastal zones. Not only are temperature regimes very spatially variable on the mesoscale, but frequent mesoscale wind flows (urban heat islands, mountain/valley winds, land/sea breezes) require vertical wind profile climatologies. EMSU special radiosonde stations have only slightly filled the void. Since radiosonde technology is highly expensive in terms of both equipment and manpower, remote sensing technology seems more likely to yield mesoscale time-continuous data in a cost effective manner. Vertical wind measurements via laser or acoustic doppler anemometry will be feasible in the near future. At this time, continuous estimates of mixing depths using

lidars and acoustic sounders are now quite routine, especially the latter. The installation of an acoustic sounder along the western shore of Lake Michigan by UWM in 1974 gave rise to the acquisition of data for a "climatological" study of mixing depths near a large lake during various synoptic regimes. A complete survey of the field of acoustic sounding technology can be found in Hall (1972), and Thompson (1975), among others.

An example of the complex thermal regimes found in the Lake Michigan coastal zone was acquired at Waukegan, Illinois during a five-day period of sustained onshore stable flow. Figure 9-1 shows analyses of wiresonde vertical temperature profiles at the shoreline and at 3 km inland on one of the days. An intense elevated inversion was present at the shoreline power plant. The shallow surface based neutral layer was due to the air's passage over a narrow rim of warm water just offshore. By the time the air traveled 3 km inland, the inversion had partially burned off, but as afternoon onshore flow increased, the capping inversion could still be found. Figure 9-2, using data taken on the prior day when conditions were very similar, shows how these complex lake-induced thermal patterns can lead to potential errors in diffusion estimates. If one were to use the table presented in Turner (1969) to convert surface data into P-G stability classes at Milwaukee airports some 6 and 16 km inland, one sees highly unstable A, B, and C conditions suggested. Yet a quick analysis of wiresonde vertical temperature lapse rates converted into P-6 equivalent classes (Pendergast and Crawford, 1974) at the shoreline and 3 km

inland reveals that while indeed the immediate surface layer may be remodified, intensely stable layers remain aloft. Thus the use of surface data to infer dispersion conditions at the altitudes of elevated plumes under the influence of lake effects is highly questionable at best. An acoustic sounder, while not providing quantitative data (in the configuration used) allows one to monitor continuously the approximate depth of the mixed layer at any given point at relatively little cost.

THE ACOUSTIC SOUNDER

The AeroVironment Model 300 acoustic sounder was operated at ground level some 3 km inland at Waukegan and atop a 15 m high building in Milwaukee about 1 km inland. The sounder, which had an input power of 35 watts, transmitted typically at 100 microsecond pulses at 1600 Hz, and was enclosed within an 8 ft high plywood/lead sound baffle lined with convoluted urethane. The data were recorded on facsimile type paper with 15 cm vertical scale (either 500 or 1000 m mode) at the rate of 32 mm per hour, and were cut into 24-hour (Midnight to Midnight local time) strips. Since the sounder operated in a monostatic mode, the signal return was generated only by temperature fluctuations on the order of half the wavelength, typically 20 cm.

With some experience, and especially with the vast amount of ancillary data available, it became quite straight forward to interpret the traces obtained. Figure 9-3a is a trace taken at Milwaukee, 13 July 1974, on a day with brisk offshore southwest winds and strong sunshine. The nocturnal radiation inversion,

approximately 200 m deep, was plainly visible and began burning off by 0700 CDT, and the top of the mixed layer went above the 500 m full-scale by 1100 CDT. The vertical streak lines visible (though poorly in reproduction) mark the characteristic signature of thermal convective plumes rising from the surface superadiabatic layer. Vector-vane σ_θ values suggested surface P-G classes B and C during the bulk of the daylight hours.

Figure 9-3b was taken under very different conditions, namely stable onshore flow of fog on 6 May 1975. The echo returns appear to represent the top of the fog layer where turbulent interactions are taking place. Heating during the day caused the layer to expand from 300 m to 400 m around noon only to return to its original depth by evening. Figure 9-3c, taken 24 June 1974 at 3 km, occurred during stable onshore flow, but clear skies. This was the first of five consecutive days of continuous stable northeast flow. Though the sunshine was strong, remodification of the lake air was sufficiently slow so that a mixing depth of more than 500 m was never attained at this site throughout the entire period. Vector vane σ_θ readings, even during mid-day suggested no better than P-G class D at its most unstable. Apparently the extremely limited vertical depth of the mixed layer prevented the development of vertical convective plumes, thus limiting the energy of turbulent wind fluctuations in the surface layer. This was noted many times throughout the summer. Thus a sounder, especially within 10 km of the shoreline, can be used to monitor the upper limit to which near surface effluents can mix at a given point, which is also the time profile of the top of the TIBL. Rapid changes in mixing depth

with the onset of lake breezes will of course also be noted (Figure 9-3d). On 17 June 1974, weak southwest flow prevailed during the day and the mixing depth rose above 1000 m by early afternoon. But a late-onsetting lake breeze front passed the sounder at 1715 CDT. The frontal slope as well as mixing depths reduced to about 400 m are evident.

A CLIMATOLOGY OF MIXING DEPTHS

As discussed by Rizzo (1975), it is possible to use a sounder to compile a climatology of shoreline mixing depths. During the period 2 July - 15 September 1974, 1618 hours of mixing depth heights were extracted from the sounder traces (at the 1 km inland Milwaukee site). Wind directions and speeds were available from the co-located vector vane and cloud cover conditions were noted from the nearby Milwaukee NWS station, as well as logs and photographs.

Thus for each hour, Rizzo cataloged apparent sounder-derived mixing depths (when an echo present), wind direction, cloud cover (clear, scattered, broken, or overcast) and time after surface or sunset. On those afternoons when the mixing depth exceeded sounder range (500 m) or the returns were too weak or diffuse to allow assigning a specific value, a mixing depth was assumed if the flow was offshore. Figure 9-4 includes a curve of mixing depths rising to Holzworth's published mean summer afternoon maximum depth for clear or scattered clouds (1200 m). For days with broken or overcast conditions, 1000 m was assumed to be the maximum depth.

Figure 9-4 then is a graph of the measured (and partially assumed) hourly mixing depth heights for offshore flow during clear or scattered cloud conditions plotted in terms of hours after sunrise and hours after sunset. It is rather as one expects to find. The contrast with Figure 9-5, the measured mixing depths during stable onshore flow (clear and scattered) is notable indeed. In addition to the mixing depths or base of the elevated inversion being generally in the 175-250m range,there is virtually no diurnal fluctuation. The same pattern holds forth during broken and cloudy onshore flow. Thus it can be said that during stable onshore flow, at any given point, it remains "nighttime" for as long as the condition persists, with mixing depths severely limited and changing only slowly over time.

A mixing depth wind rose (Figure 9-6) was prepared which shows, as expected, that night values are lower than day values for viatually all directions during clear and scattered cloud conditions. More importantly is the directional dependence of daytime mixing depths between onshore and offshore flow (with a lesser but detectable nocturnal analog). Mean daytime (clear and scattered) mixing depths (for all hours, not just maximum) for southwest flow is 656 m as opposed to 240 m for northeast flow (a factor of 2.73 times greater). During the peak hours of afternoon heating, it is likely the difference becomes a factor of 5 or more. It should be noted that the UWM campus is on a small peninsula and both due north and south winds have considerable over water fetch.

During this period the mean mixing depth over Milwaukee at

1 km inland for all hours and all wind and sky conditions was 300 m. For daytime offshore flow it averaged 480 m compared to 240 m for onshore. Thus any regional dispersion model based on radiosonde derived mixing depths (which is devoid of any lake suppressive effects) would likely underestimate mixing depths at this point by a factor of two, and all other factors aside, underestimate pollution concentrations from local sources by the same factor. It must be pointed out that these data are only valid for this exact point due to the extreme variability of lake effects upon TIBL height. However, the sounder has proven itself highly useful and it would appear that a network of several sounders in a line normal to the shoreline in perhaps two seasons would provide an adequate estimate of lake suppression of mixing depths on both a day-by-day as well as seasonal basis.

There is of course an overiding question as to whether or not the structures seen on the sounder trace do in fact properly define the top of the mixed layer. Schubert (1975) suggests that sounders tend to yield estimates less than those of conventional temperature sounding techniques (although that is not to imply the data are not more accurate). On several occasions when the UITS-equipped Cessna 182 flew nearby the sounder, a comparison was run between the $\varepsilon^{1/3}$ and the sounder patterns (Figure 9-7). On a section of the 4 September 1974 trace, a shallow but intense nocturnal inversion layer was present below 100 m. Turbulent fluctuations caused by mechanical eddies were sufficient to cause a strong sounder return. Sections of the

$\varepsilon^{1/3}$ trace as the airplane flew at different levels from the shoreline inland are superimposed. The 0800 CDT data shows that above the inversion the air was virtually smooth ($\varepsilon^{1/3}$ less than 0.3 $cm^{2/3}sec^{-1}$) due to the lack of both convective and mechanical turbulence. By 0915 CDT, just before the onset of a lake breeze, heating had allowed the mixed layer to grow over 500 m. Values of $\varepsilon^{1/3}$ were almost everywhere above 1.0 $cm^{2/3}sec^{-1}$. Other studies show that the intensity of the sounder return is fairly well correlated, thus linking the aircraft derived TIBL profiles to the sounder estimated mixing depths. Figure 9-8, from mid-afternoon, 16 July 1974, clearly shows the top of the sounder return separates the surface layers with $\varepsilon^{1/3}$ values above 1.0 $cm^{2/3}sec^{-1}$ from the layer aloft with $\varepsilon^{1/3}$ less than 0.3 $cm^{2/3}sec^{-1}$.

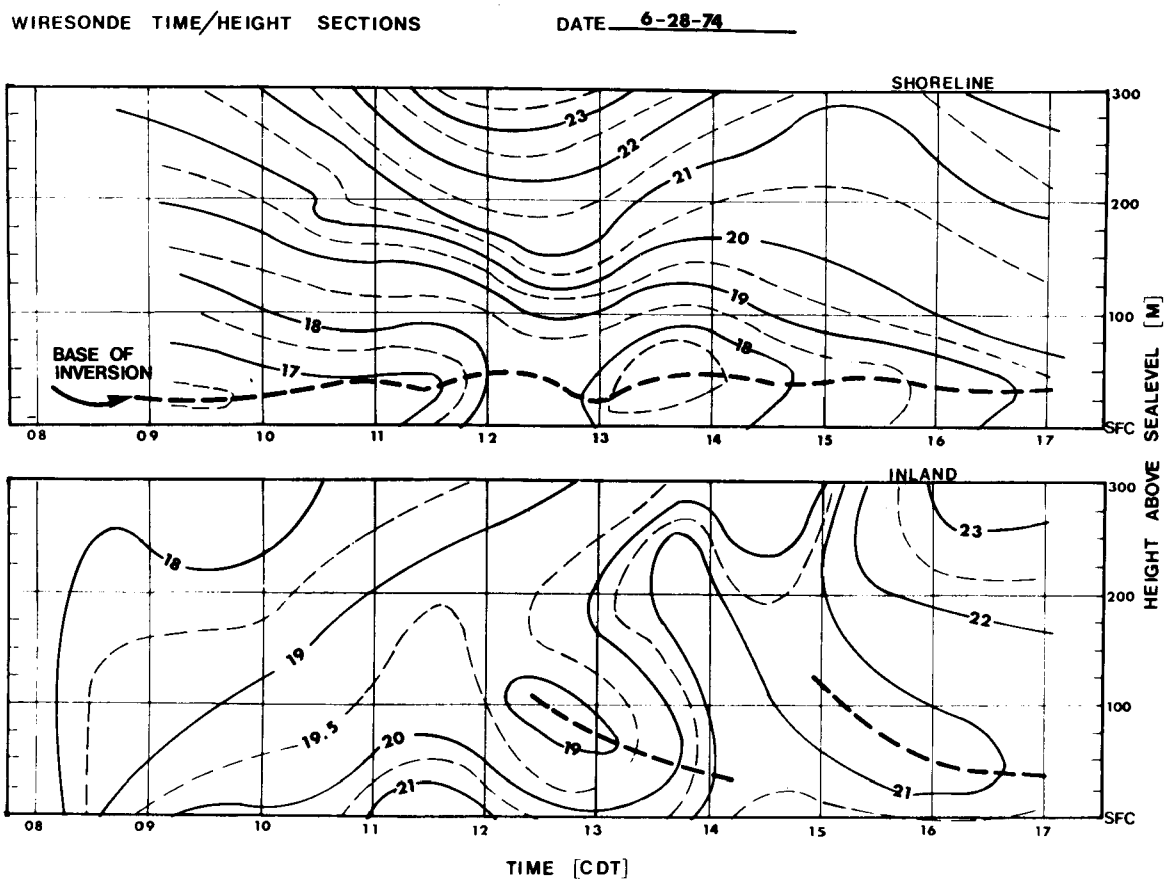

Figure 9-1. Temperature cross sections for 28 June 1974 at Waukegan Power Plant (top) and 3 km inland (bottom) by smoothing plots of hourly wiresonde runs. (Isotherms every 0.5 °C. Heavy line indicates base of elevated inversions.)

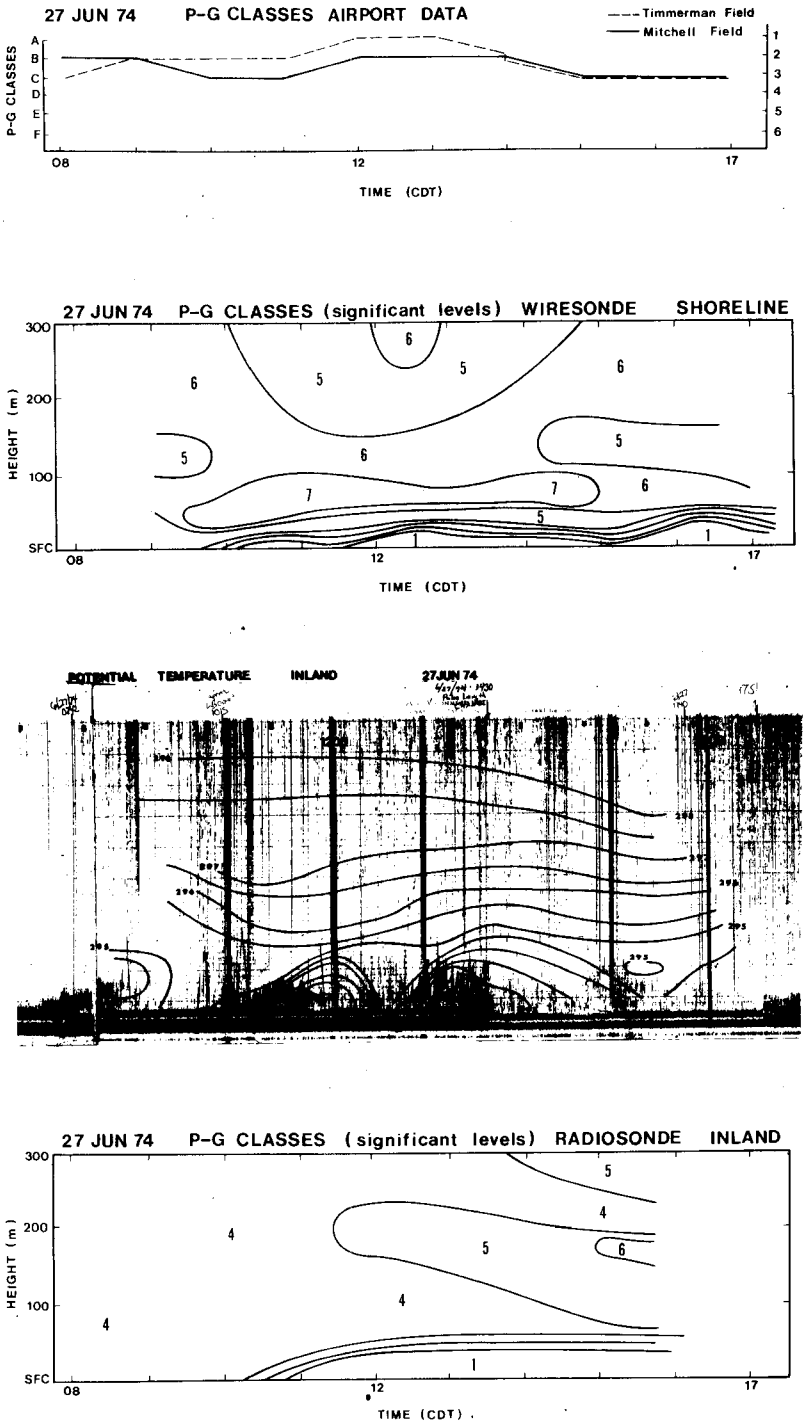

Figure 9-2. Measurements of shoreline meteorological conditions made 27 June 1974.

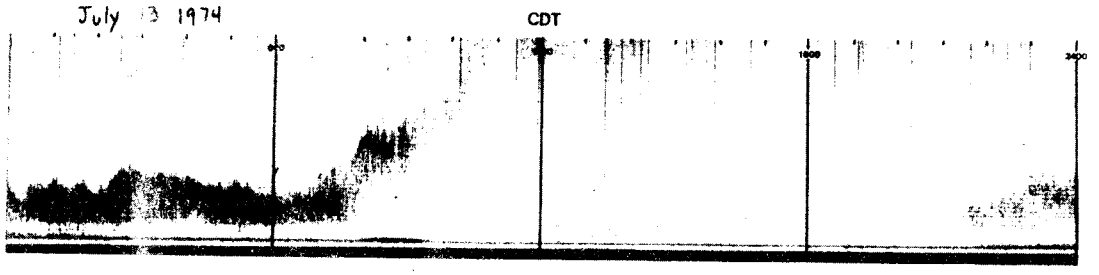

Figure 9-3a. Acoustic sounder trace, Milwaukee, 13 July 1974.

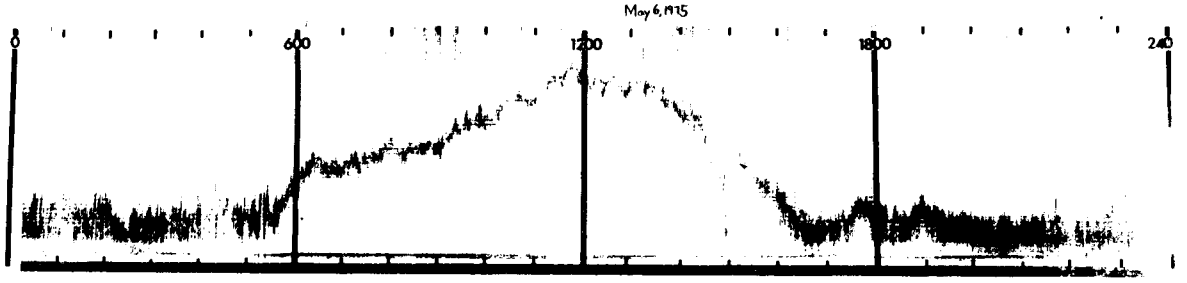

Figure 9-3b. Acoustic sounder trace, 6 May 1975.

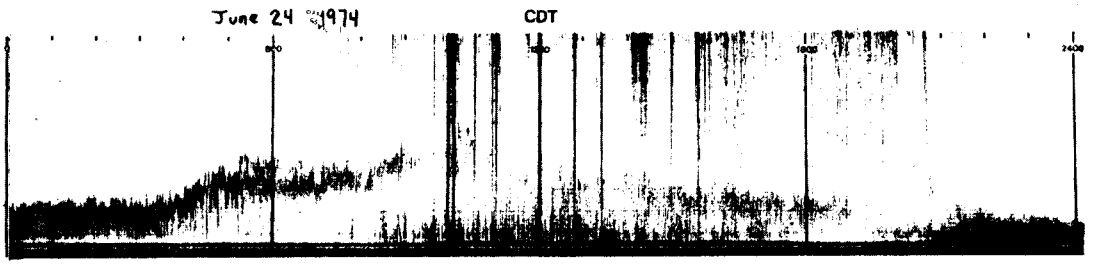

Figure 9-3c. Acoustic sounder trace, Waukegan, 24 June 1974.

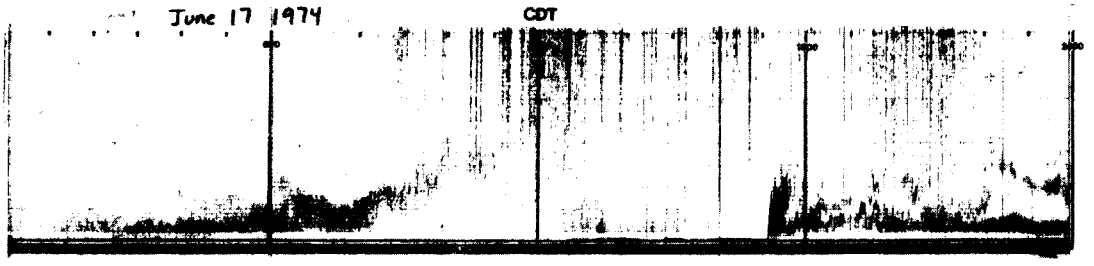

Figure 9-3d. Acoustic sounder trace, Waukegan, 17 June 1974.

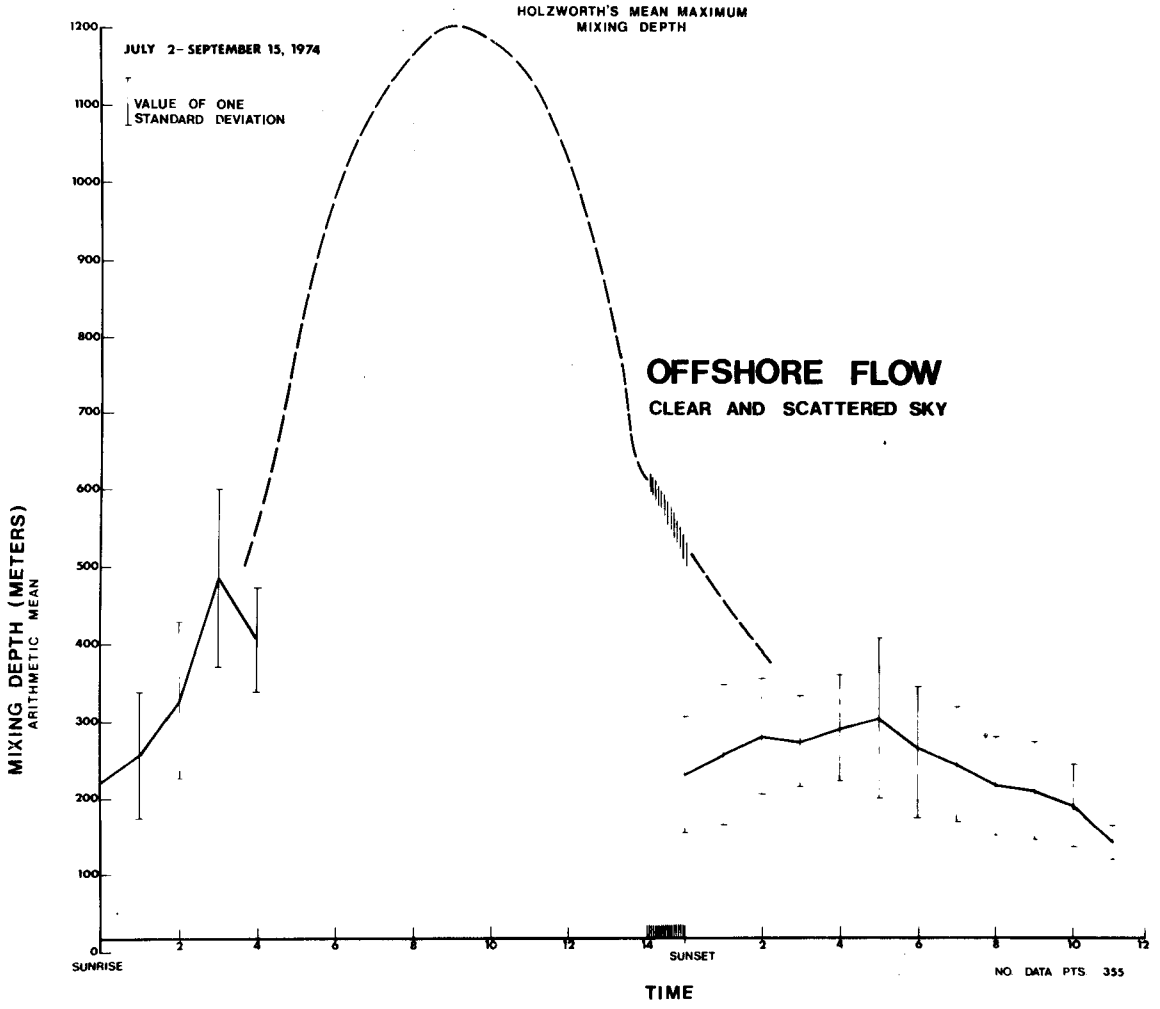

Figure 9-4. Mixing depth vs. time (offshore flow, clear and scattered sky).

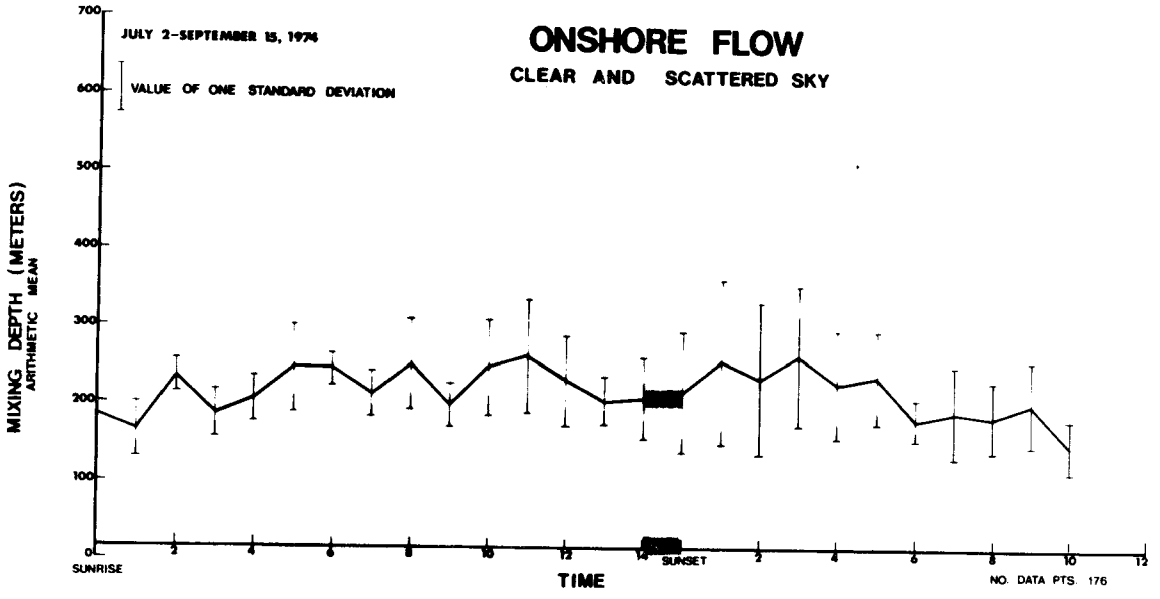

Figure 9-5. Mixing depth vs. time (onshore flow, clear and scattered sky).

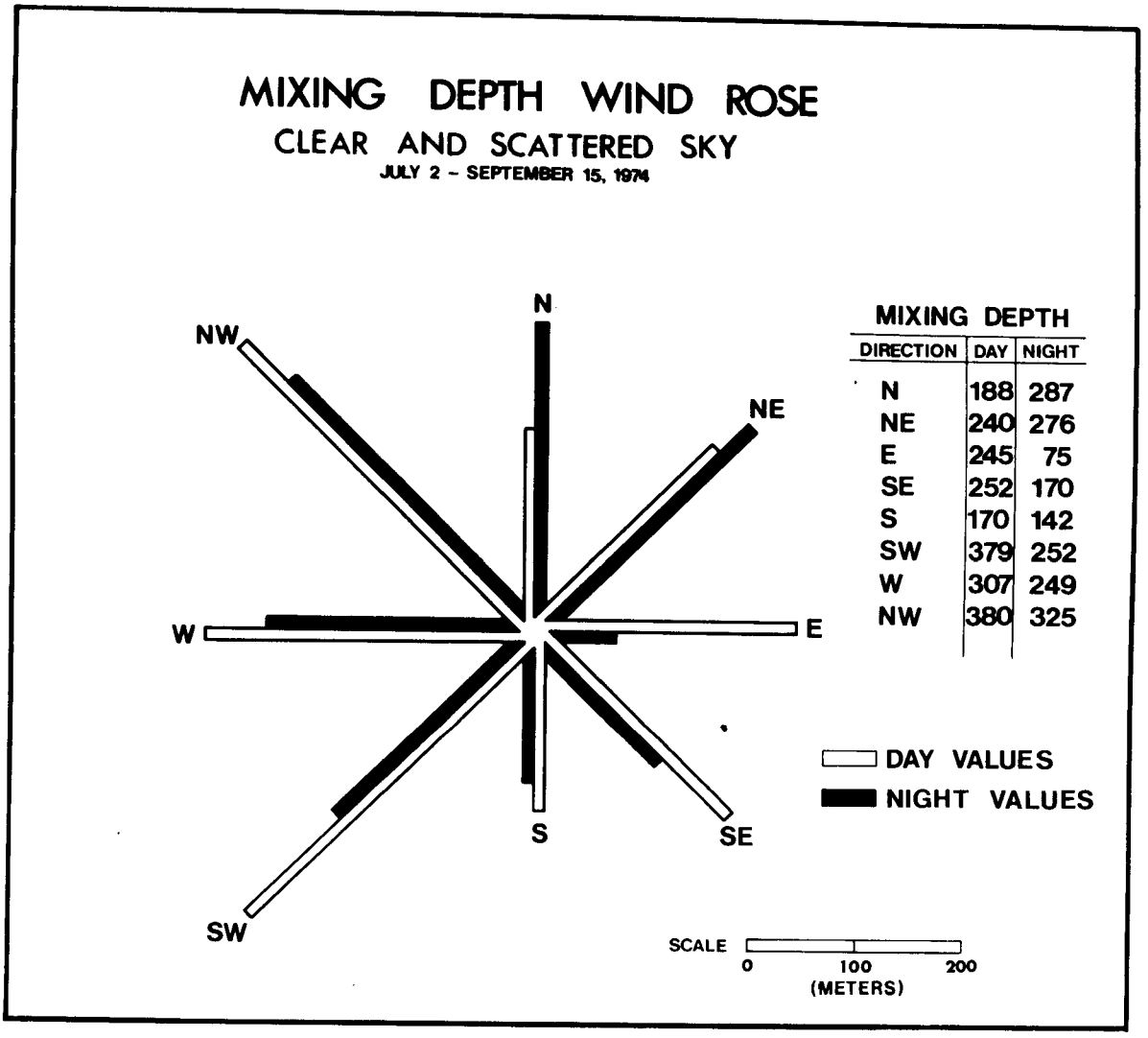

Figure 9-6. Mixing depth wind rose with adjusted data (clear and scattered sky).

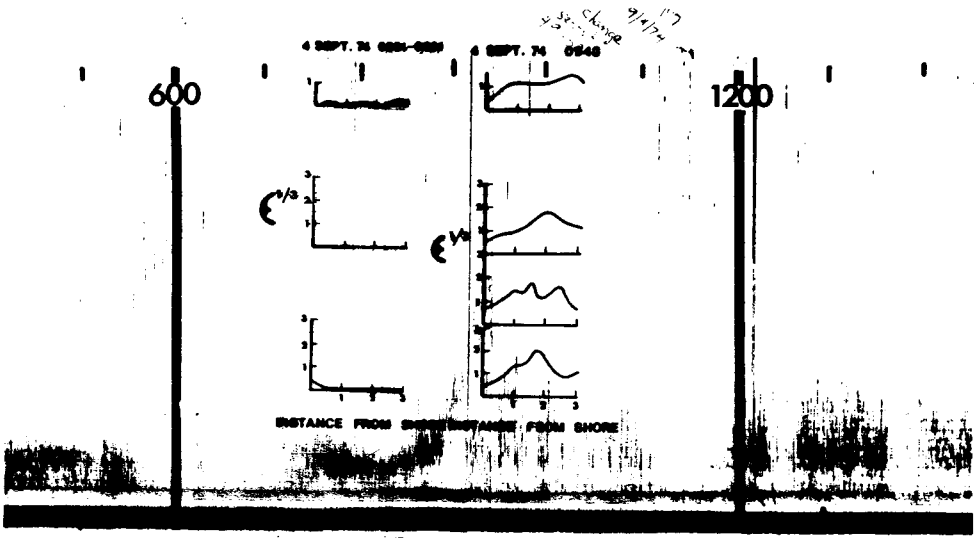

Figure 9-7. Acoustic sounder trace with turbulence data (September 4, 1974).

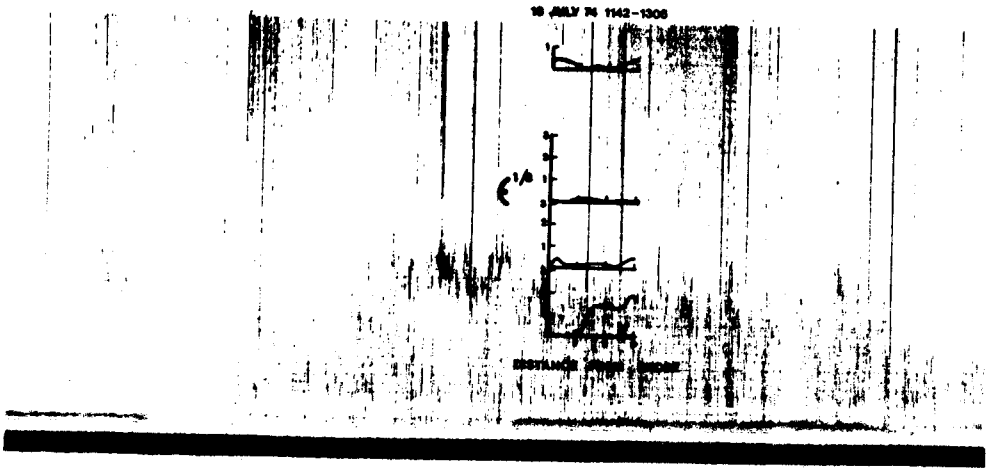

Figure 9-8. Acoustic sounder trace with turbulence data (16 July 1974).

SECTION 10

LAKE BREEZE STRUCTURE

GENERAL COMMENTS

Since, by meteorological standards, the lake/sea breeze is comparatively easy to observe and has aspects appealing to numerical modelers, there has developed an extensive literature on the subject. Baralt and Brown (1965) and Jehn (1973) have indexed literally hundreds of articles. Upon considering the basic nature of these dirunal mesoscale flows, it is obvious they would have a profound effect upon both air pollution dispersion and transport. Figure 10-1 shows a schematic of an idealized land breeze cell, collecting urban pollutants in its offshore flow, some of which rises in the offshore convergence zone into the return layer aloft, then partially returning into the urban area. The sea or lake breeze (which are dynamically equivalent and often of comparable strength on the Great Lakes) would act in reverse, only this circulation is characteristically more vigorous (Figure 10-2). Urbanized shoreline areas during daytime may appear to experience adequate ventilation, yet the combination of partial recirculation of pollutants as well as restricted mixing depths could cause locally serious air pollution potentials.

It was not however until the mid-1960's that the air quality aspects of shoreline mesoscale regimes began to be appreciated. Lyons and Olsson (1972) were among the first to illustrate how the complex wind and thermal patterns dramatically and consistently effect shoreline air quality.

Numerical models of the sea breeze began very modestly indeed with studies such as that of Haurwitz (1947). As computational power increased they advanced in complexity (Pearce, 1955), and finally with Estoque (1961, 1962) began to achieve a certain resemblance to reality, including showing the effects of environmental winds upon the locally developed circulation. Moroz (1967) extended Estoque's model to the Great Lakes. McPherson (1970) was able to make many improvements, including the inclusion of shoreline irregularities in his model of the Texas coast sea breeze. The model of Neumann and Mahrer (1971, 1975) allowed the prediction of surface pressure fields after the abandonment of the hydrostatic approximation. Pielke (1974a, 1974b) simulated in three dimensions the sea breeze of the Florida peninsula, and its convection patterns, with an eight-level primitive equation model, and a detailed boundary layer parameterization scheme. The 11 km grid used, while less than in many preceeding models, and adequate for his purposes, also resulted in much of the detail of the circulation being masked. Typically, most models underestimate vertical motions in the convergence zone by a factor of two to an order of magnitude or more. Some of the strongest lake breeze frontal motions computed were in the model of Sheih and Moroz (1975) which found upward of 95 cm/sec. Numerical models to date have not been configured to provide three-dimensional trajectories of air motion, which of course is the relevant parameter for air pollution studies. The model now under development by Dieterle and Tingle (1976) at Brookhaven appears to be the first to have this capability.

Observational studies of sea/lake breezes, while numerous, were rarely of sufficeint scope to provide adequate data to allow verification of models being developed. The study of Fischer (1960) on the New England coast was perhaps the earliest major program. The Texas coast (Hsu, 1969), the eastern shore of Lake Michigan (Olsson, et al., 1968) and the Chicago area (Lyons and Olsson, 1973) said major field programs, however, even these collected only fragmentary information relevant for modeling purposes. Figure 10-3 is a summary of literature reports regarding the structure of well developed lake (sea) breezes. Keen (1976) discusses these in great detail.

The land breeze is even more limited in terms of numerical modeling and relevant complimentary observational programs. What is known about the nocturnal analog of the lake/sea breeze is summarized in Figure 10-4 (also taken from Keen, 1976). Reports by Olsson et al. (1969) on the eastern Lake Michigan shore, Feit (1969) on the Texas coast, and radar observations by Meyer (1971) along the Atlantic coast) are among the more complete studies. In general numerical models have been plagued by difficulties in parameterizing the nocturnal boundary layer, which has led to generally unsatisfactory results.

The bottom line is that models, while clearly becoming increasingly better able to simulate the real atmosphere, are not yet of sufficient precision and versatility to allow direct applications to mesoscale air pollution transport problems. Observational programs, costly and difficult to manage, have generally

failed to provide sufficient verification of models, although improvements continue here also.

The lake breeze observations made on the western shore of Lake Michigan in 1974 were useful inasmuch as they confirmed many of the findings of Lyons and Olsson (1973) in Chicago, but more importantly provided raw data for an attempt at a purely kinematical approach to estimating air pollution transport within complex three-dimensional time dependent coastal flows. The basic observational results are summarized below, after Keen (1976).

THE LAKE BREEZE OF 4 SEPTEMBER 1974

By far the best lake breeze studied during the rather poor summer season of 1974 occurred on 4 September. In many ways it resembled that discussed by Lyons and Olsson (1973) and provides for some interesting comparisons.

A large unseasonably cold cP high pressure system drifted south of Lake Michigan on 4 September 1974 (Figure 10-5 shows the noon synoptic chart and SMS-1 visible satellite). The pressure gradient over the southern basin of the lake that day never exceeded 1.2 mb/200 km. Clear skies and light winds produced an intense nocturnal radiation inversion. Surface low temperatures at dawn set numerous records (2 °C to 7 °C). The development of intense lake breezes after unusually cool nites, contrary to what might be expected, is often quite common. It appears these air masses are thermally unstable in the lowest layers which aids the development of intense upward convective heat transport over land during the day. Figure 10-6 shows lake surface water temperatures

increasing from 10 °C on the western shore to 21 °C on the eastern shore. Also shown are the 0600 CDT surface observations. A shallow but well defined land breeze was present along the entire shoreline, persisting for two to three hours after sunrise. Visual observations of the Milwaukee urban smoke dome combined with the acoustic sounder trace (Figure 10-7) suggested the top of this inversion (and perhaps the land breeze inflow) to be about 100 m. Peak offshore wind speeds were about 2.3 m/sec. Aircraft observations above this layer found the air to be non-turbulent ($\varepsilon^{1/3}$ less than 0.3 $cm^{2/3}sec^{-1}$), with extremely low aerosol concentrations. Figure 10-8 shows a plume from a fertilizer plant in a rural area south of Milwaukee draining into the lake in the waning moments of the land breeze (about 0830 CDT). Vector vane σ_θ observations suggested P-G stability classes D and E existed even in the urban area within the land breeze outflow before dawn (0620 CDT). The plume from the OCPP, visible to the south in Figure 10-8, was nearly vertically into a small cumulus of its own making base about 800 m, with the effluent then drifting generally northward.

The sounder trace, as well as the smoke photographs, revealed that convective plumes began to develop over land about 0830 CDT. The aircraft first detected a developing lake breeze wind shift zone by the appearance of white caps about 3 km offshore at 0850 CDT. By 0945 CDT, the front began moving rapidly inland, undercutting the now vertically mixing urban smoke pall and injecting it into the return flow layer aloft. The windshift

line (Figure 10-9) at first moved at 7-8 km/hr inland, but gradually slowed to about 3 km/hr by mid-afternoon, finally becoming indistinguishable approximately 30 km inland at sunset. At 1100 CDT pibals revealed the inflow layer to be about 500-600 m deep with a 1200 m thick return flow layer above (Figure 10-10). Maximum inflow velocities of 4.0 m/sec were achieved at 150 m above the lakeshore around 1400 CDT. The surface inflow layer winds showed the apparent effect of the Coriolis acceleration by shifting from northeast to southeast as the day wore on.

Cumulus clouds associated with the frontal convergence zone gradually moved further inland during the day (Figure 10-11). The Landsat image also shows cumulus and altocumulus over the lake, the remnants of the vigorous convection present over the warm lake water on the edge of the land breeze outflow. This remained vigorous for more than an hour after the lake breeze onset. This represents a vivid illustration of the fact that shoreline circulations are driven by differences in upward heat transport between land and water - even if they are positive over both. Due to the weak synoptic pressure gradient, the lake breeze convergence zone was detectable along the entire shoreline of Lake Michigan.

TETROON OBSERVATIONS

Three tetroons were released on 4 September 1974. Figure 10-12 is the plan view of their trajectories. Figure 10-13 is a cross-sectional view of the same trajectories.

The first tetroon, launched at 0850 CDT, initially

moved toward the southeast in the land breeze outflow, but at 10 minutes into the flight it met the lake breeze convergence zone and was lifted to about 600 m. For the following 30 minutes it oscillated between 600 and 700 m, drifting northeastward, after which it slowly began to sink and move back toward land. The maximum lakeward fetch of the tetroon was 10 km. After 74 minutes it was lost from the view of one of the tracking theodolites, to be recovered later than afternoon at the position marked in Figure 10-12. This helical trajectory is similar to that found by Lyons and Olsson (1973).

Tetroon two was launched at 1048 CDT shortly after the onset of the lake breeze. It drifted slightly south of west, with the lake breeze, performing a cycloidal loop at about 25 minutes into the launch. The floating height, between 400-500 m, was in the upper part of the lake breeze inflow layer. Oscillations of of this nature have been observed by Angell (1975) and Pack et al. (1972) in a Los Angeles sea breeze study. By 50 minutes into the launch the tetroon had reached the lake breeze convergence zone (20 km inland) and rose rapidly in the updraft, disappearing from sight in haze. This tetroon was found on the ground the following morning at the position marked in the figure.

The third tetroon was weighed off to float at a lower altitude than the previous two, and 10 minutes after launch (1310 CDT) it leveled off at 400 m, drifting slowly toward the west. Sudden updrafts took the tetroon to 500 m and 700 m but after 70 minutes into the launch, it began to settle back to its floating

altitude. By 90 minutes the tetroon was more than 25 km from the tracking theodolites and was occasionally lost from the view of theodolite 1. (The trajectory path from 95 minutes to 110 minutes was extrapolated between those missing observations.) After 110 minutes, both theodolites lost sight of the balloon, it was recovered in a field just north of I94 later that afternoon.

Cross sections of dry bulb temperature and humidity profiles from the RASOT package attached to the 1048 CDT tetroon are given in Figure 10-14. The temperature profile went from a relatively smooth to a highly fluctuating trace as the thermal internal boundary layer (TIBL) grew to balloon altitude. The humidity trace roughly paralleled the dry-bulb curve, indicating that the periodic fluctuations were associated with penetrative convective thermals, estimated to be between 200 and 300 m in width.

AIRCRAFT OBSERVATIONS

Three flights were made in the instrumented Cessna 182 aircraft on 4 September. The first flight was between 0835 and 0948 CDT, the second between 1118 and 1215 CDT and the third flight was from 1351 to 1542 CDT. East-west transects were flown from approximately 8 km offshore to about 30 km inland. The flight of 1351-1542 CDT was meteorologically the most interesting and will therefore be the focus of discussion. By 1400 CDT the lake breeze had penetrated 20-25 km inland and distinct areas of turbulence and particulate concentrations were observed along the flight tracks.

The $\varepsilon^{1/3}$ profile in Figure 10-15 shows a pattern with smooth air over the lake (values 0.3 $cm^{2/3}sec^{-1}$) overland within 8 km of the lakeshore. The TIBL upper limit (1.0 $cm^{2/3}sec^{-1}$) is not confined to the inflow layer. The effect of forced convection in the lake breeze convergence is marked by a "column" of air several kilometers wide with $\varepsilon^{1/3}$ above 2.5 $cm^{2/3}sec^{-1}$. Temperatures frequently fall within this updraft zone - and indication of strong vertical motion. The bending of the isopleths first inland in the lake breeze inflow layer and then lakeward at the base of the return flow suggests that turbulence was also being advected eastward in the return flow aloft while dissipating.

The various features of the lake breeze are strikingly illustrated by the aerosol cross sections (Figure 10-16 and Figure 10-17). For particles in the size range 0.3-1.3 μm, nominal terminal velocities from 0.01 cm/sec. In effect they drift with the air motions. Particles in the size range 7.0-9.0 μm have nominal terminal velocities between 0.5 and 1.1 cm/sec in calm air and would tend to settle much more rapidly than the smaller particles. Figures 10-16 and 10-10 show the distribution of the two size ranges of aerosol particles obtained from flight transects between 1351 and 1541 CDT. Analyses were made from the Rustrack charts of the Royco particle counter with a full-scale deflection being plotted at 100 in the case of the 0.3-1.3 μm range, and as 10 in the case of the 7-9 μm range. These illustrations are not indications, therefore, of absolute particle counts but rather of patterns of the fine and giant aerosol distributions in the lake

breeze circulation.

Figure 10-16 is a plot of aerosols in the 0.3-1.3 μm range and clearly evident is the effect of the TIBL which starts at the shoreline and quickly begins urban scale fumigation of the pollutants stored in the upper portion of the inflow within 3 km. That the upper half of the inflow over the lake (as determined by shoreline pibals) is as heavily polluted is strong additional evidence that much of the return flow mass gradually settles back into the onshore flow layer causing at least partial recirculation of pollutants. In addition, pollutants from sources in the Milwaukee industrial valley (80 isopleth) were being advected inland and mixed upward in the turbulent lower portions of the inflow layer. The bending of the isopleths eastward in the region of the frontal zone together with low particle values (relatively clean air) on the landward side of the front, suggests that strong subsidence was present just ahead of the front. With the pollution advected lakeward in the return flow experiencing a steady decay in turbulence (Figure 10-15) the dipping of the isopleths into the inflow layer suggests the presence of subsidence and implies recirculation. This is supported by the pattern found in Figure 10-17 where in this region the air is clean in terms of giant aerosols.

The pattern of the 7-9 μm range particles (Figure 10-17) does not show the patterns found in the fine aerosol analysis. This range of aerosols is produced largely by mechanical abrasion and geographically random sources accounting for their non-uniform distribution. Notable,though,is the high concentration of large

aerosols at very low levels over the lake. In all probability this represents the fall-out of these aerosols into the lake and is further evidence of the size sorting hypothesis by Lyons and Olsson (1973). The importance of this to dry deposition lake pollution has been noted by Lyons and Keen (1976).

Thus 4 September represents a well documented lake breeze. The observed wind, temperature and turbulence fields can be used to test existing or developmental numerical models, and plans are underway to do just this. An immediate use was as input for the UWM Kinematic Diagnostic Model (Keen, 1976).

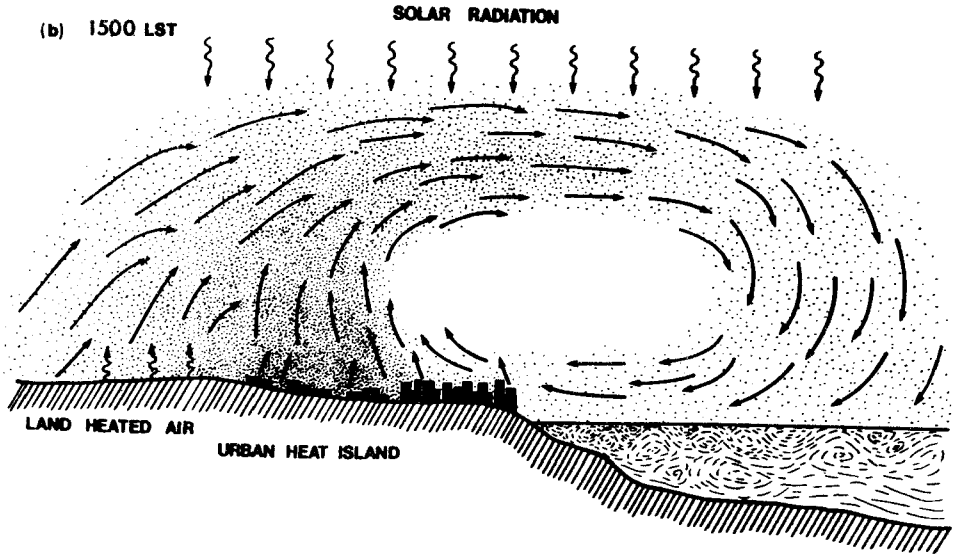

Figure 10-1. A depiction of the Classical Land Breeze at about 0500 LST, driven by differential radiational cooling and showing the urban pollution plume advected over the lake. The dashed line shows the top of the land breeze outflow layer.

THE CLASSICAL LAKE BREEZE

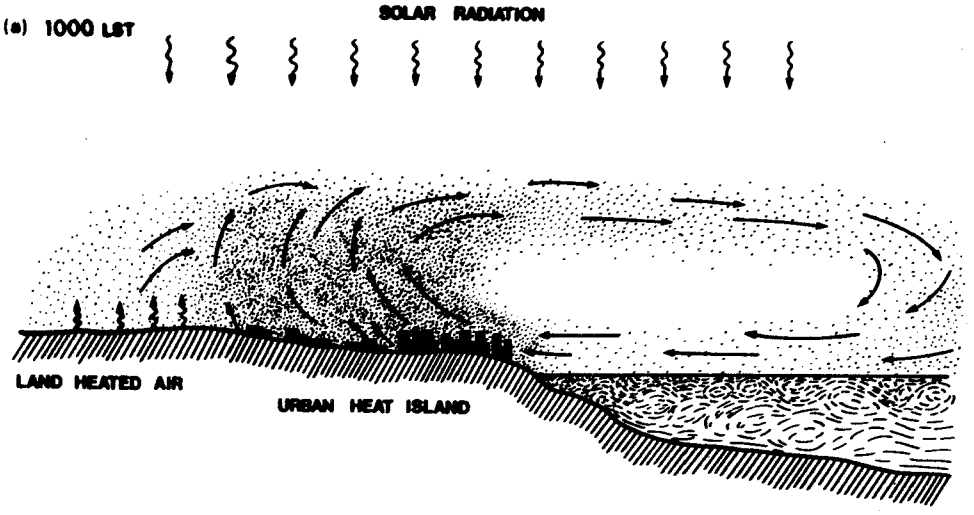

Figure 10-2. A depiction of the Classical Lake or Sea Breeze, fully mature, at about 1500 LST, driven by differential radiational heating, with elemental motions of air pollution transport noted.

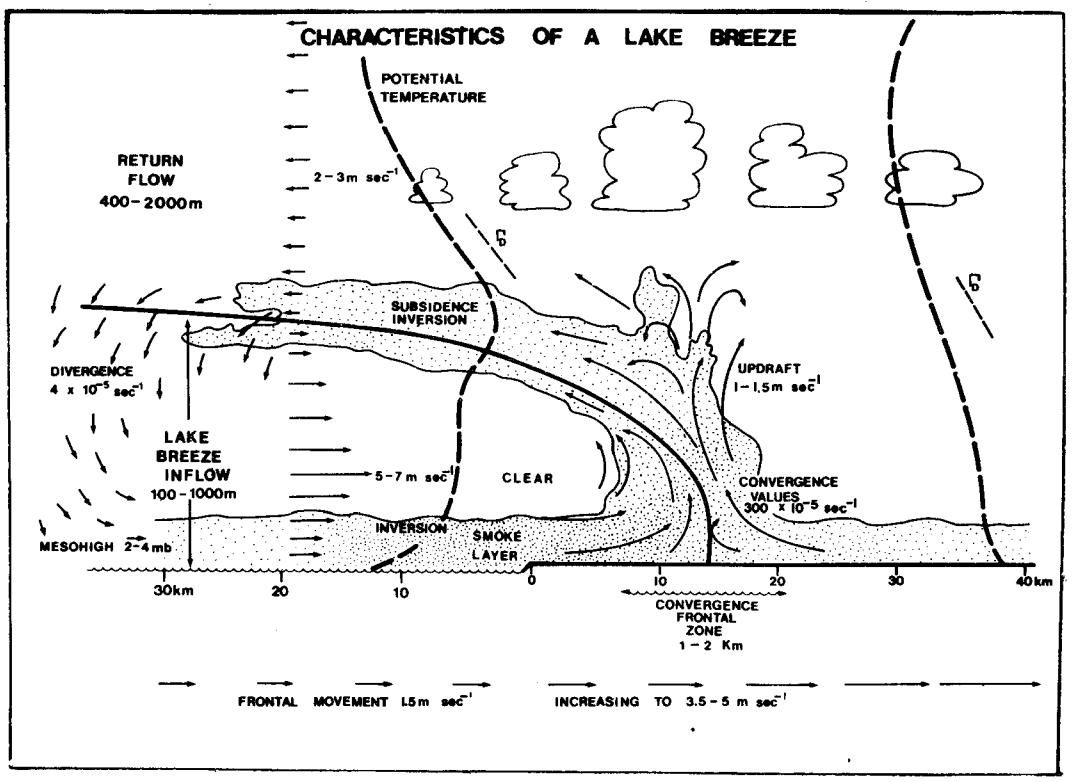

Figure 10-3. Summary of the observed characteristics of a well developed lake breeze during mid-afternoon.

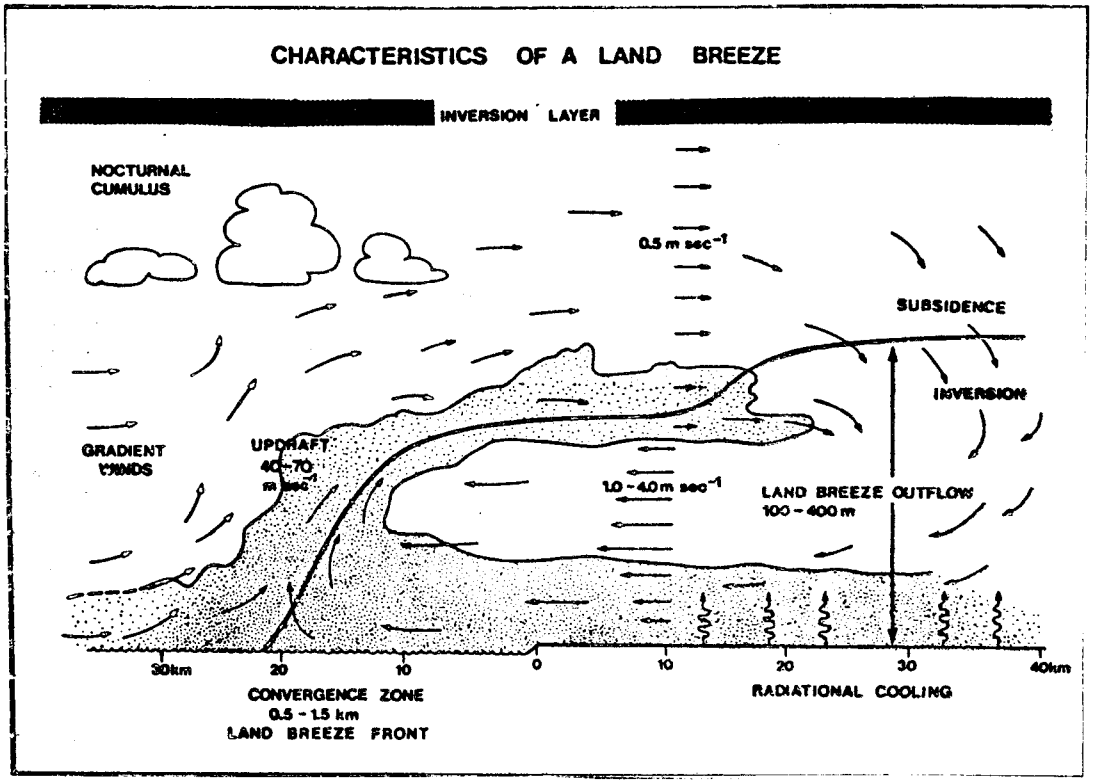

Figure 10-4. Summary of the observed characteristics of a land breeze near dawn.

Figure 10-5. The 1200 CDT SMS-1 satellite photograph on which is superimposed the 1200 CDT surface isobars and frontal positions.

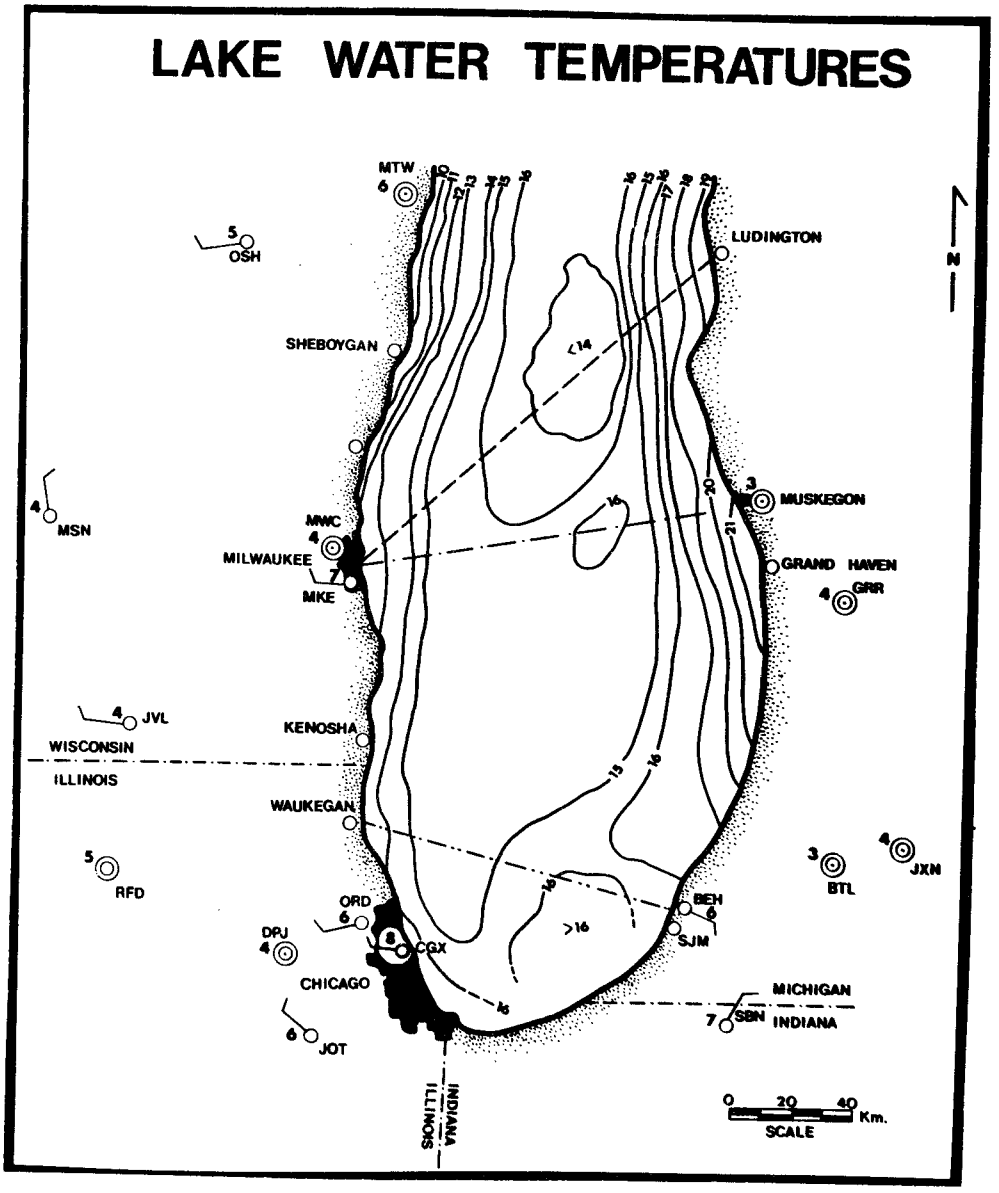

Figure 10-6. Lake water isotherms (°C), compiled from (i) 4 ship transects on 2, 3, 4 and 7 September, (ii) mean daily water intake temperatures at Sheboygan, Milwaukee, Grand Haven, and Muskegon, (iii) averaged from an infrared airborne radiation thermometer from a flight on 6 September 1974. The dotted lines indicate the routes of the ships. Surface winds and temperatures (°C) are for 0600 CDT for 4 September 1974. Each wind barb equals 1 m/sec.

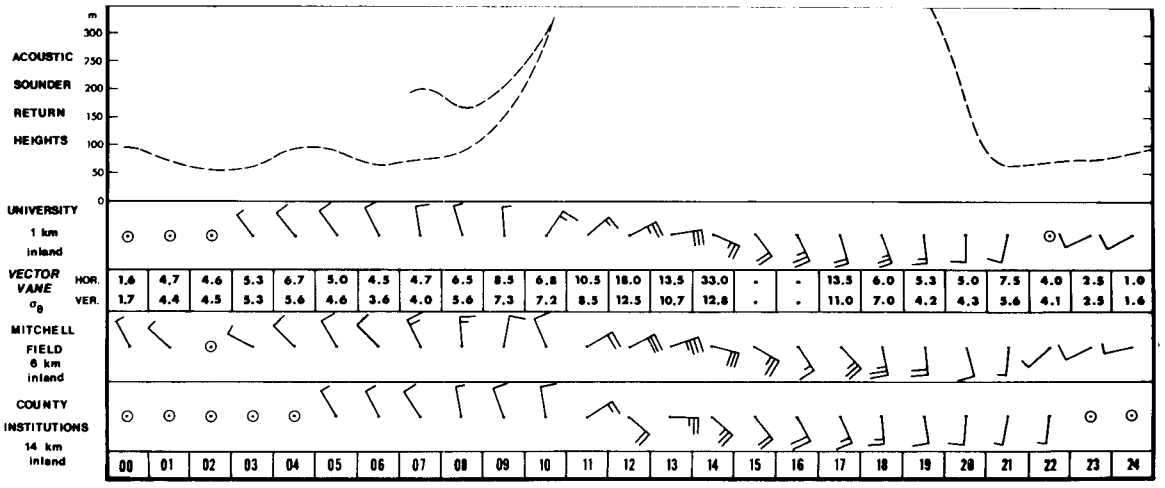

Figure 10-7. Summary diagram of the acoustic sounder return heights and the wind velocities at each hour during 4 September 1974. The vector vane values are in degrees and each wind barb is equal to 1 m/sec.

Figure 10-8. Photograph, looking south along Lake Michigan shore, 0830 CDT, 4 September 1974 as low level plume drifts lakeward in land breeze, power plant effluent rises vertically into light gradient flow above, and cumulus convection is present distant offshore.

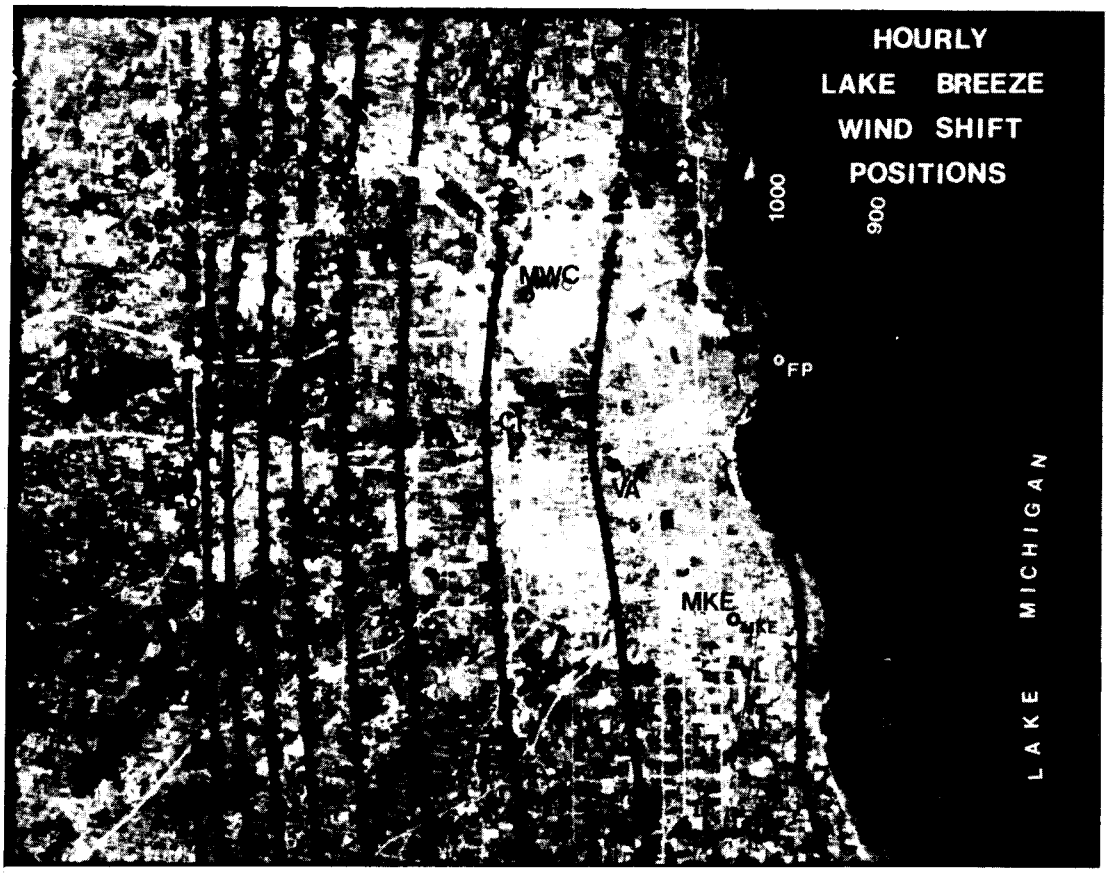

Figure 10-9. Hourly lake breeze wind shift positions on 4 September 1974. Initially the lake breeze traveled inland at between 8 and 9 km/hour but in the late afternoon slowed to under 3 km/hour. FP= filtration plant, VH = Veterans Hospital, CI = County Institutions. Mitchell Field, Timmerman Field and Waukesha are marked by MKE, MWC, and WAU respectively.

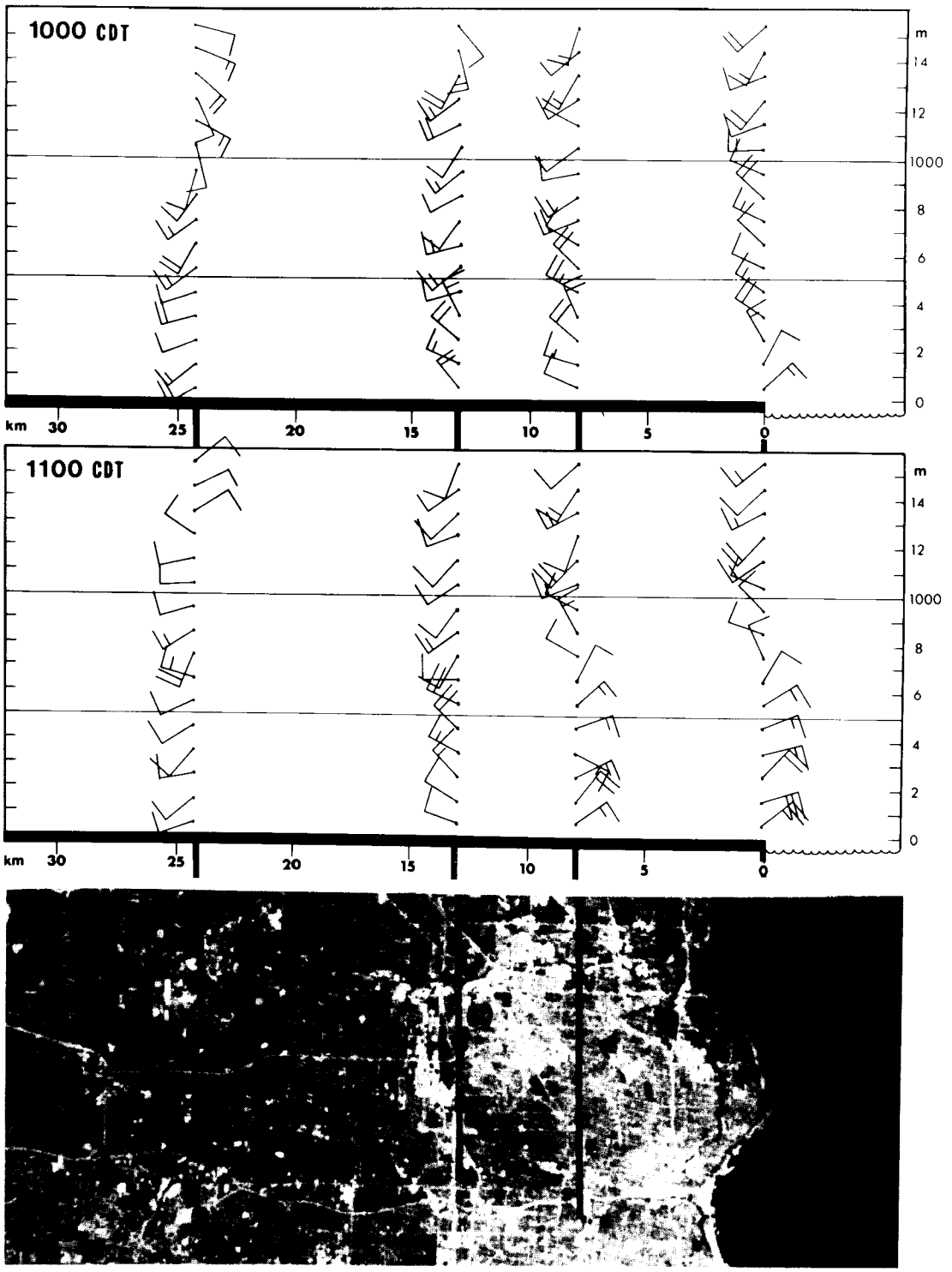

Figure 10-10. The 1000 CDT and 1100 CDT pibal soundings on 4 September 1974; 1 barb equals 1.0 m/sec. Pibal sites located on Landsat image.

Figure 10-11. Composite photograph of 3 frames from Landsat-1 of the western shoreline of Lake Michigan at 1103 CDT, 4 September 1974. Band 5 is shown. Note the inland penetration of the lake breeze by the line of cumulus clouds paralleling the coast and the clear zone within the lake breeze.

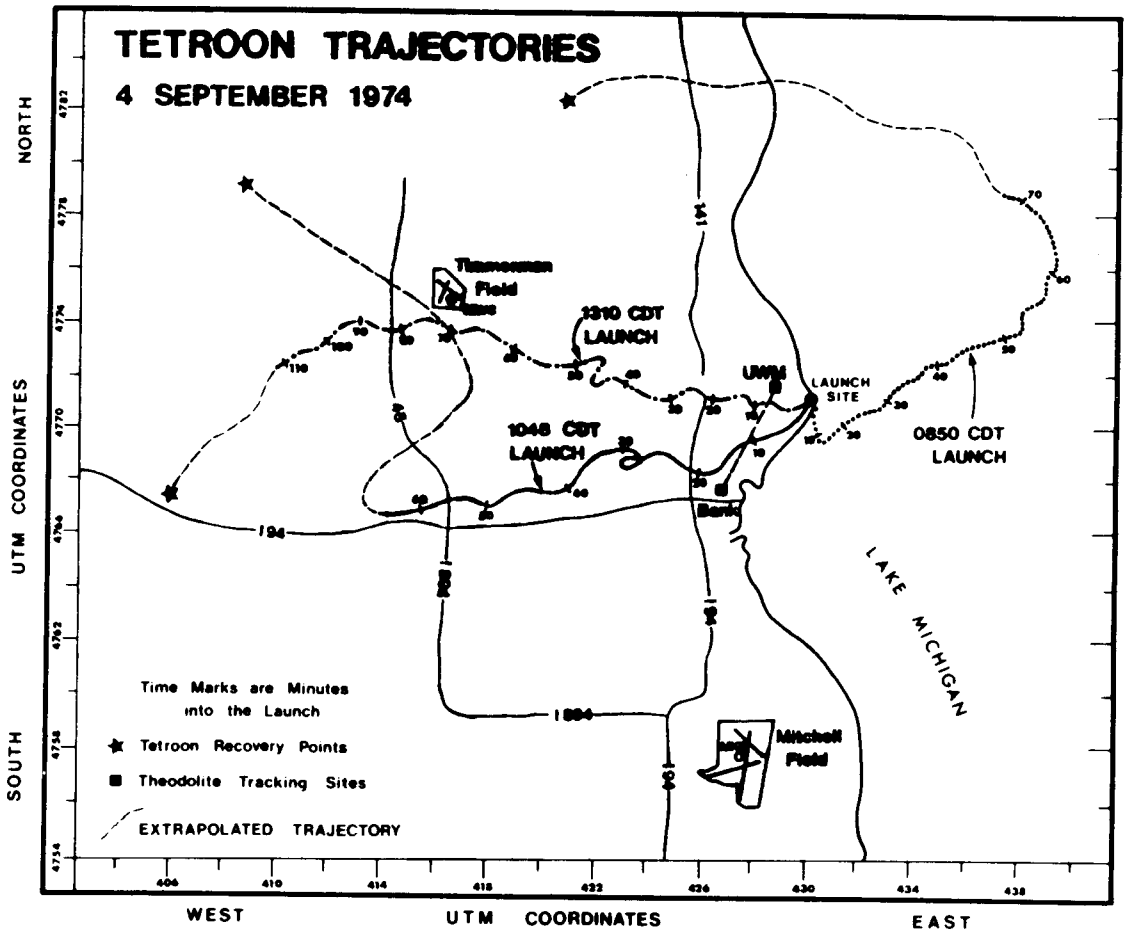

Figure 10-12. Plan view of the trajectories of 3 tetroons launched on 4 September 1974. The 0850 CDT tetroon drifted in the lake breeze return flow before dropping into the inflow layer after 60 minutes. The 1048 CDT and 1310 CDT tetroons drifted with the lake breeze before disappearing from view. The theodolite base line was between the UWM campus and the First Wisconsin Center - a distance measured by laser at 3740.2 m.

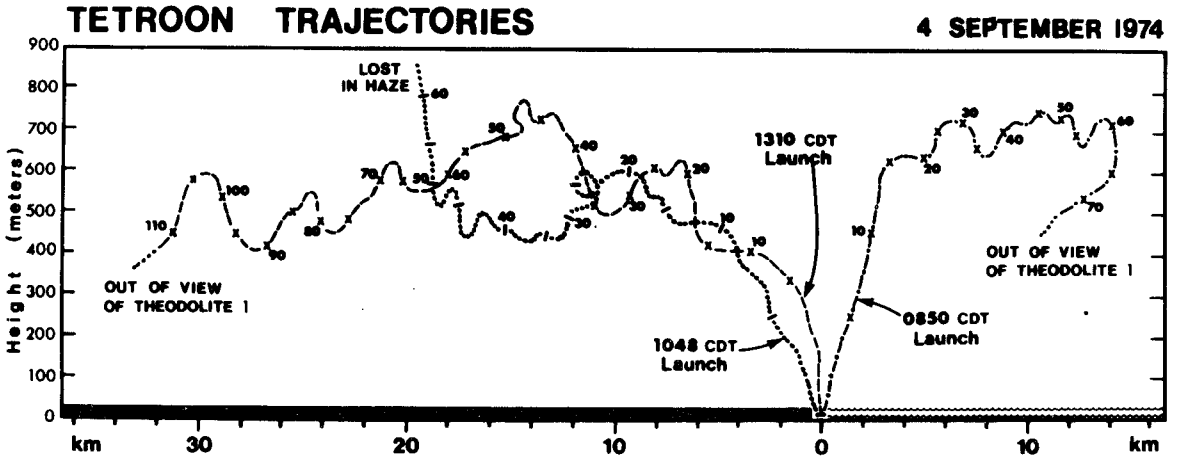

Figure 10-13. Cross sectional view of the trajectories of the three tetroons. The weigh-off height of the 0850 CDT and 1048 CDT tetroons was 500 m while the 1310 CDT tetroon was 400 m. Note the cycloidal oscillation in the 1048 CDT tetroon at about 26 minutes into the launch.

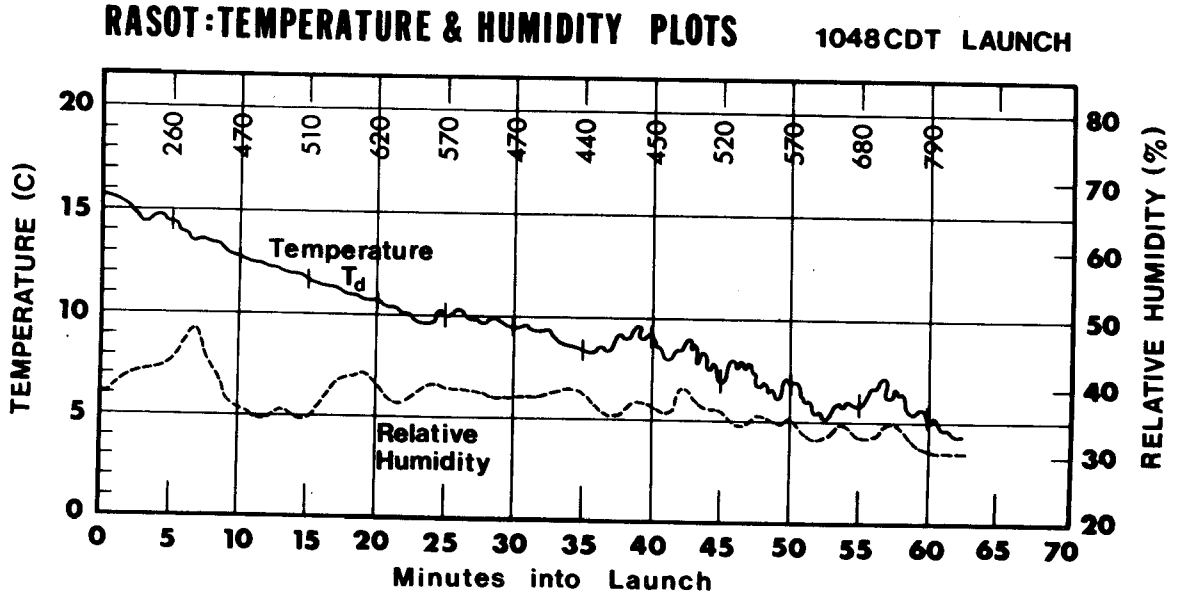

Figure 10-14. Temperature (dry bulb) and humidity profiles from the RASOT package attached to the 1048 CDT tetroon. Times shown are elapsed time into the launch. Diagonal numbers at the top of the diagram give the heights (m) of the tetroons at 5-minute intervals.

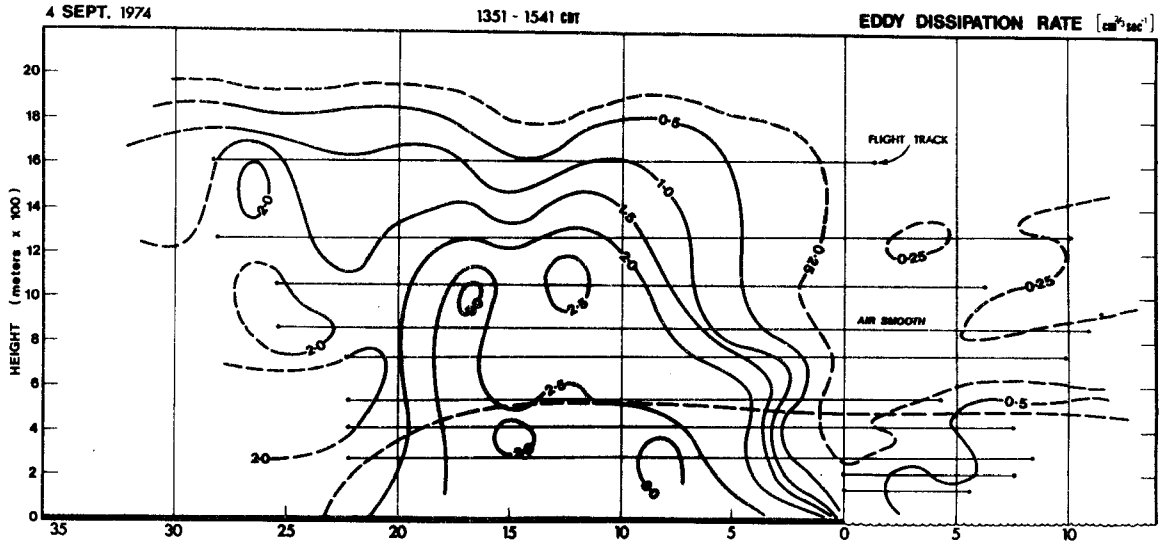

Figure 10-15. Measurements of Eddy Dissipation Rate ($\varepsilon^{1/3}$) $cm^2/3\ sec^{-1}$) on a traverse along Wisconsin Avenue. The inflow layer of the lake breeze is shown as a dotted line.

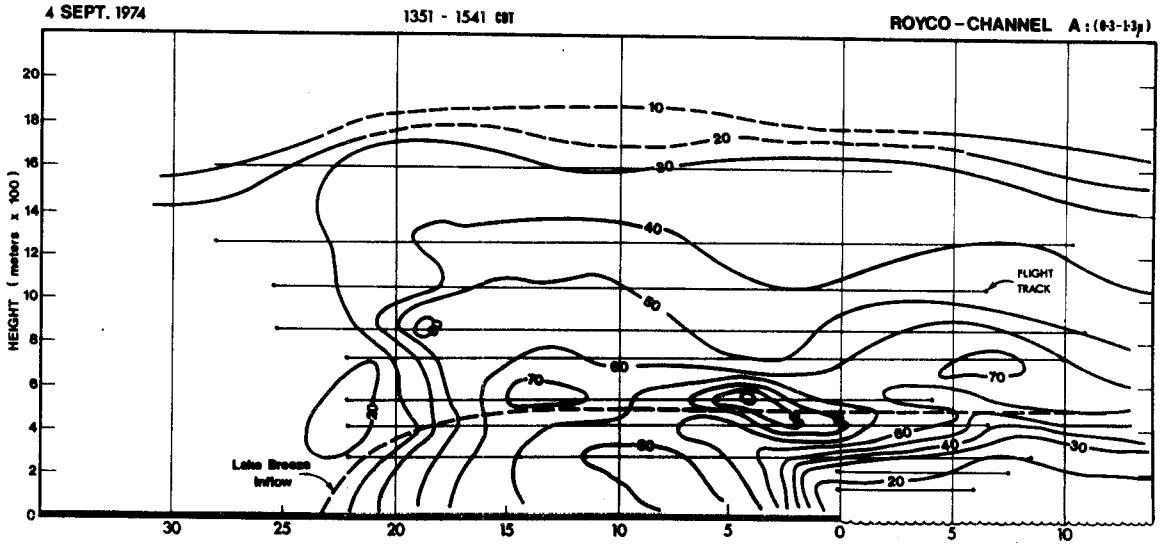

Figure 10-16. The pattern of distribution of the 0.3-1.3 μm range aerosols between 1351 and 1541 CDT. The numbers represent the percent scale deflection on the Rustrack recorder with a full deflection being recorded as 100.

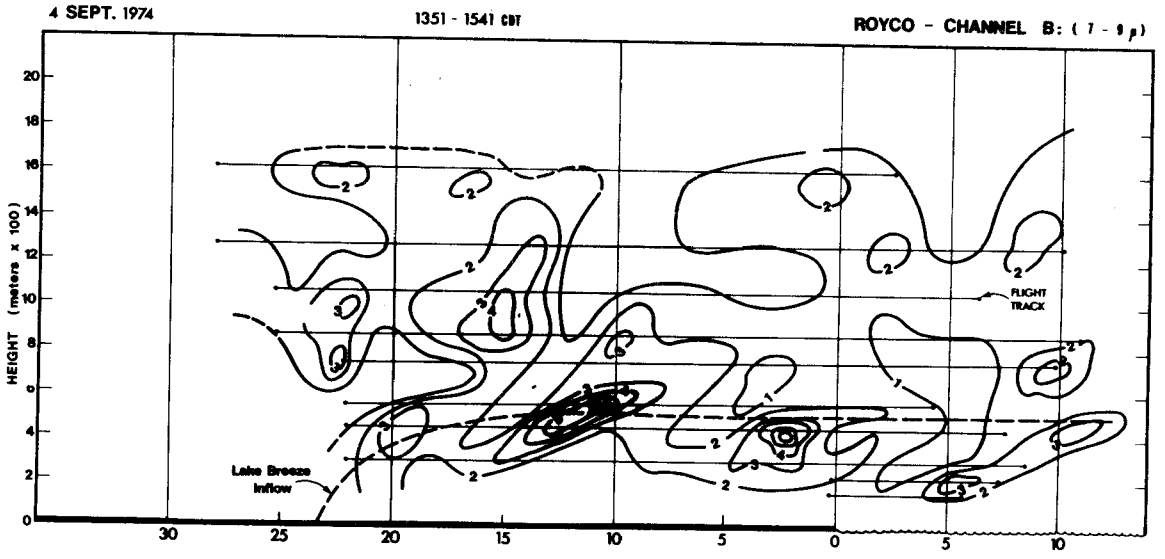

Figure 10-17. The pattern of distribution of the 7-9 μm range aerosols between 1351 and 1541 CDT. Full scale deflection in this case was recorded as 10.

SECTION 11

THE KINEMATIC DIAGNOSTIC MODEL

RATIONALE AND SCOPE

The kinematic diagnostic model (KDM) of a lake breeze-land breeze system uses observed data as input rather than a computed flow field. This largely avoids the scale-ratio problems faced in numerical models, and provides a straightforward method of analyzing the trajectories of particles within the circulation system. By assuming that the breezes are laminar flows and ignoring the effects of microscale turbulence, a model can simulate the mean transport wind, which determines a plume centerline. While the simulation may represent a rather unsophisticated approach to the problem, it is felt it also reveals with great clarity the great complexity of shoreline circulations.

The lake breeze-land breeze sequence on 4 September 1974 was chosen as a case study. Computational restrictions had to be balanced against spatial and temporal resolution requirements, and the following compromises resulted:

(i) The horizontal computational area extends 35 km inland and 15 km into the lake, making a total length of 51 km across the coast.

(ii) The vertical computational area extends to 2200 m, with calculations nominally starting at 1 m above ground.

(iii) Horizontal resolution would be refined to 250 m.

(iv) Vertical resolution would be 100 m.

(v) The coastline would be considered straight.

(vi) The individual soundings would be plotted on a cross-sectional plane, normal to the shore.

(vii) A 24-hour lake breeze-land breeze cycle would be considered, and by repitition, trajectories of up to 48 hours could be computed.

DATA RECTIFICATION AND PREPARATION

The individual pibal soundings at the four observing stations yielded 'u' and 'v' component winds at 100 m height increments above each station. These component winds were separately plotted to scale on cross-sectional maps of 1 km horizontal and 100 m vertical scales. Isotachs were then drawn over an area of 51 km in the horizontal and 2200 m in the vertical. As no soundings were made further than 24 km inland nor over the lake, isotach values in these areas were estimated. Before 0800 CDT and after 1600 CDT, no hourly soundings were made and the cross sections were estimated from surface recording anemometers and detailed knowledge of the behavior of the night time wind flow was not as important as its gross features.

With hourly 'u' and 'v' component isotach fields compiled for the 24-hour period beginning 0500 CDT 4 September, further interpolations were made at sections between hours, as often as every 15 minutes, primarily to describe the inland movement of the lake breeze frontal zone in more detail. This was necessary

since u component velocities in the frontal zone varied from strong negative values on one side (easterly flow) to weaker positive values on the other (westerly flow) over an area of less than 2 km, and further, since the horizontal advance of the front through time was not uniform. In total 65 u-component sections and 24 v-component sections were prepared.

Digitization of the individual sections was accomplished by using a Bendix Datagrid precision digitizer connected to a card punch. Measurements were made to a thousandth of an inch and point values were taken about 0.5 cm apart (approximately 800 m) along single isotachs. Depending on the complexity of the section, the u-component points varied in number between 860 and 1500 points per section. Since the v-component sections were not as complex, these varied in number between 650 and 800 points per section. Approximately 24,000 cards were used for data storage in the 89 sections digitized.

The Computer Sciences-Statistics Center of the University of Wisconsin-Madison provided graphics routines for two-dimensional interpolation, smoothing, and refining, including four interpolation routines called RANGRD, INTERP, INTRP and INTRPB. These routines do not interpolate in the classical sense, but rather use algorithms to find the values at every point on a rectangular grid given a set of N arbitrary values with corresponding x, z locations in a two-dimensional domain. Keen (1976) gives a complete discussion and should be consulted for details.

The interpolation routine INTRP took the arbitrarily spaced data points on each time section and produced point values at

each of 1173 points in a 51 X 23 grid matrix, and for this a smoothing routine called SMOOTH was used. The horizontal scale is in kilometers and the vertical scale in hundreds of meters. In order to achieve the desired horizontal resolution of 250 m, each sectional matrix had to be subjected to a refining technique to produce a final matrix of 201 X 23. For this the routine REFN1 was used, which finds the values at new grid points by bilinear interpolation in a two-dimensional domain from the values supplied in an existing grid of either equally or unequally spaced rows and columns.

The output from REFN1 produced a rectangular grid matrix with 201 horizontal spacings (of 250 m in actual resolution) and 23 vertical spacings (of 100 m in actual resolution). In total 4,623 node point values per section were obtained.

One more data manipulation is necessary before any trajectories could be produced. The period of analysis for this study was 24 hours, in which time sections were made at 15 minute intervals during the daytime hours and 30 minutes or 60 minute intervals during the nighttime hours. Since a final resolution of 15 minutes was desired, a further series of interpolations had to be made. In this case a simple linear interpolation between the two time periods was used.

After these matrices at intermediate times were calculated, 96 u-component matrices and 96 v-component matrices were available at 15 minute intervals for a 24-hour period. By now 887,616 discrete values have been calculated to produce a time series of matrices, 201 (0.25 km) by 23 (100 m) at 15 minute intervals.

The data were stored on tape in files and it was now possible to proceed with particle trajectory analysis.

TRAJECTORY CALCULATIONS

The Mainline Program was written to be independent of the data series, so that the technique can be used with a data series in which the spatial scales and/or temporal scales are different from those in the above example. For ease of description, the program will be explained with the aid of a schematic flow chart, Figure 11-1.

The first requirement is to initialize the program with the space and time scales of the study and to decide upon the number and starting time of the particles.

Input Parameters Initialize 1

xUTM, yUTM	=	The UTM coordinates of the lower left hand corner of the matrix (0.0)[2]
SCALEX, SCALEY	=	The distance between the matrix columns (in km) and between the rows (in m) (0.25, 100)
NHOURS	=	The total number of time periods to be analyzed. If a 24-hour period is desired and each time was 15 minutes apart, then (24 x 4) + 1 = 97 (193)
NREAD	=	The number of intervals in a time period
NP	=	The number of time period per hour (4)

[2]The figure in brackets following the descriptions are the input parameters used in this study.

NPTS = Total number of particles to be considered (up to 1000). (273)

START = Time at which trajectory computations are to start, i.e., the first time in 24 hour time (0500)

CORR. = Correction factor to increase or decrease the u and v vector velocities. Given as a decimal.(0)

PARTICLE POSITIONS AND DIMENSIONS

The spatial starting positions (x, y, z) of each particle are read in, followed by its fall speed (in cm sec^{-1}) and its actual start time.

INITIAL U-MATRIX V-MATRIX

The u-matrix and the v-matrix of the first time period are read in.

COMPUTE 'W' MATRIX

From the u-matrix, the w-components are calculated from the formula

$$w(z) = w_0 - \int_{z=0}^{z} \frac{\Delta u}{\Delta x}\, dz$$

where w(z) is the vertical motion at height z_1, w_0 the vertical motion at the lowest level (assumed zero for the ground), and x the distance normal to the shore. These are then stored into a w-matrix array.

MAIN LOOP I=1, NHOURS

This is the beginning of the main loop of the program. Since each matrix uses a considerable amount of core storage, a flip-flop technique was devised whereby only two time sections are in core at any one time. This is accomplished by means of a four dimensional array (VCTR(FLIP, IZ, IX, IDIM)) where the first subscript (FLIP) is used as a pointer, indicating the location of the old and the new time section.

FLIP-FLOP COUNTER INTERCHANGE MATRIX

NEW U-MATRIX V-MATRIX

The next time period is read in and the w-components of that time are calculated as above.

COMPUTE 'W' MATRIX

SUB-LOOP FOR POSITIONS J=1,NREAD

A secondary loop is now used for computing the actual positions of the particles between the main loop time period (15 minutes). In the secondary loop, positions are calculated every minutes. Since new particles may start at any time during the total computational period (24 hours), a test is included to determine whether any new particles are to start in the time interval being computed. Another test is included to stop computation of a particle if it has descended to ground level.

NEW STARTING TIME

TEST PARTICLE IMPACT

COMPUTE VELOCITY & DISTANCE FOR NEW POSITIONS

A subroutine is now called to compute the u, v and w velocities effecting each of the particles. The particles are translated at constant vector component velocities during each time period and their positions are then determined from the following formulae:

NEW x, y & z POSITIONS OF PARTIC.

NEW(km)=OLDX(km)+3600(sec)xFACTOR(1/sec)xANS(u)(m/sec)x0.001(to km)

NEWY(km)=OLDY(km)+3600(sec)xFACTOR(1/sec)xANS(v)(m/sec)x0.001(to km)

NEWZ(m)=OLDZ(m)+3600(sec)xFACTOR(1/sec)x(ANS(w)(cm/sec)-FALL(cm/sec))
x0.01 (to m)

where FACTOR is the time interval over which the velocity is held constant, i.e. 15 minutes.

Winds outside the initial 50 km by 2200 m domain were set equal to those at the boundaries.

The new x, y and z positions for each of the particles at every minute can be written out to a file from which various types of computer plots may be generated.

By means of a CalComp plotter and standard plot routines, XY, XZ, and YZ plots were made of the trajectories of the selected particles. A three-dimensional plot routine was adapted for use with this program to illustrate graphically the pattern of dispersion in a lake breeze-land breeze circulation system.

All computations were performed on the UNIVAC 1106 computer operated by the Computer Services Division of the University of Wisconsin -Milwaukee. On this system the program required 27K words of memory; for each additional particle only 21 extra words of memory were required.

The efficiency of the program is shown by considering that during a 24-hour sequence, 1,331,424 individual values are handled, of which 443,808 (the w-components) have to be calculated. These computations took between 8 and 10 minutes of computation time.

Some problems were met, however, in handling the plotting file. As an example, with 273 particles, a file was produced which contained 1,180,171 point values which on the UNIVAC 1100 series took 659 tracks of disc or approximately 800 feet of high density (1600 BPI) tape. For convenience, the file was broken into subfiles with particles being handled and plotted in groups. Although

the x, y and z positions of each particle were given every minute, plotting tests showed that a point of economic efficiency was reached when points were plotted at 6-minute intervals. Plotting them every minute more than doubled the plotting time (and cost) while longer time intervals became noticeable in departures in the trajectory paths.

A complete listing of the program and routines used is given in Appendix II of Keen (1976).

SUMMARY

Annotated flow-diagrams of the procedures followed in the development of the KDM are presented as a summary of this section using data at 1100 CDT, 4 September 1974 (Figures 11-2, 11-3, and 11-4).

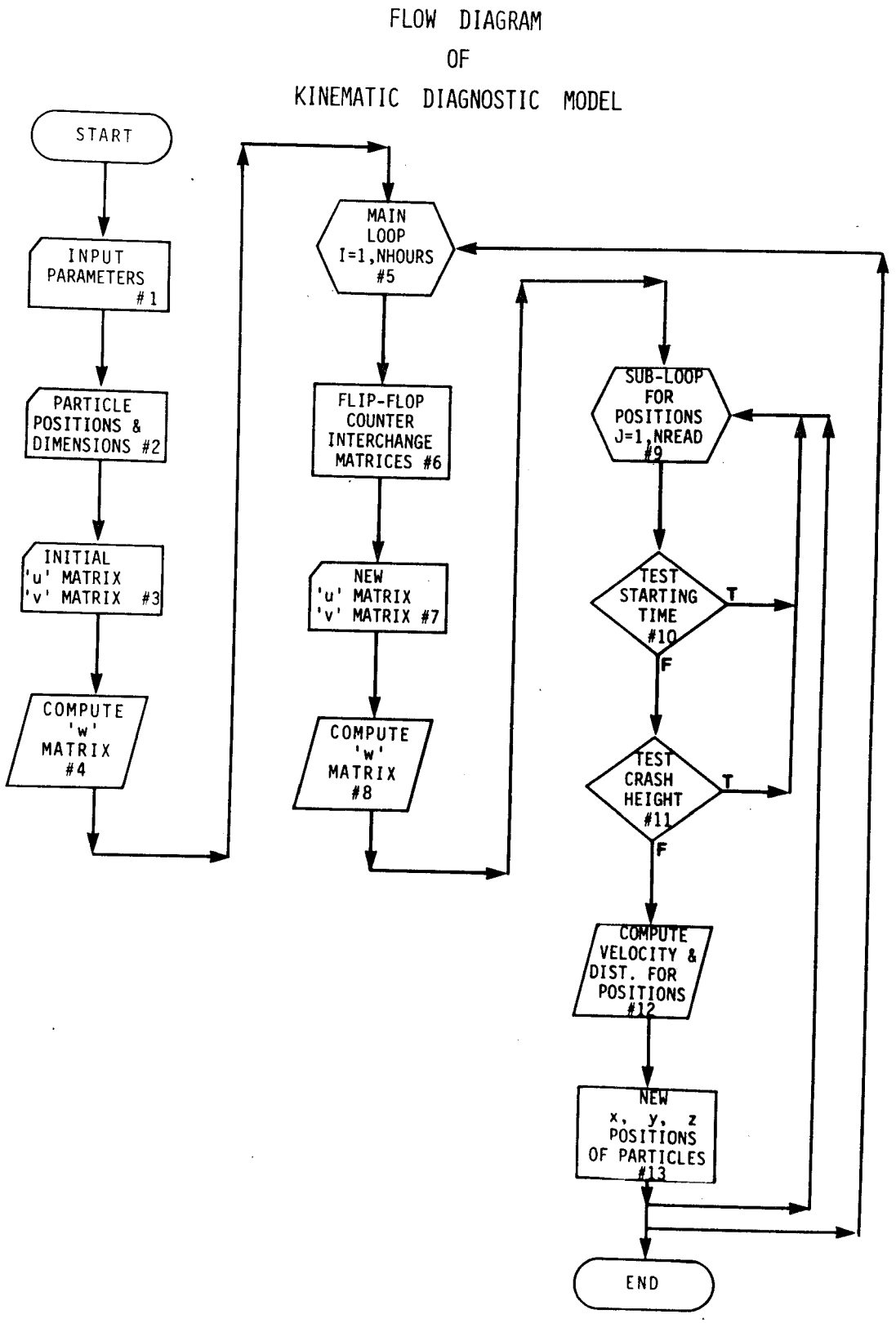

Figure 11-1. Flow diagram of the Kinematic Diagnostic Model.

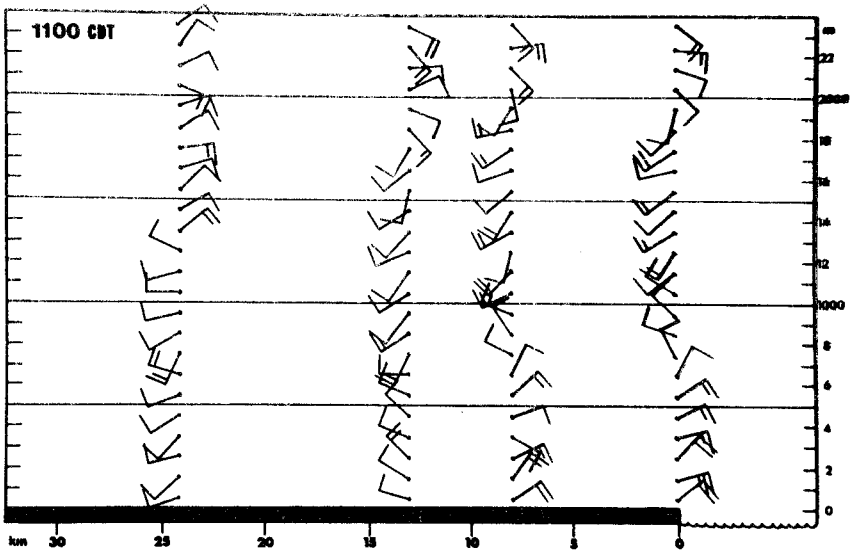

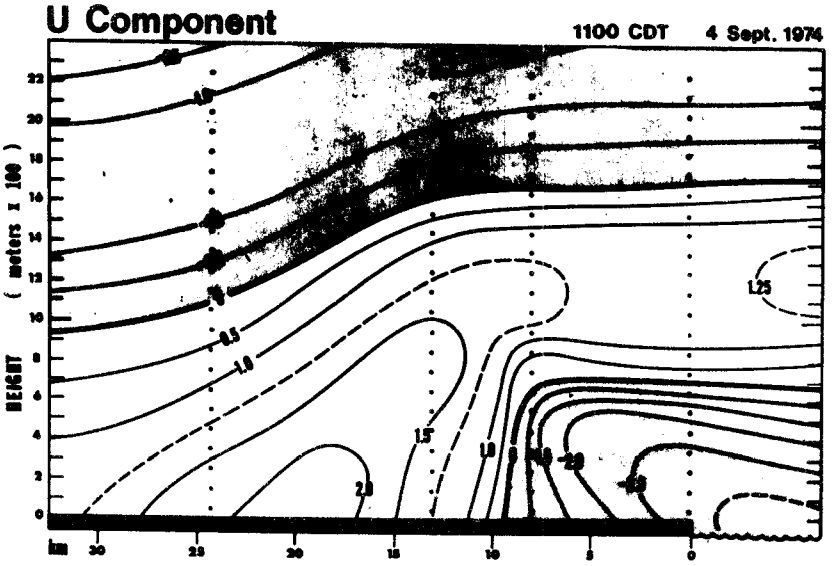

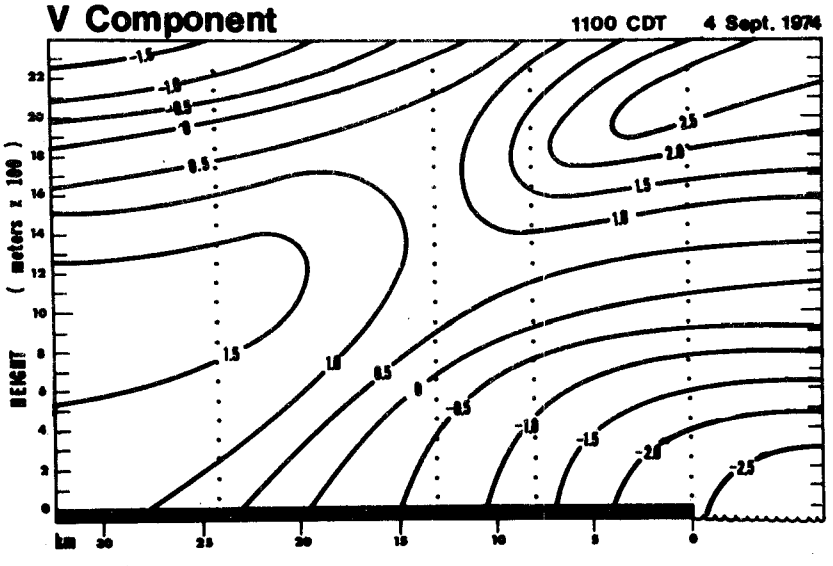

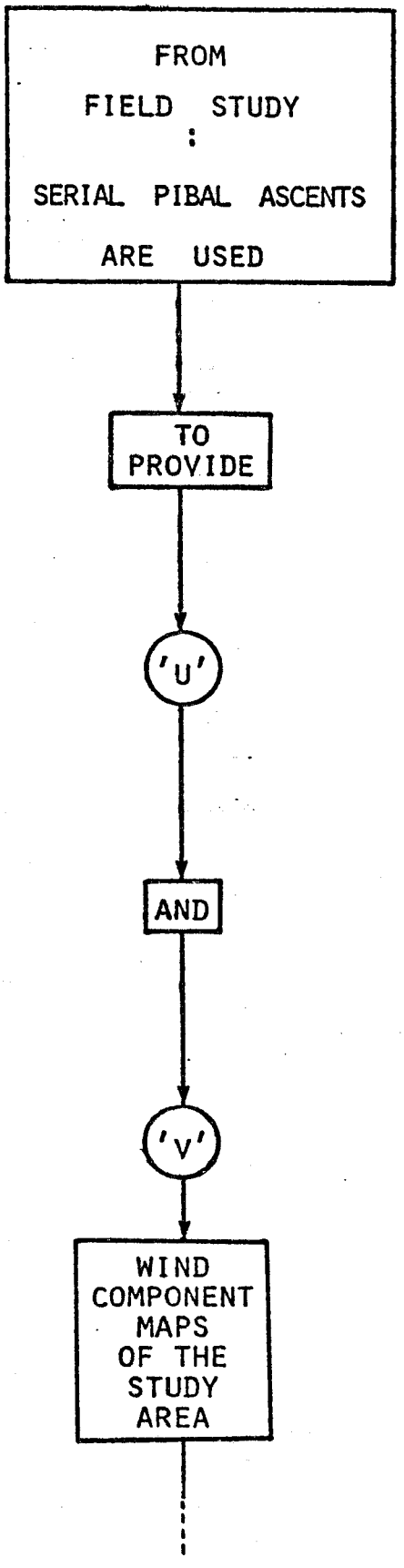

Figure 11-2. Detailed flow diagram of Kinematic Diagnostic Model.

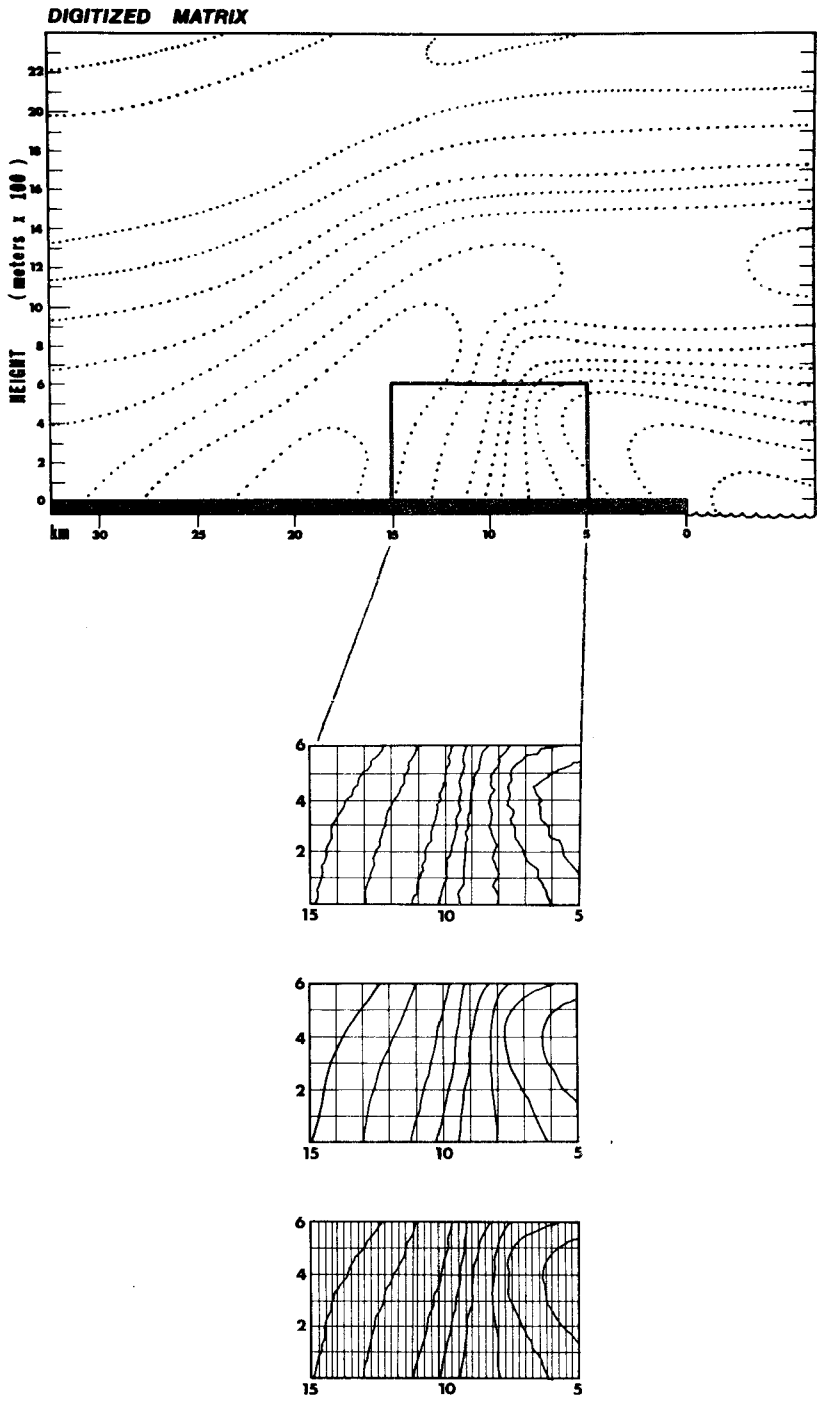

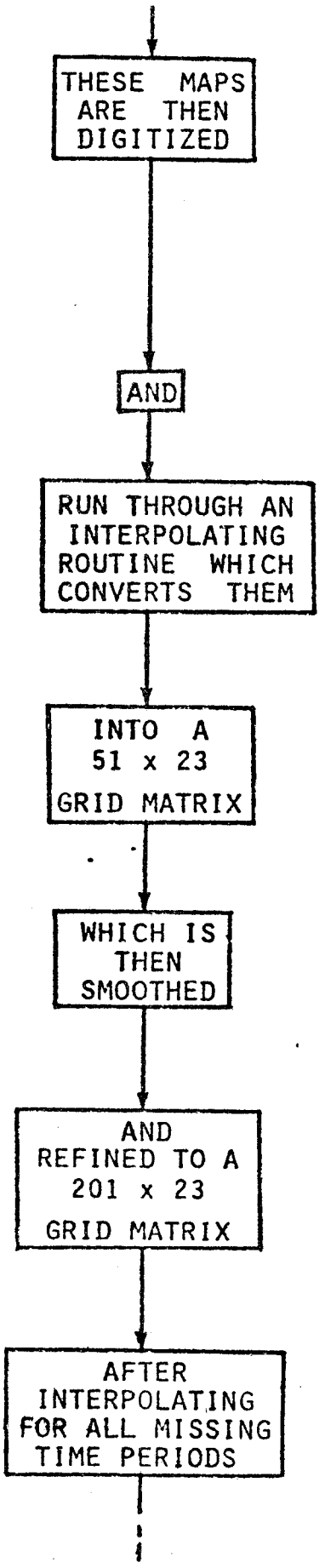

Figure 11-3. Detailed flow diagram of Kinematic Diagnostic Model, continued.

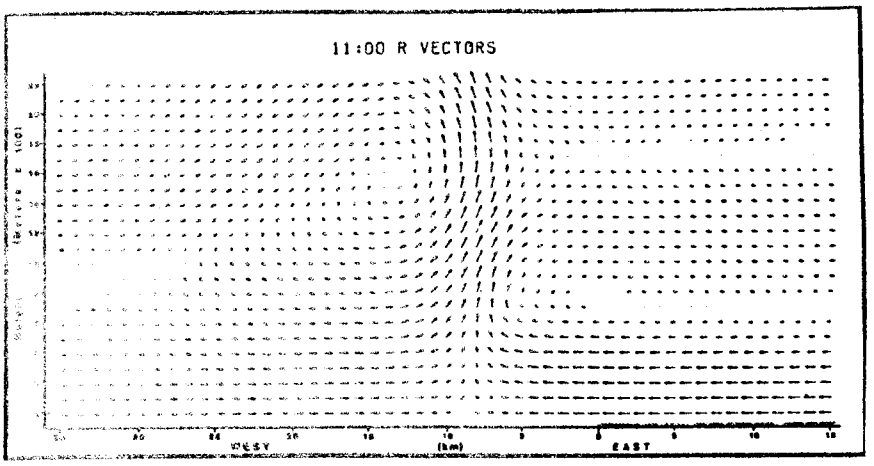

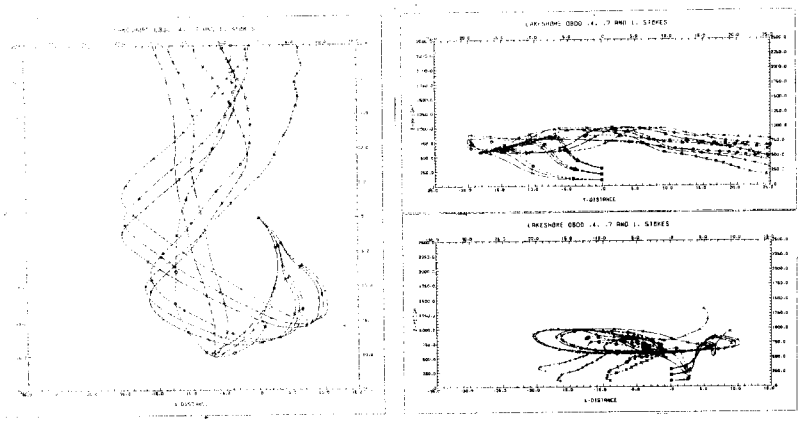

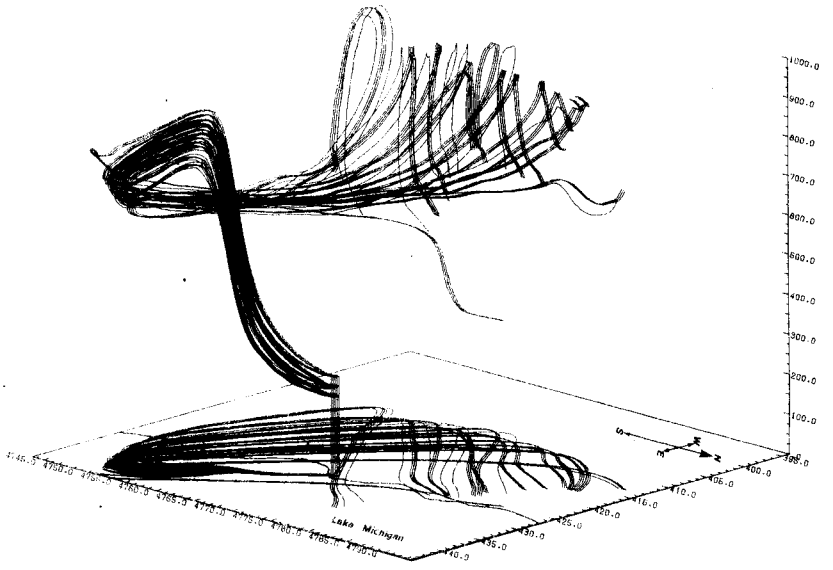

AND CALCULATING THE 'W' COMPONENT FROM THE 'U' FIELD

FROM WHICH 'UW' WIND VECTOR PLOTS MAY BE PRODUCED

THE MAINLINE PROGRAM IS RUN WHICH COMPUTES THE TRAJECTORIES OF EACH PARTICLE

STANDARD PLOTTING ROUTINES MAY BE USED TO PRODUCE

XY

YZ

XZ

PROJECTIONS

OR

3-DIMENSIONAL DISPLAYS

Figure 11-4. Detailed flow diagram of Kinematic Diagnostic Model, continued.

SECTION 12

RESULTS OF THE KDM

TRAJECTORY COMPUTATIONS

The land/lake breeze sequence of 4 September 1974 was used as a case study in the development of the Kinematic Diagnostic Model (KDM). Time integrations allowed the construction of particle trajectories, released at any point in space or time within the computation grid. Both gases and aerosols can be submitted. Aerosol deposition rates are crudely approximated by using estimates of terminal velocity (a constant vertical speed imposed upon the advected particle). Particles impacting upon the surface were "deposited" and calculations were terminated. Those passing beyond the computation perimeter could be brought back if wind conditions so dictated.

The KDM allows the simulation of transport from line sources, multi-stack sources, area and volume sources, and aerial bursts.

The use of observed data hopefully provides a more realistic wind field than that computed via complex (and expensive) numerical models, although notable data voids, such as over water, do indeed exist. The use of tetroons was in part motivated in an attempt to validate the calculated trajectories. Figure 12-1 shows the xz view of the 1048 CDT tetroon superimposed upon the 1130 CDT uw-vector cross-section plotted on the same scale. The authenticity of such cycloidal movement within the general lake breeze circulation seems probable, and while the coincidence between observed

and predicted may be rather fortuitous in this case, an inspection of the overall tetroon data (Section 10) suggests a gratifying degree of similarity in most respects.

It is felt that the KDM works best by far in the frontal convergence zone and is weakest in the overwater areas where flows were in fact merely "guesstimated." In particular it is felt that the data used for this trial underestimated overwater subsidence. On the whole the KDM is believed to be a useful tool and a starting point at refining modeling philosophies.

SIMULATION EXPERIMENTS

A gradation of particle sizes was used in the KDM trajectory simulations, spanning the gaseous state and the fine and the coarse size ranges. Fall speeds of 0.0, 0.1, 0.4, 0.7, and 1.0 cm sec^{-1} were used in the various simulations.

LINE SOURCE

Particles (0.1 and 0.4 cm sec^{-1} fall speeds) were simultaneously released at six points along a line running southwest-northeast from an inland point 13 km from the lakeshore to the most easterly release 2 km inland from the shore. The release altitude was 10 m AGL. Figure 12-2 (a) of various particulates released at 0700 CDT.

Initially the trajectories of the 0.1 and 0.4 cm/sec particles were similar. The particles responded to the land breeze and stayed within 20 m of the surface (heavier particles descended to ground level shortly after release) for several hours until

being rapidly lifted in the lake breeze convergence zone and advected first inland then lakeward with the return flow. The lighter particles (0.1 cm sec^{-1}) showed a greater lateral spread in their downwind travel than did the heavier particles. The effect of the two different fall speeds is clearly seen in the xz projections.

The release of an identical series of particles at 1200 CDT is shown in Figure 12-3. With the lake breeze convergence zone by this time nearly 16 km inland, the particles were injected into the inflow layer and were carried westward for 10-15 km before being lifted to 1200-1600 m in the frontal convergence zone. Thereafter they traveled in the lake breeze return flow layer, at least for some distance before some were affected by vortex circulations, whereupon opposite paths were taken.

If these trajectories are somewhat analagous to the behavior of automotive pollutants released that day, it is interesting to note elevated layers of NO_x were seen that afternoon over the lake. This suggests that the convergence zone acts like a chimney injecting many pollutants into the upper portion of the boundary layer. Only dynamical recirculation and fumigation in the lake breeze, or washout/fallout mechanism should involve them again with near surface processes in the short run.

MULTI-STACK LAKESHORE SOURCE

In this series of simulations five sizes of particles were considered. The particles of fall speeds 0.0 and the 0.1 cm sec^{-1} were released from 5 levels (20, 50, 100, 200, and 300 m) and the

0.4, 0.7 and 1.0 cm sec^{-1} particles at 3 levels (100, 200, and 300 m). The trajectories of the particles were calculated over a maximum period of 24 hours. Computations terminated if the particle went beyond the plotting grid, or else at 0800 CDT on the following morning (5 September 1974).

Figure 12-4 are the xy, xz, and yz projections of the trajectories of the particles simultaneously released at 0700 CDT. During the first three hours after release, all particles responded to the land breeze circulation, veering to a northerly component under the apparent effect of the Coriolis force. The most westerly pair of trajectories in Figure 12-4 are those of particles emitted at the lower two levels (20 and 50 m). The effect of greater height is to cause the trajectories (plumes) to diverge more rapidly.

During the first three hours after release the trajectories of the particles from the lower three levels (20, 50 and 100 m) closely approximates the trajectory of the low-level plume shown in the photograph in Figure 10-8, showing not only a similar directional path but also very little upward movement over the lake for the first 2-1/2 hours. By 0930, 2-1/2 hours after emission when the lake breeze was approaching shore, the particles became progressively influenced by the vertical component in the advecting convergence zone. After rising to over 700 m, they were carried in the weaker return flow, the lighter particles with a more easterly component than the heavier ones. The trajectories of the heavier particles (Figure 12-4) not only show a greater divergence

with downwind advection, but also a significant fall-out during the night hours.

Heavier particles, released at the same elevations as the latter three, were similarly advected to the north, also in a complex series of helical circulations. The greater particle sizes (greater fall speeds) produced a significant fall-out during the night, suggesting that an apparent size sorting occurred across the shoreline.

Figure 12-5 illustrates the phenomenon of split-flow depicted by Cole and Lyons (1972) in which power plant plumes with differing effective stack heights were found with radically differing orientations.

Numerous three-dimensional views such as Figure 12-5 confirmed and emphasized many features of lake breeze flows including

(i) the helical circulations that occur within the whole circulation cell;

(ii) the large lateral spread of "plume" produced by the highly complex trajectories caused partly by the different fall-out velocities of the particles, but to a greater extent by the vertical wind shear;

(iii) the partial recirculation of gases and aerosols within the circulation cell.

(iv) the size-sorting phenomena allowing particles from common sources with differing fall speeds to take often radically different trajectories.

SIZE SORTING OF PARTICLES

In an attempt to investigate size sorting of the particles within a lake-breeze system, a composite diagram was constructed from the trajectories of 180 particles. Release heights of 20, 50, 100, 150, 200, and 300 m were chosen at a lake-shore source. Particles were divided into three groups; group A comprised particles with fall speeds of 1.0 and 0.7 cm sec^{-1}, group B particles of 0.5 and 0.4 cm sec^{-1} and group C, 0.1 and 0.0 cm sec^{-1}. Particles of each size were released from each of the above noted heights at the following hours: 0700, 0900, 1100, 1300, and 1500 CDT. The trajectories were traced, and the position of every particle at 1800 CDT was marked. Figure 12-6 is the xy projection of the 1800 CDT positions. No easily recognizable grouping could be distinguished, so the x-distance (i.e. across shore) was divided into four equal zones, each 20 km wide. The over-lake zone covered a distance from 30 km to 10 km out from the lakeshore, the shore zone spanned the area 10 km on either side of the lakeshore, and the two inland zones covered distances from 10 to 30 and 30 to 50 km, respectively. The distribution of the particle groups within each zone was totaled and graphed in Figure 12-7. The most obvious variation occurs with Group A, the largest particles considered, which display a distince maximum over the lake, diminishing steadily with inland distance. Group B, particles with intermediate fall speeds, shows only a slight maximum in the shoreline zone, and no definite conclusions can be made about their distribution. Group C, the gases range, shows a maximum concentration in the inland

zone 10-30 km from the shore. For the large particles (fall speeds greater than 0.7 cm sec^{-1}), a sorting across the shore does seem apparent, suggesting that with an obvious concentration of particles over the lake, enhanced deposition in the lake should occur.

AERIAL BURST

The simulation of an aerial burst was accomplished by considering an instantaneous release of 52 particles from a position 200 m above the lakeshore. The release time chosen was 0700 CDT and trajectories were computed for a 12-hour period thereafter. A release height of 200 m was chosen because this would place the burst within the zone of maximum inflow velocities and thereby cause the plume to experience a maximum downwind divergence.

A release time of 0700 CDT was chosen to emphasize the complexity of flow within a lake breeze system as well as to illustrate the inaccuracies in the present procedure to handle an emergency situation such as an accidental release of a toxic substance. In the event of such an explosion, authorities might consider the prevailing wind direction and speed and calculate an arc 20° on either side of the mean direction, and then assumed that 95 per cent of the contaminants would be contained within this cone advecting at the speed of the mean wind. At 0700 CDT the mean wind direction was northwesterly and the mean speed estimated at 1.2 m sec^{-1}. This would imply that the contamination would travel and slowly diffuse over the lake, averting the populated shoreline areas especially the downtown area. However,

one glance at Figure 12-8 shows that just the opposite would occur. The trajectories are initially toward the southeast, but on meeting the lake breeze convergence zone, are convected into the return flow layer. There they slowly sink into the inflow layer with a northerly helical circulation advecting with the lake-breeze front and concentrating in a 10 km zone along the shoreline at approximately the same latitude as the burst origin. With the possible occurrence of fumigation within the lake breeze inflow layer it is quite likely that the contaminants could reach the ground within 6 or 7 hours after release.

The use of a model such as described above to simulate problems such as explosions, dry deposition trajectories of single or multiple particle releases, etc., is clear. It remains to improve the model technique further and to make other simulations within lake breeze systems.

In summary the KDM shows the lake breeze circulation produces transport patterns of a highly complex nature. Keen (1976) presents many more examples showing the futility of attempting to apply "conventional" methods of air quality analysis to mesoscale flow systems.

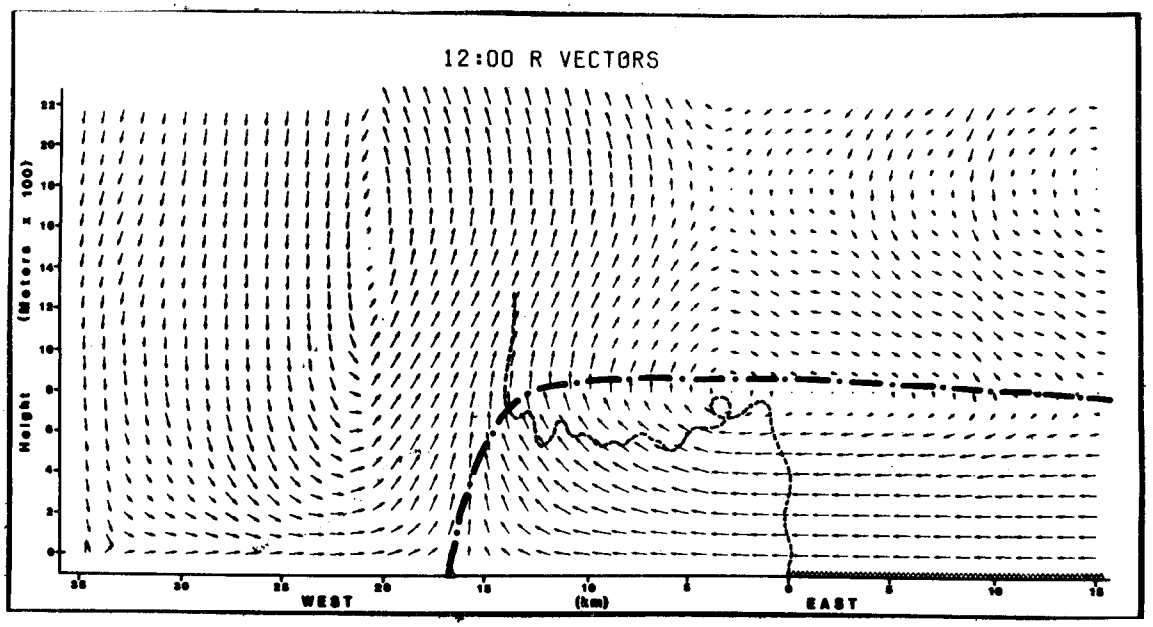

Figure 12-1. The xz plot of the 1048 CDT tetroon superimposed upon the 1130 CDT 2-dimensional uw wind vectors. The dark dotted line marks the lake breeze inflow layer.

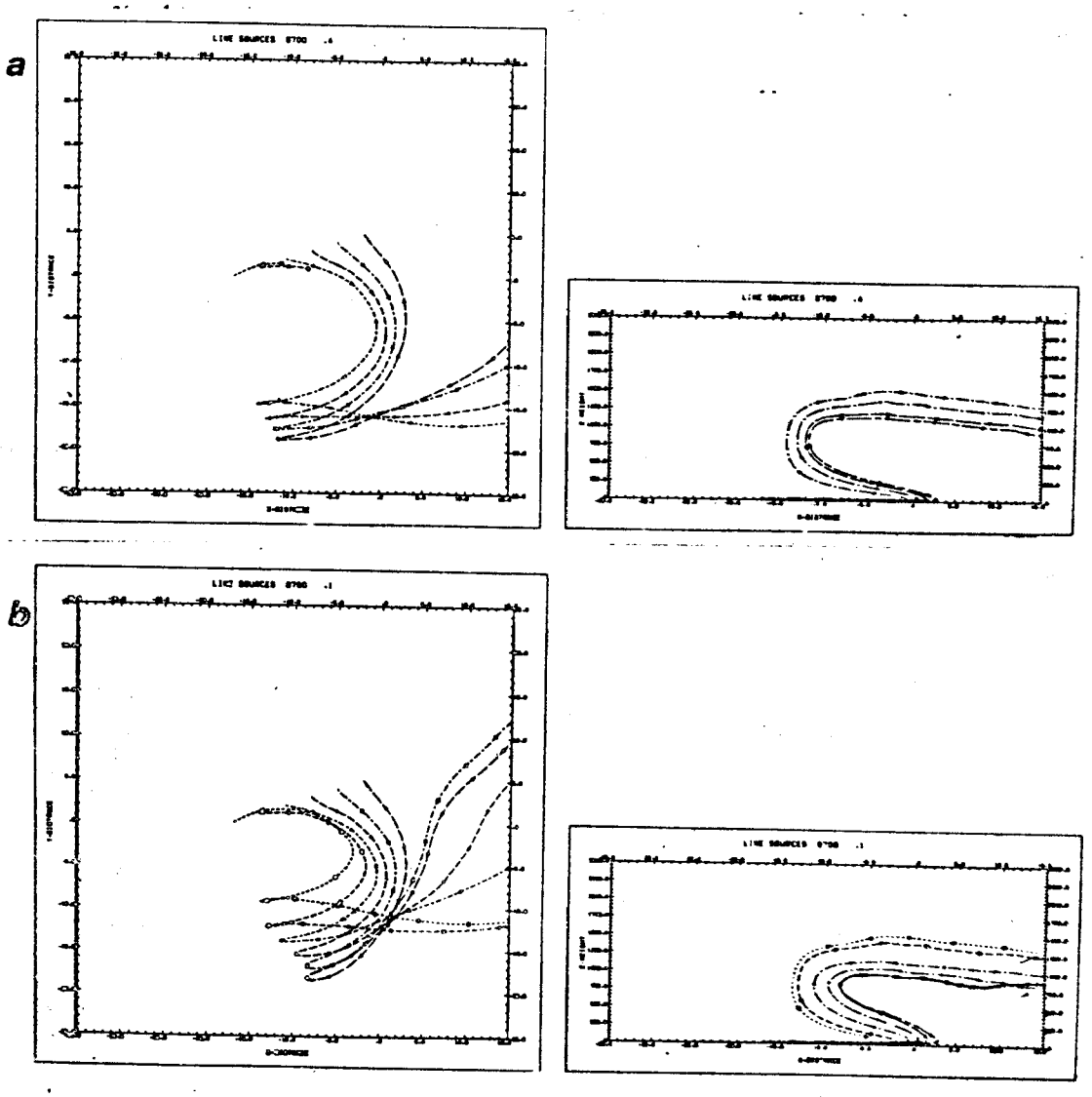

Figure 12-2. Plots of particle trajectories from a six point "line" source orientated SSW to NNE. Release time was 0700 CDT. xy (50 x 50 km) and xz (50 x 2.5 km) projections are shown and the '0' mark along the x-distance indicates the position of the shoreline. (a) shows the trajectories of the particles with a 0.4 cm sec^{-1} fall speed, (b) shows the trajectories of the particles with a 0.1 cm sec^{-1} fall speed.

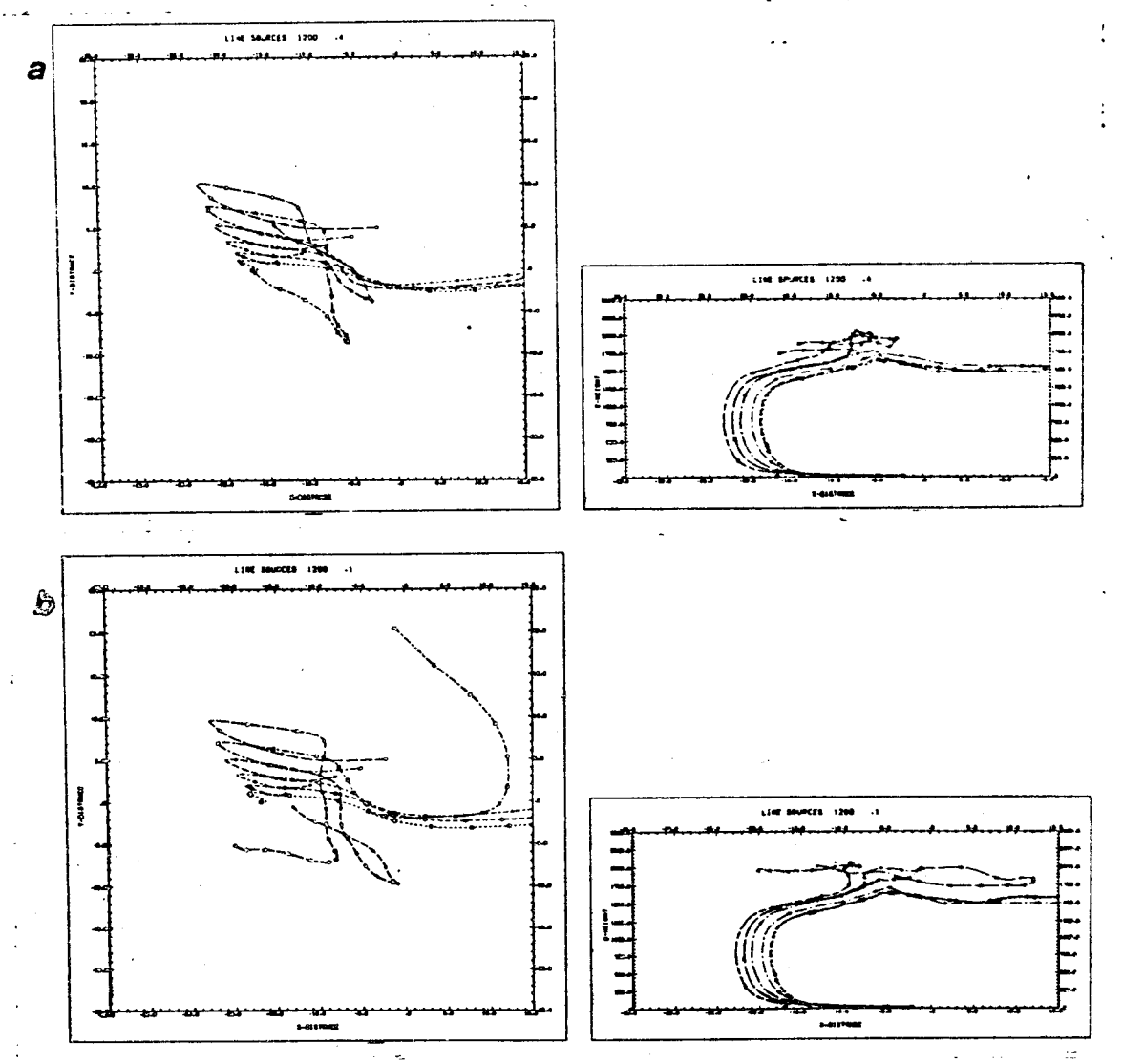

Figure 12-3. Plots of particle trajectories from a line source with a release time of 1200 CDT. (a) shows the trajectories of the particles with a 0.4 cm sec^{-1} fall speed, (b) shows the trajectories of the particles with a 0.1 cm sec^{-1} fall speed.

a

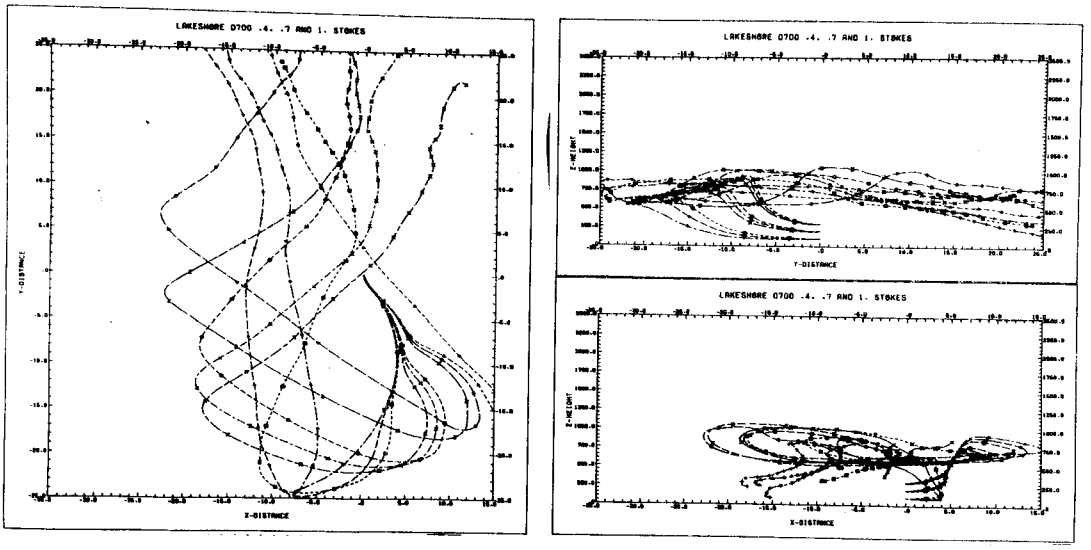

b

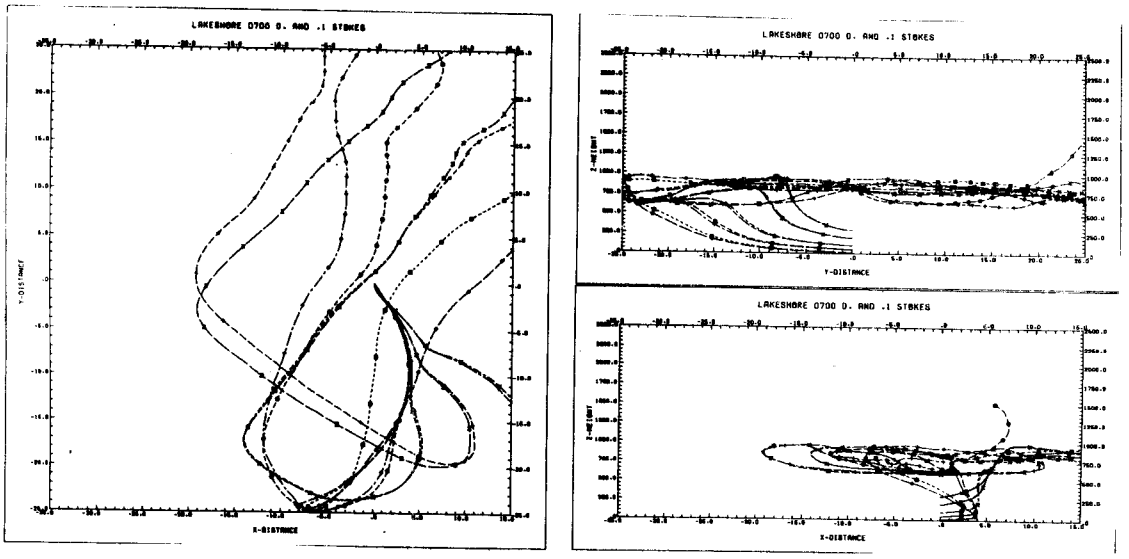

Figure 12-4. Plots of particle trajectories from a multistack source on the shore with release heights of 20, 50, 100, 200, and 300 m. Release time was 0700 CDT and trajectories were computed for an 18 hour period. (a) the xy, yz, and xz projections of the particles with fall speeds of 0.4, 0.7, and 1.0 cm sec^{-1}. (b) the xy, yz, and xz projections of the particles with fall speeds of 0.1 and 0.0 cm sec^{-1}.

a

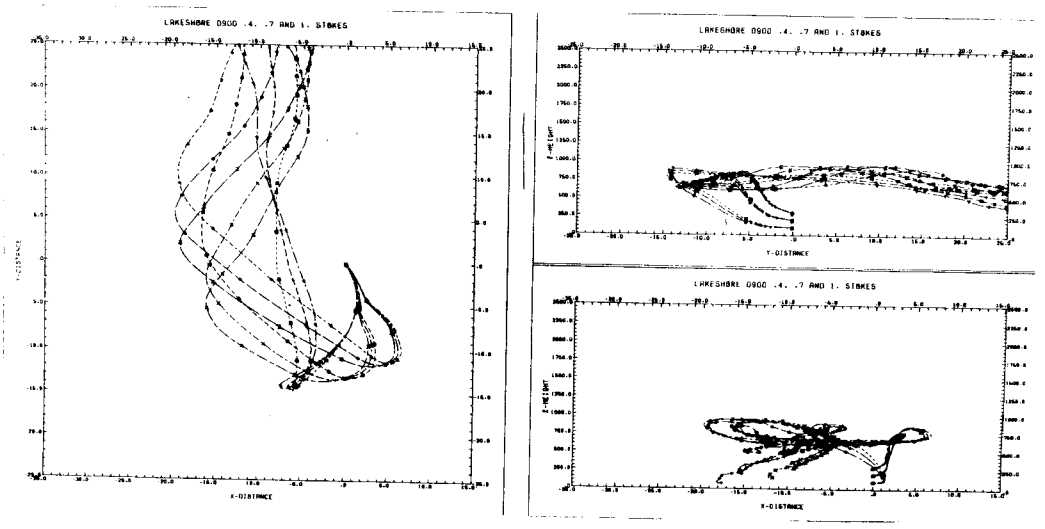

b

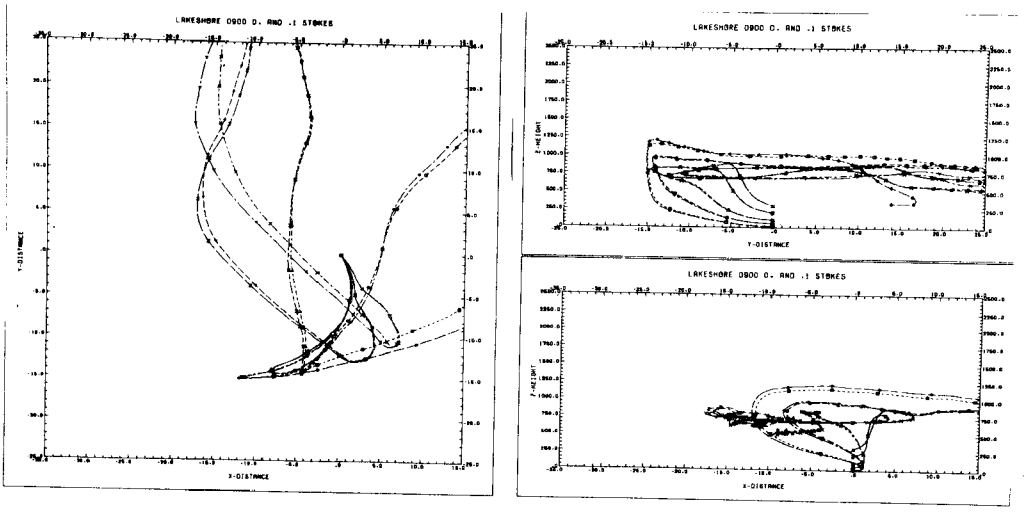

Figure 12-5. Particle trajectories from a multistack source with a release time of 0930 CDT. (a) shows the trajectories of the particles with fall speeds of 0.4, 0.7, and 1.0 cm sec^{-1}, (b) shows the trajectories of the particles with fall speeds of 0.1 and 0.0 cm sec^{-1}, (c) shows a 3-dimensional view of all the trajectories.

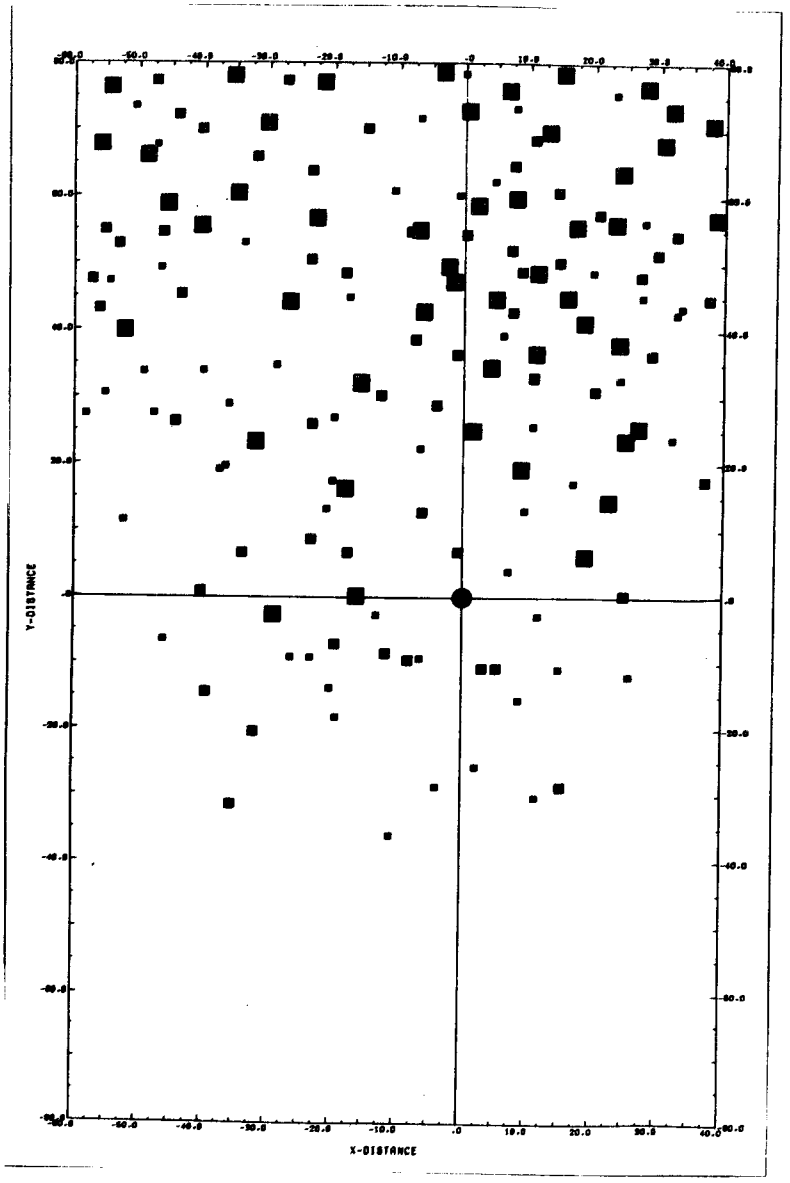

Figure 12-6. The xy projection of the positions of a series of particles at 1800 CDT. Particles were released from a multistack source on the lakeshore (marked by a large dot). The particles were grouped into 3 size ranges with the largest squares showing the positions of the particles with fall speeds of 0.7 and 1.0 cm sec^{-1}, the middle size squares mark the positions of the particles with fall speeds of 0.4 and 0.5 cm sec^{-1} and 0.0 cm sec^{-1}.

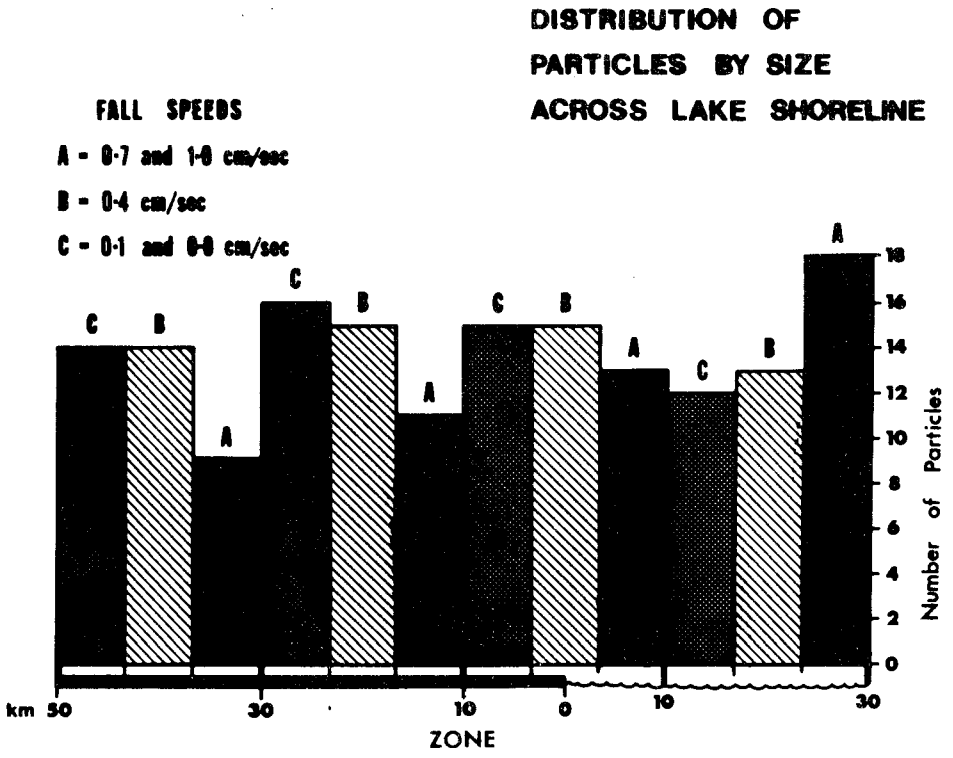

Figure 12-7. A histogram of the relative distribution of particles according to size groups across the lake shoreline. Each zone was 20 km wide and any particles having a greater than 30 km over-lake fetch or 50 km over-land fetch were disregarded.

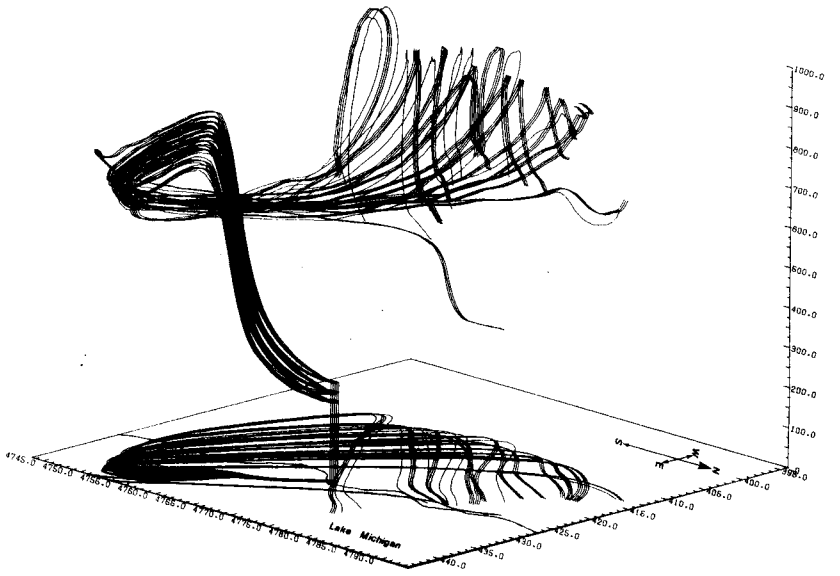

Figure 12-8. A 3-dimensional plot of a simulated aerial 'burst.' Particles were simultaneously released from a cube 200 m above the lakeshore at 0700 CDT and trajectories shown represent the travel over a period of 12 hours.

SECTION 13

LONG RANGE POLLUTION TRANSPORT

GENERAL COMMENTS

An integral part of the rationale behind the Clean Air Act of 1967-1970 was the assumption that air pollution measured at a given point emanated from "local" sources. Air Quality Control Regions (AQCRs) were established on the principle that local political jurisdictions could best cope with emissions from local sources which cause their own peculiar pollution problems. Since 1970 however, evidence has been steadily mounting that air pollution can be anything but a "local" problem. It now seems to be a certainty that certain pollutants, in particular photochemical oxidants and sulfate aerosols can and do travel considerable distances, in many cases in excess of 1000 kilometers, while undergoing complex chemical and physical transformations en route. Thus a monitor situated at any given point registers concentrations reflecting the result of local emissions, plus mesoscale and even synoptic scale transport and transformation, all commingled in a manner making it virtually impossible to separate the factions resulting from each mechanism. At least in the case of these two major pollutants, the term "natural background" has become a harder and harder one to define. Widespread occurrences of elevated rural ozone levels (Coffey and Stasiuk, 1975) attest to the viability of this chemical while traveling long distances. Although ground level SO_2 levels in cities are declining slowly

(Altshuller, 1976) increased sulfate monitoring in rural areas shows no decline, and if anything perhaps a slight rise over the last few years. Thus the reduction in near-ground level releases of SO_2, often by injection of SO_2 into the upper portion of the boundary layer via high stacks, is causing a new problem to replace an older one. Rural sulfate values several times the proposed standard are now being routinely monitored over large areas of the nation simultaneously (EPA, 1975). The Sulfate Regional Experiment (SURE) as described by Hidy, et al. (1976), is just one of several efforts now focusing on the problem of meso- and synoptic-scale air pollution. The Midwest Interstate Sulfur Transport and Transformation program (MISTT) in the St. Louis area is yet another. Already individual power plant plumes have been found traveling in a cohesive manner for distances over several hundred kilometers. The reality of meso- and synoptic-scale transport of pollutants can no longer be denied. Moreover these events do not occur on an unfrequent, but rather on a routine basis.

Various aspects of the research performed at the UWM Air Pollution Analysis Laboratory, as described below, adds several more facets to this complex phenomena.

SATELLITE DETECTION OF AIR POLLUTANTS

With the launching of Tiros I in 1960, a succession of over 40 meteorological satellites have relayed a vast amount of information gathered by an impressive array of sensors. Sensor resolution, using visible light, infrared and other wavelengths, has

consistently improved over time. The first satellite imagery, with resolutions on the order of 10-20 nautical miles, were designed to see large-scale cloud patterns, with image dynamic range so poor as to totally preclude the observation of such subtle features as smoke and haze. The ability of an orbital sensor to detect visible air pollutants however was quickly noted by 70 mm color hand-held photographs taken by astronauts as early as 1960 (see Figure 1-1). By the late 1960's, sensor resolution and spectral sensitivity had improved to the point where plumes from volcanic eruptions, Saharan dust storms, and the snoke from forest and agricultural slash burning fires could be seen. Even these, had they been interpreted in the proper light, would have been convincing proof of the frequent occurrence of long-range pollutant transport. It was not until the advent of NASA's Landsat-1 satellite however that observations of longer range pollutant transport became more routinely available. The spatial resolution of the satellite was better than 100 meters, and in addition, worked in four spectral bands: Band 4 - 0.5-0.6 μm; Band 5 - 0.6-0.7μ m; Band 6 - 0.7-0.8μm; and Band 7 - 0.8-1.1 μm. Lyons and Pease (1973) published Landsat images of the southern basin of Lake Michigan which very clearly showed plumes of smoke from Chicago-Northern Indiana sources advecting with relatively little dilution for more than 60 km northeastward over the relatively cold lake. It was found that for various reasons smoke plumes could be best detected in Landsat MSS Band 5 (the "red" band). Also of interest was that the same smoke

plumes were not as readily visible over the mottled land surface inasmuch as inherent image contrast between ground smoke was exceedingly poor (Lyons, 1975).

It had long been suspected by Wisconsin DNR officials that the Chicago metropolitan area was a major source of pollutants measured in the Southeastern Wisconsin AQCR. The original NAPCA implementation documents for this region suggested that up to 10% of the suspended particulates had Chicago as their original source. There was no easy way to prove this correlation however, in spite of the occasional observations of dense clouds of iron-oxide-red smoke drifting into the Milwaukee area from the southeast during stable cross-lake flow conditions. Figure 13-1 is an excellent example of a Landsat image of interregional pollutant transport. In this particular case the plumes drifted on southwest winds over a colder lake for distances of over 160 km with relatively little lateral diffusion. A plume σ_y of 4.5 km measured at 60 km downwind suggesting a Pasquill-Gifford stability Class E. It also appears that as distance downwind increases, the rate of lateral increase in plume width decreases. In this particular example, plumes crossed the southwestern Lake Michigan shoreline in the vicinity of Benton Harbor. Given the meteorological conditions of this date, it seems almost certain that the plume matter fumigated to the surface after a passage of only five to ten kilometers inland. Had local control officials been monitoring in this vicinity, they might have been quite perplexed at the high levels of suspended particulates, and other pollutants contained within these industrial plumes. Quite clearly there is

no way for the receptor AQCR to defend itself against the "sins of emissions" of the source AQCR, particularly if they are unaware of the phenomenon just described.

The same plumes have been implicated in regional-scale inadvertent weather modification. Specifically, Chicago industrial complex pollutants have been postulated as a cause of the LaPorte, Indiana precipitation anomoly (Changnon, 1968). As described by Lyons (1974), these plumes were "caught in the act" of apparently modifying cloud streets formed during a period of cold air advection over the southern end of Lake Michigan on 24 November 1972 (Fig. 13-2). While the satellite image does not indicate the active agents in the cloud modification (heat, moisture, cloud nuclei, ice nuclei, etc.) there seems to be little doubt that cumulus clouds began forming out of the smoke plumes considerably closer to the shoreline and that those cloud lines were also better developed. Great Lakes water management via cloud seeding has been discussed for more than five years. If large-scale inadvertent seeding is occurring from pollution sources, its effect must be clearly understood in order to assess the overall impact of advertent weather modification.

While subjective interpretation of Landsat and other satellite imagery is of tremendous value, it is generally preferable to use objective machine-oriented data analysis. As described by Lyons, Keen, and Northouse (1974), automatic image interpretation techniques were applied with success to Landsat digital data tapes. The MODCOMP II/25 computer system developed by the

UWM Robotics and Artificial Intelligence Laboratory interpreted Landsat tapes using pattern recognition techniques, specifically the cluster analysis algorithm of Eigen and Northouse (1973). Figure 13-3 shows the results. In this example water is shown by a dash (-), all land spectral signatures are suppressed and therefore blank, and those 60 by 80 meter data pixels having a spectral signature thought to be smoke are shown as filled in circles (⊗). More sophisiticated techniques would be needed in order to detect smoke over land surfaces having a wide spectrum of spectral characteristics.

On 20 August 1972 (Figure 13-4) an exceptionally well-developed lake breeze cloud system was noted over the eastern end of Lake Erie and the southern shore of Lake Ontario, along with a "smudge" over the eastern end of Lake Erie west of Buffalo, New York. This was interpreted to be the signature of smoke layers in the developing lake breeze return flow, a graphic example of the phenomenon described in the Chicago area by Lyons and Olsson (1973). As pointed out by Raynor, Hays, and Ogden (1974) any gas, aerosol, or pollen would be transported in a similarly complex manner in a lake or sea breeze circulation cell.

THE CHICAGO URBAN PLUME

During the 1974 field program conducted at Waukegan, Illinois, the major effort was concentrated on the local power plant plumes as described in the above sections. On 28 June 1974 a serendipitous measurement of the Chicago urban plume was obtained. This

case study is described in considerable detail by Lyons and Rubin (1976).

On this day, there was a brisk southeast gradient flow. Winds gradually changed from south through southeast to east, from daybreak through late afternoon. Extensive fumigation of the Waukegan power plant plume was measured. Intense elevated inversions were present over the lake from 50 to above 300 meters throughout the entire day. SMS-1 satellite imagery showed a cumulus-free zone extending several tens of kilometers inland during late afternoon. Aircraft traverses were run in east-west traverses along the Illinois-Wisconsin border throughout much of the day. The $\mathcal{E}^{1/3}$ field showed that the TIBL reached a semi-steady state after 1100 CDT, with the top of the TIBL extending to approximately 1000 meters after 20 km of inland fetch.

During the flight (1006-1154 CDT) the SO_2 plumes from the Waukegan power plant and smaller local ground sources were noted. As shown in Figure 13-5 a very concentrated plume of SO_2 with peak values above 20 pphm was present offshore at approximately 400 meters. The reasonable presumption is that this plume had emanated from the general vicinity of Gary, Indiana. More strikingly however, embedded within the overall haze was found an urban scale plume from the Chicago metropolitan area. It began approximately 15 km inland and extended to a sharp western edge approximately 28 km inland. The Chicago plume consisted of elevated values of SO_2 and fine particulates(and a noxious odor).

The Chicago urban plume had clearly traveled as a cohesive mass during the early morning hours. It was initially very

shallow, probably trapped beneath the shallow nocturnal inversion of the prior night, growing directly proportional to the penetrative convective mixing after sunrise. Aircraft measurements showed it rose almost in unison with the height of the $1.0\varepsilon^{1/3}$ isopleth. The peak concentrations of SO_2 within the plume were 145 pphm, or about 120 pphm above apparent regional "background." The fine particle concentration was a factor of five above values present within the boundary layer but outside the plume during mid-day. Visibilities outside the Chicago plume were typically 15 to 25 km, but only 5-10 km within its core. During the early afternoon the plume became more and more vertically and laterally diffuse and was found further and further westward. By the time the afternoon traverses were run, the Chicago plume was not noted within the first 30 km of the shoreline.

Using mean pibal winds within the mixed layer, a back trajectory was estimated. Air crossing the Wisconsin border at 1200 CDT was calculated to have been over industrialized extreme northwestern Indiana at 0600 CDT (100 km, 152° from Waukegan). The plume matter continued into Wisconsin where maximum hourly ozone levels (probably also associated with this plume) of almost 10 pphm were recorded between 1500-1700 CDT at Poynette, Wisconsin, some 35 km north of Madison. The amount of SO_2 entering the state of Wisconsin was considerable. An integration of plume matter contained within the 4 pphm isopleth yielded transport rate of 25 tons/hour at 1100 CDT. This would compute to an annual rate of 22,000 tons/year.

From this observation alone it is impossible to assess the annual average impact upon air quality of Wisconsin AQCRs by the Chicago metropolitan area. But given the relatively high frequency of southeasterly gradient flow in this area, and for those pollutants where federal standards are just marginally being exceeded, at least legally, the impact might be considerable.

MESOSCALE TRANSPORT OF PHOTOCHEMICAL OXIDANTS WITHIN LAKE BREEZES

The traditional "recipe" for photochemical "smog" (which is primarily ozone) that is given in textbooks includes, 1) large quantities of precursors, reactive hydrocarbons (RHC), and the oxides of nitrogen (NO_x), 2) strong solar radiation, 3) relatively high ambient temperatures, 4) relatively light wind speeds, and 5) limited mixing depths. It is assumed the RHC and NO_x precursors react in the presence of sunlight within some unspecified distance, perhaps several kilometers downwind of the sources, producing a peak of photochemical oxidants shortly after noon with a gradual fall-off to near zero by and during the following nighttime hours. As pointed out by Cole and Lyons (1972) the high emissions of primary pollutants in the Gary-Chicago-Milwaukee corridor combined with lake effects make this region a prime suspect for photochemical oxidant episodes. This was confirmed during 1971, when EPA monitored for photochemical oxidants 99 days at a suburban site 2 km inland from Lake Michigan, and 10 km north-northwest of the central business district. Maximum hourly averages of 19 pphm were reached - the highest for any city over

200,000 population monitored. On 18 days readings in excess of the 8 pphm hourly average federal standard were observed. Most interesting though was the fact that fully 94% of the exceedences occurred with winds from west-southwest through southeast, and 67% from the south through southeast alone. Inspection of the data showed frequent sharp rises in ozone after the passage of lake breeze fronts. Furthermore peak values frequently occurred during late afternoon and sometimes even early evening after sunset. These data were among the first to suggest that the source of southeastern Wisconsin't ozone might be at least in part, the Chicago metropolitan area.

During 1973 the Wisconsin DNR installed a network of air quality stations around Milwaukee and also Racine, Wisconsin, near the lakeshore, 30 km south of the Milwaukee CBD. Also an additional "rural background" installation was made at Poynette, Wisconsin.

In a 47-day period during late summer 1973, at least two or more stations in the network (excluding Poynette) reported readings greater than 8 pphm on a total of 27 days. On nine of these days episode alert dosage thresholds (40 pphm h) were obtained at one or more sites. Hourly averages as high as 27 pphm were measured at Racine. A pollution wind rose, based on the MKE mean resultant daily wind, showed that 92% of the days with standard exceedences had daytime winds from the southwest through east-southeast. Racine frequently reported the highest ozone readings, which is somewhat odd if one considers that the area only has approximately 12% of the RHC and NO_x emissions of Milwaukee

County. During 1974 and 1975 even higher values have been recorded in the Racine area. Thus with the noted strong correlation between high ozone levels and southerly winds the Chicago and northern Indiana industrial complex looms as the immediate candidate for the source of a large fration of the ozone measured in southeastern Wisconsin.

Some local patterns in ozone distribution however also emerged (Lyons and Cole, 1976). Figure 13-7 shows data taken from six monitoring sites during the 1973 summer. It appears that ozone levels near the immediate shoreline (less than 1 km) are relatively low, and then there is a sharp rise in about 1-4 km inland, with a gradual fall-off further to the west. More complete 1974 data confirm this pattern. Esser (1973) used specifically chosen bioindicator plants (Bel W-3 tobacco) to monitor photochemical oxidant patterns in the greater Milwaukee area (Figure 13-8). Analysis of his results shows that damage is relatively infrequent in the first kilometer form the shoreline but then rises sharply as one proceeds inland. A band of 25% or more damage runs north-south parallel to the shore from approximately 1.5 to 8 km inland, then there is a gradual fall-off further inland. Since higher ozone values are usually found with an onshore component of the wind, why are the values near the immediate shoreline lower?

A mechanism is proposed to explain this pattern. A typical lake breeze day dawns with a weak land breeze in progress (Figure 13-9). Pollutants produced by morning rush-hour traffic drift

offshore over the lake. Since the air becomes warmer than the lake water after sunrise, a strong low-level conduction inversion is present over the lake, perhaps 100-200 m in depth. Ship wiresonde observations (Bellaire, 1965) indicate that the offshore flowing air and its pollutants should tend to flow up and over the shallow surface inversion leaving the air near the lake relatively "clean." Lack of penetrative convection over the cold lake allows the air above the inversion to become stratified, and sunlight acts on the primary pollutants, forming ozone. The newly produced ozone cannot penetrate the surface inversion, and little scavenging of the gas occurs and concentrations increase. After the onset of the lake breeze inflow, the onshore flowing air has little ozone near the surface, with the bulk of it being stratified from perhaps 150-500 meters aloft. In a manner analogous to continuous fumigation of elevated shoreline plumes, the ozone aloft is intercepted by the deepening TIBL as the airstream moves inland. The ozone and other pollutants are fumigated to the surface in relatively high concentrations beginning 1 or 2 km inland. After perhaps 5 km inland fetch, the bulk of the ozone has been mixed within the deepening TIBL. Rapid destruction now begins by contact with the surface plus the addition of NO. Similar patterns have been discovered at the inland boundary of the west coast marine inversion by Miller and Ahrens (1969), Edinger, et al. (1972), and Blumenthal et al. (1974). While Figure 13-9 assumes that the air flow is purely two-dimensional (in the plane of the paper) it provides a reasonable explanation for the observed patterns.

The experience in southern California proves photochemical oxidants can indeed be transported for long distances. Edinger, et al. (1972) show tree damage in mountainous areas 120 km distant from the source of the primary pollutants. Blumenthal et al. (1974) computes over 100 tons per hour being advected from the Los Angeles basin to areas further east. That the Chicago metropolitan area could be acting as giant source adding to locally produced photochemical oxidants in southeastern Wisconsin is therefore not surprising. But since lake breezes have a highly complex transport wind as described above, the exact mechanism by which the transport occurs is hard to specify.

Figure 13-10 represents hypothetical air trajectories used to explain an ozone episode in southeast Wisconsin on 17 July 1973. Trajectories A and B represent air (and pollutant) motions near the surface which moved roughly northward during the day, totally unaffected by the lake. Trajectory C marks an air parcel released near the ground around 0800 LST, which drifted northward only to be undercut by the inland rushing lake breeze. Trajectory D represents a low-level release around sunrise. With the formation of the lake breeze, this air, which by now has developed a considerable photochemical oxidant burden, crosses the shoreline at Racine about 1-2 km inland, and fumigation of ozone to the surface begins (heavy line). Trajectory F is somewhat similar in behavior except it leaves the shore perhaps around 0900 LST. This parcel may fumigate further south around Kenosha. The air then rises into the return flow layer near the

lake breeze front and after traveling northeastward, it may sink back down into the upper portion of the inflow to once again fumigate while passing inland. In the case of trajectory E, this parcel is released near the shoreline within the lake breeze inflow during late morning. It spirals northward and finally fumigates over Racine late in the day.

In reality, there are an infinite variety of possible trajectories and many of them may be variations of those above. The results of the KDM would suggest the air motions, if anything, are even more complex than described in Figure 13-10. This mechanism is consistent with the simpler two-dimensional view of the lake breeze in Figure 13-9 inasmuch as it still allows for the fumigation mechanism to produce the inland ozone maximum. It also explains the late afternoon and even nighttime elevated ozone readings in Milwaukee and Racine. Parcels of air arriving in Wisconsin come from a spectrum of distances and release times. Air streaming onshore after dark, which left the Chicago area during morning rush-hour, can cause high surface ozone readings simply due to mechanical mixing of the air from above the 100 m level to the ground. This is a "mechanical fumigation" which may well be aided and abetted by "urban heat island fumigation." The lack of appreciation by some officials of the complex meteorology involved in ozone transport is emphasized by Altshuller (1975) who discovered some monitoring reports where high nocturnal ozone values were sumarily dismissed as inaccurate per se.

When the southeasterly gradient flow is strong enough so

that no lake breeze circulation is present, relatively high ozone levels still occur in the nearshore areas of southeastern Wisconsin. The primary pollutants released at the southern end of the lake still travel with relatively little vertical dilution across a cold lake, reaching the downwind shoreline with a considerable ozone burden. In this case the air trajectories are far less convoluted.

LONGER RANGE PHOTOCHEMICAL OXIDANT AND SULFATE TRANSPORT

The distinction between mesoscale and synoptic scale transport of pollutants may be almost semantical. However in the case of photochemical oxidants, it may be appropriate for photochemical reasons to classify as synoptic transport those events taking more than one day's time.

The literature is now replete with reports studying widespread rural elevated ozone levels. Rural ozone monitors within the state of Wisconsin have not been exempted from this phenomenon. During 1973 the Wisconsin DNR ozone monitor at Poynette, which is 140 km west of Lake Michigan, began collecting rural "natural background" data. During the 1973 summer at least 189 hours of episode alert dosages were recorded on a total of 24 different days, the first as early as 24 May. While the values were not as high as in the lakeshore region (maximum only 16 pphm), 8 pphm was frequently exceeded. The pollution wind rose (Figure 13-11) based on the Madison, Wisconsin resultant daytime surface winds, shows once again a strong directional preference, with 84% of the alert level hours occurring with winds from the

southwest through the east-southeast. The 41% of the events occurring with winds from the southwest quadrant cannot easily be attributed to the Chicago, Milwaukee, or Madison area urban plumes.

On 27 August 1973, typical of days with elevated rural ozone levels, there was a general southwest surface flow through the central United States around a high pressure system moving slowly through the Appalachinas. The Poynette site recorded 12 consecutive hours of alert levels beginning at 1000 LST. A backtrack of air trajectories showed these air parcels had traversed such major urban areas as Kansas City, Dallas-Fort Worth, and Houston in the previous three days. Remembering that the low-level jet stream mechanism (Bonner, 1968) has high velocity wind cores exceeding 25 m/sec within the nocturnal boundary layer, it is quite possible for materials to be advected more than 1000 km within a 12-hour period. In effect, large metropolitan areas within the eastern 2/3 of the United States can be considered as a patchwork of large volume sources of RHC and NO_x, which is vertically distributed within the daytime mixed layer. Downwind, in the absence of additional NO emissions, ozone forms, or if the sun has set, the primary pollutants stay in relatively high concentrations within the urban plumes. The development of the nocturnal radiation inversion allows frictional decoupling from the surface producing the low-level wind maximum aloft, and also encapsulating the pollutants aloft in what was the prior day's mixed layer. This also prevents further input of fresh NO. By sunrise the next morning either the primary pollutants begin forming oxidants or an existing pool of ozone is present aloft, typically stored in

a layer below the synoptic scale subsidence inversion and above the top of the prior evening's radiation inversion break-up fumigation. It has been noted on numerous occasions in Milwaukee during southwesterly flow that ozone suddenly increases at the surface during mid-morning at the time an acoustic sounder shows the rapid burn-off of the inversion with the development of convective plumes.

In effect, entire air masses can become polluted. Ripperton et al. (1974) made airborne ozone measurements during anticyclonic conditions over North Carolina, Ohio, West Virginia, and Pennsylvania, finding widespread ozone levels near or above 8 pphm rather uniformly vertically mixed within the daytime mixed layer. There was no apparent specific source of the pollutants. Air masses characterized by elevated ozone levels also have an appreciable degree of haziness. The Landsat-1 satellite has observed these widespread turbidity episodes. Figure 13-12a is a picture of the southeastern shoreline of Lake Ontario on a late winter day when the region was covered by a very clean cP air mass. The exact same region was monitored on 1 September 1973 (Figure 13-12b) during a widespread air stagnation episode. Very light southwesterly winds covered the region. Sparse precipitation and relatively shallow mixing depths allowed effluents from much of the Ohio Valley and Appalachian region to commingle for several days producing a widespread air mass turbidity which made the ground virtually invisible to the Landsat sensors. Ernst (1975) has noted in SMS imagery large hazy masses of air drifting off

the U.S. east coast. The occurrence of widespread air mass pollution was noted by Hall et al. (1973) in their study of an August 1970 air stagnation. The movement of a large volume of air characterized by visibilities severely reduced due to smoke and haze for several thousand kilometers was studied. As shown by Altshuller (1976) and Wilson et al. (1975), the haziness is largely associated with sulfate aerosols formed by complex gas phase reactions in the atmosphere. These sulfate episodes, which could also be as easily termed "smog blobs" due to their frequent coincidence with elevated ozone levels, are associated with mT anticyclones, and their attendent synoptic scale subsidence, lack of precipitation and therefore wash-out of pollutants, low visibilities, very warm temperatures, high dewpoints, low mixing depths, and light transport winds. It is noted by Husar et al. (1976) that these episodes can be present over the eastern 2/3 of the United States for up to two weeks at a time. The latter part of June and early July 1975 was characterized by a significant sulfate episode in the central and eastern U.S. Most amazingly is the fact that standard SMS satellite imagery was able to detect this event (Figure 13-13). Extremely large areas of turbid air covering many states could be tracked on a day-to-day basis by inspection of the SMS imagery.

Fortuitously and coincidentally the MISTT program was conducting field studies in St. Louis during that period. Mid-day visibilities in eastern Missouri deteriorated to about 4 km during the peak of the episode. The low visibilities were associated with relative humidities as low as 40% elimanating

consideration of fog or "water haze" situations. Aircraft and ground instruments showed degraded visibility to be widespread and not a local phenomenon. At the peak of the episode, total suspended aerosol mass was not unusually high, approximately 100 μgm/m^3. Chemical analyses however showed the total sulfate aerosol content to be as high as 35 μgm/m^3, nearly three times the proposed national standard for sulfates. Furthermore, of that, nearly 40% appeared to be comprised of sulfuric acid aerosol. A conversion of Service A teletype visibility reports to equivalent b_{scat} values (Husar, 1975) showed a very high degree of correlation between the satellite photograph turbidity producing reduced ground contrast and the geographical extent of the turbid air mass (Figure 13-14).

The rather amorphous and slowly changing shape of the "smog blob" makes the origins of the aerosols hard to determine. An attempt at plotting the path of the center of the stagnant high pressure cell was inconclusive due to minute pressure changes resulting in an apparent erratic translation from chart to chart. More illustrative however is a plot of the 1020 mb isobar position for each 1200 GMT surface map, 25 June through 30 June 1975 (Figure 13-15). Since the situation was so nearly steady-state, this ensemble can be thought of as a crude approximation of the trajectories of boundary layer air parcels. Note the general appearance of flow from the high power plant density region of the Ohio Valley into the Midwest where the "smog blob" is most obvious on 30 June. As the haze area gradually penetrated into the Minneapolis/St. Paul area, surface visibilities

degraded from 40+ km on 27 June to 5 km on 29 June. Elevated oxidant values throughout this entire region were also simultaneously recorded. An important finding is that initial studies suggest that the degree of haziness seen on the photograph is surprisingly well-correlated to mid-day surface visibility reports, which in turn has a somewhat consistent relationship to sulfate aerosol concentrations (Husar, 1975).

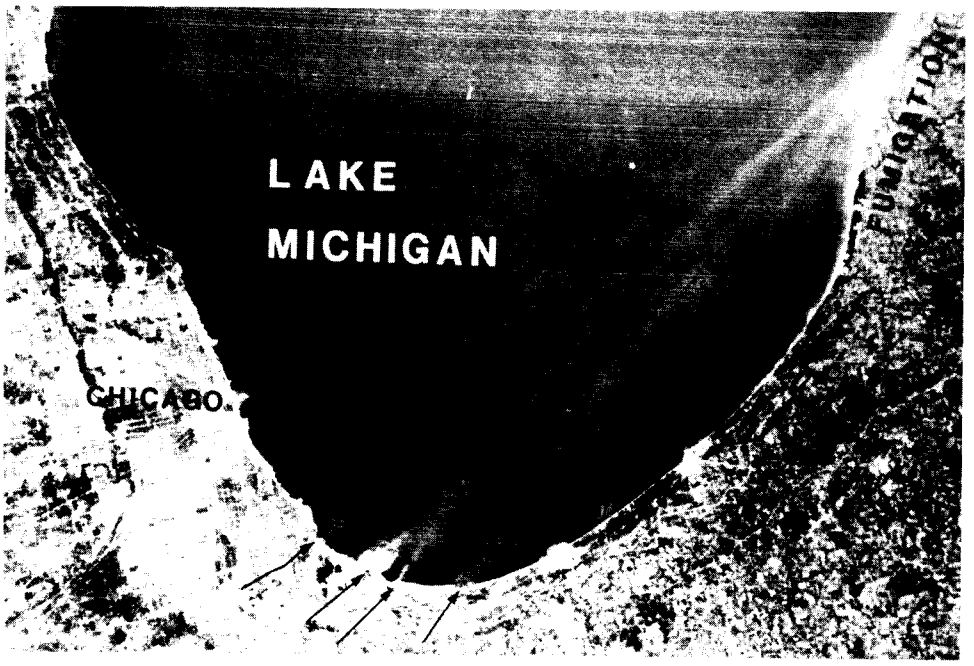

Figure 13-1. Landsat-1, Band 5 (0.6-0.7 μm) image of Chicago-Gary area, 1003 LST, 14 October 1973. Smoke plumes advect across the relatively cold lake showing little diffusion, only to fumigate on downwind shoreline near Benton Harbor, Michigan.

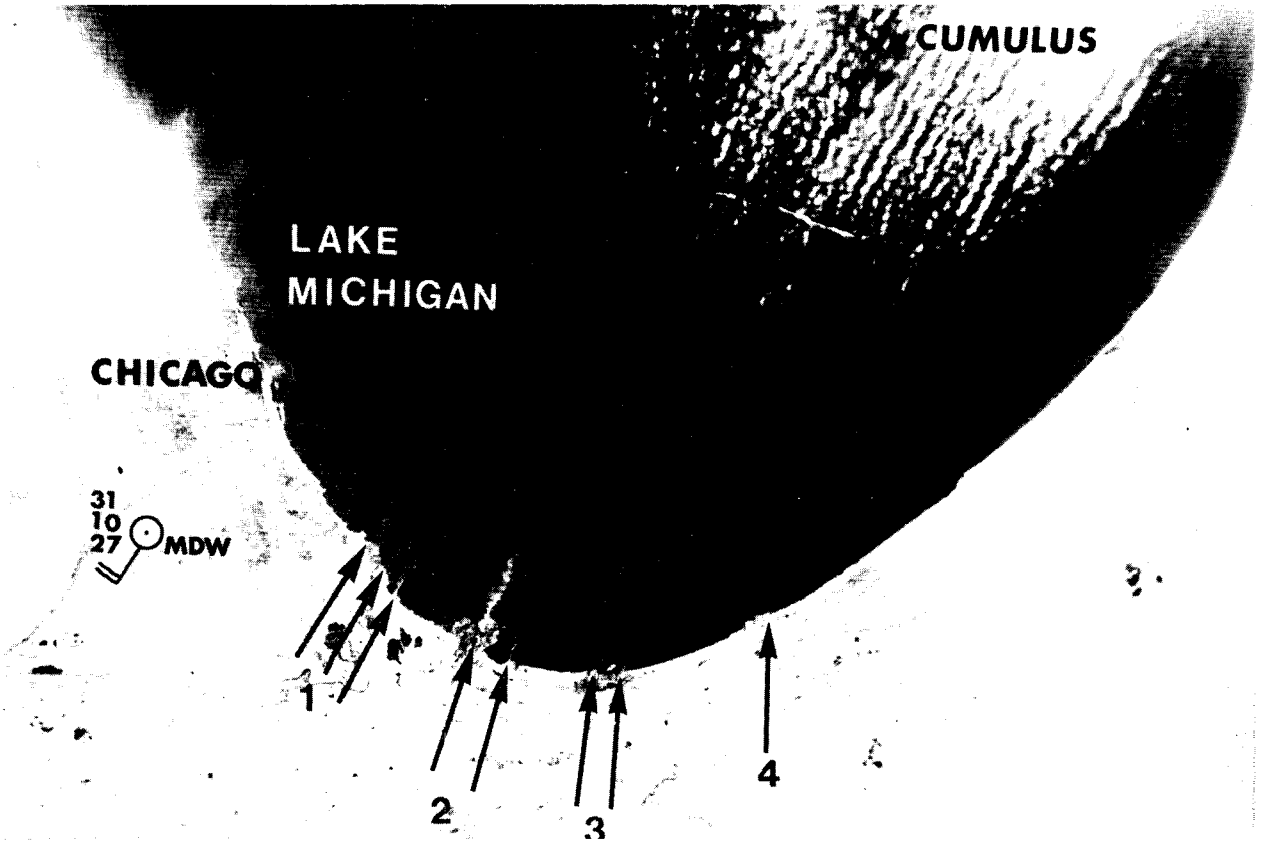

Figure 13-2. Landsat-1 image, Band 6 (0.7-0.8 μm), over southern Lake Michigan, 1003 LST, 24 November 1972. Four major particulate plumes emanate from shoreline sources. Cumulus clouds form over relatively warm lake, and those arising out of smoke plumes form closer to shore and become larger and brighter.

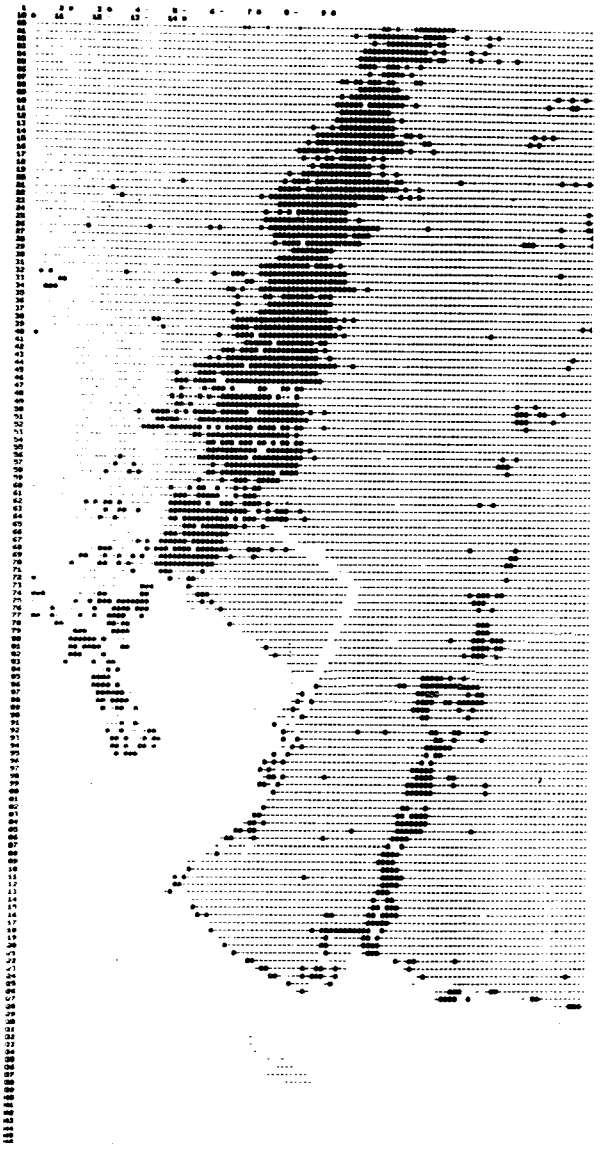

Figure 13-3. Computer processed Landsat-1 digital data, small segment of frame taken along southern Lake Michigan shoreline, 1003 LST, 1 October 1972. Lake water indicated by (-), all land signatures are suppressed (and therefore blank), and smoke is denoted by (⊗). Note man-made peninsula and breakwater protruding into lake. The plume on the left is from a steel mill complex, while the one on the right is from a cement plant.

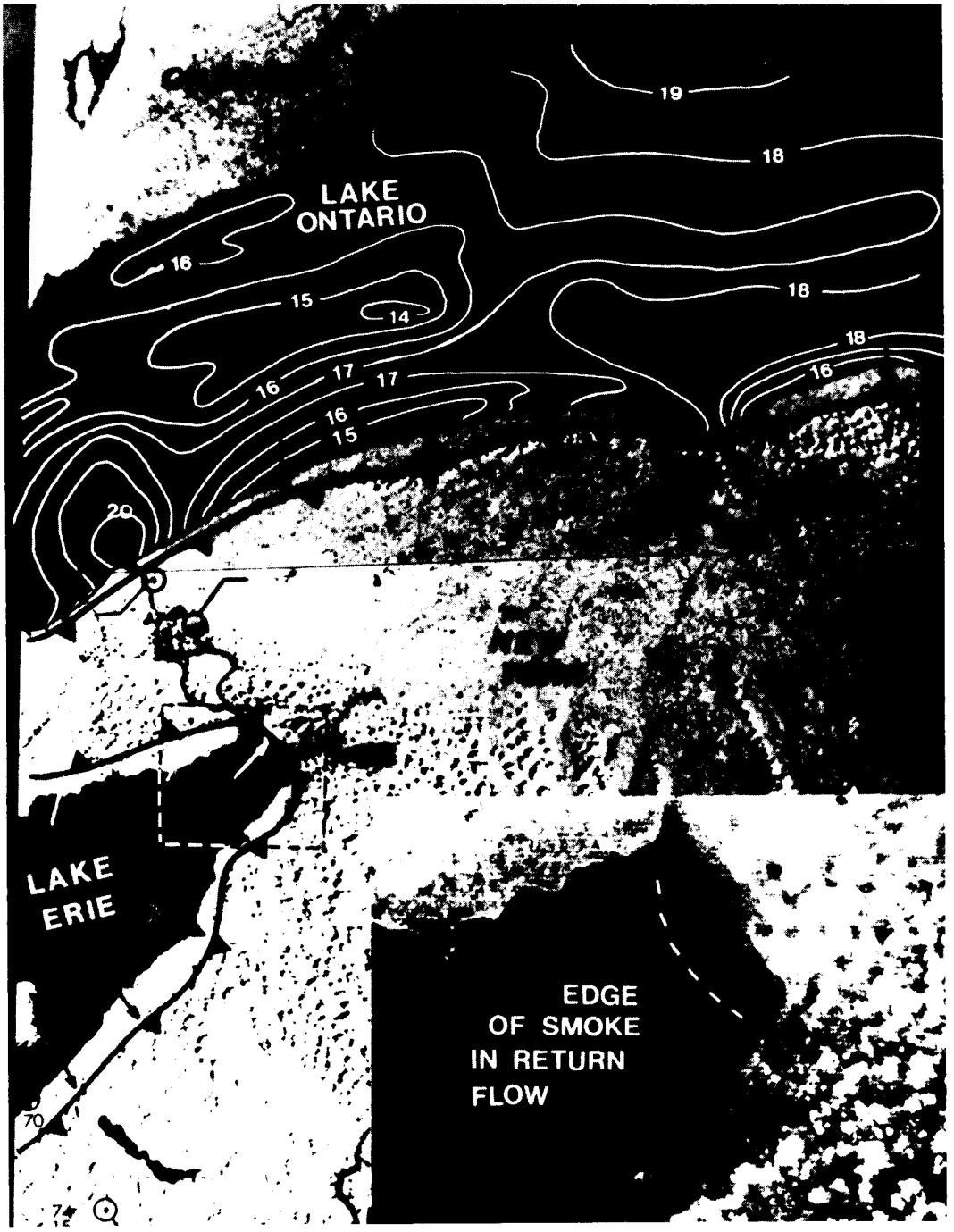

Figure 13-4. Landsat-1 image, band 6, of 20 August 1972 showing a portion of Lake Ontario and the eastern end of Lake Erie. A well defined lake breeze rings both lakes (with the front indicated). The inset is an enlargement of the Buffalo, N.Y., area over which smoke in the return flow layer can be seen extending over the lake. Water temperatures (°C) are shown for Lake Ontario and the 1000 CST hourly aviation weather data is plotted. (Each barb equals 2.5 m/sec).

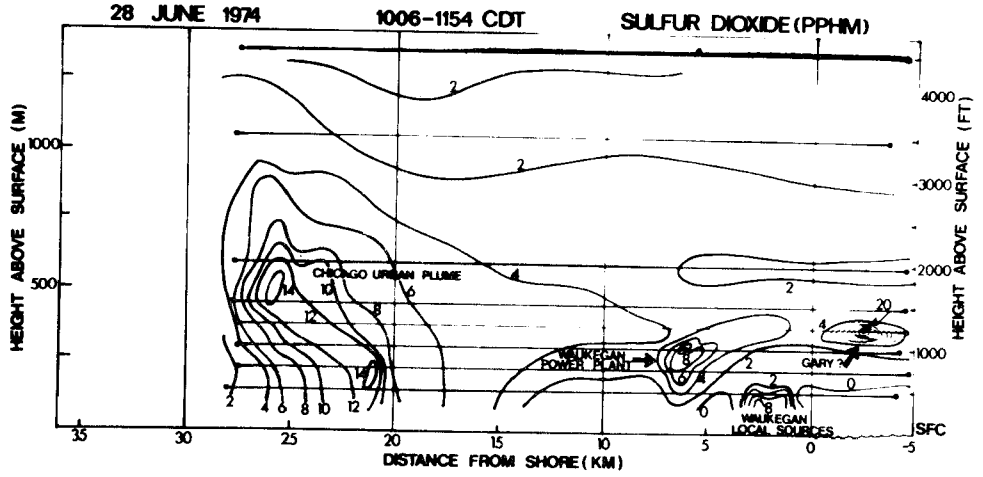

Figure 13-5. Aircraft measurements of SO_2 (pphm) profiled in an east-west path along the Wisconsin-Illinois state border, 1006-1154 CDT, 28 June 1974, surface to 1500 meters. Clearly visible are the Chicago urban plume, the plume from Waukegan's power plant, local Waukegan sources, and probably a plume emanating from Gary (with peak concentrations above 20 pphm).

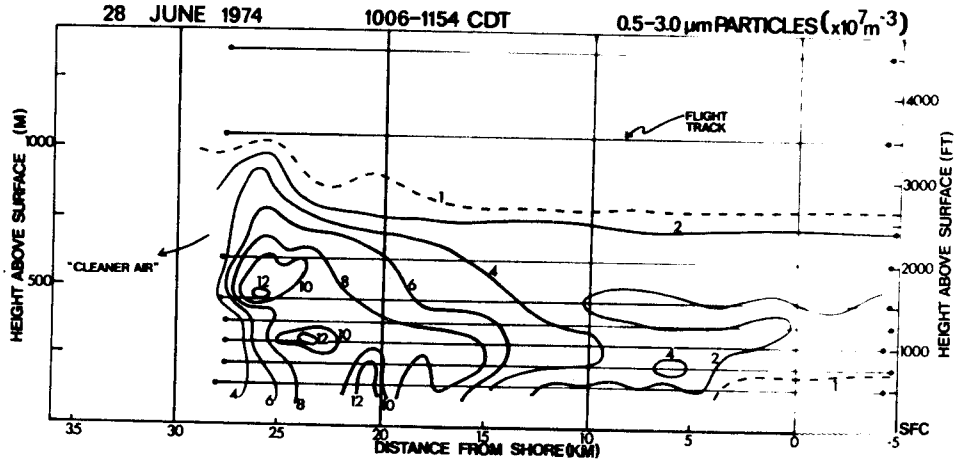

Figure 13-6. The same as 13-5, except for concentrations of aerosols in the 0.3-1.3 μm size range.

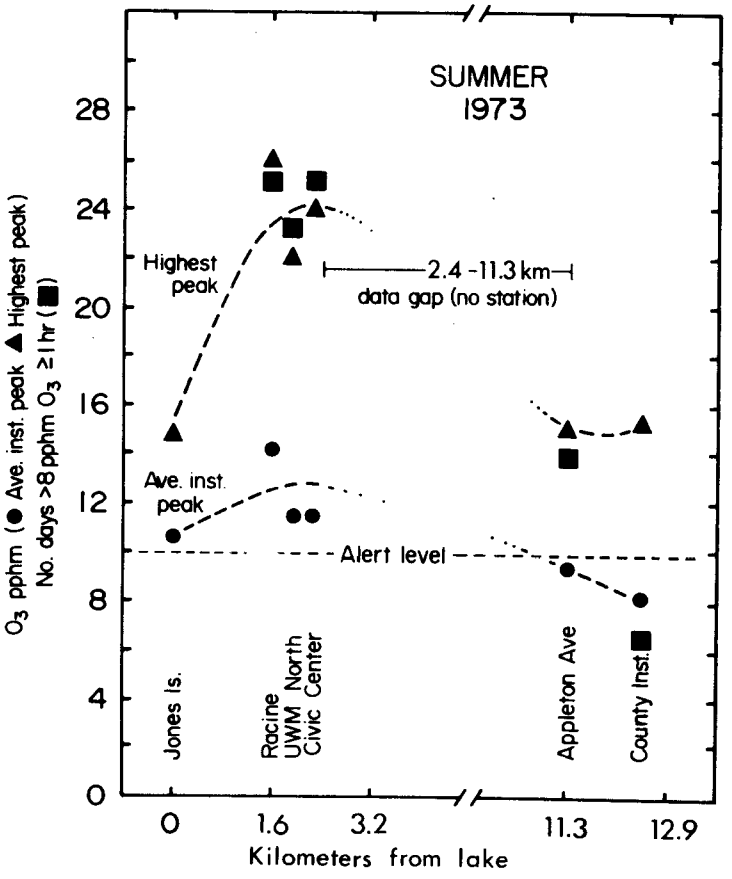

Figure 13-7. Data from six monitoring sites from 15 July through 31 August 1973 (except Jones Island which began 4 August). Data plotted as a function of distance from the lake. Dots indicate average instantaneous peaks measured on all days. Triangles are the highest instantaneous peaks recorded. Squares denote number of days with readings > 8 pphm.

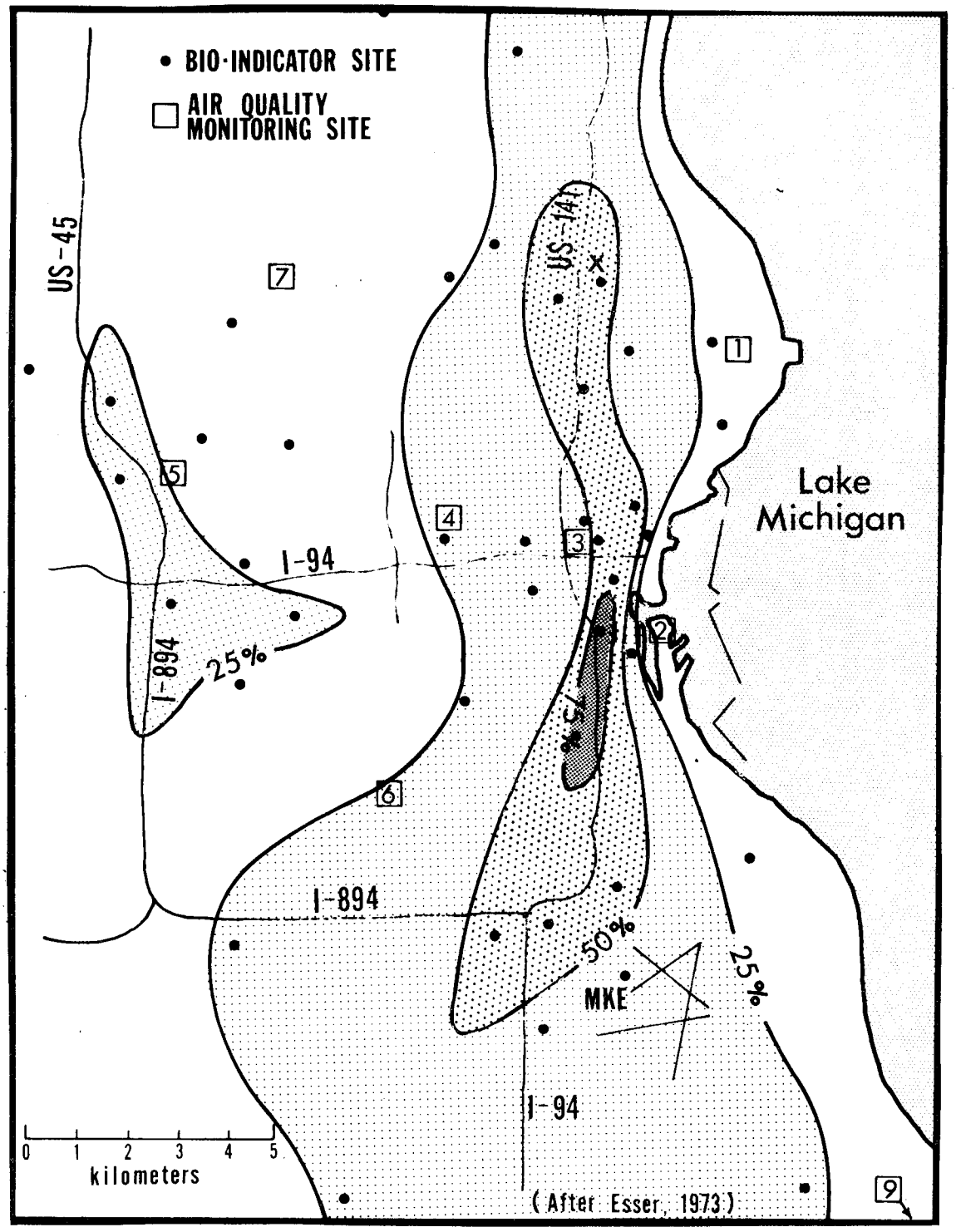

Figure 13-8. Isopleths of percentage of sensitive plants experiencing photochemical oxidant damage in Milwaukee during the summer of 1972. Wisconsin DNR air quality monitoring sensor indicated by numbers in boxes. The "X" locates the EPA monitoring site active in the summer of 1971. MKE is the National Weather Service station at Mitchell Field.

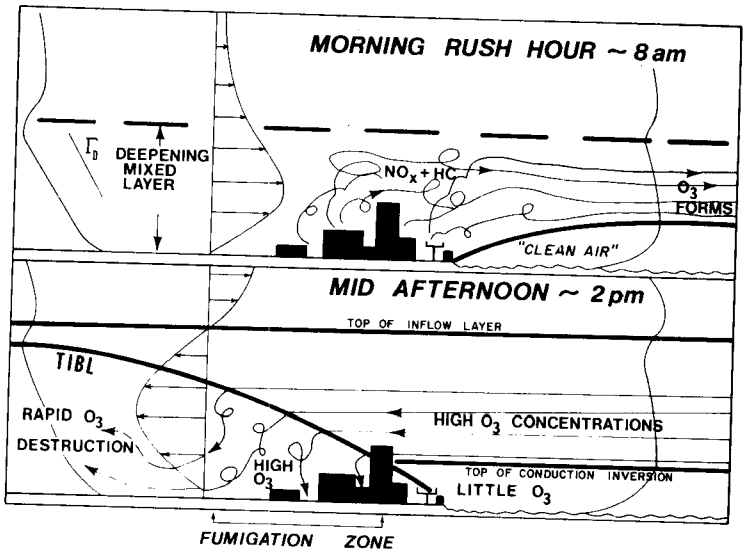

Figure 13-9. Schematic showing the mechanism by which a lake breeze causes elevated ozone levels in a narrow band parallel to the shore but several kilometers inland. This diagram refers to idealized conditions when the lake breeze flow is purely two-dimensional (in the plane of the paper).

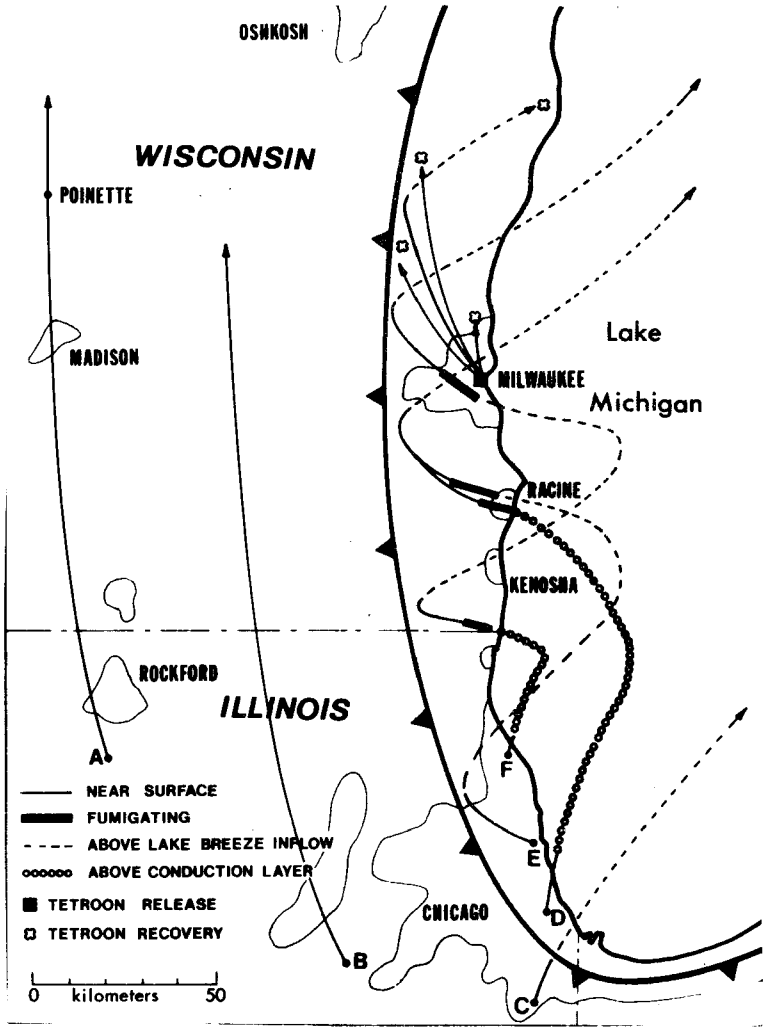

Figure 13-10. Hypothetical trajectories of air parcels (and pollutants) along the western shoreline of Lake Michigan during a lake breeze event.

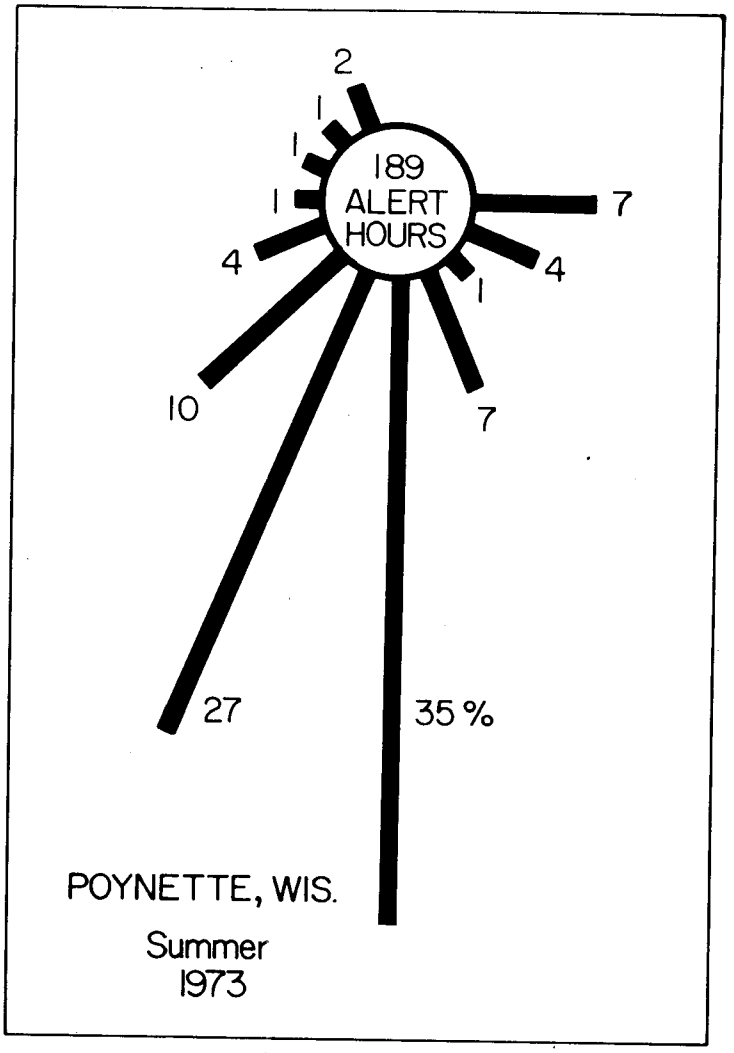

Figure 13-11. Pollution wind rose for Poynette for days on which ozone exceeded episode alert levels in summer of 1973. Winds measured at Madison, Wisconsin NWS station. Based on DNR report.

Figure 13-12a. Landsat-1 image, Band 4 (0.5-0.6μm), 0945 LST, 23 March 1973, of the eastern Lake Ontario region, on a cloud-free day with low atmospheric turbidity. Snow cover is spotty through the region. Rochester, New York indicated by ROC.

Figure 13-12b. Identical geographic area as Figure 13-12a, Landsat-1 Band 4, 0945 LST, 1 September 1973 on a cloud-free day but with highly polluted atmosphere associated with synoptic scale air stagnation sulfate episode.

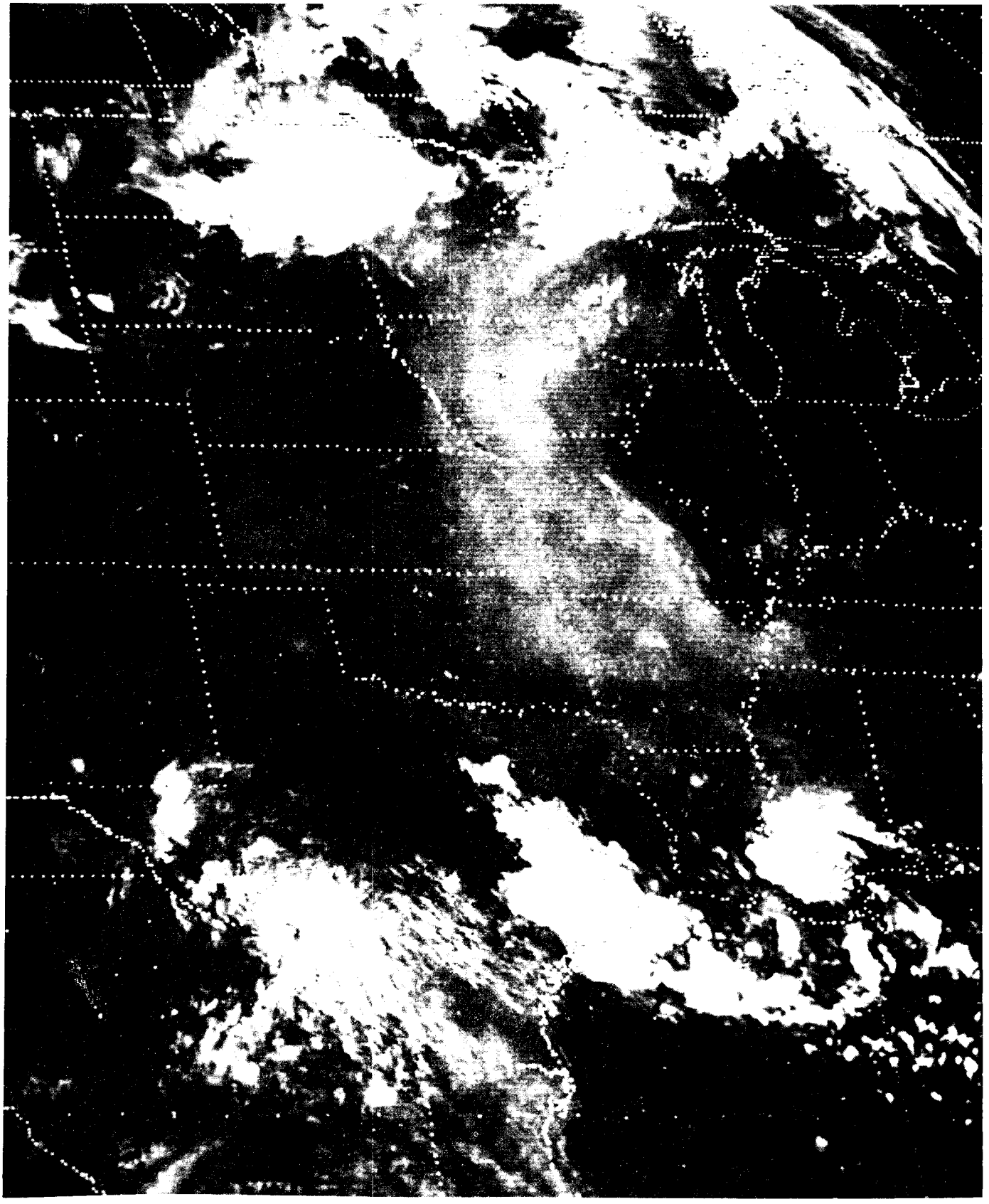

Figure 13-13. Portion of an SMS-1 visible image (1 NM resolution) taken 1445 GMT, 30 June 1975. Atmospheric turbidity over the central U.S. enhanced by re-photography of the original. Datalog print courtesy National Weather Service Forecast Office, Twin Cities, MN.

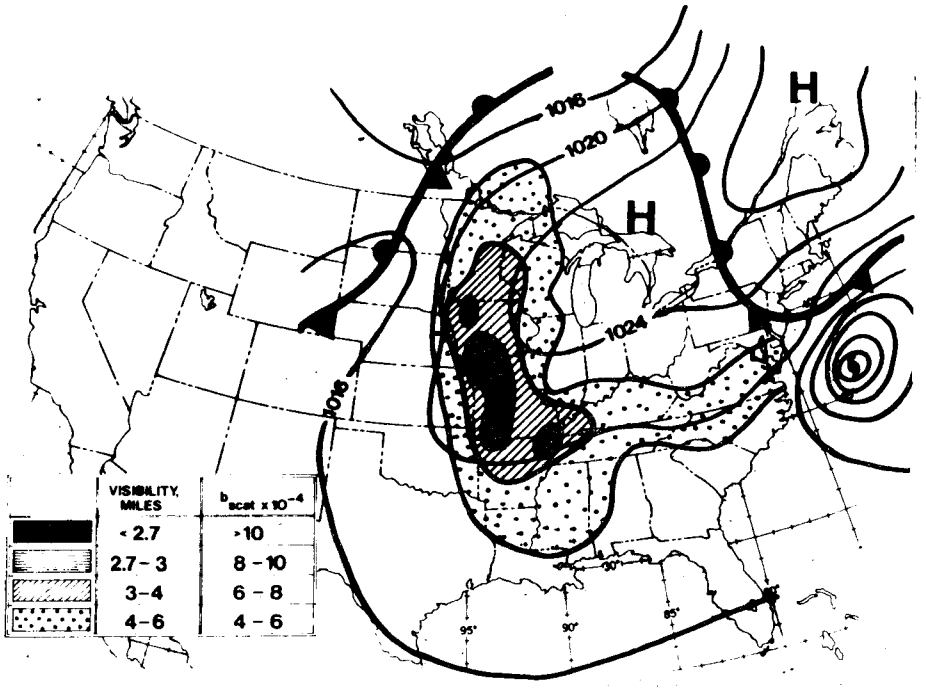

Figure 13-14. Surface synoptic chart, 1200 GMT, 30 June 1975, with contoured shadings representing areas of reduced visibility (and corresponding back-scattering coefficients) acquired from Service A network data at 1800 GMT.

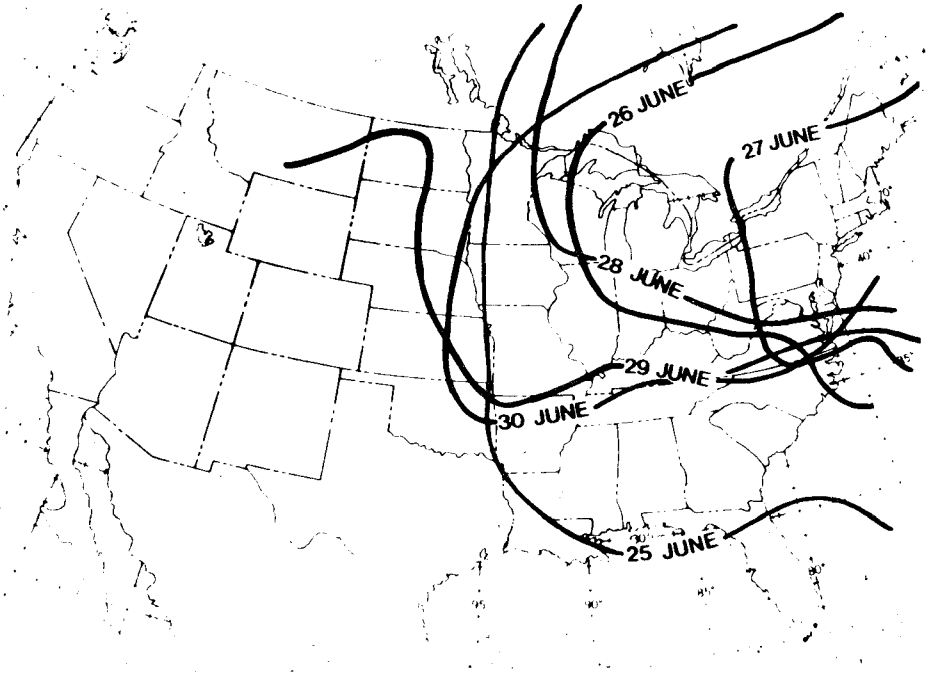

Figure 13-15. Location of the 1020 mb isobar on six consecutive 1200 GMT synoptic charts during the period 25 June - 30 June 1975.

REFERENCES

Altshuller, A.P., 1976: Regional transport and transformation of sulfur dioxide to sulfates in the U.S., J. Air Poll. Control Assoc., 26, 318-324.

Altshuller, A.P., 1975: Evaluation of oxidant results at CAMP sites in the United States. J. Air Poll. Control Assoc., 25, 19-24.

Angell, J.K., 1975: The use of tetroons for probing the atmospheric boundary layer, Atmos. Tech., 7, 38-43.

Baralt, G., and R.A. Brown, 1965: The land and sea breeze: an annotated bibliography, The University of Chicago, Satellite and Mesometeorology Research Project, 61 pp.

Bellaire, F.R., 1965: The modification of warm air moving over cold water, Proc. 8th Conf. Great Lakes Res., Intern. Assoc. Great Lakes Res., 249-256.

Bierly, E.W., 1968: An investigation of atmospheric discontinuities inducted by a lake breeze, Ph.D. dissertation, Univ. Michigan, Dept. Meteor. and Oceanogr., 150 pp.

_____, and E.W. Hewson, 1962: Some restrictive meteorological conditions to be considered in the design of stacks, J.Appl. Meteor., 1, 383-390.

Blumenthal, D.L., W.H. White, and R.L. Peace, and T.B. Smith,1974: Determination of the feasibility of the long-range transport of ozone or ozone precursors. Meteor. Res. Inc. Contract No. 68-02-1462. EPA, 92 pp. NTIS No. EPA-450/3-74-061.

Bonner, W.D., 1968: Climatology of the low-level jet. Mon. Wea. Rev., 96, 833-850.

Briggs, G.A., 1969: Plume rise, U.S. Atomic Energy Commission, TID-25075, 81 pp.

Brown, R.M. and P. Michael,1974: Measured effect of shear on plume dispersion, Preprint, Symposium on Atmospheric Diffusion and Air Pollution, Amer. Meteor. Soc., Santa Barbara, 246-250.

Changnon, Stanley, The LaPorte weather anomaly - fact or fiction?:1968, Bull. Amer. Meteor. Soc. 49, 4-11.

Coffey, P.E., and W.N. Stasiuk, 1975: Evidence of atmospheric transport of ozone into urban areas, Environ. Sci. Tech., 9, 59-62.

Cole, H.S., and W.A. Lyons, 1972: The impact of the Great Lakes on the air quality of urban shoreline areas: some practical application with regard to air pollution control policy and environmental decision making. Proc. 15th Conf. Great Lakes Res., Intern. Assoc. Great Lakes Res., 436-463.

Collins, G.F., 1971: Predicting 'Sea-breeze fumigation' from tall stacks at coastal locations, Nuclear Safety, 12, 110-114.

Dieterle, D.A. and A.G. Tingle, 1976: A numerical study of meso-scale transport of air pollutants in sea-breeze circulations. Preprints, 3rd Symposium on Atmospheric Trubulence, Diffusion and Air Quality, A.M.S., Raleigh, 436-441.

Dooley, J.C., Jr., 1976: Fumigation from power plant plumes in the lakeshore environment, UWM Air Pollution Analysis Laboratory Report No. 18, May, 119 pp.

Edinger, J.G., M.H. McCutchan, P.R. Miller, B.C. Ryan, M.J. Schroeder, and J.V. Behar, 1972: Penetration and duration of oxidant air pollution in the south caost air basin of California, J. Air Poll. Control Assoc., 22, 882-886.

EPA, 1975: Position paper on regulation of atmospheric sulfates, U.S. Environmental Protection Agency, EPA-450/2-75-007, 85 pp.

Ergen, D.J. and R.A. Northouse, 1973: Unsupervised discrete cluster analysis TR-A1-73-2, Robotics and Artificial Intelligence Lab Report, UW-Milwaukee.

Ernst, J.A., 1975: A different perspective reveals air pollution, Weatherwise, 28, 215-126.

Esser, J.T., 1973: Bio-assay of ambient pollution in Milwaukee and environs: effects of photochemical air pollution on vegetation, M.S. thesis, Botany Dept., UW-Milwaukee.

Estoque, M.A., 1962: The sea breeze as a function of the prevailing synoptic situation, J. Atm. Sci., 19, 244-250.

_____, 1961: A theoretical investigation of the sea breeze, Quart. J.R. Meteor. Soc., 87, 136-146.

Fert, D.M., 1969: Analysis of the Texas coast land breeze, Tech. Report No. 18, Atm. Sci. Group, Univ. of Texas, Austin, 52 pp.

Fisher, E.L., 1960: An observational study of the sea breeze, J. Meteor., 17, 645-660.

Hall, F.F., Jr., 1972: Temperature and wind structure studies by acoustic echo sounding,in Remote Sensing of the Troposphere, V.E. Derr, Ed., GPO, Washington, D.C.

_____, C.E. Duchon, L.G. Lee, and R.R. Hagan, 1973: Long-range transport of air pollution: a case study, August 1970, Mon. Wea. Rev., 101, 404-414.

Haurwitz, B., 1947: Comments on the sea breeze circulation, J. Meteor., 4, 1-8.

Herkoff, D., 1969: Observed temperature profiles near the Lake Michigan shoreline. Tech. Report, Dept. of Meteorology and Oceanography, Univ. of Michigan, 37 pp.

Hewson, E.W., G.C. Gill, and G.J. Walke, 1963: Smoke plume photography study, Big Rock Point nuclear plant, Charlevoix, Michigan. Pub. No. 04015-3-P, Dept. of Meteorology and Oceanography, Univ. of Michigan, Ann Arbor, unpublished.

Lyons, W.A., 1971: Low-level divergence and subsidence over the Great Lakes in summer. Proc. 14th Conf. Great Lakes Res., Intern. Assoc. Great Lakes Res., 467-487.

_____, 1974: Inadvertent weather modification by Chicago-Northern Indiana pollution sources observed by ERTS-1. Mon.Wea. Rev., 102, 503-508.

_____, 1970: Numerical simulation of Great Lakes summertime conduction inversions, Proc. 13th Conf. Great Lakes Res., Intern. Assoc. Great Lakes Res., 369-387.

_____, 1975: Satellite detection of air pollutants. Proc., Symposium on Remote Sensing Applied to Energy Related Problems, sponsored by University of Miami, John Wiley & Sons, 263-290.

_____, 1966: Some effects of Lake Michigan upon squall lines and summertime convection. Proc. 9th Conf. Great Lakes Res., Intern. Assoc. Great Lakes Res., 259-273.

_____, 1975a: Turbulent diffusion and pollutant transport in shoreline environments, in Lectures on Air Pollution and Environmental Impact Analysis, A.M.S., Boston, 136-208.

_____, and H.S. Cole, 1973: Fumigation and plume trapping on the shores of Lake Michigan during stable onshore flow. J. of Appl Meteor., 12, 494-510.

_____, and H.S. Cole, 1976: Photochemical oxidant transport: mesoscale lake breeze and synoptic-scale aspects, J. Appl. Meteor., 15, 733-743.

_____, and J.C. Dooley, Jr., 1974: Study of fumigation of sulfur oxides from the Waukegan, Illinois power plant. Report submitted to Commonewalth Edison Company, Chicago.

_____, J.C. Dooley, C.S. Keen, J.A. Schuh, and K.R. Rizzo, 1974: Detailed field measurements and numerical models of SO_2 from power plants in the Lake Michigan shoreline environment, Contract Report to Wisconsin Electric Power Co., by Air Pollution Analysis Laboratory, UW-Milwaukee, Milwaukee, Wisconsin, 218 pp.

_____, and C.S. Keen, 1976a: Particulate transport in a Great Lakes coastal environment. In Proceedings, Workshop on Atmospheric Transport and Removal Processes, 2nd ICMSE Conf. on the Great Lakes, Argonne National Laboratory.

_____, C.S. Keen, and R.A. Northouse, 1974: ERTS-1 satellite observations of mesoscale air pollution dispersion around the Great Lakes, preprints, Symposium on Atmospheric Diffusion and Air Pollution, A.M.S., Santa Barbara, 273-280.

_____, and L.E. Olsson, 1973: Detailed mesometeorological studies of air pollution dispersion in the Chicago lake breeze, Mon. Wea. Rev., 101, no. 5, 387-403.

_____, and L.E. Olsson, 1972: Mesoscale air pollution transport in the Chicago lake breeze, J. Air Poll. Control Assoc., 22, 876-881.

_____, and S.R. Pease, 1973: Detection of particulate air pollution plumes from major-point sources using ERTS-1 imagery, Bull. Amer. Meteor. Soc., 54, 1163-1170.

_____, and S.R. Pease, 1972: 'Steam Devils' over Lake Michigan during a January arctic outbreak, Mon. Wea. Rev., 100, 235-237.

_____, and E.M. Rubin, 1976: Aircraft measurements of the Chicago urban plume at 100 km downwind, Preprints, 3rd Symposium on Atmospheric Trubulence, Diffusion, and Air Quality, A.M.S., Raleigh, 358-365.

_____, and J.W. Wilson, 1968: The control of summertime cumuli and thunderstorms by Lake Michigan during non-lake breeze conditions, Res. Paper No. 74, Satellite and Mesometeorology Res. Proj., Univ. of Chicago, 38 pp.

Hidy, G.M., P.K. Mueller, E.Y. Tony, J.R. Mahoney, and N.E. Gaut, 1976: Design of the sulfate regional experiment (SURE), Final Report of Research Project 485, Electric Power Research Institute.

Hirt, M.S., 1. Shenfeld, G. Lee, H. Whaley, and S.D. Jurtors, 1971: A study of the meteorological conditions which developed a classic "fumigation" inland from a large lake shore source, Paper 71-132, 64th Annual Meeting, Air Poll. Control Assoc.

Holzworth, G.C., 1967: Mixing depths, wind speeds, and air pollution potential for selected locations in the United States, Journal of Applied Meteorology, 6.

_____, 1972: Mixing heights, wind speeds, and potential for urban air pollution throughout the contiguous United States, Envir. Protection Agency, Office of Air Programs, Pub. No. AP-101, xi, 118 pp.

Hsu, S.A., 1969: Mesoscale structure of the Texas coast sea breeze, Report No. 16, NSF Grant GA-3674, Univ. of Texas at Austin, Atmospheric Sciences Group, 237 pp.

Husar, R.B., 1975: On the origin of large scale haziness over the Midwestern United States: anatomy of an air pollution episode in St. Louis, unpub. report, Air Poll. Res. Lab., Washington Univ., St. Louis, 10 pp.

_____, N.V. Gillani, J.D. Husar, C.C. Paley, and P.N. Turcu, 1976: Long-range transport of pollutants observed through visibility contour maps, weather maps, and trajectory analysis, Preprints, 3rd Symposium on Atmospheric Turbulence, Diffusion and Air Quality, A.M.S., Raleigh, 344-347.

Jehn, K.H., 1973: A sea breeze bibliography, 1664-1972, Report No. 37, University of Texas, Atm. Science Group, 51 pp.

Keen, C.S., 1976: Trajectory analyses of mesoscale air pollution transport in the Lake Michigan shoreline environment, Ph.D. dissertation, Univ. Wis.-Milwaukee, also Special Report No. 29, Center for Great Lakes Studies, 235 pp.

Lavoie, R.L., A mesoscale numerical model of lake-effect storms, J. Atm. Sci., 29, 1025-1040.

Lenschow, D.H., 1973: Two examples of planetary boundary layer modification over the Great Lakes, J. Atmos. Sci., 30, 568-581.

MacCready, P.B., Jr., 1964: Standardization of gustiness values from aircraft. J. Appl. Meteor., 3, 439-449.

McPherson, R.D., 1970: A numerical study of the effect of a coastal irregularity on the sea breeze, J. Appl. Meteor., 9, 767-777.

Meyer, J.H., 1971: Radar observations of land breeze fronts, J. Appl. Meteor., 10, 1224-1232.

Miller, A., and C.D. Ahrens, 1969: Ozone within and below the west coast temperature inversion, Peport No. 6, San Jose State College, Dept. of Meteor., 74 pp.

Moroz, W.J., 1967: A lake breeze on the eastern shore of Lake Michigan: Observations and model, J. Atmos. Sci., 24, 337-355.

Munn, R.E., 1959: The application of an air pollution climatology to town planning, Inter. J. Air Poll., 1, 276-278.

Neumann, J., and Y. Mahrer, 1971: A theoretical study of the land and sea breeze circulations, J. Atmos. Sci., 28, 532-542.

_____, and _____, 1975: A theoretical study of the lake and land breezes of circular lakes, Mon. Wea. Rev., 103, 474-485.

Ogawa, Y., W.H. Hoydysh, and R. Griffith, 1973: A laboratory simulation of sea breeze effects, TR 115, New York Univ., Environ. Res. Labs, 175 pp.

Olsson, L.E., 1969: Lake effects on air pollution dispersion, Ph.D. dissertation, Dept. of Meteorology and Oceanography, Univ. of Michigan, 216 pp.

Pearce, R.P., 1955: The calculation of a sea breeze circulation in terms of the differential heating across the coast line, Quart. J.R. Meteor. Soc., 81, 351-381.

Pendergast, M.M., and T.V. Crawford, 1974: Actual standard deviations of vertical and horizontal wind direction compared to estimates from other measurements, Preprint, Symposium on Atmospheric Diffusion and Air Pollution, A.M.S., Santa Barbara, 1-7.

Pielke, R.A., 1974a: A comparison of three-dimensional and two-dimensional numerical predictions of sea breezes, J. Atm. Sci., 31, 1577-1585.

_____, 1974b: A three-dimensional numerical model of the sea breeze over south Florida, Mon. Wea. Rev., 102, 115-139.

Raynor, G.S., T.V. Hayes, and E.C. Ogden, 1974: Mesoscale transport and dispersion of airborne pollens, J. Appl. Meteor., 13, 87-95.

_____, P. Michael, R.M. Brown, and S. Sethuraman, 1974: A research program on atmospheric diffusion from an oceanic site. Preprint, Symposium on Atmospheric Diffusion and Air Pollution, A.M.S., Santa Barbara, 289-295.

Ripperton, L.A., J.B. Tommerdahl, and J.J.B. Worth, 1974: Airborne ozone measurements study, Paper 74-42, presented at 67th Annual Meeting, Air Poll. Control Assoc, Denver, 19 pp.

Rizzo, K.R., 1975: Determining the mixing depth climatology using an acoustic sounder in a lakeshore environment, M.S. thesis, UW-Milwaukee, also, Special Report No. 28, Center for Great Lakes Studies, 78 pp.

Schubert, J.F., 1975: Climatology of the mixed layer using acoustic methods, 3rd Symposium on Meteorological Observations and Instrumentation, Preprint, A.M.S., 10-13 February, Washington, D.C.

Schuh, J.A., 1975: A mesoscale model of continuous shoreline fumigation and lid trapping in a Wisconsin shoreline environment, M.S. thesis, UW-Milwaukee, also Special Report No. 27, Center for Great Lakes Studies,107 pp.

Sheih, C.M., and W.J. Moroz, 1975: Mathematical modeling of lake breeze, Atmos. Environ., 9, 1-12.

Thomson, D.W., 1975: ACDAR Meteorology: the application and interpretation of atmospheric acoustic sounding measurements, Preprint, 3rd Symposium on Meteorological Observations and Instruments, A.M.S., Washington, D.C.

Turner, D.B., 1969: Workbook of atmospheric dispersion estimates, Rev. ed., U.S. Dept. Health, Education, and Welfare, 84 pp.

Van der Hoven, I., 1967: Atmospheric transport and diffusion at coastal sites, Nuclear Safety, 8, No. 5, K.E. Cowser, Ed., 490-493.

Warner, J., and J.W. Telford, 1967: Convection below cloud base, J. Atm. Sci., 24, 374-382.

Weisman, B., and M.S. Hirt, 1975: Dispersion governed by the thermal internal boundary layer, Paper 75-26.3, presented at 68th Annual Meeting, Air Pollution Control Assoc., Boston, 13 pp.

Wilson, W.E., R.J. Charlson, R.B. Husar, K.T. Whitby, and B. Blumenthal, 1976: Sulfates in the atmosphere, Paper 76-30-06, 69th Annual Meeting, Air Poll. Control Assoc., Portland, 20 pp.

APPENDIX

Publications generated via support from the U.S. Environmental Protection Agency, Grant No. R-800873.

1972

"Climatology and Prediction of the Chicago Lake Breeze," 20-minute color film, presented, American Meteorological Society Conference on Weather Analysis and Forecasting, Portland, Oregon, also Journal of Applied Meteorology, 11, 1255-1270.

"Mesoscale Air Pollution Transport in the Chicago Lake Breeze" with L.E. Olsson, Journal of the Air Pollution Control Association, 22, 876-881. Also APAL Report No. 3.

"Detailed Mesometeorological Studies of Air Pollution Dispersion in the Chicago Lake Breeze," with L.E. Olsson, Monthly Weather Review, 101, 387-403. Also APAL Report No. 8.

"The Impact of the Great Lakes on the Air Quality of Urban Shoreline Areas: Some Practical Applications with regard to Air Pollution Control Policy and Environmental Decision Making," with H.S. Cole, Proc. 15th Conf. Great Lakes Res., IAGLR, 436-463. Also APAL Report No. 4.

1973

"Fumigation and Plume Trapping on the Shores of Lake Michigan During Stable Onshore Flow," Journal of Applied Meteorology, 12, 494-510, Also APAL Report No. 2.

"ERTS-1 Views the Great Lakes," with S.R. Pease, presented to 16th Conf. Great Lakes Research, IAGLR, also NASA, Goddard Space Flight Center, Greenbelt, MD., Proceedings, "Symposium on Significant Results Obtained from ERTS-1 Satellite," Vol. I, Sec. A, 847-854, Also GLUMP Report No. 15.

"Detection of Particulate Air Pollution Plumes from Major Point Sources Using ERTS-1 Imagery," with S.R. Pease, Bulletin of the American Meteorological Society, 54, 1163-1170. Also APAL Report No. 10.

"The Use of ERTS-1 Imagery in Air Pollution and Mesometeorlogical Studies Around the Great Lakes," with R.A. Northouse, NASA, Goddard Space Flight Center, Greenbelt, MD, Proceedings, Third ERTS Symposium," also, APAL Report No. 11.

"Mesoscale Despersion Regimes on the Shores of the Great Lakes: Observations and Models," with H.S. Cole, J.A. Schuh, and C.S. Keen, 20 minute color film, presented Annual Meeting, American Geophysical Union, San Francisco.

1974

"Inadvertent Weather Modification by Chicago-Northern Indiana Pollution Sources Observed by ERTS-1, Monthly Weather Review, 102, 1163-1170, Also APAL Report No. 9.

"Great Lakes Springtime Conduction Fogs: ERTS-1 Observations and Models," with S.R. Pease, 20-minute color film, presented Annual Meeting, American Meteorological Society, Honolulu.

"Numerical Modeling of Mesoscale Suspended Particulates and Sulfur Oxide Patterns in an Urban Great Lakes Shoreline Environment," with J.A. Schuh, preprints, AMS 5th Conference, Weather Analysis and Forecasting, St. Louis, also APAL Report No. 7.

"The Use of Monitoring Network and ERTS-1 Data to Study Interregional Pollution Transport in the Chicago-Gary-Milwaukee Corridor," with H.S. Cole, presented Annual Meeting, Air Pollution Control Association, Denver, Paper 74-241, also APAL Report No. 12, 25 pp.

"ERTS-1 Satellite Observations of Mesoscale Air Pollution Dispersion Around the Great Lakes," with C.S. Keen and R.A. Northouse, preprints AMS/WMO Symposium on Atmospheric Diffusion, Turbulence, and Air Pollution, Santa Barbara, 273-280, also APAL Report No. 13.

"Study of Fumigation of Sulfur Oxides from the Waukegan, Illinois Power Plant," with J.C. Dooley, Final Report to Commonwealth Edison Co., 75 pp.

1975

"Detailed Field Measurements and Numerical Models of SO_2 from Power Plants in the Lake Michigan Shoreline Environment," with J.C. Dooley, C.S. Keen, J.A. Schuh, and K.R. Rizzo, Final Report to Wisconsin Electric Power Company, 218 pp.

"Satellite Detection of Air Pollutants," Remote Sensing Energy-Related Studies,T.N. Veziroglu, Ed.,John Wiley & Sons, New York, 263-290.

"Turbulent Diffusion and Pollutant Transport in Shoreline Environments," invited contribution, Workshop on Meteorology and Environmental Assessment, American Meteorological Society, Boston, 105-177. (Invited lecture/paper).

1976

"Single Theodolite Pibal Observations on the Western Shoreline of Lake Michigan: Summers 1973 and 1974," with S. Hentz, J.C. Dooley, C.S. Keen, GLUMP Project Report No. 16, 190 pp.

"Particulate Transport in a Great Lakes Coastal Environment," with C.S. Keen, invited paper, Proceedings, 2nd ICMSE Conference on the Great Lakes, workshop on atmospheric transport and removal processes, Argonne National Laboratory, 23 pp.

"Computed 24-Hour Trajectories for Aerosols and Gases in a Lake/Land Breeze Circulation Cell on the Western Shore of Lake Michigan," with C.S. Keen, preprints, Sixth Conference on Weather Analysis and Forecasting, American Meteorological Society, Albany, NY, 6 pp.

"Photochemical Oxidant Transport: Mesoscale Lake Breeze and Synoptic Scale Aspects," with H.S. Cole, Journal of Applied Meteorology, 15 (in press), pp. 733-743.

"Aircraft Measurements of the Chicago Urban Plume at 100 km Downwind," with E.M. Rubin, Preprints, Third Symposium on Turbulence, Diffusion, and Air Pollution, American Meteorological Society, Raleigh, N. Carolina, pp. 358-365.

"Meteorological Aspects of Air Quality," Bulletin of the American Meteorological Society, 57, 205-206.

"SMS/GOES Visible Images Detect Synoptic-Scale Air Pollution Episode," with R.B. Husar, submitted to Monthly Weather Review.

Graduate Theses produced via support from the U.S. Environmental Protection Agency, Grant No. R-800873.

Ph.D.

Keen, Cecil S., 1976: Trajectory Analyses of Mesoscale Air Pollution Transport in the Lake Michigan Shoreline Environment. University of Wisconsin-Milwaukee, Department of Geography, published as Special Report No. 29, UWM Center for Great Lakes Studies, April, 235 pp.

M.S.

Dooley, John C., Jr., 1976: Fumigation from Power Plant Plumes in the Lakeshore Environment. University of Wisconsin-Milwaukee, College of Engineering and Applied Science, Published as Air Pollution Analysis Laboratory Report No. 19, July, 119 pp.

Rizzo, Kenneth R., 1975: Determining the Mixing Depth Climatology Using an Acoustic Sounder in a Lakeshore Environment. University of Wisconsin-Milwaukee, College of Engineering and Applied Science, Published as Special Report No. 28, UWM Center for Great Lakes Studies, December, 78 pp.

Schuh, Jerome A., 1975: A Mesoscale Model of Continuous Shoreline Fumigation and Lid Trapping in a Wisconsin Shoreline Environment. University of Wisconsin-Milwaukee, College of Engineering and Applied Science, Published as Special Report No. 27, UWM Center for Great Lakes Studies, December, 107 pp.

TECHNICAL REPORT DATA
(Please read Instructions on the reverse before completing)

1. REPORT NO.	2.	3. RECIPIENT'S ACCESSION NO.
EPA-600/4-77-010		

4. TITLE AND SUBTITLE	5. REPORT DATE
MESOSCALE AIR POLLUTION TRANSPORT IN SOUTHEAST WISCONSIN	February 1977
	6. PERFORMING ORGANIZATION CODE
7. AUTHOR(S)	8. PERFORMING ORGANIZATION REPORT NO.
Walter A. Lyons	
9. PERFORMING ORGANIZATION NAME AND ADDRESS	10. PROGRAM ELEMENT NO.
University of Wisconsin-Milwaukee Air Pollution Analysis Laboratory College of Engineering and Applied Science Milwaukee, Wisconsin 53201	1AA603
	11. CONTRACT/GRANT NO.
	R-800873
12. SPONSORING AGENCY NAME AND ADDRESS	13. TYPE OF REPORT AND PERIOD COVERED
Environmental Sciences Research Laboratory - RTP, N.C. Office of Research and Development U.S. Environmental Protection Agency Research Triangle Park, N.C. 27711	Final 1972-1976
	14. SPONSORING AGENCY CODE
	EPA/600/09

15. SUPPLEMENTARY NOTES

16. ABSTRACT During the period 1970-1976, the University of Wisconsin-Milwaukee's Air Pollution Analysis Laboratory (College of Engineering and Applied Science) engaged in extensive studies on the mesometeorology of the Great Lakes. This report highlights the important findings of this research that are air pollution-related. An extensive field study on the western shore of Lake Michigan during the summer of 1974 essentially validated the GLUMP Fumigation Model, which was calibrated for multi-plume power plants. Studies of lake meteorology showed that, even during supposedly "steady-state" onshore gradient flows, complicated wind patterns occurred including the development of low-level jet streams associated with intense inversion layers. The acoustic sounder was found to be highly useful in showing the structure of the lake-shore environment. Also, satellite data were highly useful in monitoring mesoscale, regional and synoptic scale transport. Individual plumes were detected for more than 150 km over Lake Michigan, and a major sulfate haze aerosol episode was imaged over the central U.S. A model was proposed to explain the inland band of elevated ozone levels running parallel to the shoreline, and the Chicago metropolitan area was shown to be a major contributor to the high oxidant levels recorded in southeastern Wisconsin. On one occasion, aircraft monitoring of the Chicago urban plume revealed interstate transport of 25 tons per hour of SO_2 from Illinois into Wisconsin. The findings suggest that the concept of Air Quality Control Regions has to be severely modified ~~or abandoned altogether and showed the inapplicability of most existing short term~~ prediction models in coastal zones.

17. KEY WORDS AND DOCUMENT ANALYSIS

a. DESCRIPTORS	b. IDENTIFIERS/OPEN ENDED TERMS	c. COSATI Field/Group
*Air pollution Ozone Sulfur dioxide *Meteorology *Atmospheric circulation Sea breezes *Mathematical models Electric power plants Meteorological satellites Plumes	Great Lakes Southeast Wisconsin	13B 07B 04B 12A 10B 22B 21B

18. DISTRIBUTION STATEMENT	19. SECURITY CLASS *(This Report)*	21. NO. OF PAGES
RELEASE TO PUBLIC	UNCLASSIFIED	238
	20. SECURITY CLASS *(This page)*	22. PRICE
	UNCLASSIFIED	

EPA Form 2220-1 (9-73)